

ROZPRAWA DOKTORSKA



INSTYTUT CHEMII BIOORGANICZNEJ
Polskiej Akademii Nauk

***Opracowanie allelo-selektywnej strategii
terapeutycznej dla chorób poliglutaminowych
z wykorzystaniem wektorowych narzędzi
technologii interferencji RNA***

mgr inż. Anna Kotowska-Zimmer

Praca wykonana w Zakładzie Inżynierii Genomowej
pod opieką dr hab. Marty Olejniczak, prof. ICHB PAN

Poznań 2022

*Składam najserdeczniejsze
podziękowania mojej Promotor
dr hab. Marcie Olejniczak, prof. ICHB PAN
za opiekę naukową, przekazaną wiedzę,
cenne uwagi merytoryczne
oraz okazaną życzliwość,
wrozumiałość i cierpliwość*

*Dziękuję **Koleżankom i Kolegom**
z Zakładów Inżynierii Genomowej
i Biotechnologii Medycznej
za cenne rady i miłą atmosferę w pracy*

*Moim najbliższym, **Rodzicom i Adamowi**
za możliwość rozwoju i nieustanne wsparcie
w najtrudniejszych momentach
również pragnę ogromnie podziękować*

Spis treści

Wykaz skrótów	2
Lista publikacji będących częścią rozprawy	3
Lista publikacji niebędących częścią rozprawy	3
Streszczenie	4
Abstract	6
Wprowadzenie	8
Choroby poliglutaminowe	8
Strategie terapeutyczne w chorobach poliglutaminowych	10
Strategia celowania w powtórzenia CAG	14
Cel pracy doktorskiej	17
Opis publikacji wchodzących w skład rozprawy doktorskiej	18
<i>Universal RNAi Triggers for the Specific Inhibition of Mutant Huntingtin, Atrophin-1, Ataxin-3, and Ataxin-7 Expression</i>	18
<i>Artificial miRNAs as therapeutic tools: Challenges and opportunities</i>	22
<i>A CAG repeat-targeting artificial miRNA lowers the mutant huntingtin level in the YAC128 model of Huntington's disease</i>	25
Dyskusja	30
Bibliografia	36

Załączniki:

Oświadczenia określające wkład w powstanie prac naukowych wchodzących w skład rozprawy doktorskiej

Prace naukowe wchodzące w skład rozprawy doktorskiej

Wykaz skrótów

5'UTR, 3'UTR – nieulegające translacji regiony mRNA znajdujące się po stronie 5' lub 3' sekwencji kodującej białko (ang. *untranslated region*)

AGO – białko z rodziny Argonaute

ASO – oligonukleotyd antysensowy (ang. *antisense oligonucleotide*)

DRPLA - zanik zębatoczerwienny pallidoniskowzgórzowy (ang. *dentatorubral-pallidoluysian atrophy*)

HD – choroba Huntingtona (ang. *Huntington's Disease*)

NGS- sekwencjonowanie nowej generacji (ang. *Next-Generation Sequencing*)

nt – nukleotyd

poliQ – poliglutamina

pre-miRNA – prekursor mikroRNA

pri-miRNA – pierwotny transkrypt mikroRNA, pierwotny prekursor mikroRNA

pz – pary zasad

RISC – kompleks wyciszający indukowany przez RNA (ang. *RNA-induced silencing complex*)

RNAi – interferencja RNA (ang. *RNA interference*)

SBMA –rdzeniowo-opuszkowy zanik mięśni, choroba Kennedy'ego (ang. *Spinal and Bulbar Muscular Atrophy*)

SCA – ataksja rdzeniowo-mózdkowa (ang. *spinocerebellar ataxia*)

siRNA – krótkie interferujące RNA (ang. *small interfering RNA*)

shRNA – krótkie RNA tworzące strukturę typu spinki (ang. *short hairpin RNA*)

SNP – polimorfizm pojedynczego nukleotydu (ang. *single nucleotide polymorphism*)

Lista publikacji będących częścią rozprawy

1. **Kotowska-Zimmer A**, Ostrovska Y, Olejniczak M (2020). *Universal RNAi Triggers for the Specific Inhibition of Mutant Huntingtin, Atrophin-1, Ataxin-3, and Ataxin-7 Expression*. *Molecular Therapy – Nucleic Acids*, 19: 562-571.
DOI: 10.1016/j.omtn.2019.12.012, IF– 8,886
2. **Kotowska-Zimmer A**, Pewinska M, Olejniczak M (2021). *Artificial miRNAs as therapeutic tools: Challenges and opportunities*. *WIREs RNA*, 12:e1640.
DOI: 10.1002/wrna.1640, IF– 9,957
3. **Kotowska-Zimmer A**, Przybyl L, Pewinska M, Suszynska-Zajczyk J, Wronka D, Figiel M, Olejniczak M (2022). *A CAG repeat-targeting artificial miRNA lowers the mutant huntingtin level in the YAC128 model of Huntington's disease*. *Molecular Therapy – Nucleic Acids*, 28: 702-715.
DOI: 10.1016/j.omtn.2022.04.031, IF– 8,886

Lista publikacji niebędących częścią rozprawy

1. Olejniczak M, **Kotowska-Zimmer A**, Krzyzosiak W (2018). *Stress-induced changes in miRNA biogenesis and functioning*. *Cellular and Molecular Life Sciences*, 75: 177–191.
DOI: 10.1007/s00018-017-2591-0, IF- 7,014*

DOI - Digital Object Identifier

IF – Impact Factor zgodnie z rokiem opublikowania (JCR)

Streszczenie

Choroby poliglutaminowe (poliQ) są grupą genetycznych chorób neurodegeneracyjnych, których wspólną cechą jest występowanie mutacji polegającej na ekspansji powtórzeń CAG w określonych genach. Mutacja ta prowadzi do powstania toksycznego białka z wydłużonym ciągiem poliglutaminowym. Do grupy chorób poliQ zaliczamy chorobę Huntingtona (HD), ataksje rdzeniowo-mózdkowe typu 1, 2, 3, 6, 7 i 17 (SCAs), zanik zębatoczerwienny pallidoniskowzgorzowy (DRPLA) oraz rdzeniowo-opuszkowy zanik mięśni (SBMA). W zależności od choroby, dochodzi do degeneracji neuronów w różnych regionach mózgu, a co za tym idzie do wystąpienia różnorodnych objawów neurologicznych, jak i emocjonalnych, które pojawiają się najczęściej w czwartej dekadzie życia. Na wystąpienie choroby wpływa liczba powtórzeń CAG w określonym genie, która różni się w przypadku każdej z chorób, np. dla HD jest to >40 powtórzeń CAG, natomiast dla SCA3 >60. Niestety, mimo wielu lat badań nad skuteczną terapią, choroby te są w dalszym ciągu nieuleczalne, a łagodzone są jedynie ich objawy. Jedną z bardziej obiecujących strategii terapeutycznych, mających na celu ograniczenie rozwoju choroby, jest technologia interferencji RNA (RNAi). Wyniki licznych eksperymentów *in vitro*, jak i *in vivo*, potwierdziły skuteczność stosowania narzędzi tej technologii, takich jak siRNA (ang. *small interfering RNA*), shRNA (ang. *short-hairpin RNA*) i amiRNA (ang. *artificial miRNA*) w wyciszaniu ekspresji zmutowanych genów. W związku z tym, głównym celem mojej pracy doktorskiej był rozwój strategii terapeutycznej, polegającej na selektywnym wyciszaniu ekspresji zmutowanych genów, odpowiedzialnych za rozwój chorób poliQ, przy pomocy wektorowych narzędzi technologii RNAi, celujących w powtórzenia CAG.

W pierwszym etapie badań zaprojektowałam serię cząsteczek typu shRNA ze wstawionymi sekwencjami siRNA celującymi w powtórzenia CAG i posiadającymi niesparowania w określonych pozycjach z sekwencją docelową, co umożliwiło działanie allelo-selektywne na drodze inhibicji translacji.

Ich efektywność oraz allelo-selektywność sprawdziłam w komórkowych modelach chorób poliQ, takich jak HD, SCA3, SCA7 i DRPLA. Wykazałam, że cząsteczki te są precyzyjnie docinane w komórkach, powodują specyficzne obniżenie poziomu zmutowanych białek i nie wywołują istotnych efektów niespecyficznych w liniach komórkowych. Ze względu na to, że doniesienia literaturowe pokazują, że cząsteczki

shRNA mogą być toksyczne w zastosowaniu *in vivo*, w kolejnych etapach prac podjęłam się zgłębienia i analizy wiedzy dotyczącej cząsteczek amiRNA oraz zaprojektowania i przetestowania własnych cząsteczek tego typu. W pracy przeglądowej, której jestem głównym autorem, zebrana została najbardziej aktualna wiedza dotycząca biogenezy miRNA, cech strukturalnych i sekwencyjnych cząsteczek pri-miRNA wpływających na ich obróbkę komórkową, a także zasady projektowania cząsteczek amiRNA i wykorzystane tego typu narzędzi w potencjalnych terapiach chorób neurodegeneracyjnych, nowotworowych i wirusowych. Zdobyta wiedza pozwoliła mi na zaprojektowanie cząsteczek amiRNA, mających obniżyć poziom zmutowanej HTT w linii komórkowej fibroblastów HD. Cząsteczka działająca najbardziej efektywnie i selektywnie posiadała tę samą wstawkę siRNA, co działający najefektywniej shRNA, czyli posiadający substytucję A w 8 pozycji od końca 5' cząsteczki. Wstawiona była w kadłub pri-miR-136, który wykazuje homogeną obróbkę komórkową. Obie cząsteczki, shRNA jak i amiRNA, zostały przeze mnie przetestowane w mysim modelu HD, YAC128. Wykazałam, że obie cząsteczki powodują efektywne i allelo-selektywne obniżenie poziomu zmutowanej HTT. Potwierdziłam również, że cząsteczki shRNA mogą powodować wystąpienie efektów toksyczności u myszy. Działanie cząsteczki amiRNA nie spowodowało wystąpienia tego typu efektów. Barwienia immunofluorescencyjne skrawków mózgu myszy nie wykazały aktywacji mikrogleju i astrocytów po iniekcji wektora AAV5 niosącego amiRNA. Ponadto cząsteczka ta spowodowała zmniejszenie ilości agregatów HTT w prążkowie myszy. Zaobserwowana została także częściowa poprawa fenotypu u tych zwierząt.

Podsumowując, zaprojektowane przeze mnie cząsteczki shRNA i amiRNA, celujące w powtórzenia CAG, efektywnie i allelo-selektywne obniżają poziom zmutowanych białek poliQ. Ponadto działanie cząsteczki amiRNA, w porównaniu do shRNA jest bezpieczne w organizmie myszy i prowadzi do poprawy fenotypu chorych zwierząt.

Abstract

Polyglutamine diseases (polyQ) are a group of genetic, neurodegenerative disorders that share a common feature of the presence of a mutation associated with the expansion of CAG repeats in specific genes. This mutation leads to the formation of toxic protein containing an abnormally elongated polyglutamine tract. To the group of polyQ diseases, we can include Huntington's Disease (HD), spinocerebellar ataxias type 1, 2, 3, 6, 7, and 17 (SCA), dentatorubral-pallidoluysian atrophy (DRPLA), and spinal and bulbar muscular atrophy (SBMA). Depending on the disease, neurons degenerate in different regions of the brain, and thus various neurological and psychological symptoms occur in most cases in the fourth decade of life. The occurrence of the diseases is influenced by the number of CAG repeats in the certain genes, which depends on the disease, e.g. for HD it is >40 CAG repeats, and for SCA3 >60. Unfortunately, despite many years of research, these diseases are incurable and only their symptoms are alleviated. One of the most promising therapeutic strategies that aim to reduce the development of these diseases is RNA interference (RNAi). Results of many *in vitro* and *in vivo* experiments confirmed the effectiveness of RNAi tools, such as siRNA (small interfering RNA), shRNA (short-hairpin RNA), and amiRNA (artificial miRNA) in the silencing of the expression of mutant genes.

Therefore, the main goal of my dissertation was to develop a therapeutic strategy that selectively silences the expression of mutant genes which cause polyQ diseases, with the use of vector-based tools of RNAi technology targeting CAG repeats.

In the first step of the study, I designed a series of shRNAs with embedded siRNAs targeting repeats and containing mismatches at certain positions to the target sequence, which allowed for an allele-selective effect by inhibiting translation.

I tested their efficiency and allele-selectivity in cellular models of polyQ diseases such as HD, SCA3, SCA7, and DRPLA. I showed that they are precisely processed in cells, cause a specific silencing of mutant proteins, and do not cause overt toxicity in cell lines. Due to the fact, that the literature shows the toxicity of shRNAs *in vivo*, in the next steps of my study I undertook to investigate and analyze the knowledge of amiRNA as well as design and test my amiRNAs. In the review, in which I am the main author, the most up-to-date knowledge of miRNA biogenesis, structural and sequence features of pri-miRNAs affecting their cell processing, as well as the rules of designing amiRNAs and the use of

this type of tools in potential therapies of neurodegenerative, cancer and viral diseases were collected. The acquired knowledge allowed me to design amiRNAs that were embedded into 4 different backbones to silence the level of mutant HTT in the HD fibroblast. The most efficient and selective molecule contained the same siRNA insert as the most effective shRNA containing A substitution at the 8th position from the 5' end of the molecule. This amiRNA was embedded into the pri-miR-136 backbone, which shows the homogenous processing in cells. I tested both molecules, shRNA, and amiRNA in the mouse model of HD, YAC128. I showed that both of them cause efficient and allele-selective reduction of mutant HTT. I also confirmed that shRNAs can be toxic in mice. In the case of amiRNA, it did not cause any overt symptoms of toxicity. The immunofluorescence stainings of mouse brain sections did not show micro- and astrogliosis after mice injection with AAV5 carrying amiRNA. Moreover, this molecule led to a reduction in the number of HTT aggregates in the mice striatum. A partial improvement in some motor and learning deficits was also observed.

In conclusion, CAG-targeting shRNAs and amiRNAs designed by me, efficiently and allele-selectively silence the expression of mutant proteins. In addition, amiRNAs compared to shRNAs are safe in mice and lead to the partial improvement of the YAC128 phenotype.

Wprowadzenie

Choroby poliglutaminowe

Choroby poliglutaminowe (poliQ) są grupą rzadkich, neurodegeneracyjnych chorób genetycznych spowodowanych ekspansją powtórzeń CAG w regionach ulegających translacji odpowiednich genów, powodując powstawanie ciągów poliglutaminowych. Prowadzi to do nabycia toksycznych właściwości przez białka^{1,2}. Charakterystyczne jest również występowanie agregatów składających się z fragmentów białek zawierających wydłużone ciągi poliQ. Funkcja tych agregatów nie jest do końca poznana, w związku z tym nie można jednoznacznie stwierdzić czy przyczyniają się one do postępującej neurodegeneracji, czy wręcz przeciwnie - pełnią funkcję ochronną poprzez gromadzenie toksycznych fragmentów białek³⁻⁶. Do chorób poliQ zaliczamy: chorobę Huntingtona (HD), ataksje rdzeniowo-mózdkowe typu 1, 2, 3, 6, 7 i 17 (SCA), zanik zębato-czerwienny pallidoniskowzgórzowy (DRPLA), które są dziedziczone w sposób autosomalnie dominujący oraz rdzeniowo-opuszkowy zanik mięśni (choroba Kennedy'ego, SBMA) spowodowany przez mutację sprzężoną z chromosomem X, na który chorują wyłącznie mężczyźni⁷. Na wystąpienie choroby wpływa liczba powtórzeń CAG w określonym genie, która różni się w zależności od choroby, dla HD jest to >40 powtórzeń CAG, dla SCA3 >60 a dla DRPLA >48⁸⁻¹¹. Objawy pojawiają się zazwyczaj w czwartej dekadzie życia, jednakże w przypadku HD, może wystąpić również młodzieńcza postać choroby, objawiająca się już przed 20 rokiem życia, co związane jest z większą liczbą powtórzeń CAG w genie huntingtyny (> 60)^{9,12,13}. Badania wykazały, że w przypadku chorób poliQ większa liczba powtórzeń CAG wiąże się z wcześniejszym ujawnieniem się choroby i jej silniejszymi objawami^{14,15}. Dodatkowo mutacja tego typu jest niestabilna, co powoduje zmiany liczby powtórzeń pomiędzy pokoleniami, jak również pomiędzy różnymi typami komórek i tkanek u tej samej osoby. Związane jest to z tendencją do tworzenia przez powtórzenia trójnukleotydowe alternatywnych struktur, takich jak spinki do włosów, czy do przesunięcia nici DNA (slipped-strands), które prowadzą do zmian długości ciągów i mogą występować podczas replikacji, naprawy, rekombinacji i transkrypcji¹⁶⁻¹⁸. Mutacje w genach kodujących białka poliQ przyczyniają

się do zaburzenia wielu procesów komórkowych, w których naturalnie biorą udział. Przykładem może być huntingtyna (HTT), która odpowiada za oddziaływanie z czynnikami transkrypcyjnymi, transport pęcherzyków i organelli wzdłuż aksonów, sygnalizację postsynaptyczną oraz pełni funkcje neuroprotektoryjne. Ważną jej rolą jest transport i transkrypcyjna regulacja neurotroficznego czynnika pochodzenia mózgowego (ang. *brain-derived neurotrophic factor*, BDNF), który jest istotny w przeżyciu neuronów prążkowania i kory mózgowej¹⁹⁻²¹. W przypadku mutacji HTT może dojść m.in. do deregulacji transkrypcji, dysfunkcji mitochondriów, stresu oksydacyjnego, ekscytotoksyczności pozasynaptycznej oraz zaburzenia transportu pęcherzykowego^{22,23}. Ataksyna-3 (ATXN3) jest kolejnym białkiem o istotnym znaczeniu w komórkach. Pełni funkcję enzymu deubikwitynującego, który wiąże i niszczy łańcuchy poliubikwitynowe. Jest ona składnikiem systemu ubikwityna-proteasom (ang. UPS, *ubiquitin-proteasome system*) oraz pełni funkcje regulatorowe w autofagii²⁴, czyli bierze udział w procesach mających na celu kontrolę jakości i degradację białek^{25,26}. Ponadto potwierdzono, że zaangażowana jest w regulację transkrypcji²⁷. Mutacja ATXN3 może prowadzić do hamowania aktywności proteasomu poprzez nagromadzenie nieprawidłowo sfałdowanych białek²⁸. Innymi negatywnymi skutkami mutacji mogą być deregulacja transkrypcji, zaburzenia w transporcie aksonalnym i autofagii²⁹.

Pomimo że geny kodujące białka poliQ ulegają ekspresji w komórkach całego ciała, degeneracja dotyczy głównie komórek nerwowych. Każda z tych chorób posiada charakterystyczny, unikalny wzór neurodegeneracji w określonym regionie mózgu. W przypadku HD jest to wczesna i znaczna degeneracja w prążkowie i korze mózgu, w SCA3 degeneracja komórek w mózdzku i zwojach podstawnych, dla SCA7 zwyrodnienie receptorów siatkówki, a w SBMA występuje znaczna degeneracja neuronów ruchowych i patologia mięśni szkieletowych. Degeneracja w tych rejonach wpływa na występowanie specyficznych objawów, np. w HD obserwuje się m.in. niekontrolowane ruchy, drżenie kończyn, zmniejszenie napięcia mięśni i zaburzenia pamięci; w przypadku ataksji są to problemy z utrzymaniem równowagi, trudności z koordynacją ruchową, zaburzenia chodu i mowy^{7,30-32}. Objawy te znacznie obniżają pacjentom jakość życia, sprawiając, że chory musi być pod stałą opieką.

Strategie terapeutyczne w chorobach poliglutaminowych

W przypadku chorób poliQ nie ma skutecznej terapii, a leczenie jest ograniczone jedynie do łagodzenia objawów chorobowych. Najbardziej zaawansowane badania prowadzone są dla choroby Huntingtona. Część potencjalnych terapeutów celujących w HTT jest już na etapie badań klinicznych. W przypadku innych chorób poliQ badania nie są prowadzone na tak dużą skalę, a testy kliniczne obejmują tylko nieliczną grupę podejść terapeutycznych. Jedynym lekiem stosowanym w HD, zaakceptowanym przez amerykańską Agencję Żywności i Leków (FDA) jest tetrabenazyna stosowana w łagodzeniu hiperkinetycznych zaburzeń motorycznych³³. Nie powoduje ona jednak cofnięcia objawów chorobowych, co w przypadku pacjentów byłoby bardzo pożądane. W związku z tym wiele zespołów prowadzi badania nad potencjalnymi terapiami, które pozwalałyby na to, albo nawet nie dopuściły do rozwinięcia się choroby. Stosowane są różne strategie, w tym celowanie w powstałe toksyczne białko. Możliwe jest to, między innymi, poprzez wykorzystanie endogennych szlaków komórkowych, w których zwiększa się efektywność degradacji nieprawidłowo sfałdowanego białka lub agregatów. Pozwala to na usunięcie toksycznego czynnika z komórki, głównie poprzez modulowanie szlaków UPS i autofagii³⁴⁻³⁷. Do tej pory jednak podejścia takie nie weszły w etap badań klinicznych. Dlatego też najbardziej obiecującą strategią wydaje się celowanie w zmutowane geny lub ich transkrypty, tak aby nie dopuścić do powstania toksycznego białka lub obniżyć jego poziom w organizmie, a tym samym zapobiec wystąpieniu dalszych szkodliwych efektów. Może to być osiągnięte przez zastosowanie technologii, takich jak edycja DNA, niskocząsteczkowe modulatory obróbki RNA, antysensowe oligonukleotydy (ASO) lub narzędzia technologii interferencji RNA (RNAi), do których zaliczamy krótkie interferujące RNA (ang. *small interfering RNA*, siRNA), krótkie spinki RNA (ang. *short hairpin RNA*, shRNA) i sztuczne mikroRNA (ang. *artificial miRNAs*, amiRNA). Dwie ostatnie technologie celujące w RNA, po uzyskaniu obiecujących wyników w eksperymentach *in vivo*, weszły w fazę badań klinicznych (Tab. 1).

Cząsteczki ASO testowane przez naukowców z firm Wave Life Sciences (WVE-120101 i WVE-120102) i Roche (GENERATION-HD1; tominersen; RG6042) były na najbardziej zaawansowanym etapie badań klinicznych. Celując w sekwencje komplementarne w mRNA *HTT*, powodowały włączenie mechanizmu degradacji transkryptu przez RNAzę H, a co za tym idzie obniżenie poziomu toksycznej *HTT*.

W przypadku Wave Life Sciences cząsteczki celowały tylko w zmutowaną formę HTT, rozróżniając allel zmutowany od normalnego na podstawie SNP związanego z mutacją. Natomiast strategia wykorzystywana przez Roche miała powodować obniżenie poziomu zmutowanej, jak i prawidłowej HTT. W 2021 roku badania kliniczne z zastosowaniem obu typów cząsteczek zostały zatrzymane, w I/II (Wave Life Sciences) i III fazie (Roche). Pacjenci, którzy otrzymali tominersen, uzyskiwali gorsze wyniki w badaniach, niż pacjenci z placebo. Ponadto obserwowano powiększenie komórek bocznych zależne od podania leku oraz wodogłowie u kilku pacjentów otrzymujących częstsze dawki tego terapeutycznego. Wyniki z wcześniejszej fazy badań wykazały, że cząsteczka ta może spowodować obniżenie poziomu HTT w płynie mózgowo-rdzeniowym (ang. CSF, *cerebrospinal fluid*) o 44%.





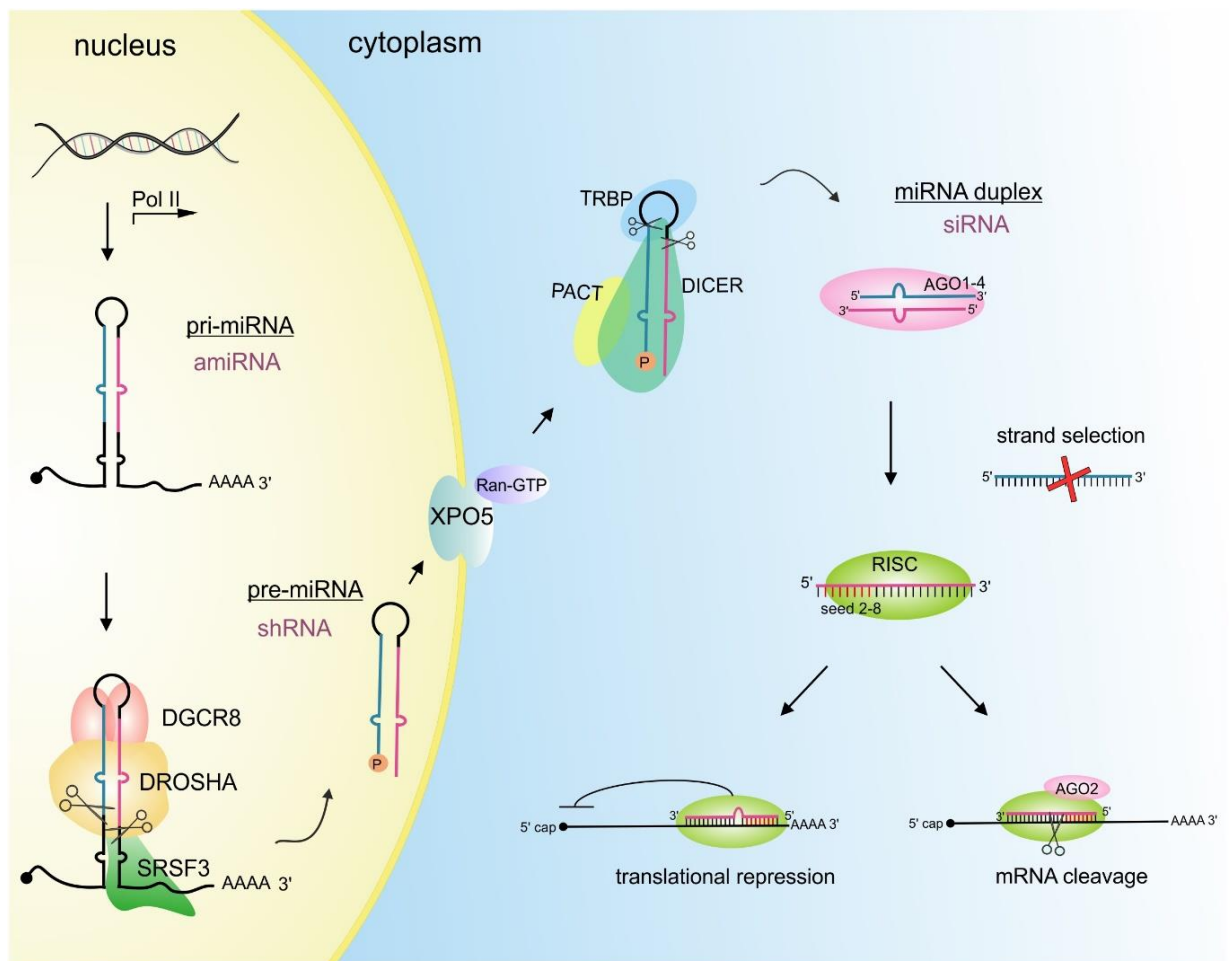
Firma	Technologia	Strategia	Nazwa terapeutycznego	Faza badań klinicznych
	ASO	nieselektywna	RG6042 (HTTRx)	I/IIa – ukończona III - wstrzymana
	ASO	selektywna	WVE-120101 WVE-120102 WVE-003	I/IIa – zakończona I/IIa – rozpoczęta w 2021 r.
	RNAi	nieselektywna	AMT-130	I/IIa – rozpoczęta w 2021 r.
	RNAi	nieselektywna	VY-HTT01	w planach

Tabela 1. Porównanie badań klinicznych dla HD wykorzystujących cząsteczki celujące w RNA

Powstaje jednak pytanie, czy taki poziom wyciszenia jest bezpieczny? Redukcji ulega HTT zmutowana, ale też i prawidłowa, która pełni określone funkcje. Niepowodzenie tominersenu może w tym przypadku wynikać z przekroczenia bezpiecznego progu obniżania poziomu HTT, jednak jest to kwestia do dalszych analiz. Jeśli chodzi o cząsteczki WVE-120101 i WVE-120102, mimo comiesięcznego podawania terapeutycznego, zespół badawczy nie zaobserwował istotnego obniżenia poziomu HTT w płynie mózgowo-rdzeniowym. Postęp choroby u pacjentów, którym podano ASO, był taki sam jak u pacjentów z placebo. Skłoniło to zespół Wave Life Sciences do pracy nad kolejną cząsteczką celującą w inny SNP (WVE-003) i rozpoczęcia w tym samym roku badań klinicznych z jej wykorzystaniem. Ponadto nowy ASO posiada modyfikację w strukturze, aby poprawić jego działanie u pacjentów. Jak widać, mimo zaawansowania badań nad tego typu cząsteczkami, jest jeszcze wiele do wyjaśnienia. Dużym problemem w przypadku ASO jest również konieczność częstego podawania tej cząsteczki, która w przypadku HD musi zostać podana dooponowo przynajmniej raz na dwa miesiące. Aby ominąć ten problem, korzystnym rozwiązaniem jest zastosowanie narzędzi technologii RNAi, podawanych w formie wektorowej, co zostało wykorzystane m.in. przez firmę Uniqure i pozwoliło na rozpoczęcie przez nią pierwszej fazy badań klinicznych. Technologia RNAi wykorzystuje naturalną ścieżkę biogenezy miRNA, a narzędzia w niej stosowane, takie jak amiRNA, shRNA i siRNA odpowiadają cząsteczkom pri-miRNA, pre-miRNA i miRNA. Każda z nich włącza się w ścieżkę biogenezy miRNA na odpowiednim etapie (Ryc.1). Ponadto różnią się one sposobem dostarczania do komórek, budową i czasem działania (Tab. 2). Cząsteczka siRNA, ze względu na prostotę projektowania i wprowadzania do komórek, jest najczęściej stosowanym narzędziem do wyciszenia ekspresji genów. W tym przypadku, jak i w przypadku ASO problemem jest jednak krótki okres półtrwania związany ze stosunkowo szybką degradacją i „rozcieńczanie” efektu związane z podziałami komórkowymi³⁸. Na osiągnięcie dłuższego okresu działania może pozwolić chemiczna i strukturalna modyfikacja narzędzi siRNA, jak np. stworzona w ostatnim czasie biwalentna cząsteczka składająca się z dwóch połączonych cząsteczek siRNA, która pozwoliła na utrzymujące się przez sześć miesięcy obniżenie HTT w mózgu myszy będącej modelem HD³⁹. Dla osiągnięcia efektu trwającego znacznie dłużej korzystne jest zatem stosowanie podejścia wektorowego, w którym cząsteczka shRNA lub amiRNA wprowadzana jest do organizmu za pomocą wirusa, najczęściej związanego z adenowirusami (AAV), a jej ekspresja po jednorazowym podaniu trwa przez wiele lat. Cząsteczki te cięte są

w komórkach odpowiednio przez enzymy Dicer lub Drosha i Dicer do dojrzałego siRNA^{40,41}. Warto dodać, że najbezpieczniejszym typem cząsteczki technologii RNAi jest amiRNA. Cząsteczki shRNA, ze względu na to, że osiągają wysokie poziomy ekspresji, mogą prowadzić do wysycania maszynerii białkowej biogenezy miRNA, szczególnie białka XPO5^{42,43}. Zbyt wysoki poziom tego typu cząsteczek może również skutkować wystąpieniem efektów niespecyficznych zależnych od sekwencji (ang. *off-target*), a tym samym do toksyczności w organizmie. Poziom amiRNA w komórkach jest stosunkowo niski, często porównywalny do endogennie występujących miRNA, ze względu na dwuetapową obróbkę komórkową. Cząsteczki te ulegają ekspresji spod promotorów polimerazy RNA II (Pol II), a najczęściej stosowanym jest CMV. Podczas projektowania amiRNA w miejsca sekwencji nici wiodącej i pasażerskiej w pri-miRNA wstawia się działające sekwencje siRNA. Jednym z przykładów tego typu terapeutyków, jest miHTT, który jako pierwszy został wykorzystany w badaniach klinicznych nad HD.



Rycina 1. Schemat szlaku biogenezy miRNA .

Naukowcy z firmy Uniqure zaprojektowali i przetestowali amiRNA (AMT-130) celujący w sekwencję komplementarną znajdującą się w eksonie 1 *HTT*, tak aby obniżyć poziom białka normalnego, jak i zmutowanego. Zastosowano kadłub pri-miR-451, który podlega niekanonicznej obróbce, niezależnej od enzymu Dicer, przez co nie pasażerska się nie uwalnia, zmniejszając ryzyko powstania efektów niespecyficznych. Częsteczka ta dostarczana jest bezpośrednio do mózgu pacjenta za pomocą wektora AAV5. Badania przedkliniczne prowadzone na wielu modelach zwierzęcych, w tym na myszach, szczurach i świniami pokazały, że podejście to jest efektywne i bezpieczne⁴⁴⁻⁴⁶. Wstępne wyniki zebrane od 4 pierwszych pacjentów po roku od iniekcji potwierdziły brak występowania skutków ubocznych, jednakże poziom HTT w CSF był na tyle zróżnicowany, że nie potwierdzono jeszcze efektywności obniżenia białka u tych pacjentów. Jednakże w tym przypadku, jak i w przypadku firmy Roche ponownie powstaje pytanie, czy w dłuższej perspektywie czasowej obniżanie całkowitego poziomu białka przyniesie więcej korzyści niż zastrzeżeń.

Strategia celowania w powtórzenia CAG

Ze względu na nie w pełni poznane funkcje prawidłowych białek poliQ oraz ich wpływ na przebieg choroby, nie można mieć pewności, że długotrwałe obniżenie ich poziomu będzie całkowicie bezpieczne. Doniesienia literaturowe pokazują natomiast, że usunięcie genu *Htt* z genomu myszy w trakcie embriogenezy jest letalne^{47,48}, a delecja genu we wczesnym okresie pourodzeniowym prowadzi do postępującej degeneracji neuronów i bezpłodności⁴⁹. Mimo że eksperymenty, w których dokonywano delecji *Htt* u dorosłych myszy⁵⁰, jak i u małych⁵¹ nie wykazały negatywnych efektów, to badania *in vitro* wprowadzają pewne wątpliwości. Wykazano, że delecja lub wyciszenie ekspresji prawidłowej *HTT* może mieć negatywny wpływ na transport cząsteczek w komórkach neuroblastomy i aksonach neuronów korykalnych^{21,52}. Jest to szczególnie ważne ze względu na to, że prawidłowa *HTT* bierze udział w produkcji i transporcie BDNF, który jest istotny dla życia komórek prądkowia²¹.

W przypadku ATXN3 wykazano, że myszy pozbawione tego białka są nadal płodne i żyją tak samo długo, jak myszy całkowicie zdrowe^{53,54}. Zaobserwowano jednak, że w ich tkankach jest wyższy poziom ubikwitynowanych białek niż w przypadku myszy

zdrowych⁵³. Zostało również wykazane w danio pręgowanym (*Danio rerio*) oraz w myszach, że usunięcie *Atxn3* może powodować dysfunkcję siatkówki oka⁵⁵.

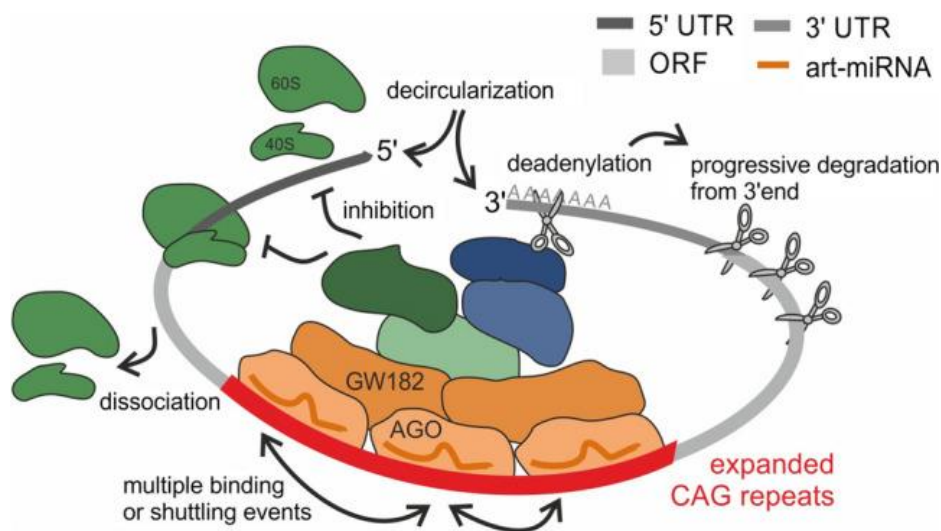
Kolejnym przykładem białka, którego redukcja może być niekorzystna dla zdrowia, jest *ATXN7*. Wyniki badań wykazały, że w muszkach owocówkach (*Drosophila melanogaster*) delecja tego białka powoduje poważne zwyrodnienie siatkówki, a w przypadku danio pręgowanego wadę rozwojową gałki ocznej oraz fotoreceptorów⁵⁶. Natomiast usunięcie prawidłowej *Atxn1* u myszy może prowadzić do problemów neurobehawioralnych, w tym uczenia się przestrzennego oraz motorycznego⁵⁷.

W związku z tym najbezpieczniejszą strategią wydaje się mimo wszystko allelo-selektywne celowanie w zmutowane warianty, bez wpływu na wariant niezmutowany.

W przypadku chorób poliQ regionami dzięki którym można rozróżnić allele, mogą być jednonukleotydowe polimorfizmy (SNP) sprzężone z mutacją lub same regiony powtórzeń CAG. Pierwsza z tych strategii ma jednak pewne ograniczenia, ponieważ jest skierowana tylko do pewnej grupy chorych, którzy posiadają jeden z występujących heterozygotycznie SNP, a nie do wszystkich pacjentów. Szacuje się, że 5 cząsteczek siRNA celujących w 3 różne SNP byłoby potrzebnych, aby leczyć 75% pacjentów HD⁵⁸. W takim przypadku wielu chorych nie zostanie objętych leczeniem ze względu na brak polimorfizmu lub jego homozygotyczność. Ponadto każda taka cząsteczka wymaga niezależnych badań klinicznych oraz dokładnego genotypowania pacjenta, aby dobrać odpowiedni typ terapeutyku do posiadanego SNP. Mimo to cząsteczki ASO wykorzystujące tę strategię do terapii choroby Huntingtona wkroczyły w fazę badań klinicznych. Warto zaznaczyć, że cząsteczka WVE-003 przeznaczona jest dla ok. 40% pacjentów.

Z tego względu druga strategia, czyli celowanie w powtórzenia CAG jest bardziej uniwersalna, ponieważ potencjalnie wszyscy pacjenci cierpiący na choroby poliQ mogliby z niej skorzystać. Niezależne badania prowadzone w naszym instytucie oraz przez zespół profesora Davida Coreya doprowadziły do powstania allelo-selektywnych cząsteczek siRNA, celujących w powtórzenia CAG^{59,60}. Strategia celowania w ciąg powtórzeń wykorzystuje różnicę w długości ciągu w allelu normalnym i zmutowanym. W allelu zmutowanym znajduje się więcej miejsc wiązania dla cząsteczki terapeutycznej niż w allelu prawidłowym. W związku z tym, do wariantu zmutowanego przyłącza się kilka kompleksów RISC, co powoduje efektywne blokowanie translacji (ryc. 2)⁶¹. Ponadto ważnym aspektem tej strategii jest wstawienie niesparowania pomiędzy nicią wiodącą siRNA a sekwencją docelową, przez co cząsteczka taka nie działa jak typowy

siRNA (ang. *siRNA-like mechanism*), który degradowuje mRNA, ale w sposób podobny do miRNA (ang. *miRNA-like mechanism*), czyli powoduje zablokowanie translacji. Takie kooperatywne działanie wielu cząsteczek z niesparowaniami po związaniu z sekwencją docelową powoduje powstanie stabilnej blokady dla maszynerii translacyjnej. W przypadku allelu normalnego, oddziaływanie siRNA z sekwencją docelową jest na tyle słabe, że kompleks RISC ulega szybszemu oddysocjowaniu, a translacja może dalej zachodzić.



Rycina 2. Schemat allelo-selektywnego działania cząsteczki celującej w powtórzenia CAG. (Ciesiolka A. CMLS 2021)

Cel pracy doktorskiej

Od wielu lat prowadzone są badania nad skuteczną terapią chorób poliQ. Niestety nadal choroby te są nieuleczalne, a pacjentom oferuje się jedynie łagodzenie objawów. Do mutacji, polegającej na ekspansji powtórzeń CAG i odpowiedzialnej za wystąpienie choroby dochodzi w jednym określonym genie, co czyni ją idealnym celem dla narzędzi technologii RNAi.

Celem mojej pracy doktorskiej był rozwój strategii terapeutycznej, polegającej na selektywnym wyciszaniu ekspresji zmutowanych genów, odpowiedzialnych za rozwój chorób poliQ, przy pomocy wektorowych narzędzi technologii RNAi, celujących w powtórzenia CAG.

W związku z tym w swojej pracy projektowałam i testowałam cząsteczki shRNA oraz amiRNA, wykorzystując różne modele chorób poliglutaminowych. Poszczególne etapy badań obejmowały:

1. Projektowanie cząsteczek shRNA oraz testowanie ich efektywności i specyficzności w modelach komórkowych chorób poliQ, takich jak HD, DRPLA, SCA3 i SCA7.
2. Zebranie i analizę najnowszych informacji dotyczących projektowania i zastosowania cząsteczek amiRNA w terapii chorób człowieka.
3. Zaprojektowanie cząsteczek amiRNA celujących w powtórzenia CAG oraz testowanie ich efektywności i specyficzności w modelach komórkowych HD.
4. Wybór najbardziej efektywnej cząsteczki amiRNA oraz analizę jej efektywności wyciszania i bezpieczeństwa w mysim modelu HD.

Opis publikacji wchodzących w skład rozprawy doktorskiej

Universal RNAi Triggers for the Specific Inhibition of Mutant Huntingtin, Atrophin-1, Ataxin-3, and Ataxin-7 Expression

Autorzy:

Anna Kotowska-Zimmer, Yuliya Ostrovska, Marta Olejniczak

Główny cel pracy:

Opracowanie i przetestowanie allelo-selektywnych cząsteczek shRNA (short-hairpin) celujących w powtórzenia CAG do wyciszenia ekspresji genów kodujących zmutowaną huntinginę, atrofinę-1, ataksynę-3 i ataksynę-7.

Opis pracy:

Wcześniejsze badania prowadzone w naszym instytucie doprowadziły do powstania efektywnych i allelo-selektywnych cząsteczek siRNA celujących w powtórzenia CAG, które występują w genach odpowiedzialnych za powstawanie chorób poliQ. Składały się one z powtórzeń CUG i zawierały substytucję U>A lub U>G w określonej pozycji. Działanie każdej z cząsteczek było uzależnione od typu i pozycji substytucji⁵⁹.

Ze względu na to, że działanie cząsteczek siRNA w komórce nie jest stałe, aby wydłużyć czas ich działania, w ramach swoich badań zaprojektowałam 4 wektorowe cząsteczki shRNA. Trzon każdej z nich stanowiły sekwencje najbardziej efektywnych siRNA, celujących w powtórzenia CAG, a pętla pochodziła z naturalnie występującego hsa-miR-23. Konstrukty ulegały ekspresji spod promotora H1.

Cząsteczki shRNA ulegają cięciu w komórkach przez enzym Dicer do cząsteczek siRNA. W związku z tym, pierwszym etapem prac było sprawdzenie jak nasze cząsteczki są docinane w komórkach przez ten enzym. Komórki HEK293T zostały transfekowane

plazmidami z shRNA, a następnie RNA wyizolowany z komórek został poddany analizom głębokiego sekwencjonowania. Wyniki pokazały, że **każda z cząsteczek ulega precyzyjnej obróbce**, a nie pasażerska uwalniana jest tylko w niewielkiej ilości. W przypadku każdej z cząsteczek nić wiodąca i pasażerska uwalniana była w podobnych stosunkach, z przeważającą ilością nici wiodącej, która osiągnęła 99% dla cząsteczki shA2R, shG2 i shG4. W przypadku cząsteczki shA2R1 stosunek ten był niższy i wynosił 96%. Większość produktów cięcia miała długość 19-24 nt. Dojrzałe cząsteczki siRNA różniły się głównie długością ciągu nukleotydów U na końcu 3' w przypadku cząsteczek shA2 i shG2, ponadto 90% cząsteczek uzyskanych z tych konstruktyw posiadało substytucję w pozycji 8 od końca 5' dojrzałej cząsteczki siRNA. Produkty cięcia cząsteczki shA2R1 różniły się na końcu 5', co doprowadziło do powstania cząsteczek z substytucją nukleotydu A w pozycji 8 (69%) i w pozycji 9 (25%). Natomiast z cząsteczki shG4 uwolnionych zostało 95% produktów z substytucjami w pozycjach 8 i 14.

Następnie cząsteczki zostały przetestowane pod kątem ich efektywności i selektywności. W pierwszym etapie został zastosowany system reporterowy z lucyferazą do pomiaru zdolności obniżania poziomu białka przez cząsteczki shRNA. W tym celu wykorzystane zostały konstrukty, w których ekspresji ulegał 1 ekson *HTT* zawierający dwie różne długości ciągów CAG (16 i 85). Każda z cząsteczek shRNA spowodowała efektywne obniżenie poziomu ekspresji konstruktów zawierającego dłuższy ciąg CAG, a najwyższe wyciszenie osiągające 75% zostało uzyskane przez cząsteczkę shA2R. Analiza wartości IC50 (ilość cząsteczki powodująca obniżenie poziomu białka do 50%) wykazała, że cząsteczki shG2, shA2R i shA2R1 są bardziej skuteczne przy mniejszej dawce niż cząsteczka shG4. Ponadto w żadnym przypadku ekspresja konstruktów z 16 powtórzeniami CAG nie została obniżona do 50% nawet po zastosowaniu najwyższych dawek cząsteczek. Pomiar allelo-selektywności, liczony jako stosunek wartości IC50 (16CAG/85CAG) wykazał, że cząsteczkami o najwyższej selektywności są shG2 i shA2R.

W kolejnym etapie cząsteczki były podawane do komórek fibroblastów w postaci wektorów lentiwirusowych. Efektywność wszystkich wektorów została sprawdzona w **4 różnych modelach chorób poliQ: HD, SCA3, SCA7 i DRPLA** oraz dodatkowo najbardziej efektywna cząsteczka, shA2R, w 3 innych liniach komórkowych HD różniących się liczbą powtórzeń CAG (fibroblasty 44/21Q, 151/21Q, mysie prekursor neuronarne 111/7Q) za pomocą metody western blot. Przy zastosowaniu wektora

z cząsteczką shA2R uzyskane zostało maksymalne 90% wyciszenie zmutowanej huntingtyny. Każda z cząsteczek w różnych modelach komórkowych posiadała inny wzór wyciszenia, jednakże w każdym przypadku **udało się osiągnąć efektywne i selektywne wyciszenie zmutowanego białka.**

Cząsteczka shA2R została dodatkowo przetestowana pod kątem wystąpienia potencjalnych efektów niespecyficznych. Przeprowadzone zostały analizy bioinformatyczne mające na celu znalezienie genów zawierających sekwencje komplementarne do dojrzałej cząsteczki siRNA, ponieważ taki typ oddziaływania może spowodować obniżenie ekspresji genów innych niż docelowy. Wyniki wykazały, że w genomie człowieka jest 5 genów z pełną komplementarnością do dojrzałej cząsteczki i wszystkie z nich ulegają ekspresji w mózgu, jednak na niskim lub średnim poziomie. Do analiz wybraliśmy te, które ulegają ekspresji w fibroblastach, czyli *SLC16A*, *PEG3*, *MINK1*. W przypadku każdego z nich sekwencja komplementarna znajdowała się w innym rejonie mRNA, a analizy RT-qPCR pokazały, że obniżeniu uległ tylko poziom mRNA i białka PEG3, odpowiednio o 50% i 30%, co mogło być związane z komplementarnością w rejonie 3'UTR. Jednakże efekty *in vivo* związane z wyciszeniem ekspresji tego genu są trudne do przewidzenia, głównie ze względu na to, że w ciągu życia jedynie allel ojcowski jest aktywny. Ponadto do jego najwyższej ekspresji dochodzi przede wszystkim w jajnikach, jądrach i łożysku.

Sprawdzony został także poziom białek kodowanych przez geny posiadające czyste lub poprzerywane ciągi powtórzeń CAG (TBP, FOXP2, RPL14). W żadnym przypadku nie doszło do obniżenia poziomu białka, co potwierdza mechanizm blokowania translacji przez nasze cząsteczki, które efektywnie działają na ekspresję genów zawierających wyłącznie długie i nieprzerwane ciągi CAG.

Przeprowadzone przeze mnie eksperymenty wykazały, że **zastosowanie cząsteczek shRNA celujących w powtórzenia CAG powoduje efektywne obniżenie poziomu docelowych białek w modelach komórkowych chorób poliQ, bez wystąpienia istotnych efektów niespecyficznych.**

Wkład pracy doktoranta

Mój wkład pracy w powstanie tej publikacji obejmował:

- Projektowanie i wykonanie konstruktywów genetycznych do ekspresji shRNA oraz systemu reporterowego;
- Udział w przeprowadzeniu części testów reporterowych oraz analizę i opracowanie uzyskanych wyników;
- Przygotowanie i scharakteryzowanie (MOI) wektorów lentiwirusowych do transdukcji linii komórkowych;
- Transdukcję, izolację materiału biologicznego i wykonanie znacznej większości eksperymentów western blot w celu określenia poziomu białek oraz RT-qPCR w celu określenia poziomu transkryptów, a także analizę uzyskanych wyników;
- Przygotowanie prób do sekwencjonowania małych RNA metodą NGS i udział w analizie wyników;
- Wykonanie wszystkich rycin do publikacji i przygotowanie materiałów suplementarnych;
- Udział w pisaniu publikacji obejmujący opis wyników i metodologii.

Artificial miRNAs as therapeutic tools: Challenges and opportunities

Autorzy:

Anna Kotowska-Zimmer, Marianna Pewińska, Marta Olejniczak

Główny cel pracy:

Analiza dostępnej wiedzy na temat cząsteczek amiRNA, zaproponowanie reguł dotyczących ich projektowania, a także ocena dotychczasowych eksperymentów z wykorzystaniem tego typu narzędzi technologii RNAi pod kątem ich ograniczeń w potencjalnych terapiach.

Opis pracy:

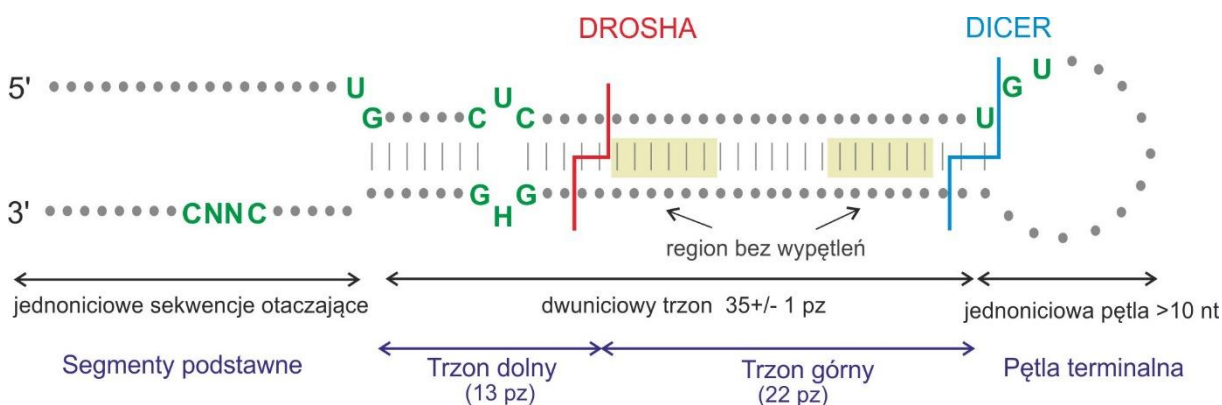
W pracy tej zostały zebrane najważniejsze informacje dotyczące projektowania efektywnych cząsteczek amiRNA, opierając się na wynikach uzyskanych z analiz endogennych pri-miRNA. Ponadto zestawione zostały podejścia terapeutyczne z ich zastosowaniem, a także rozpoczęte badania kliniczne.

Technologia interferencji RNA jest wykorzystywana od ponad dwudziestu lat do poznawania funkcji genów, jak i do celów terapeutycznych. W kontekście terapii, na szczególną uwagę zasługują cząsteczki amiRNA, które projektowane są na podstawie naturalnych pri-miRNA, które w miejscu miRNA posiadają wstawione cząsteczki siRNA specyficzne do sekwencji docelowej. Prawidłowe wstawienie siRNA w kadłub endogennego pri-miRNA zapewnia mu precyzję wycinania i transport. Jak pokazują wyniki badań, cząsteczki tego typu są **bezpieczniejsze od innych narzędzi RNAi**, ze względu na to, że w znacznym stopniu odzwierciedlają procesy występujące w komórce, a białkowa maszyna biogenezy miRNA nie ulega wysyceniu⁶². Najczęściej dostarczane są poprzez wektory wirusowe, a ekspresji ulegają spod promotorów polimerazy RNA II (Pol II), co zapewnia im długotrwałą ekspresję i możliwość stałego obniżania poziomu docelowych genów. Dodatkowo można stosować promotory o ekspresji tkankowo-specyficznej lub indukowalne, co może pozytywnie wpłynąć na

bezpieczeństwo, ponieważ cząsteczka terapeutyczna będzie ulegała ekspresji jedynie w miejscu docelowym lub w określonym czasie.

Ostatnie wyniki prac naukowych podkreślają **istotną rolę sekwencji i struktur pri-miRNA** wykorzystywanych jako kadłuby w ulepszaniu działania narzędzi amiRNA⁶³.

Cząsteczki amiRNA, tak jak pri-miRNA, zbudowane są z dwuniciowego trzonu, dwóch jednoniciowych sekwencji otaczających oraz pętli apikalnej. Trzon składa się z części górnej o długości 22 pz, licząc od pętli terminalnej oraz części dolnej zbudowanej z 13 pz, licząc od sekwencji otaczających (Ryc. 3). Wielkość pętli, długość trzonu oraz występowanie podstawnych (CNNC, UG) i apikalnych motywów sekwencji (UGU) wpływa na obróbkę amiRNA w komórkach poprzez ułatwienie kompleksowi Mikroprocesora rozpoznania substratu i odpowiednie ustawieniu go do cięcia. Dodatkowo, bardzo ważny jest skład nukleotydowy cząsteczki, ponieważ jak wiadomo, Drosha i Dicer unikają cięcia w miejscach bogatych w nukleotydy G⁶⁴.



Rycina 3. Cechy strukturalne cząsteczek pri-miRNA (Kotowska-Zimmer A., WIREs RNA, 2021).

Ze względu na skomplikowaną budowę pri-miRNA, aby zaprojektować cząsteczkę amiRNA, tak żeby była efektywnie docinana w komórkach i wyciszała ekspresję genów, należy wziąć pod uwagę wszystkie wymienione aspekty związane z sekwencją, jak i strukturą. Ponadto istotne jest, aby sprawdzić, jak zaprojektowana cząsteczka jest docinana w komórkach. Badania wykazały, że nawet jeśli stosowany jest jeden z najbardziej powszechnie stosowanych kadłubów (pri-miR-30 lub pri-miR-155) to wstawienie do niego cząsteczki siRNA może spowodować nieefektywną obróbkę enzymatyczną, doprowadzić do tego, że zamiast nici wiodącej, do kompleksu zostanie włączona nić pasażerska (ang. *arm switching*) albo do postania heterogennych

produktów, niekoniecznie z przewagą tego, który jest oczekiwany⁶⁵. Jest to szczególnie niebezpieczne w sytuacji, gdy powstające produkty będą różniły się na końcu 5' cząsteczki siRNA, a co za tym idzie, będą miały różne sekwencje „seed”. Zwiększa to ryzyko regulacji innych genów niż docelowe.

Liczne eksperymenty przedkliniczne wykazały, że cząsteczki amiRNA mogą być stosowane jako potencjalne narzędzia terapeutyczne w leczeniu chorób, np. neurodegeneracyjnych, nowotworowych czy infekcji wirusowych. Jak pokazuje literatura, niestety w większości przypadków zaprojektowane cząsteczki nie są dokładnie charakteryzowane pod kątem precyzji ich cięcia, a także poziomu ekspresji w komórkach, co w dłuższym okresie po podaniu może przyczynić się do wystąpienia efektów niespecyficznych, zależnych i niezależnych od sekwencji. Dlatego równie ważna jest analiza poziomu transkryptów, które mogły ulec deregulacji po zastosowaniu potencjalnego terapeutyku. Wyniki z głębokiego sekwencjonowania zawsze powinny być potwierdzone przez zastosowanie innych metod, takich jak RT-qPCR lub western blot, co pozwoli na uzyskanie szerszego obrazu potencjalnych efektów ubocznych.

Wkład pracy doktoranta

Mój wkład pracy w powstanie tej publikacji obejmował:

- Zebranie i analizę dostępnej literatury na temat biogenezy miRNA, projektowania i dostarczania cząsteczek amiRNA oraz wykorzystania cząsteczek amiRNA w terapii chorób neurodegeneracyjnych (rozdziały 2-6);
- Udział w pisaniu publikacji;
- Wykonanie wszystkich rycin i tabeli głównej.

A CAG repeat-targeting artificial miRNA lowers the mutant huntingtin level in the YAC128 model of Huntington's disease

Autorzy:

Anna Kotowska-Zimmer, Łukasz Przybył, Marianna Pewińska, Joanna Suszyńska-Zajczyk, Dorota Wronka, Maciej Figiel and Marta Olejniczak

Główny cel pracy:

Porównanie efektywności i selektywności wektorowych narzędzi technologii RNAi typu shRNA i amiRNA celujących w zmutowane ciągi powtórzeń CAG do wyciszenia ekspresji huntingtyny w mysim modelu choroby Huntingтона.

Opis pracy:

Wyniki badań *in vivo* pokazują, że najbezpieczniejszymi narzędziami technologii RNAi są cząsteczki amiRNA, które w największym stopniu odzwierciedlają naturalne procesy zachodzące w komórkach. Ponadto, gdy są dobrze zaprojektowane, mogą być tak efektywne, jak cząsteczki shRNA, jednak bez wywoływania efektów toksycznych.

Analiza literatury dotyczącej biogenezy miRNA oraz cech strukturalnych pri-miRNA i ich wpływu na obróbkę komórkową, pozwoliły mi na zaprojektowanie własnej serii cząsteczek amiRNA celujących w powtórzenia CAG. Na podstawie wyników z wcześniejszych eksperymentów dotyczących cząsteczek siRNA i shRNA celujących w ciągi powtórzeń CAG, wybrałam 2 cząsteczki siRNA, A2 i G4, które zostały wstawione w 4 różne kadłuby (pri-miR-136, pri-miR-155, pri-miR-122, pri-miR-451) wyselekcjonowane na podstawie analiz literatury i bazy miRBase (<http://www.mirbase.org/>). Obróbka tych pri-miRNA jest dobrze poznana i każdy z nich wykazuje korzystny stosunek nici wiodącej do pasażerskiej. W dodatku pri-miR-451 podlega niekanonicznej obróbce, niezależnej od enzymu Dicer, co skutkuje tym, że nić pasażerska się nie uwalnia. W przypadku pri-miR-136, badania przeprowadzone

w naszym instytucie, wykazały, że jest on precyzyjnie cięty i powstają z niego homogenne produkty, co powinno być korzystną cechą w potencjalnej terapii.

Zastosowanie różnych kadłubów w projektowaniu amiRNA spowodowane było faktem, że w zależności od kadłuba i wstawki siRNA, dojrzały produkt może się różnić, co może powodować problemy z uzyskaniem odpowiedniej efektywności i selektywności.

Wszystkie zaprojektowane cząsteczki zostały dostarczone za pomocą wektorów lentiwirusowych do komórek fibroblastów pochodzących od pacjentów HD (68/17Q). Cząsteczką najbardziej efektywną i wykazującą działanie allelo-selektywne była cząsteczka w kadłubie pri-miR-136 ze wstawką A2 (amiR136-A2; 50% wyciszenia białka zmutowanego). Dodatkowo przetestowana została ona w linii komórkowej, zawierającej krótsze ciągi powtórzeń (47/15Q). W tym przypadku również zostało osiągnięte istotne statystycznie obniżenie poziomu zmutowanego białka.

W kolejnym etapie sprawdzona została efektywność cząsteczki amiR136-A2 w systemie reporterowym z wykorzystaniem konstruktów, zawierających 1 ekson *HTT* z różnymi długościami ciągów CAG (16, 40 i 57), co **potwierdziło jej działanie allelo-selektywne**. Wyniki głębokiego sekwencjonowania RNA wyizolowanego z komórek HEK293T po transfekcji plazmidem zawierającym konstrukt **amiR136-A2** wykazały, że nic wiodąca uwalniana była z ramienia 5', co stanowiło ~80% odczytów. Około 70% dojrzałych cząsteczek posiadało substytucję w 8 pozycji, licząc od 5' końca siRNA, a główny produkt cięcia miał długość 22 nt. Wzór docinania był zatem podobny do tego otrzymanego w przypadku cząsteczki shA2, jednakże ilość odczytów dla dojrzałej cząsteczki siRNA otrzymanej z amiR136-A2 była 10 razy niższa niż w przypadku shA2 i odpowiadała poziomowi endogennych miRNA.

Kolejnym etapem badań były eksperymenty *in vivo* z wykorzystaniem myszy YAC128, które są modelem choroby Huntingtona. Model ten posiada zmutowaną, ludzką huntingtynę ze 125 powtórzeniami CAG. Do dostarczenia konstrukt do mózgu myszy został wybrany wektor wirusowy AAV5 ze względu na jego tropizm do komórek nerwowych. Do optymalizacji dostarczania i dystrybucji wektora w mózgu myszy został zastosowany wektor wirusowy, z którego dochodziło do ekspresji GFP (ang. *green fluorescent protein*). Zwierzęta zostały poddane iniekcji 3 dawkami wektora (1×10^9 , 1×10^{10} , 1×10^{11} gc) do prądkowia prawej półkuli mózgu (po 3 na grupę). Po 4 tygodniach od iniekcji zostały pobrane mózgi myszy, a ze skrawków zostały wykonane preparaty do oceny dystrybucji wirusa metodą mikroskopii fluorescencyjnej. Zgodnie z oczekiwaniami, najlepsza dystrybucja i transdukcja komórek została uzyskana po

zastosowaniu najwyższej dawki wirusa, gdzie do ekspresji genu kodującego GFP doszło w komórkach prążkowiec, hipokampu oraz części komórek kory mózgowej.

Po zoptymalizowaniu dostarczania wektora wirusowego, zostały wygenerowane wektory AAV niosące potencjalnie terapeutyczne cząsteczki shA2 i amiR136-A2 oraz kontrolne shSCR i amiR136-SCR. Cząsteczki shRNA ulegały ekspresji spod promotora H1, a cząsteczki amiRNA spod promotora CAG. Kasety ekspresyjne nie zawierały GFP, aby wyeliminować ryzyko wystąpienia odpowiedzi immunologicznej u myszy. Przeprowadzone były eksperymenty krótkoterminowe oraz długoterminowe. Eksperyment krótkoterminowy trwał 4 tygodnie i miał na celu porównanie efektywności cząsteczek shA2 oraz amiR136-A2 w obniżaniu poziomu HTT w różnych regionach mózgu. W przypadku każdej z cząsteczek naceLOWanych na powtórzenia CAG uzyskano w prążkowiec **obniżenie poziomu zmutowanego białka** wynoszące ok. 30% w porównaniu do myszy traktowanych konstrukcjami kontrolnymi. W hipokampie wyciszenie HTT było zbliżone do tego uzyskanego w prążkowiec i wyniosło 30% dla shA2 i 20% dla amiR136-A2, co może być związane z bliskim położeniem obu struktur. Jeśli chodzi o korę mózgu, wyciszenie zostało uzyskane tylko po traktowaniu cząsteczką amiR136-A2 i wyniosło 20%.

Kolejnym etapem badań, był eksperyment trwający 20 tygodni. Miał on na celu sprawdzenie efektów długoterminowych, takich jak bezpieczeństwo, poprawa fenotypu oraz czy dłuższy czas od iniekcji wpłynie na poprawę efektywności cząsteczek. W tym przypadku, wektor został podany do obu półkul, w dwóch różnych dawkach dla każdej z cząsteczek. Co 4 tygodnie wykonywane było ważenie myszy oraz testy behawioralne, takie jak test na Rotarodzie, test prętów statycznych oraz dwukrotnie test w zlewce i jednorazowo test siły mięśni.

Po upływie 20 tygodni od iniekcji, do analiz RNA, DNA i białka zostały pobrane struktury mózgu, do analiz immunohistochemicznych całe mózgi, do ważenia organy obwodowe, takie jak śledziona, nerka, serce.

Analiza western blot wykazała najwyższe obniżenie poziomu HTT w prążkowiec, następnie w hipokampie, a najniższe w korze mózgu. W przypadku niższej dawki wektora średnia efektywność w prążkowiec wynosiła ok. 30% dla cząsteczek shA2 oraz amiR136-A2. Przy zastosowaniu wyższej dawki wektora, **obniżenie poziomu zmutowanego białka w prążkowiec wyniosło ok. 50% dla obu cząsteczek, natomiast poziom białka prawidłowego nie został obniżony**. Myszy YAC128 odzwierciedlają wiele cech występujących w HD, w tym również występowanie agregatów HTT w komórkach

prążkowie i kory. Analizy immunohistochemiczne pokazały, że w skrawkach mózgu myszy traktowanych cząsteczką amiR136-A2 **dochodzi do zmniejszenia ilości agregatów, nawet do 50%** w zależności od dawki wektora.

Sprawdzone zostały również potencjalne efekty niespecyficzne działania cząsteczki amiR136-A2. Analizie zostały poddane poziomy 2 białek kodowanych przez geny zawierające ciągi CAG, takie jak *Rbm33* (10 CAG) i *Hcn1* (>30 CAG *poprzerywanych 4 powtórzeniami CAA*). Poziom żadnego z nich nie uległ zmianie po iniekcji wektorem AAV5 niosącym amiR136-A2.

Ponadto przeprowadzona została analiza bioinformatyczna mająca na celu wytypowanie genów zawierających sekwencję w pełni komplementarną do wstawki A2. Znalezionych zostało 6 takich genów (*Golga4*, *Soga3*, *Maml1*, *Ccdc177*, *Th* i *Ppp1r3f*). Każdy z nich posiadał sekwencję komplementarną do wstawki w otwartej ramce odczytu, a gen *Golga4* dodatkowo w regionie 3'UTR. Analizy wyników RT-qPCR wykazały, że jedynie ekspresja *Golga4* została obniżona, co najprawdopodobniej związane było z lokalizacją sekwencji komplementarnej do siRNA, jednakże wynik wyciszenia nie był istotny statystycznie.

Aby sprawdzić, czy nasze cząsteczki powodują wystąpienie zapalenia w układzie nerwowym, wykonałam barwienia immunohistochemiczne skrawków mózgu przeciwciałami przeciwko markerom reakcji immunologicznej, takimi jak marker aktywacji mikrogleju (IBA1) i astrogleju (GFAP). Dodatkowo sprawdziłam poziom ekspresji mRNA *Iba1* i *Gfap*. Po obserwacji serii skrawków i analizie wyników z RT-qPCR **potwierdziłam brak aktywacji immunologicznej**. Dodatkowo nie zaobserwowałam degeneracji neuronów (NeuN, DARPP-32). Po zważeniu narządów obwodowych uzyskane wyniki wskazywały na obniżenie masy śledziony myszy traktowanych amiR136-A2 w porównaniu do myszy nietraktowanych i traktowanych amiR136-SCR, **uzyskując wynik odpowiadający myszom zdrowym**.

W przypadku testów behawioralnych, myszy traktowane cząsteczką shA2 radziły sobie lepiej w teście na Rotarodzie oraz w teście prętów statycznych (głównie pręt o średnicy 17mm) w porównaniu do myszy traktowanych cząsteczką kontrolną shSCR. **Częściowa poprawa fenotypu** została również zaobserwowana u myszy traktowanych cząsteczką amiR136-A2, a istotne statystycznie różnice dotyczyły testu prętów statycznych (17mm). Natomiast w testach zlewki jak i siły mięśni, myszy traktowane shA2 jak i amiR136-A2 nie wykazały poprawy.

Wyniki badań wskazują, że cząsteczka **amiR136-A2 efektywnie i allelo-selektywnie** obniża poziom **zmutowanego białka** oraz **agregatów HTT nie powodując** przy tym wystąpienia **efektów niespecyficznych. Powoduje ona również częściową poprawę fenotypu.**

Wkład pracy doktoranta

Mój wkład pracy w powstanie tej publikacji obejmował:

- Projektowanie cząsteczek amiRNA, tworzenie lentiwirusów i testowanie ich efektywności w modelu komórkowym fibroblastów HD (68/17Q) z wykorzystaniem techniki western blot oraz analizę uzyskanych wyników;
- Analizę wyników głębokiego sekwencjonowania do określenia obróbki komórkowej amiR136-A2 i ilości dojrzałych cząsteczek;
- Genotypowanie myszy do uzyskania odpowiedniej kohorty myszy YAC128;
- Wykonanie procedury iniekcji grupy myszy wektorami AAV5 niosącymi GFP, jak również cząsteczki shRNA i amiRNA;
- Pobór tkanek z grupy zwierząt; izolację RNA, DNA i białka z tkanek;
- Wykonanie wszystkich analiz western blot na tkankach pobranych z mózgow oraz części RT-qPCR;
- Wykonanie wszystkich preparatów pochodzących z mysich mózgow, immunobarwień oraz zdjęć mikroskopowych, a także ich analiz;
- Wykonanie rycin do publikacji;
- Udział w pisaniu publikacji i odpowiedzi na recenzje.

Dyskusja

W ostatnich latach można zaobserwować intensywne prace wykorzystujące różnorodne podejścia mające na celu stworzenie leku dla pacjentów cierpiących na nieuleczalne choroby neurodegeneracyjne. Brane są pod uwagę strategie allelo-selektywne, jak i nieselektywne. Selektowność w przypadku chorób poliglutaminowych można osiągnąć poprzez celowanie w SNP sprzężony z mutacją lub bezpośrednio w powtórzenia CAG. Opisanym zostało wiele badań *in vivo*, w których efektywnie wyciszono ekspresję genów poliQ w sposób nieselektywny z wykorzystaniem cząsteczek shRNA i amiRNA^{51,66-68}. Mimo że wykazano bezpieczeństwo częściowej redukcji poziomu huntingtyny typu dzikiego (ok. 45%) w prądkowiu dorosłych zesusów w ciągu 5 miesięcy po wprowadzeniu shRNA za pomocą AAV2, to nadal nie są znane długoterminowe konsekwencje obniżenia poziomu prawidłowych białek u pacjentów. W związku z tym, wyciszenie ekspresji tylko zmutowanego wariantu genu wydaje się wciąż najbezpieczniejszą opcją terapii.

Selektywne celowanie w SNP lub powtórzenia CAG jest jednak bardziej wymagającym podejściem. W przypadku SNP efektywne wyciszenie ekspresji genów uzyskano w komórkowych i zwierzęcych modelach HD⁶⁹ i SCA3⁷⁰, natomiast celowanie w powtórzenia CAG jak dotąd nie zostało w tak szerokim zakresie przetestowane, ograniczając się głównie do eksperymentów *in vitro*^{44,59,71}.

Dlatego też pierwszym etapem moich badań było przetestowanie serii cząsteczek shRNA celujących w powtórzenia CAG, zaprojektowanych na bazie siRNA, które zostały opracowane w naszym instytucie⁵⁹. Mimo że sekwencja bogata w nukleotydy GC i nieposiadająca nukleotydów A i U na końcach 5' odbiega od standardowych reguł projektowania cząsteczek siRNA, to nie spowodowało to zaburzenia ich działania. Każdy z zaprojektowanych shRNA ulegał precyzyjnemu docinaniu w komórce przez enzym Dicer, skutkując powstaniem dojrzałego siRNA z substytucją A lub G głównie w 8 pozycji od 5' końca. Badania nad wykorzystaniem siRNA wykazały, że typ niesparowania, jak i jego pozycja są istotne w preferencyjnym obniżaniu poziomu zmutowanego białka^{60,72}. Prowadzone przeze mnie badania pokazały, że allelo-selektowność zależy głównie od modelu choroby poliQ oraz dawki użytego shRNA. W przypadku modelu HD zaobserwowałam istotną różnicę między allelo-selektownością po użyciu cząsteczek z substytucją A i G. Cząsteczka shA2R spowodowała znaczną

redukcję poziomu białka zmutowanego, natomiast cząsteczka shG2 obniżyła poziom obu białek. Jednakże zależności takiej nie zaobserwowałam w modelach komórkowych SCA3, SCA7 i DRPLA, gdzie w każdym przypadku obniżenie poziomu białka było selektywne, mimo iż długości ciągów były zbliżone do tych w modelu HD. Świadczyć to może o tym, że na efektywność, jak i selektywność cząsteczki może wpływać nie tylko obecność niesparowania w konkretnej pozycji, ale również lokalizacja ciągu w transkrypcie, sekwencja go otaczająca, a także stosunek ilości danej cząsteczki do ilości transkryptu docelowego w komórce.

Wątpliwości co do tej strategii może budzić stosunkowo duża ilość transkryptów w komórkach ludzkich zawierających powtórzenia CAG i CUG, co może powodować niespecyficzne obniżanie poziomu innych ważnych białek, głównie w mózgu. W genomie człowieka zidentyfikowano 159 genów zawierających powyżej 6 powtórzeń CAG, w tym 29 genów z liczbą ciągów CAG powyżej 15. W większości z nich, ciągi powtórzeń zlokalizowane są w rejonach kodujących genów, które biorą udział przede wszystkim w transkrypcji i neurogenezie. Posiadają głównie aktywność koaktywatorów transkrypcji oraz są odpowiedzialne za wiązanie kwasów nukleinowych⁷³⁻⁷⁵. W przypadku powtórzeń CTG, zidentyfikowane zostały 104 geny, z czego 5 posiada powyżej 10 takich powtórzeń. Białka kodowane przez geny zawierające powtórzenia CTG związane są głównie z błoną komórkową, prawdopodobnie ze względu na hydrofobowe właściwości leucyny. Analizy wykazały, że genów posiadających powyżej 20 powtórzeń CAG lub CTG jest niewiele, a dopiero takie ciągi mogłyby być potencjalnym celem dla naszych cząsteczek⁷³. W związku z tym, w swoich badaniach sprawdziłam, czy poziom innych białek, zawierających czyste bądź poprzerywane ciągi CAG ulegają obniżeniu po traktowaniu najbardziej efektywnym shRNA. Wyniki moich badań wykazały, że do obniżenia poziomu białka dochodzi tylko w przypadku obecności w genach bardzo długich i nieprzerwanych powtórzeniami CAA ciągów CAG. Jest to zgodne z innymi badaniami nad cząsteczkami siRNA działającymi jak miRNA celującymi w tego typu powtórzenia^{59,60}.

Badania *in vivo* wykazały, że stosowanie cząsteczek typu shRNA może być toksyczne ze względu na wysycenie ścieżki biogenezy miRNA w związku ze zwiększoną konkurencją o białka biorące udział w powstawaniu i transporcie dojrzałych miRNA, a w szczególności o białko XPO5^{42,43,62,76,77}. Wykorzystanie takiej cząsteczki pod kontrolą silnego promotora U6 może również powodować ostrą neurotoksyczność, ze względu na wytworzenie znacznej ilości nici antysensowego RNA⁶². W przypadku moich

badaniach zastosowany został promotor H1, który uznawany jest za słabszy⁷⁸. Analiza NGS wykazała, że ilość nici wiodącej powstającej w trakcie obróbki cząsteczki shA2R jest porównywalna do poziomu komórkowego najbardziej licznych miRNA, czyli hsa-miR-221-3p i hsa-miR-191. Niestety pomimo zastosowania słabszego promotora cząsteczka shA2 wykazywała toksyczność *in vivo*.

Zmiana promotora na słabszy jest jedną z możliwości obejścia problemu wysycenia komórkowej maszynerii białkowej biogenezy miRNA. Inną opcją może być zastosowanie cząsteczek amiRNA, które swoją budową przypominają naturalne pri-miRNA i ulegają w komórce dwuetapowej obróbce^{44,62,79}. Projektowanie cząsteczek amiRNA jest bardziej skomplikowane, ze względu na fakt, że podczas docinania takiej cząsteczki więcej czynników wpływa na precyzję cięcia niż w przypadku shRNA, co może sprawiać problemy z uzyskaniem dobrej efektywności oraz allelo-selektywności. Pierwszym z etapów, mających na celu stworzenie przez mnie takich złożonych cząsteczek było zgłębienie i zebranie wiedzy w pracy przeglądowej na temat optymalizacji i zastosowania amiRNA głównie w terapiach chorób neurodegeneracyjnych, wirusowych i nowotworowych. Wiedza dotycząca biogenezy miRNA jest od wielu lat uzupełniana, co powinno przyczyniać się do lepszego zrozumienia licznych procesów zachodzących w komórce, a co za tym idzie, projektowanie cząsteczek o potencjale terapeutycznym, które opierają się na budowie naturalnych cząsteczek, również powinno stać się łatwiejsze. Literatura wskazuje jednak, że do badań wykorzystywane są głównie te same kadłuby pri-miRNA, takie jak pri-miR-30 i pri-miR-155, a prace naukowe z innymi kadłubami są bardzo nieliczne. Przeciwnieństwem są badania przeprowadzane na roślinach, gdzie narzędzia amiRNA są bardzo szeroko rozwijane i dopracowywane w celu ulepszenia plonów oraz ochrony przeciwwirusowej⁸⁰. Ponadto w przypadku potencjalnej terapii, wielu naukowców dąży głównie do osiągnięcia wysokiego poziomu wyciszenia ekspresji genów, nie przywiązując uwagi do efektów niespecyficznych, które mogą powstać po wprowadzeniu terapeutyku do organizmu. Analiza wielu prac badawczych wykazała, że jednym z najważniejszych aspektów przy optymalizacji sztucznych miRNA jest sprawdzenie, jak są one docinane w komórkach przez enzymy Drosha i Dicer oraz na jak wysokim poziomie jest ich ekspresja.

Niestety, mimo że ich efektywność testowana jest w badaniach przedklinicznych wielu chorób, to w większości przypadków obróbka komórkowa jak i ilość powstających cząsteczek nie są analizowane. Uzyskanie wielu różnych produktów siRNA w wyniku

cięcia jednej cząsteczki amiRNA oraz niekorzystny stosunek powstającej nici wiodącej do pasażerskiej mogą skutkować obniżeniem poziomu białek niebędących docelowymi. Heterogenność końca 5' skutkować będzie przesunięciem sekwencji „seed” i regulacją poziomów ekspresji innych transkryptów. W przypadku izomirów końca 3' może dochodzić do zmiany ich efektywności i stabilności w komórce. Odziaływanie końca 3' miRNA z sekwencją docelową może wpływać na stabilizację i wzmocnienie wiązania miRNA z sekwencją docelową szczególnie w przypadku niepełnej komplementarności sekwencji „seed”⁸¹. Dodatkowo analiza poziomu dojrzałego siRNA w porównaniu do naturalnych miRNA występujących w komórce pozwala na oszacowanie ryzyka wystąpienia wysycenia ścieżki biogenezy miRNA.

W przypadku zastosowania technologii RNAi w badaniach terapeutycznych, poza problemem dotyczącym prawidłowego zaprojektowania cząsteczek amiRNA i ich bezpieczeństwa, ważnym aspektem jest również dostarczanie tych cząsteczek do miejsca docelowego. Najczęściej do tego celu wykorzystywane są wektory AAV o różnych serotypach, wykazujące tropizm do konkretnych tkanek. Są one bezpieczne, gdyż nie są patogenne dla ludzkiego organizmu i nie wywołują odpowiedzi immunologicznej. Ponadto nie integrują do genomu gospodarza, przez co ryzyko mutacji jest na bardzo niskim poziomie⁸².

Wiedza pochodząca z literatury pozwoliła mi na zaprojektowanie serii różnych amiRNA i na zwrócenie uwagi na motywy sekwencyjne i strukturalne, które są szczególnie istotne przy obróbce enzymatycznej takich cząsteczek.

Na podstawie bazy miRbase oraz wcześniej opublikowanych prac, do stworzenia własnych cząsteczek amiRNA wybrałam cztery kadłuby pri-miRNA, z których nic wiodąca uwalniana jest z nici 5', a nic pasażerska nie powstaje lub powstaje w bardzo niewielkiej ilości. Interesującym kadłubem, który został wybrany do testowania, jest niekanoniczny pri-miR-451, który nie podlega docinaniu przez enzym Dicer, ale przez AGO. W jego przypadku nie dochodzi do powstawania nici pasażerskiej, co jest bardzo korzystne w przypadku wybrania go do terapii⁸³. Na podstawie badań wykonywanych w naszym zakładzie wiadomo, że homogenne produkty powstają w wyniku biogenezy pri-miR-136⁶⁴. Kadłub ten również został wybrany do moich badań. Jego wcześniejsza szczegółowa analiza obróbki pozwoliła na zachowanie efektywności i selektywności cząsteczki z niego uwalnianej w badaniach *in vitro* i *in vivo*.

W miejsce dojrzałego miRNA-136 została wstawiona cząsteczka siRNA A2. Wyniki NGS potwierdziły powstawanie cząsteczki takiej samej jak w przypadku shA2R, czyli

z substytucją A w pozycji 8 od 5' końca. Ponadto ilość dojrzałego siRNA była około 10 razy niższa niż w przypadku cząsteczki powstającej po wprowadzeniu do komórek shA2R. Przeprowadzone przeze mnie badania pozwoliły na porównanie bezpieczeństwa i efektywności wektorowych cząsteczek typu shRNA i amiRNA celujących w powtórzenia CAG wprowadzonych za pomocą wirusa AAV5 do myszy YAC128. Eksperymenty *in vivo* potwierdziły, że narzędzia RNAi typu shRNA mogą być toksyczne po wprowadzeniu do żywego organizmu, najprawdopodobniej poprzez wysycenie maszynerii białkowej biogenezy miRNA lub poprzez efekt off-target. Mniejsza ilość powstającej dojrzałej cząsteczki z amiR136-A2 nie spowodowała wystąpienia objawów toksyczności u myszy. W dodatku, mimo uzyskania mniejszych ilości siRNA, efektywność obniżania poziomu zmutowanej HTT była porównywalna w przypadku shA2 i amiR136-A2 i wynosiła około 50% po 20 tygodniach od podania wektora. Ponadto ilość dojrzałego siRNA po traktowaniu amiR136-A2 pozwoliła na uzyskanie obniżenia ilości agregatów HTT w komórkach mózgu o 50%, a jak wiadomo, agregaty HTT są cechą charakterystyczną w występowaniu choroby Huntingtona.

Ciekawym, jak i obiecującym wynikiem było uzyskanie obniżenia masy śledziony w myszach po iniekcji wysoką dawką amiRNA do poziomu masy śledziony myszy zdrowych. Jest to istotne, ze względu na fakt, że myszy YAC128 mają tendencję do przybierania na wadze w czasie. Literatura pokazuje, że ekspresja zmutowanej *HTT* może prowadzić do zwiększenia masy organów, z wyjątkiem mózgu i jąder, prawdopodobnie poprzez mechanizmy zachodzące w komórkach mózgu^{84,85}.

Droga do badań klinicznych, poprzez optymalizację cząsteczki terapeutycznej *in vitro*, poprzez testowanie jej na różnych modelach komórkowych, a potem badania przedkliniczne na małych i większych zwierzętach, jest często bardzo długa i skomplikowana. Mimo uzyskania przeze mnie obiecujących wyników jest jeszcze wiele do ulepszenia. Jedną z kwestii jest sposób dostarczania cząsteczki do mózgu tak, aby był on jak najbardziej bezpieczny, a większość komórek docelowych miała dostarczony terapeutyk. Uzyskane rozbieżności w obniżeniu poziomu HTT między osobnikami, jak i niska efektywność inhibicji translacji w korze mózgu świadczy o tym, że dostarczanie i dystrybucja wektora wirusowego powinny być poprawione. Ważnym aspektem jest też zastosowanie jak najniższej dawki leku tak, aby uzyskać jak najskuteczniejszy efekt terapeutyczny. Wprowadzane przeze mnie cząsteczki były w bardzo wysokich dawkach i mimo że amiR136-A2 nie spowodował w trakcie tych 20 tygodni eksperymentu efektów niespecyficznych, z terapeutycznego punktu widzenia należałoby tę dawkę zmniejszyć

do minimum, co będzie przedmiotem moich dalszych badań w projekcie Preludium 20. Będę chciała tak zoptymalizować cząsteczkę, aby z kadłuba pri-miR-136 uwalniana była większa ilość dojrzałych siRNA. Inną drogą mającą na celu zwiększenie efektywności obniżania poziomu HTT będzie zastosowanie dodatkowej cząsteczki częściowo komplementarnej do sekwencji *HTT*, która miałaby wzmocnić blokadę translacji białka. Cząsteczka taka byłaby wprowadzana w postaci dodatkowego wektora lub w postaci tandemowego amiRNA, w przypadku którego do ekspresji dwóch różnych siRNA dochodziłoby z jednego konstrukt. Zaletą tandemowych cząsteczek jest to, że podejście takie może być tańsze ze względu na to, iż zastosowany byłby tylko jeden wektor. Ponadto stosowanie kilku różnych siRNA może zmniejszyć ryzyko wystąpienia efektu „off-target” wywołanego przez cząsteczkę podaną w wysokiej dawce^{86,87}.

Cząsteczka AMT-130, wykorzystująca strategię wektorową i będąca obecnie w fazie I/IIa badań klinicznych (NCT0412049) z pewnością otwiera drogę do badań klinicznych innym cząsteczkom amiRNA dostarczonym za pomocą wektorów wirusowych, w tym naszej. Należy podkreślić, że uzyskanie allelo-selektywności oraz uniwersalności poprzez celowanie w powtórzenia CAG jest dodatkową zaletą w porównaniu do nieselektywnej cząsteczki AMT-130, a przeprowadzone przeze mnie badania na modelu mysim zbliżają naszą strategię do wejścia w etap kliniczny. Co więcej, zarówno metoda inhibicji ekspresji genów przy pomocy wektorowych cząsteczek RNAi celujących w powtórzenia CAG jak również same cząsteczki są chronione patentami ICHB PAN i skomercjalizowane.

Bibliografia

1. Novak MJU, Tabrizi SJ. Huntington's disease. *BMJ*. 2010;340:c3109. doi:10.1136/bmj.c3109
2. Marsh JL, Walker H, Theisen H, et al. Expanded polyglutamine peptides alone are intrinsically cytotoxic and cause neurodegeneration in *Drosophila*. *Hum Mol Genet*. 2000;9(1):13-25. doi:10.1093/hmg/9.1.13
3. Arrasate M, Mitra S, Schweitzer ES, Segal MR, Finkbeiner S. Inclusion body formation reduces levels of mutant huntingtin and the risk of neuronal death. *Nature*. 2004;431(7010):805-810. doi:10.1038/nature02998
4. Perutz MF, Windle AH. Cause of neural death in neurodegenerative diseases attributable to expansion of glutamine repeats. *Nature*. 2001;412(6843):143-144. doi:10.1038/35084141
5. Becher MW, Kotzuk JA, Sharp AH, et al. Intranuclear neuronal inclusions in Huntington's disease and dentatorubral and pallidolusian atrophy: correlation between the density of inclusions and IT15 CAG triplet repeat length. *Neurobiol Dis*. 1998;4(6):387-397. doi:10.1006/nbdi.1998.0168
6. Legleiter J, Mitchell E, Lotz GP, et al. Mutant Huntingtin Fragments Form Oligomers in a Polyglutamine Length-dependent Manner in Vitro and in Vivo. *J Biol Chem*. 2010;285(19):14777-14790. doi:10.1074/jbc.M109.093708
7. Katsuno M, Tanaka F, Adachi H, et al. Pathogenesis and therapy of spinal and bulbar muscular atrophy (SBMA). *Prog Neurobiol*. 2012;99(3):246-256. doi:10.1016/j.pneurobio.2012.05.007
8. MacDonald ME, Ambrose CM, Duyao MP, et al. A novel gene containing a trinucleotide repeat that is expanded and unstable on Huntington's disease chromosomes. *Cell*. 1993;72(6):971-983. doi:10.1016/0092-8674(93)90585-E
9. Ross CA. Polyglutamine pathogenesis: emergence of unifying mechanisms for Huntington's disease and related disorders. *Neuron*. 2002;35(5):819-822. doi:10.1016/s0896-6273(02)00872-3
10. Da Silva JD, Teixeira-Castro A, Maciel P. From Pathogenesis to Novel Therapeutics for Spinocerebellar Ataxia Type 3: Evading Potholes on the Way to Translation. *Neurotherapeutics*. 2019;16(4):1009-1031. doi:10.1007/s13311-019-00798-1
11. Ashizawa T, Öz G, Paulson HL. Spinocerebellar ataxias: prospects and challenges for therapy development. *Nat Rev Neurol*. 2018;14(10):590-605. doi:10.1038/s41582-018-0051-6

12. Quarrell OWJ, Nance MA, Nopoulos P, Paulsen JS, Smith JA, Squitieri F. Managing juvenile Huntington's disease. *Neurodegener Dis Manag*. 2013;3(3):10.2217/nmt.13.18. doi:10.2217/nmt.13.18
13. Nance MA, Myers RH. Juvenile onset Huntington's disease—clinical and research perspectives. *Ment Retard Dev Disabil Res Rev*. 2001;7(3):153-157. doi:10.1002/mrdd.1022
14. Carroll LS, Massey TH, Wardle M, Peall KJ. Dentatorubral-pallidolusian Atrophy: An Update. *Tremor Hyperkinetic Mov*. 2018;8:577. doi:10.7916/D81N9HST
15. Swami M, Hendricks AE, Gillis T, et al. Somatic expansion of the Huntington's disease CAG repeat in the brain is associated with an earlier age of disease onset. *Hum Mol Genet*. 2009;18(16):3039-3047. doi:10.1093/hmg/ddp242
16. Cohen-Carmon D, Meshorer E. Polyglutamine (polyQ) disorders. *Nucleus*. 2012;3(5):433-441. doi:10.4161/nucl.21481
17. Khristich AN, Mirkin SM. On the wrong DNA track: Molecular mechanisms of repeat-mediated genome instability. *J Biol Chem*. 2020;295(13):4134-4170. doi:10.1074/jbc.REV119.007678
18. Schmidt MHM, Pearson CE. Disease-associated repeat instability and mismatch repair. *DNA Repair*. 2016;38:117-126. doi:10.1016/j.dnarep.2015.11.008
19. Zuccato C, Cattaneo E. Huntington's Disease. In: Lewin GR, Carter BD, eds. *Neurotrophic Factors*. Handbook of Experimental Pharmacology. Springer; 2014:357-409. doi:10.1007/978-3-642-45106-5_14
20. Zuccato C, Ciammola A, Rigamonti D, et al. Loss of huntingtin-mediated BDNF gene transcription in Huntington's disease. *Science*. 2001;293(5529):493-498. doi:10.1126/science.1059581
21. Gauthier LR, Charrin BC, Borrell-Pagès M, et al. Huntingtin Controls Neurotrophic Support and Survival of Neurons by Enhancing BDNF Vesicular Transport along Microtubules. *Cell*. 2004;118(1):127-138. doi:10.1016/j.cell.2004.06.018
22. Schulte J, Littleton JT. The biological function of the Huntingtin protein and its relevance to Huntington's Disease pathology. *Curr Trends Neurol*. 2011;5:65-78.
23. Jones L, Hughes A. Pathogenic Mechanisms in Huntington's Disease. In: Brotchie J, Bezdard E, Jenner P, eds. *International Review of Neurobiology*. Vol 98. Pathophysiology, Pharmacology, and Biochemistry of Dyskinesia. Academic Press; 2011:373-418. doi:10.1016/B978-0-12-381328-2.00015-8
24. Herzog LK, Kevei É, Marchante R, et al. The Machado–Joseph disease deubiquitylase ataxin-3 interacts with LC3C/GABARAP and promotes autophagy. *Aging Cell*. 2020;19(1):e13051. doi:10.1111/acel.13051
25. Matos CA, de Almeida LP, Nóbrega C. Machado–Joseph disease/spinocerebellar ataxia type 3: lessons from disease pathogenesis and clues into therapy. *J Neurochem*. 2019;148(1):8-28. doi:10.1111/jnc.14541

26. Pohl C, Dikic I. Cellular quality control by the ubiquitin-proteasome system and autophagy. *Science*. 2019;366(6467):818-822. doi:10.1126/science.aax3769
27. Li F, Macfarlan T, Pittman RN, Chakravarti D. Ataxin-3 Is a Histone-binding Protein with Two Independent Transcriptional Corepressor Activities*. *J Biol Chem*. 2002;277(47):45004-45012. doi:10.1074/jbc.M205259200
28. Bence NF, Sampat RM, Kopito RR. Impairment of the ubiquitin-proteasome system by protein aggregation. *Science*. 2001;292(5521):1552-1555. doi:10.1126/science.292.5521.1552
29. Evers MM, Toonen LJA, van Roon-Mom WMC. Ataxin-3 Protein and RNA Toxicity in Spinocerebellar Ataxia Type 3: Current Insights and Emerging Therapeutic Strategies. *Mol Neurobiol*. 2014;49(3):1513-1531. doi:10.1007/s12035-013-8596-2
30. Seidel K, Siswanto S, Brunt ERP, den Dunnen W, Korf HW, Rüb U. Brain pathology of spinocerebellar ataxias. *Acta Neuropathol (Berl)*. 2012;124(1):1-21. doi:10.1007/s00401-012-1000-x
31. Fan HC, Ho LI, Chi CS, et al. Polyglutamine (PolyQ) diseases: genetics to treatments. *Cell Transplant*. 2014;23(4-5):441-458. doi:10.3727/096368914X678454
32. Lieberman AP, Shakkottai VG, Albin RL. Polyglutamine Repeats in Neurodegenerative Diseases. *Annu Rev Pathol*. 2019;14:1-27. doi:10.1146/annurev-pathmechdis-012418-012857
33. Paleacu D. Tetrabenazine in the treatment of Huntington's disease. *Neuropsychiatr Dis Treat*. 2007;3(5):545-551.
34. Kegel KB, Kim M, Sapp E, et al. Huntingtin expression stimulates endosomal-lysosomal activity, endosome tubulation, and autophagy. *J Neurosci Off J Soc Neurosci*. 2000;20(19):7268-7278.
35. Ravikumar B, Vacher C, Berger Z, et al. Inhibition of mTOR induces autophagy and reduces toxicity of polyglutamine expansions in fly and mouse models of Huntington disease. *Nat Genet*. 2004;36(6):585-595. doi:10.1038/ng1362
36. Harding RJ, Tong Y feng. Proteostasis in Huntington's disease: disease mechanisms and therapeutic opportunities. *Acta Pharmacol Sin*. 2018;39(5):754-769. doi:10.1038/aps.2018.11
37. Tomoshige S, Nomura S, Ohgane K, Hashimoto Y, Ishikawa M. Discovery of Small Molecules that Induce the Degradation of Huntingtin. *Angew Chem Int Ed Engl*. 2017;56(38):11530-11533. doi:10.1002/anie.201706529
38. Bramsen JB, Laursen MB, Nielsen AF, et al. A large-scale chemical modification screen identifies design rules to generate siRNAs with high activity, high stability and low toxicity. *Nucleic Acids Res*. 2009;37(9):2867-2881. doi:10.1093/nar/gkp106

39. Alterman JF, Godinho BMDC, Hassler MR, et al. A divalent siRNA chemical scaffold for potent and sustained modulation of gene expression throughout the central nervous system. *Nat Biotechnol.* 2019;37(8):884-894. doi:10.1038/s41587-019-0205-0
40. Bartel DP. MicroRNAs: genomics, biogenesis, mechanism, and function. *Cell.* 2004;116(2):281-297. doi:10.1016/s0092-8674(04)00045-5
41. O'Brien J, Hayder H, Zayed Y, Peng C. Overview of MicroRNA Biogenesis, Mechanisms of Actions, and Circulation. *Front Endocrinol.* 2018;9. doi:10.3389/fendo.2018.00402
42. Grimm D, Streetz KL, Jopling CL, et al. Fatality in mice due to oversaturation of cellular microRNA/short hairpin RNA pathways. *Nature.* 2006;441(7092):537-541. doi:10.1038/nature04791
43. Borel F, van Logtenstein R, Koornneef A, et al. In vivo knock-down of multidrug resistance transporters ABCC1 and ABCC2 by AAV-delivered shRNAs and by artificial miRNAs. *J RNAi Gene Silenc Int J RNA Gene Target Res.* 2011;7:434-442.
44. Miniarikova J, Zanella I, Huseinovic A, et al. Design, Characterization, and Lead Selection of Therapeutic miRNAs Targeting Huntingtin for Development of Gene Therapy for Huntington's Disease. *Mol Ther Nucleic Acids.* 2016;5:e297. doi:10.1038/mtna.2016.7
45. Evers M, Miniarikova J, Juhas S, et al. AAV5-miHTT Gene Therapy Demonstrates Broad Distribution and Strong Human Mutant Huntingtin Lowering in a Huntington's Disease Minipig Model. *Mol Ther J Am Soc Gene Ther.* 2018;26(9):2163-2177. doi:10.1016/j.ymthe.2018.06.021
46. Caron NS, Southwell AL, Brouwers CC, et al. Potent and sustained huntingtin lowering via AAV5 encoding miRNA preserves striatal volume and cognitive function in a humanized mouse model of Huntington disease. *Nucleic Acids Res.* 2020;48(1):36-54. doi:10.1093/nar/gkz976
47. Nasir J, Floresco SB, O'Kusky JR, et al. Targeted disruption of the Huntington's disease gene results in embryonic lethality and behavioral and morphological changes in heterozygotes. *Cell.* 1995;81(5):811-823. doi:10.1016/0092-8674(95)90542-1
48. Zeitlin S, Liu JP, Chapman DL, Papaioannou VE, Efstratiadis A. Increased apoptosis and early embryonic lethality in mice nullizygous for the Huntington's disease gene homologue. *Nat Genet.* 1995;11(2):155-163. doi:10.1038/ng1095-155
49. Dragatsis I, Levine MS, Zeitlin S. Inactivation of Hdh in the brain and testis results in progressive neurodegeneration and sterility in mice. *Nat Genet.* 2000;26(3):300-306. doi:10.1038/81593
50. Wang G, Liu X, Gaertig MA, Li S, Li XJ. Ablation of huntingtin in adult neurons is nondeleterious but its depletion in young mice causes acute pancreatitis. *Proc Natl Acad Sci U S A.* 2016;113(12):3359-3364. doi:10.1073/pnas.1524575113

51. Grondin R, Kaytor MD, Ai Y, et al. Six-month partial suppression of Huntingtin is well tolerated in the adult rhesus striatum. *Brain J Neurol.* 2012;135(Pt 4):1197-1209. doi:10.1093/brain/awr333
52. Her LS, Goldstein LSB. Enhanced Sensitivity of Striatal Neurons to Axonal Transport Defects Induced by Mutant Huntingtin. *J Neurosci.* 2008;28(50):13662-13672. doi:10.1523/JNEUROSCI.4144-08.2008
53. Schmitt I, Linden M, Khazneh H, et al. Inactivation of the mouse Atxn3 (ataxin-3) gene increases protein ubiquitination. *Biochem Biophys Res Commun.* 2007;362(3):734-739. doi:10.1016/j.bbrc.2007.08.062
54. Switonski PM, Fiszer A, Kazmierska K, Kurpisz M, Krzyzosiak WJ, Figiel M. Mouse Ataxin-3 Functional Knock-Out Model. *Neuromolecular Med.* 2011;13(1):54-65. doi:10.1007/s12017-010-8137-3
55. Toulis V, García-Monclús S, de la Peña-Ramírez C, et al. The Deubiquitinating Enzyme Ataxin-3 Regulates Ciliogenesis and Phagocytosis in the Retina. *Cell Rep.* 2020;33(6):108360. doi:10.1016/j.celrep.2020.108360
56. Carrillo-Rosas S, Weber C, Fievet L, Messaddeq N, Karam A, Trottier Y. Loss of zebrafish Ataxin-7, a SAGA subunit responsible for SCA7 retinopathy, causes ocular coloboma and malformation of photoreceptors. *Hum Mol Genet.* 2019;28(6):912-927. doi:10.1093/hmg/ddy401
57. Matilla A, Roberson ED, Banfi S, et al. Mice Lacking Ataxin-1 Display Learning Deficits and Decreased Hippocampal Paired-Pulse Facilitation. *J Neurosci.* 1998;18(14):5508-5516. doi:10.1523/JNEUROSCI.18-14-05508.1998
58. Pfister EL, Kennington L, Straubhaar J, et al. Five siRNAs Targeting Three SNPs May Provide Therapy for Three-Quarters of Huntington's Disease Patients. *Curr Biol.* 2009;19(9):774-778. doi:10.1016/j.cub.2009.03.030
59. Fiszer A, Olejniczak M, Galka-Marciniak P, Mykowska A, Krzyzosiak WJ. Self-duplexing CUG repeats selectively inhibit mutant huntingtin expression. *Nucleic Acids Res.* 2013;41(22):10426-10437. doi:10.1093/nar/gkt825
60. Hu J, Liu J, Corey DR. Allele-selective inhibition of huntingtin expression by switching to an miRNA-like RNAi mechanism. *Chem Biol.* 2010;17(11):1183-1188. doi:10.1016/j.chembiol.2010.10.013
61. Kilikevicius A, Meister G, Corey DR. Reexamining assumptions about miRNA-guided gene silencing. *Nucleic Acids Res.* 2021;50(2):617-634. doi:10.1093/nar/gkab1256
62. McBride JL, Boudreau RL, Harper SQ, et al. Artificial miRNAs mitigate shRNA-mediated toxicity in the brain: Implications for the therapeutic development of RNAi. *Proc Natl Acad Sci U S A.* 2008;105(15):5868-5873. doi:10.1073/pnas.0801775105

63. Fang W, Bartel DP. The menu of features that define primary microRNAs and enable de novo design of microRNA genes. *Mol Cell*. 2015;60(1):131-145. doi:10.1016/j.molcel.2015.08.015
64. Galka-Marciniak P, Olejniczak M, Starega-Roslan J, Szczesniak MW, Makalowska I, Krzyzosiak WJ. siRNA release from pri-miRNA scaffolds is controlled by the sequence and structure of RNA. *Biochim Biophys Acta BBA - Gene Regul Mech*. 2016;1859(4):639-649. doi:10.1016/j.bbagr.2016.02.014
65. Medley JC, Panzade G, Zinovyeva AY. microRNA strand selection: Unwinding the rules. *WIREs RNA*. 2020;n/a(n/a):e1627. doi:https://doi.org/10.1002/wrna.1627
66. Harper SQ, Staber PD, He X, et al. RNA interference improves motor and neuropathological abnormalities in a Huntington's disease mouse model. *Proc Natl Acad Sci U S A*. 2005;102(16):5820-5825. doi:10.1073/pnas.0501507102
67. Drouet V, Perrin V, Hassig R, et al. Sustained effects of nonallele-specific Huntingtin silencing. *Ann Neurol*. 2009;65(3):276-285. doi:10.1002/ana.21569
68. Martier R, Sogorb-Gonzalez M, Stricker-Shaver J, et al. Development of an AAV-Based MicroRNA Gene Therapy to Treat Machado-Joseph Disease. *Mol Ther - Methods Clin Dev*. 2019;15:343-358. doi:10.1016/j.omtm.2019.10.008
69. Drouet V, Ruiz M, Zala D, et al. Allele-specific silencing of mutant huntingtin in rodent brain and human stem cells. *PLoS One*. 2014;9(6):e99341. doi:10.1371/journal.pone.0099341
70. Alves S, Nascimento-Ferreira I, Auregan G, et al. Allele-specific RNA silencing of mutant ataxin-3 mediates neuroprotection in a rat model of Machado-Joseph disease. *PLoS One*. 2008;3(10):e3341. doi:10.1371/journal.pone.0003341
71. Monteys AM, Wilson MJ, Boudreau RL, Spengler RM, Davidson BL. Artificial miRNAs Targeting Mutant Huntingtin Show Preferential Silencing In Vitro and In Vivo. *Mol Ther - Nucleic Acids*. 2015;4:e234. doi:10.1038/mtna.2015.7
72. Hu J, Liu J, Yu D, Chu Y, Corey DR. Mechanism of allele-selective inhibition of huntingtin expression by duplex RNAs that target CAG repeats: function through the RNAi pathway. *Nucleic Acids Res*. 2012;40(22):11270-11280. doi:10.1093/nar/gks907
73. Kozlowski P, de Mezer M, Krzyzosiak WJ. Trinucleotide repeats in human genome and exome. *Nucleic Acids Res*. 2010;38(12):4027-4039. doi:10.1093/nar/gkq127
74. Butland SL, Devon RS, Huang Y, et al. CAG-encoded polyglutamine length polymorphism in the human genome. *BMC Genomics*. 2007;8:126. doi:10.1186/1471-2164-8-126
75. Albà MM, Santibáñez-Koref MF, Hancock JM. The comparative genomics of polyglutamine repeats: extreme differences in the codon organization of repeat-encoding regions between mammals and *Drosophila*. *J Mol Evol*. 2001;52(3):249-259. doi:10.1007/s002390010153

76. Martin JN, Wolken N, Brown T, Dauer WT, Ehrlich ME, Gonzalez-Alegre P. Lethal toxicity caused by expression of shRNA in the mouse striatum: implications for therapeutic design. *Gene Ther.* 2011;18(7):666-673. doi:10.1038/gt.2011.10
77. Beer S, Bellovin DI, Lee JS, et al. Low-level shRNA Cytotoxicity Can Contribute to MYC-induced Hepatocellular Carcinoma in Adult Mice. *Mol Ther.* 2010;18(1):161-170. doi:10.1038/mt.2009.222
78. Mäkinen PI, Koponen JK, Kärkkäinen AM, et al. Stable RNA interference: comparison of U6 and H1 promoters in endothelial cells and in mouse brain. *J Gene Med.* 2006;8(4):433-441. doi:10.1002/jgm.860
79. Silva JM, Li MZ, Chang K, et al. Second-generation shRNA libraries covering the mouse and human genomes. *Nat Genet.* 2005;37(11):1281-1288. doi:10.1038/ng1650
80. Carbonell A, Daròs JA. Design, Synthesis, and Functional Analysis of Highly Specific Artificial Small RNAs with Antiviral Activity in Plants. *Methods Mol Biol Clifton NJ.* 2019;2028:231-246. doi:10.1007/978-1-4939-9635-3_13
81. Moore MJ, Scheel TKH, Luna JM, et al. miRNA–target chimeras reveal miRNA 3'-end pairing as a major determinant of Argonaute target specificity. *Nat Commun.* 2015;6(1):8864. doi:10.1038/ncomms9864
82. Wang D, Tai PWL, Gao G. Adeno-associated virus vector as a platform for gene therapy delivery. *Nat Rev Drug Discov.* 2019;18(5):358-378. doi:10.1038/s41573-019-0012-9
83. Kretov DA, Walawalkar IA, Mora-Martin A, Shafik AM, Moxon S, Cifuentes D. Ago2-Dependent Processing Allows miR-451 to Evade the Global MicroRNA Turnover Elicited during Erythropoiesis. *Mol Cell.* 2020;78(2):317-328.e6. doi:10.1016/j.molcel.2020.02.020
84. Van Raamsdonk JM, Gibson WT, Pearson J, et al. Body weight is modulated by levels of full-length Huntingtin. *Hum Mol Genet.* 2006;15(9):1513-1523. doi:10.1093/hmg/ddl072
85. Slow EJ, van Raamsdonk J, Rogers D, et al. Selective striatal neuronal loss in a YAC128 mouse model of Huntington disease. *Hum Mol Genet.* 2003;12(13):1555-1567. doi:10.1093/hmg/ddg169
86. Jackson AL, Linsley PS. Recognizing and avoiding siRNA off-target effects for target identification and therapeutic application. *Nat Rev Drug Discov.* 2010;9(1):57-67. doi:10.1038/nrd3010
87. Kittler R, Surendranath V, Heninger AK, et al. Genome-wide resources of endoribonuclease-prepared short interfering RNAs for specific loss-of-function studies. *Nat Methods.* 2007;4(4):337-344. doi:10.1038/nmeth1025

***Oświadczenia określające wkład w powstanie
prac naukowych wchodzących w skład
rozprawy doktorskiej***

Poznań, 24.05.2022

mgr inż. Anna Kotowska-Zimmer
Zakład Inżynierii genomowej
Instytut Chemii Bioorganicznej PAN
Ul. Noskowskiego 12/14
61-704 Poznań

OŚWIADCZENIE KANDYDATA O WŁASNYM WKŁADZIE W PUBLIKACJE NAUKOWE WCHODZĄCE
W SKŁAD ROZPRAWY DOKTORSKIEJ

Tytuł artykułu naukowego: „*Universal RNAi Triggers for the Specific Inhibition of Mutant Huntingtin, Atrophin-1, Ataxin-3, and Ataxin-7 Expression*”


Autorzy: Kotowska-Zimmer A, Ostrowska Y, Olejniczak M

Czasopismo: Molecular Therapy – Nucleic Acids

Data opublikowania: 06-03-2020

Oświadczam, że mój wkład autorski w artykuł naukowy o tytule: „*Universal RNAi Triggers for the Specific Inhibition of Mutant Huntingtin, Atrophin-1, Ataxin-3, and Ataxin-7 Expression*” polegał na:

- Projektowaniu i wykonaniu konstruktów genetycznych do ekspresji shRNA oraz systemu reporterowego,
- Udziale w przeprowadzeniu części testów reporterowych oraz analizie i opracowaniu uzyskanych wyników;
- Przygotowaniu i scharakteryzowaniu (MOI) wektorów lentiwirusowych do transdukcji linii komórkowych;
- Transdukcji, izolacji materiału biologicznego i wykonaniu znacznej większości analiz poziomu białek metodą western-blot oraz analizy poziomu transkryptów metodą RT-qPCR;
- Przygotowaniu prób do sekwencjonowania małych RNA metodą NGS i udziale w analizie wyników tych badań;
- Wykonaniu wszystkich rycin do publikacji i przygotowaniu materiałów suplementarnych;
- Udziale w pisaniu publikacji obejmującym opis wyników.



Podpis kandydata

Poznań, 24.05.2022

**Oświadczenie autora korespondencyjnego
o udziale doktoranta w powstaniu artykułu naukowego**

Niniejszym potwierdzam, że w publikacji:

Kotowska-Zimmer A, Ostrowska Y, Olejniczak M (2020). Universal RNAi Triggers for the Specific Inhibition of Mutant Huntingtin, Atrophin-1, Ataxin-3, and Ataxin-7 Expression. *Molecular Therapy – Nucleic Acids*, 19: 562-571. PMID: 31927329

jestem autorem korespondencyjnym oraz, że wkład autorski w ww. publikację mgr inż. Anny Kotowskiej-Zimmer polegał na wykonaniu większości eksperymentów, analizie wyników badań, pomocy w pisaniu manuskryptu, przygotowaniu rycin oraz materiałów suplementarnych.

Doktorantka zaprojektowała i wykonała konstrukty genetyczne do ekspresji shRNA oraz systemu reporterowego; przygotowała i scharakteryzowała (MOI) wektory lentiwirusowe do transdukcji linii komórkowych; wspólnie z Julią Ostrowską wykonała analizy efektywności cząsteczek shRNA w systemie reporterowym. Wykonała ponadto większość eksperymentów na komórkach fibroblastów HD, SCA3, SCA7 i DRPLA, tj. transdukcje wirusowe, izolację materiału biologicznego, analizę poziomu białek metodą western blot oraz analizy poziomu transkryptów metodą RT-qPCR. Doktorantka przygotowała próbki do sekwencjonowania małych RNA metodą NGS i brała udział w analizie wyników tych badań.

Mój udział w tworzeniu tej publikacji polegał na opracowaniu koncepcji badań, wykonaniu analiz metodą northern blot, interpretacji wyników badań, napisaniu manuskryptu i opracowaniu materiałów suplementarnych. Ponadto nadzorowałam prace eksperymentalne i zdobyłam finansowanie na te badania.



Podpis autora korespondencyjnego

Poznań, 24.05.2022

mgr inż. Anna Kotowska-Zimmer
Zakład Inżynierii genomowej
Instytut Chemii Bioorganicznej PAN
Ul. Noskowskiego 12/14
61-704 Poznań

OŚWIADCZENIE KANDYDATA O WŁASNYM WKŁADZIE W PUBLIKACJE NAUKOWE WCHODZĄCE
W SKŁAD ROZPRAWY DOKTORSKIEJ

Tytuł artykułu naukowego: „*Artificial miRNAs as therapeutic tools: Challenges and opportunities*”

Autorzy: Kotowska-Zimmer A, Pewinska M, Olejniczak M

Czasopismo: Wiley Interdisciplinary Reviews: RNA

Data opublikowania: 01-01-2021

Oświadczam, że mój wkład autorski w artykuł naukowy o tytule: „*Artificial miRNAs as therapeutic tools: Challenges and opportunities*” polegał na:

- Zebraniu i analizie dostępnej literatury na temat biogenezy miRNA, projektowania i dostarczania cząsteczek amiRNA oraz wykorzystania cząsteczek amiRNA w terapii chorób neurodegeneracyjnych (rozdziały 2-6).
- Udziale w pisaniu publikacji;
- Wykonaniu wszystkich rycin i tabeli głównej.

Anna Kotowska-Zimmer

Podpis kandydata

Poznań, 24.05.2022

**Oświadczenie autora korespondencyjnego
o udziale doktoranta w powstaniu artykułu naukowego**

Niniejszym potwierdzam, że w publikacji:

Kotowska-Zimmer A, Pewinska M, Olejniczak M (2021). Artificial miRNAs as therapeutic tools: Challenges and opportunities. WIREs RNA, 12:e1640. PMID: 33386705

jestem autorem korespondencyjnym oraz, że wkład autorski w ww. publikację mgr inż. Anny Kotowskiej-Zimmer polegał na zebraniu i analizie dostępnej literatury na temat biogenezy miRNA, projektowania i dostarczania cząsteczek amiRNA oraz wykorzystania cząsteczek amiRNA w terapii chorób neurodegeneracyjnych (rozdziały 2-6). Doktorantka brała udział w pisaniu manuskryptu publikacji i wykonała wszystkie ryciny i tabelę 1.

Mój udział w tworzeniu tej publikacji przeglądowej polegał na przygotowaniu koncepcji pracy i napisaniu ostatecznej wersji manuskryptu. Jako autor korespondencyjny zostałam zaproszona do przygotowania tej publikacji przez edytorów czasopisma WIREs RNA.



Podpis autora korespondencyjnego

Poznań, 24.05.2022

mgr inż. Anna Kotowska-Zimmer
Zakład Inżynierii genomowej
Instytut Chemii Bioorganicznej PAN
Ul. Noskowskiego 12/14
61-704 Poznań

OŚWIADCZENIE KANDYDATA O WŁASNYM WKŁADZIE W PUBLIKACJE NAUKOWE WCHODZĄCE
W SKŁAD ROZPRAWY DOKTORSKIEJ

Tytuł artykułu naukowego: „*A CAG repeat-targeting artificial miRNA lowers the mutant huntingtin level in the YAC128 model of Huntington's disease*”

Autorzy: Kotowska-Zimmer A, Przybyl L, Pewinska M, Suszynska-Zajczyk J, Wronka D, Figiel M, Olejniczak M

Czasopismo: Molecular Therapy – Nucleic Acids

Data opublikowania: 05-05-2022

Oświadczam, że mój wkład autorski w artykuł naukowy o tytule: „*A CAG repeat-targeting artificial miRNA lowers the mutant huntingtin level in the YAC128 model of Huntington's disease*” polegał na:

- Projektowaniu cząsteczek amiRNA, tworzeniu lentiwirusów i testowaniu ich efektywności w modelu komórkowym fibroblastów HD (68/17Q) z wykorzystaniem techniki western blot oraz analizie uzyskanych wyników;
- Analizie wyników głębokiego sekwencjonowania do określenia obróbki komórkowej amiR136-A2 i ilości dojrzałych cząsteczek;
- Genotypowaniu myszy do uzyskania odpowiedniej do eksperymentów kohorty myszy YAC128;
- Nastrzykiwaniu części myszy wektorami AAV niosącymi GFP, jak również cząsteczki shRNA i amiRNA;
- Poborze tkanek z części myszy;
- Wykonaniu wszystkich analiz poziomu białka metodą western blot na tkankach pobranych z mysiego mózgu oraz części analiz poziomu transkryptów metodą RT-qPCR ;
- Wykonaniu wszystkich skrawków pochodzących z mysich mózgów, immunobarwień oraz zdjęć mikroskopowych, a także ich analiz;
- Wykonaniu rycin do publikacji;
- Udziale w pisaniu publikacji.



Podpis kandydata

Poznań, 24.05.2022

**Oświadczenie autora korespondencyjnego
o udziale doktoranta w powstaniu artykułu naukowego**

Niniejszym potwierdzam, że w publikacji:

Kotowska-Zimmer A, Przybyl L, Pewinska M, Suszynska-Zajczyk J, Wronka D, Figiel M, Olejniczak M (2022). A CAG repeat-targeting artificial miRNA lowers the mutant huntingtin level in the YAC128 model of Huntington's disease. *Molecular Therapy – Nucleic Acids*, 28: 702-715

jestem autorem korespondencyjnym oraz, że wkład autorski w ww. publikację mgr inż. Anny Kotowskiej-Zimmer polegał na wykonaniu większości eksperymentów, analizie wyników badań, pomocy w pisaniu manuskryptu i odpowiedzi na uwagi recenzentów, przygotowaniu wszystkich rycin oraz materiałów suplementarnych.

Doktorantka zaprojektowała cząsteczki amiRNA, przygotowała i scharakteryzowała konstrukty genetyczne oraz wektory lentiwirusowe, testowała ich efektywność w modelu komórkowym fibroblastów HD (68/17Q) z wykorzystaniem techniki western blot. Przeprowadziła analizę obróbki komórkowej amiR136-A2 i ilości dojrzałych cząsteczek siRNA względem endogennych miRNA, wykorzystując dane z głębokiego sekwencjonowania małych RNA. Doktorantka wykonywała również eksperymenty z wykorzystaniem modelu mysiego HD, tj. genotypowanie myszy YAC128 w celu uzyskania odpowiedniej kohorty zwierząt do eksperymentu; wykonywanie procedur iniekcji stereotaktycznej wektorów AAV5 (wspólnie z Łukaszem Przybyłem); pobór tkanek oraz izolację RNA, DNA i białka. Wykonała wszystkie analizy pomiaru liczby kopii wirusa w tkankach mózgu, analizy poziomu białka metodą western blot, analizy immunohistochemiczne oraz część eksperymentów RT-qPCR.

Mój udział w tworzeniu tej publikacji polegał na opracowaniu koncepcji badań, interpretacji wyników, napisaniu manuskryptu i opracowaniu materiałów suplementarnych. Ponadto nadzorowałam prace eksperymentalne i zdobyłam finansowanie na te badania.



Podpis autora korespondencyjnego

*Prace naukowe wchodzące w skład rozprawy
doktorskiej*

Universal RNAi Triggers for the Specific Inhibition of Mutant Huntingtin, Atrophin-1, Ataxin-3, and Ataxin-7 Expression

Anna Kotowska-Zimmer,¹ Yuliya Ostrovska,¹ and Marta Olejniczak^{1,2}

¹Department of Genome Engineering, Institute of Bioorganic Chemistry, Polish Academy of Sciences, Noskowskiego 12/14, 61-704 Poznan, Poland; ²Dystrogen Gene Therapies, 1415 W 37th Street, Chicago, IL, USA

The expansion of CAG repeats within the coding region of associated genes is responsible for nine inherited neurodegenerative disorders including Huntington's disease (HD), spinocerebellar ataxias (SCAs), and dentatorubral-pallidoluysian atrophy (DRPLA). Despite years of research aimed at developing an effective method of treatment, these diseases remain incurable and only their symptoms are controlled. The purpose of this study was to develop effective and allele-selective genetic tools for silencing the expression of mutated genes containing expanded CAG repeats. Here we show that repeat-targeting short hairpin RNAs preferentially reduce the levels of mutant huntingtin, atrophin-1, ataxin-3, and ataxin-7 proteins in patient-derived fibroblasts and may serve as universal allele-selective reagents for polyglutamine (polyQ) diseases.

INTRODUCTION

Polyglutamine (polyQ) diseases are a group of inherited autosomal dominant neurological disorders caused by the expansion of unstable CAG repeats in translated regions of the respective genes. There are 9 known polyQ diseases, including Huntington's disease (HD), six spinocerebellar ataxias (SCA) types 1, 2, 3, 6, 7, 17; dentatorubral-pallidoluysian atrophy (DRPLA); and spinal and bulbar muscular atrophy (SBMA). The common pathogenic factor in this group of disorders is toxic protein with a polyQ domain that forms intracellular aggregates and causes neuronal degeneration and death. The pathology related to polyQ diseases develops in the specific brain areas characteristic of each disorder, e.g., striatum and cerebral cortex in HD, or cerebellum, basal ganglia, brainstem, and spinal cord in SCA3.¹⁻⁴

Although no causal therapy is currently available and only symptomatic treatment is offered to patients, many therapeutic approaches are being tested to reverse or slow the progression of the disease.^{5,6} Because the pathogenesis of polyQ diseases is associated with the presence of toxic proteins, the most direct therapeutic strategies involve silencing of the specific gene expression with the use of antisense oligonucleotides (ASO) and RNA interference (RNAi), preventing mutant protein aggregation, inhibiting the cleavage of polyQ proteins and inducing mutant protein degradation.⁶⁻⁹ Other promising results were obtained by targeting downstream cellular effects,

such as reduction of mitochondrial dysfunction and oxidative stress or decrease of inflammation.¹⁰⁻¹³ Recently successful editing of *HTT* and *ATXN3* genes with the use of the CRISPR-Cas9 system was demonstrated.¹⁴⁻¹⁸ However, safety issues related to the permanent modification of the genome and off-target effects need to be resolved before clinical application of therapy.

In recent years, groundbreaking research has been conducted on HD therapy. Of particular importance are three publications reporting three different technologies.¹⁹⁻²¹ The first publication summarizes the results of a Phase 1/2a clinical trial with repeated injections of ASO in early manifest HD patients.¹⁹ In the second study, the authors demonstrate efficient allele-selective transcriptional repression of the mutant *HTT* with the use of zinc finger protein transcription factors (ZFP-TF) in cell cultures and mouse models.²⁰ Finally, in the last study, a single injection of fully modified small interfering RNA (siRNA) (divalent siRNA, di-siRNA) into the cerebrospinal fluid resulted in potent, sustained gene silencing in the central nervous system (CNS) of mice and nonhuman primates.²¹

Because the function of the wild-type polyQ proteins and their roles through patient lifetime is incompletely understood, the safest therapeutic strategy is to target mutant variants, leaving the normal proteins intact. For polyQ disease genes, the regions differentiating the alleles that can be selectively targeted are single-nucleotide polymorphisms (SNPs) linked to the repeat expansions and the repeat region itself. The first strategy has some limitations because SNPs that are targets for ASOs are present only in a selected group of patients.²²⁻²⁴ However, a Phase 1b/2a clinical trial of allele-selective ASOs targeting two SNPs (rs362307 and rs362331) in early manifest HD patients is ongoing (<https://www.clinicaltrials.gov/>, ClinicalTrials.gov: NCT03225833 and NCT03225846). A more universal strategy, applicable for all patients, is based on the difference between

Received 22 July 2019; accepted 11 December 2019;
<https://doi.org/10.1016/j.omtn.2019.12.012>

Correspondence: Marta Olejniczak, Department of Genome Engineering, Institute of Bioorganic Chemistry, Polish Academy of Sciences, Noskowskiego 12/14, 61-704 Poznan, Poland.

E-mail: marta.olejniczak@ibch.poznan.pl



the repeat tract length in the normal and mutant alleles. By using different types of CAG-targeting oligonucleotides in different polyQ models, the David Corey group showed the potency of this strategy in allele-selective silencing of mutant proteins.^{25–29} In our previous study, we demonstrated successful silencing of mutant huntingtin expression using a CAG repeat-targeting strategy and RNAi tools.³⁰ The introduction of selective modifications into siRNA sequences creates mismatches with mRNA targets and activation of microRNA (miRNA)-like translation inhibition mechanisms.^{27,30,31} Preferential silencing of mutant alleles is achieved by binding of more silencing complexes to long CAG repeat tracts.

The activity and allele selectivity of selected chemically modified CAG-targeting siRNA oligonucleotides were also confirmed in SCA3, SCA7, and DRPLA models.^{26,32–34} However, in preclinical and clinical applications, RNAi triggers are generally delivered as viral vectors to provide long-term expression and broad distribution of reagents in affected brain regions. Vector-based short hairpin RNAs (shRNAs) and artificial miRNAs expressed in cells from Pol III (typically H1 promoter of RNase P or U6 small nuclear RNA [snRNA] promoter) or Pol II promoters mimic pre- and pri-miRNA precursors, respectively. They are processed in cells by miRNA biogenesis machinery to form mature siRNA. Transcribed shRNAs are transported from nucleus to the cytoplasm by the Exportin-5/Ran guanosine triphosphate (GTP) complex and undergo single step processing by endoribonuclease Dicer. Processing is, however, imprecise and depends on the sequence and structure of a molecule and generates a heterogeneous pool of siRNAs.³⁵ Therefore, the activity of siRNAs, especially those containing selective sequence modifications, is not always reflected in corresponding vector-based RNAi triggers.^{36,37}

In the current study, we analyzed the efficacy and allele selectivity of CAG repeat-targeting reagents expressed in cells as shRNAs. We demonstrated that shRNAs efficiently silence the expression of mutant *HTT*, *ATN1*, *ATXN3*, and *ATXN7* genes in patient-derived fibroblasts. We confirmed that shRNAs are processed in cells by Dicer into a pool of siRNA with a predominance of the desired guide strand variant, which did not induce a significant off-target effect in a fibroblast model of the disease.

RESULTS

Preferential Inhibition of Mutant Huntingtin Expression by CAG-Targeting shRNAs

The CAG repeat-targeting strategy uses reagents comprising complementary CUG repeats. Therefore, in the first step, we designed shRNAs with a stem consisting of pure CUG/CUG and CAG/CUG repeats (Figure S1A). The hairpin, comprising CUG repeats, is processed by Dicer with low efficiency, likely due to the instability of the stem structure containing periodic U:U mismatches (Figure S1B). This results in low activity toward CAG-containing transcripts. More typical CAG/CUG shRNA with perfectly paired stem is processed into a pool of siRNA with high efficiency; however, its silencing activity is non-allele selective (Figure S1C).

In our previous study, we demonstrated that siRNAs containing specific interruptions in the CUG sequence (U > A and U > G type) are selective toward mutant huntingtin in cellular models of HD.³⁰ siRNA efficacy and selectivity were dependent on the type of modification and their number and position within the siRNA guide strand. The most active A2 siRNA was designed to form two variants of shRNAs (driven by the H1 promoter), namely, A2R and A2R1, comprising the hsa-miR-23 loop and CAG/CUG stem with a single U > A modification. We confirmed that shRNAs were processed in cells by Dicer into a pool of 19–24 nt siRNA and efficiently reduced mutant huntingtin levels by 90%, leaving the normal huntingtin intact.³⁰

To examine the allele selectivity of other siRNA variants expressed from genetic vectors in this study, we designed two other shRNAs containing single (shG2) or two (shG4) U > G substitutions at specific positions of the CUG repeat strand, resulting in the formation of the G-A mismatches with the target transcript.

To analyze the products of shRNAs processing by Dicer, we transfected HEK 293T cells with plasmids encoding shRNAs and performed NGS analysis of small RNA. As expected, the analyzed reagents exhibit similar strand biases, with a considerable predominance of the guide siRNA strands originating from the 3' arm, reaching more than 99% for shA2R (Figure 1A), shG2, and shG4 and 96% for shA2R1 (Figure S2). Corresponding siRNAs derived from the shA2R and shG2 differed mainly in length of the U-tail at their 3' ends, whereas 90% of molecules contain an A or G substitution at position 8 from the 5' end (5'-CTGCTGCNGCTGCTGCTGCTT-3'). siRNAs derived from shA2R1 were represented by two main variants shifted at the 5' end, which resulted in A substitution at position 8 (69%) and position 9 (25%) from the 5' end. In the case of shG4, the main variant represented by 95% of siRNAs contains G substitution at positions 8 and 14 from the 5' end (Figure S2).

To evaluate the potency of the shRNA constructs *in vitro*, we cotransfected them into HEK 293T cells together with luciferase (Luc) reporters bearing either the human *HTT* exon 1 encompassing 85 CAG repeats (mutant, 85CAG_Luc) or 16 CAG repeats (normal, 16CAG_Luc). We obtained significant repression of the luciferase expression after the transfection of 85CAG_Luc with all of the shRNA constructs; the knockdown effect was stronger than 60% for all shRNAs with shA2R being the most efficient and inducing $\pm 75\%$ silencing of mutant *HTT* (Figures 1B and 1C). An analysis of the half maximal inhibitory concentration (IC₅₀) values indicates that shG2, shA2R, and shA2R1 are more potent than shG4 and knock down the tested 85CAG_Luc reporter by 50% in concentration of 10 ng, 13.5 ng, and 16.3 ng, respectively (Figure 1C). The 16CAG_Luc reporters were not knocked down by 50% even in the highest concentration of shRNAs tested (500 ng). The highest allele selectivity measured as the ratio of the IC₅₀ values (IC₅₀16CAG_Luc/IC₅₀85CAG_Luc) was achieved when shG2 (>50) and shA2R (>37) were used (Figure 1C).

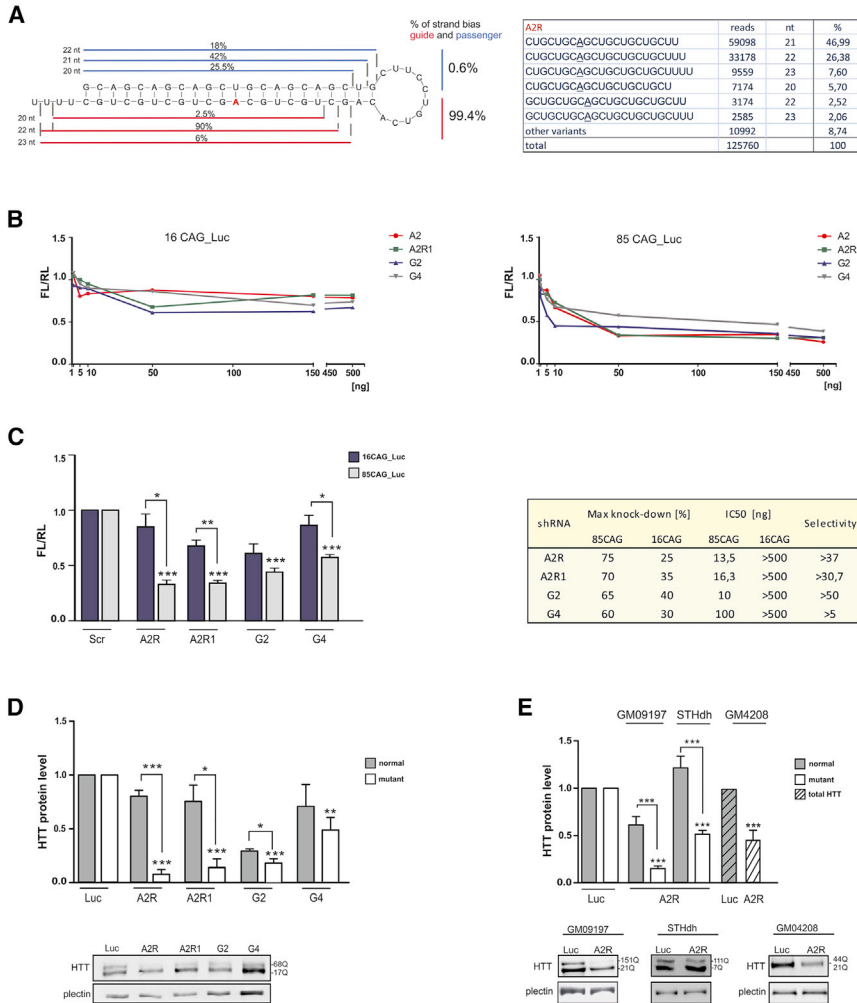


Figure 1. Cellular Processing of shA2R and Silencing Activity of CAG-Targeting shRNAs in HD Models

(A) Next-generation sequencing analysis of the shA2R processing pattern in HEK 293T cells. The guide strand is indicated in red, and the passenger strand is indicated in blue. Cleavage sites are presented on both strands corresponding to the length of released siRNA variants (content and length are noted on the left site). The table presents the results of total quantity reads, length, and percentage content of the sequence composition of released strands after NGS analysis. (B) Knockdown of Luciferase (Luc) reporters containing exon 1 of the *HTT* gene with 16 CAG repeats (16CAG_Luc) or 85 CAG repeats by shA2R, A2R1, G2, and G4. The *HTT* gene fragment was fused to the firefly luciferase (FL) gene and renilla luciferase (RL) was used as an internal control. HEK 293T cells were co-transfected with 50 ng of Luc reporters and 1, 5, 10, 50, 150, or 500 ng of shRNA constructs. FL and RL were measured 2 days post-transfection and FL was normalized to RL expression. A scrambled construct (shScr) served as a negative control and relative repression of luciferase expression following the transfection of the shScr reporter was set at 1. (C) The graph represents the results of Luc reporters' knockdown by shRNA constructs used in the concentration of 50 ng (1 × 1 ratio of Luc reporter and shRNA). Maximal knockdown by four shRNAs (%), the half maximal inhibitory concentration (IC₅₀), and allele selectivity is demonstrated in the table. The value of IC₅₀ indicates a concentration (ng) of a shRNA construct that is required for 50% Luc reporter knockdown. The selectivity was calculated as the IC₅₀ ratio of 16CAG_Luc/85CAG_Luc. (D) Western blot analysis of HTT levels in HD patient-derived fibroblasts (cell line GM04281, 17/68Q) at 7 days posttransduction with LV in MOI of 10, containing shA2R, shA2R1, shG2, and shG4 expression cassettes. Signal intensities of the protein level were normalized to plectin protein levels and compared using a one-sample t test. (E) Western blot analysis of HTT levels in different cell lines: human HD fibroblasts (GM09197 – 21/151Q, GM04208 – 21/41Q) and HD mouse striatal precursor cell line STHdh (7/111Q). Because the difference between normal and mutant protein in the cell line GM04208 (21/41Q) is low and separation of these two variants is very difficult, we measured total huntingtin level as described in the graph. The shLuc construct was used as a control reference in both graphs. The graph bars represent the mean value of protein levels ± SEM. The p values are indicated by asterisks (*p < 0.05, **p < 0.01, ***p < 0.001). All experiments were repeated at least three times.

Next, we analyzed the silencing efficiency of the shRNAs in a cellular model of HD. shRNAs were introduced into HD patient-derived fibroblasts (GM04281; 68 CAG repeats/mutant allele, 17 CAG repeats/wild-type allele) by lentiviral transduction, and protein was isolated at 7 days posttransduction. Analysis of huntingtin levels by western blotting demonstrated ~70% and 50% reduction of mutant protein levels by shG2 and shG4, respectively (Figure 1D). However, in the case of shG2, the normal huntingtin was also significantly reduced by ~60%. Interestingly, the only difference between allele-selective shA2R and nonselective shG2 is the type of substitution within the CUG guide strand (U > A versus U > G). As confirmed by NGS, these molecules are processed into similar siRNA variants with nucleotide substitution at position 8. The transcript level measured by quantitative real-time PCR did not decrease after lentiviral (LV) shRNA transduction (Figure S3), and this finding may indicate a predominance

of the translation inhibition mechanism of action suggested in other studies using miRNA-like siRNA.

Next, we examined the inhibition of HTT and allele selectivity in other HD cellular models with different numbers of CAG tracts (fibroblasts GM04208 with 21/44 CAG, GM09197 with 21/151 CAG, and mouse neuronal precursors STHdh with 7/111 Q) (Figure 1E). In all cases, shA2R preferentially silenced the expression of the mutant *HTT* gene; however, the transduction efficiency of the STHdh cell line was lower than that for human fibroblasts, which is reflected in the total silencing efficiency.

CAG-Targeting shRNAs Silence the Expression of *ATN1*, *ATXN3*, and *ATXN7* Genes

To determine whether CAG-targeting shRNAs could be considered universal therapeutics for polyQ diseases, we transduced DRPLA

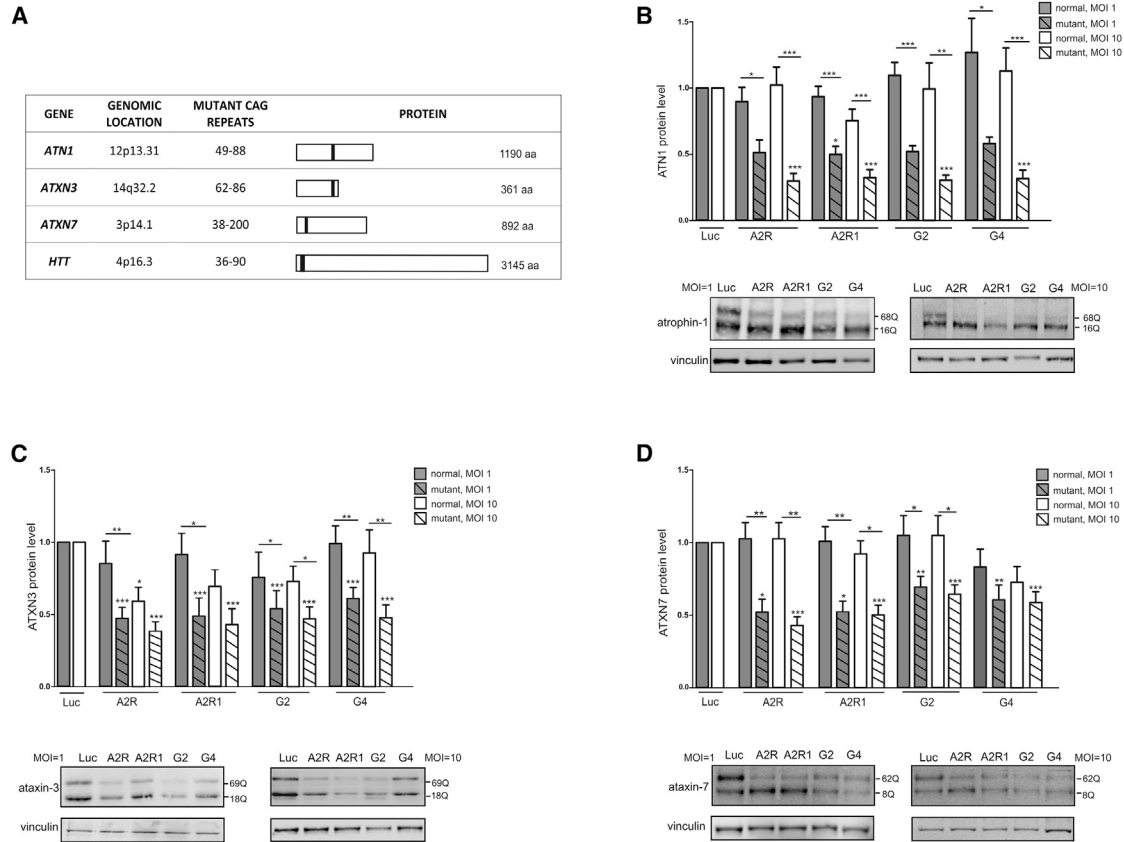


Figure 2. Analysis of Efficacy and Allele Selectivity of CAG-Targeting shRNAs in Cellular Models of DRPLA, SCA3, and SCA7

(A) Characterization of polyQ models used in this study. (B–D) Western blot analysis of atrophin-1 levels in DRPLA patient-derived fibroblasts (16/68Q) (B), ataxin-3 levels in SCA3 patient-derived fibroblasts (18/69Q) (C), and ataxin-7 levels in SCA7 patient-derived fibroblasts (8/62Q) (D). Protein was isolated at 7 days posttransduction with two concentrations of LV (MOI of 1 and 10) containing shA2R, shA2R1, shG2, and shG4 expression cassettes. The shLuc construct (Luc) was used as a negative control. Signal intensities of the protein level were normalized to vinculin protein level and compared using a one-sample t test. The graph bars represent the mean value of protein levels \pm SEM. The p values are indicated by asterisks (* $p < 0.05$, ** $p < 0.01$, *** $p < 0.001$). All experiments were repeated at least three times.

(16/68 CAG), SCA3 (18/69 CAG), and SCA7 (8/62 CAG) patient-derived fibroblasts with two concentrations of LV (multiplicity of infection [MOI] of 1 and 10) expressing shA2R, shA2R1, shG2, and shG4. These models differ in terms of CAG tract localization within specific genes, chromosomal environment and localization of causative genes, and the threshold of pathogenic repeat number (Figure 2A).

DRPLA is caused by the expansion of the CAG tract to ≥ 49 repeats in the *ATN1* gene localized at 12p13.31. In patient-derived fibroblasts containing 16/68 CAG repeats, all tested shRNAs demonstrated allele-selective silencing of mutant atrophin-1 by $\sim 50\%$ in lower concentration of LVs and $\sim 70\%$ in MOI of 10 (Figure 2B). Stronger discrimination between alleles was observed in higher concentration of LV particles.

SCA3, also known as Machado-Joseph disease (MJD), is caused by the expansion of the CAG tract to more than 62 repeats within exon 10 of the *ATXN3* gene localized at chromosome 14q32.1. In contrast to the HD model, shRNAs of A- and G-type showed a similar pattern of ac-

tivity and preferentially silenced the expression of the mutant allele to $\sim 50\%$ of the control level (Figure 2C). However, silencing efficacy and allele selectivity was lower than for the HD and DRPLA models, and the most efficient shA2R reduced mutant and normal ataxin-3 by $\sim 60\%$ and $\sim 40\%$, respectively. Generally, the silencing efficiency increased slightly with a higher dose of LV particles and also resulted also in lower allele selectivity.

Another example of polyQ diseases is SCA7 caused by the expansion of >38 CAG repeats at the *ATXN7* gene localized on chromosome 3p14.1. Similar to HD, the abnormal polyQ tract is localized in the N-terminal part of the protein. In a fibroblast model containing 8 and 62 CAG repeats, shA2R demonstrated the greatest efficacy and allele discrimination, with normal ataxin-7 unaffected and mutant silenced nearly by 60% (Figure 2D). In contrast to DRPLA and SCA3 models, and similar to HD model, shG4 decreased the level of normal and mutant ATXN7 by approximately 20% and 40%, respectively. However, overall ATXN-7 target silencing by analyzed shRNAs was the lowest among all polyQ models.

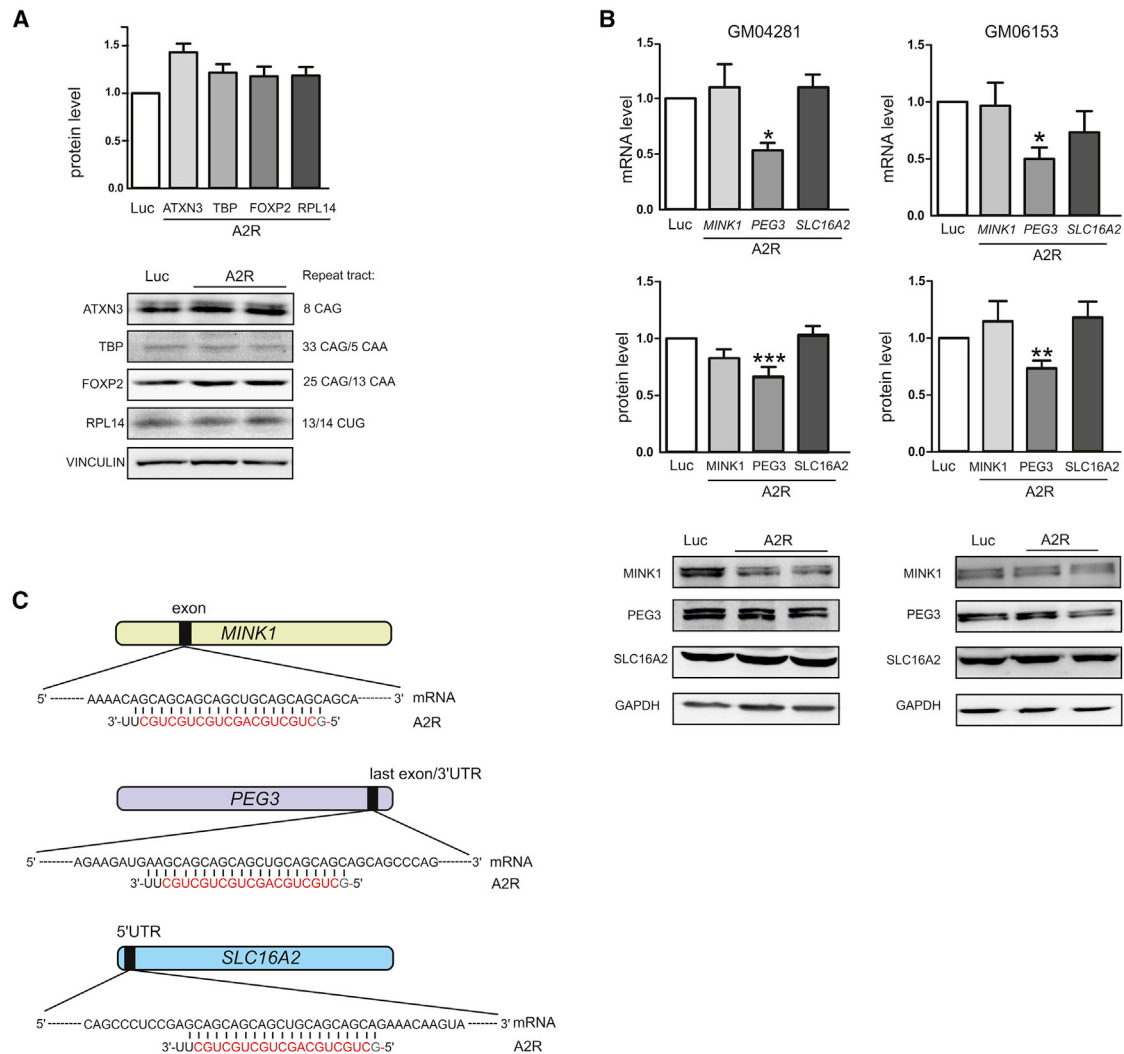


Figure 3. Evaluation of Off-Target Effects Induced by the shA2R in Human Fibroblasts

(A) Western blot analysis of selected proteins containing pure or interrupted CAG repeats in respective genes. Protein level was analyzed after transduction of HD fibroblasts (GM04281) with LV in MOI of 10 containing shA2R expression cassette. The signal intensities of the protein level were normalized to vinculin level and compared using a one-sample t test. (B) Analysis of mRNA transcript level (quantitative real-time PCR) and protein level (western blotting) of predicted off-target genes: *MINK1*, *PEG3*, and *SLC16A2*. Analysis was performed in HD (GM04281) and SCA3 (GM06153) patient-derived fibroblasts treated with LV in MOI of 10 containing shA2R expression cassette. GAPDH was used as a reference protein. (C) The localization of the target sequence within the *MINK1*, *PEG3*, and *SLC16A2* transcripts with full complementarity to the shA2R reagent. The shLuc (Luc) construct was used as a control reference. The graph bars represent the mean value of protein or transcript levels \pm SEM. The p values are indicated by asterisks (* $p < 0.05$, ** $p < 0.01$, *** $p < 0.001$). All experiments were repeated at least three times.

Although in each polyQ model, the shRNAs demonstrated different patterns of silencing, shA2R seems to be a candidate universal therapeutic tool for these diseases.

CAG-Targeting shRNA Does Not Generate Significant Off-Target Effects

An important challenge for therapeutic molecules that target CAG repeats is the existence of other genes that contain similar repetitive regions.³⁸ Previously, we demonstrated the gene selectivity of CAG-targeting siRNAs by analyzing the cellular levels of other

proteins encoded by genes containing pure or interrupted CAG repeats (ATXN3; TATA-box binding protein, TBP, and FOXP2) and CTG repeats (EIF2AK3, RPL14, and LRP8).³⁰ The Corey group²⁷ observed no inhibition of TBP, androgen receptor, AAK-1, POU3F2, or FOXP2 at high concentrations of CAG-targeting oligonucleotides. In this study, we confirmed these results by analyzing TBP (33 CAG with 5 CAA interruptions), FOXP2 (25 CAG with 13 CAA), RPL14 (13/14 CUG), and ATXN3 (8 CAG) protein levels in HD fibroblasts treated with shA2R. None of these proteins was inhibited (Figure 3A). This finding

supports the translation inhibition mechanism by miRNA-like siRNA in which only longer, uninterrupted CAG tracts are efficiently blocked by RISC-CUG.

We also performed bioinformatic analysis (BLAST NCBI and Ensembl blast) of mRNA targets that are fully complementary to the shA2R guide strand because this type of interaction may induce AGO2-mediated mRNA cleavage and unintended reduction of some transcript levels (Table S1). Guide strands released from shA2R (with U > A substitution at position 8 or 9) have 5 mRNA targets with full complementarity of 21 nt, 7 targets with 20 nt complementarity, 1 target with 19 nt, and 7 targets with 18 nt complementarity. Misshapen-like kinase 1 (MINK1), paternally expressed gene 3 (PEG3) and solute carrier family 16 member 2 (SLC16A2) transcripts were expressed in fibroblasts, and we analyzed their levels by qPCR after shA2R treatment. Of these three transcripts, only the PEG3 level was decreased by ~50% in HD and SCA3 fibroblasts (Figure 3B). A protein level analysis confirmed that only PEG3 is down-regulated by ~30% in human fibroblasts (Figure 3B). Interestingly, the sequences complementary to the siRNA guide strand are localized in different parts of these genes: in the 5' UTR (SLC16A2), in exons (MINK1), or the last exon/3' UTR (PEG3), depending on the splice variant of the PEG3 transcript (Figure 3C). The effects of PEG3 silencing *in vivo* are difficult to predict because this protein is predominantly expressed in the ovary, testis, and placenta. The maternal allele of PEG3 is inactive, and only the paternal allele is functional throughout the lifetime of mammals.^{39,40} Human PEG3 carries 12 zinc finger DNA-binding motifs and may play a role in transcription, cell proliferation, and p53-mediated apoptosis. Therefore, the level of PEG3 and other potential off-target transcripts expressed in the CNS should be carefully evaluated in a more relevant model *in vivo*.

DISCUSSION

Here, we demonstrated the efficacy and allele selectivity of CAG-targeting shRNAs in four models of polyQ diseases. These results are an important step toward the development of universal drugs for polyQ diseases with the use of RNAi tools and repeat-targeting strategy. One of the most important features/advantages of the proposed strategy, distinguishing it from the currently developed approaches, is the preferential silencing of mutant proteins. Both huntingtin and other polyQ proteins are widely expressed in the CNS and in the periphery. These proteins play important functions, such as axonal vesicular trafficking (HTT), transcription regulation (HTT, ATN-1, ATXN-7), deubiquitination (ATXN-3), and the stabilization of the cytoskeletal network (ATXN-7).[41–43] It has been demonstrated that the partial reduction of the wild-type huntingtin (~45%) in the striatum of adult rhesus monkeys treated with AAV2-shRNA is tolerated for at least 5 months without causing motor dysfunction or marked pathology.[44] However, we still do not know the consequences of the knockdown of normal polyQ proteins in patient brains that lasts for decades.[45] Therefore, the development of therapeutic approaches based on the selective inhibition of only mutant protein with leaving the wild-type intact for normal cellular function would

be a desirable option for clinical studies. It has been proved recently that such an idea is feasible. Zinc finger proteins (ZFPs) linked to the Krüppel-associated box (KRAB) transcriptional repression domain were used to directly bind mutant CAG repeats in the *HTT* gene and repress transcription in an allele-selective way.[20] Although repression was highly dependent on the length of the polyCAG tract, these ZFPs selectively repressed 100% of fully-penetrant mutant *HTT* alleles and preserved the normal *HTT* expression in more than 86% of patients.

Contrary to the principles of designing functional siRNAs,⁴⁶ our shRNAs consist of repetitive, GC-rich sequences that do not contain an A or U at the 5' end of the siRNA guide strand or AU richness at the 5' one-third region of the siRNA guide strand.⁴⁷ Nonetheless, all shRNAs are efficiently processed by Dicer, resulting in desired strand bias and siRNA guide strands mostly with an A or G substitution at position 8 from the 5' end. Both siRNA and miRNA identify and bind to their targets primarily through the seed region (2–7 nt), wherein base-pairing at nucleotide 8 can subsequently stabilize the duplex. The use of synthetic siRNA oligonucleotides has shown that the mismatch type and its position are crucial for the preferential silencing of the mutant proteins in the CAG-repeat targeting strategy.^{27,30,31} In our study, we demonstrated that allele selectivity depends mainly on the target (polyQ model) and shRNA concentration and less on the mismatch type (A versus G). However, in case of the HD model, we observed a significant difference between the selectivity of shA2R and shG2, which differ only in mismatch type. shA2R and shA2R1 induced strong allele selectivity in fibroblasts whereas shG2 silenced both alleles. Interestingly, shG2 was the most potent and selective reagent in the luciferase tests with the IC₅₀ of 10 ng for the 85CAG_Luc reporter. It may be explained by the small RNA NGS data showing that the number of reads from the G2 siRNA guide strand significantly outperforms those for other reagents (Figure S2).

The stability of the duplex formed between the guide siRNA strand and the target transcript is important for the miRNA-like translation inhibition mechanism. Therefore, we concluded that mismatched nucleotide at position 8 is important to ensure unstable interactions with normal tract and otherwise more stable interactions of multiple siRISC with expanded CAG repeats, which results in preferential silencing of mutant alleles. By comparing the allele selectivity of shRNAs in four polyQ models with similar lengths of the repeat tract, we demonstrated that other factors, such as localization of the CAG repeats within transcripts, flanking sequence composition, or target transcript to shRNA ratio, may further influence and modulate the efficacy and selectivity of silencing.

The shRNAs, which mimic natural pre-miRNAs, belong to the first generation of genetic RNAi triggers. Delivered to cells as viral vectors, these molecules allow for longer-lasting silencing effects compared to synthetic siRNAs or ASOs. There are a number of studies describing the successful use of shRNAs in the non-allele-selective silencing of polyQ genes.^{44,48–50} Designing shRNA in an allele-selective

strategy utilizing SNP or the difference in CAG tract length is more demanding. The activity of SNP-targeting shRNAs was demonstrated in cellular and animal models of HD,⁵¹ SCA3,^{52,53} and SCA7,⁵⁴ whereas CAG-targeting genetic vectors have not been extensively studied to date.^{30,36,37}

The high level of shRNA expression was shown to overload the endogenous miRNA biogenesis pathway⁴² and induced strong toxicity *in vivo*.^{55–57} Interestingly, not all shRNA vectors expressed under the strong U6 promoter were able to induce neurotoxicity in a mouse model of HD.⁵⁵ The toxic shRNAs generated higher levels of antisense siRNA strands compared with nontoxic shRNA. In this study, we used a weaker RNA Pol III promoter (H1), and the number of reads in NGS study corresponding to the A2R siRNA guide strand was similar to the highly abundant miRNAs, e.g., hsa-miR-221-3p and miR-191, and about two times lower than for miR-30a (Figure S4). The problem of the saturation of the miRNA biogenesis pathway by overexpression of shRNAs may also be overcome by the use of artificial miRNAs, the second generation of siRNA expressing vectors, which mimic the pri-miRNAs.^{55,58} However, the poorly controlled two-step processing of these molecules in cells further complicates the design of efficient and allele-selective molecules. In addition, direct comparison of shRNA- and artificial miRNA-based strategies revealed that shRNAs are more potent than the artificial miRNAs in mediating gene silencing *in vitro* and *in vivo*.⁵⁸

The idea of one drug toward all polyQ diseases is very attractive for the pharma industry and patients suffering from these rare diseases. As we demonstrated, each polyQ model exhibited a slightly different pattern of silencing after treatment with the same shRNAs; however, shA2R selectively silenced mutant proteins in all tested models. This molecule does not produce passenger strand, which might induce off-target effects, is selective toward target genes, and does not induce significant degradation of other complementary transcripts in human fibroblast. In summary, our study supports the idea of employing CAG-targeting strategy for the treatment of polyQ diseases. We demonstrated that preferential repression of mutant proteins by vector-based RNAi tools is feasible; however, further studies performed in more relevant cellular and animal models are necessary to get this strategy on road to clinics.

MATERIALS AND METHODS

Cell Culture

Fibroblasts from HD patients (GM04208, 21/44 CAG; GM04281, 17/68 CAG; GM09197, 21/151 CAG in the *HTT* gene), SCA3 patient (GM06153, 18/69 CAG in the *ATXN3* gene), SCA7 (GM03561, 8/62 CAG in the *ATXN7* gene), and DRPLA patient (GM13717, 16/68 in the *ATN1* gene) were obtained from the Coriell Cell Repositories (Camden, NJ, USA) and grown in minimal essential medium (Sigma-Aldrich, St. Louis, MO, USA) supplemented with 10% fetal bovine serum (FBS) (Sigma-Aldrich) and antibiotics (Sigma-Aldrich). HEK 293T cells were grown in Dulbecco's modified Eagle's medium (Sigma-Aldrich) supplemented with 8% (FBS) (Sigma-Aldrich), antibiotics (Sigma-Aldrich) and L-glutamine (Sigma-Aldrich). Mouse

striatal cell lines (STHdh), were purchased from the Coriell Cell Repositories and grown in a medium containing DMEM (GIBCO), FBS (Sigma-Aldrich), G418, and penicillin/streptomycin, with incubator conditions of 5% CO₂ and 33°C. All cell lines used in this study are listed in the Table S2.

Plasmids and Viral Vectors

The shRNA expression cassettes were generated from DNA oligonucleotides (Sigma-Aldrich, see sequences in Table S3). shRNAs, under an H1 polymerase III promoter, comprised a 22-bp stem and 10-nt miR-23 loop. We used shScr (scrambled) or shLuc, which targets the luciferase gene, as negative controls of silencing. Pairs of oligonucleotides were annealed and ligated into the pGreenPuro (System Biosciences, Palo Alto, CA, USA) expression plasmid and verified through sequencing. For lentivirus production, the plasmids were cotransfected with the packaging plasmids pPACKH1-GAG, pPACKH1-REV, and pVSVG (System Biosciences) in HEK 293TN cells. The medium was collected at days 2 and 3, and the viral supernatants were passed through 0.45- μ m filters and concentrated using PEGit Virus Precipitation Solution (System Biosciences). The lentiviral vectors were resuspended in Opti-MEM (GIBCO), and the virus titers (TU/mL) were determined through flow cytometry (Accuri C6, BD Biosciences) based on copGFP expression. The transduction of fibroblasts was performed at a MOI of 1 and/or 10 in the presence of polybrene (4 μ g/mL). Total RNA and protein were harvested at 7 days posttransduction.

Luciferase Assays

For luciferase assays, HEK 293T cells were seeded in a 24-well plate at a density of 10⁵ cells per well, in DMEM 1 day prior to transfection. Cells were cotransfected with shRNA expression constructs and luciferase reporters that contain both the firefly luciferase (FL) and Renilla luciferase (RL) genes (pmirGLO plasmid, Promega). Transfection was performed with Lipofectamine 2000 (Invitrogen, Thermo Fisher Scientific) according to the manufacturer's protocol. Exon 1 of the *HTT* gene with 85 or 16 CAG was fused upstream the FL gene. 48 h post-transfection, cells were harvested using Passive Lysis Buffer 1 \times (Promega) according to the manufacturer's instruction. Measurements of RL and FL activity were performed using Dual-Luciferase Reporter Assay (Promega). FL was normalized to RL expression. A scrambled construct (shScr) served as a negative control and was set at 1. The value of IC₅₀ was calculated as a concentration of shRNA needed to reach half-maximum silencing of mutant and/or normal allele. Allele selectivity ratio for each shRNA was calculated by dividing the IC₅₀ of the 16CAG_Luc reporter against the IC₅₀ of the 85CAG_Luc reporter.

Western Blotting

The western blot analysis for HTT protein was performed as previously described.³⁰ Briefly, 25 μ g of total protein was run on a Tris-acetate sodium dodecyl sulfate (SDS)-polyacrylamide gel (1.5 cm, 4% stacking gel/4.5 cm, 5% resolving gel, acrylamide:bis-acrylamide ratio of 49:1) in XT Tricine buffer (Bio-Rad, Hercules, CA, USA) at 135 V in an ice-water bath. After electrophoresis, the proteins were wet-transferred overnight to a nitrocellulose membrane (Sigma-Aldrich).

The primary and secondary antibodies were used in a PBS/0.1% Tween-20 buffer containing 5% nonfat milk. The immunoreaction was detected using Western Bright Quantum HRP Substrate (Advanta, Menlo Park, CA, USA). The protein bands were scanned directly from the membrane using a camera and quantified using Gel-Pro Analyzer (Media Cybernetics). Plectin was used as a reference protein.

For 25 µg of total protein SCA3, SCA7, and DRPLA electrophoresis, we used NuPAGE Tris-Acetate 3%–8% Protein Gels (Thermo Fisher Scientific) in NuPAGE Tris-Acetate SDS Running Buffer (Thermo Fisher Scientific). Next the proteins were wet-transferred to a nitrocellulose membrane (Sigma-Aldrich). The primary and secondary antibodies were used in a TBS/0.1% Tween-20 buffer containing 5% nonfat milk. The immunoreaction was detected as described below. Vinculin and GAPDH were used as reference proteins.

The resolution of 25 µg of total protein containing TBP (40 kDa), FOXP2 (80 kDa), RPL14 (25 kDa), MINK1 (150 kDa), PEG3 (179 kDa), SLC16A2 (60 kDa), and reference-GAPDH (40 kDa) proteins for simultaneous analysis on a single gel was performed on polyacrylamide gels (1.5 cm, 5% stacking gel/4.5 cm, 12% resolving gel, acrylamide:bis-acrylamide ratio of 29:1) in XT Tricine buffer (Bio-Rad, Hercules, CA, USA) at 120 V at room temperature. The proteins were wet-transferred to a nitrocellulose membrane (Sigma-Aldrich). The immunodetection steps were performed as described below using PBS/0.1% Tween-20 buffer containing 5% nonfat milk. A list of all antibodies used is provided in [Table S4](#).

RNA Isolation and Reverse-Transcription Polymerase Chain Reaction (PCR)

Total RNA was isolated from fibroblast cells using TRI Reagent (BioShop, Burlington, Canada) according to the manufacturer's instructions. The RNA concentration was measured using a NanoDrop spectrophotometer. A total of 500 ng of RNA was reverse transcribed at 55°C using Superscript III (Life Technologies) and random hexamer primers (Promega, Madison, WI, USA). The quality of the reverse transcription (RT) reaction was assessed through polymerase chain reaction (PCR) amplification of the GAPDH gene. Complementary DNA (cDNA) was used for qPCR using SsoAdvanced Universal SYBR R Green Supermix (Bio-Rad, Hercules, CA, USA) with denaturation at 95°C for 30 s followed by 40 cycles of denaturation at 95°C for 15 s and annealing at 60°C for 30 s. The melt curve protocol was subsequently performed for 5 s at 65°C, followed by 5 s increments at 0.5°C from 65°C to 95°C with specific primers on the CFX Connect Real-Time PCR Detection System (Bio-Rad). Data preprocessing and normalization were performed using Bio-Rad CFX Manager software (Bio-Rad). The quantitative real-time PCR primer sequences for HTT, PEG3, MINK1, and SLC16A2 are listed in the [Table S5](#).

Small RNA Next-Generation Sequencing and Data Analysis

Total RNA was isolated (TRI reagent) from HEK 293T cells at 24 h post transfection, and the RNA quality was analyzed with an Agilent 2100 Bioanalyzer (RNA Nano Chip, Agilent). Small RNA

sequencing was performed by CeGaT (Tubingen, Germany) using an Illumina HiSeq2500, 1 × 50 bp. Demultiplexing of the sequencing reads was performed with Illumina bcl2fastq (2.19). Adapters were trimmed with Skewer (version 0.2.2).⁵⁹ The reads in FASTQ format were then subjected to length filtering using a custom Python script, retaining only sequences longer than 15 nucleotides. Then, the reads were filtered for quality using the fastq_quality_filter tool from the FASTX-Toolkit package (http://hannonlab.cshl.edu/fastx_toolkit/). We applied $-q20$ and $-p9$ parameters, by which only reads with 95% of bases with Phred quality score ≥ 20 were retained. With quality filtering, between 5% and 6% of reads per sample were discarded. Then, we removed data redundancy with fastx_collapse from the same package. The reads were finally mapped against sequences of our shRNA constructs using Bowtie, with no mismatches allowed. Finally, with in-house Python script, the alignments were parsed and displayed in a graphical form for manual inspection.

Northern Blotting

Total RNA (35 µg) isolated from HEK 293T cells was resolved on denaturing polyacrylamide gels (12% PAA, 19:1 acrylamide/bis, and 7.5 M urea) in 0.5× TBE. The RNA was transferred to a GeneScreen Plus hybridization membrane (PerkinElmer) using semidry electroblotting (Sigma-Aldrich). The membrane was probed with a specific 21 nt DNA probe composed of CAG repeats and labeled with [γ 32P] ATP (5,000 Ci/mmol, Hartmann Analytics) using OptiKinase (USB) according to the manufacturer's instructions.⁶⁰ The hybridization was performed at 37°C overnight in a buffer containing 5 × SSC, 1% SDS, and 1× Denhardt's solution. The radioactive signals were quantified through phosphorimaging (Multi Gauge v3.0, Fujifilm).

Statistical Analysis

All experiments were repeated at least three times. The statistical significance of silencing was assessed using a one-sample t test, with an arbitrary value of 1 assigned to the cells treated with control shLuc. Selected data were compared using an unpaired t test. The two-tailed p values of < 0.05 were considered significant.

SUPPLEMENTAL INFORMATION

Supplemental Information can be found online at <https://doi.org/10.1016/j.omtn.2019.12.012>.

AUTHOR CONTRIBUTIONS

A.K.-Z., Y.O., and M.O. conducted the experiments. M.O. designed the experiments and wrote the paper.

CONFLICTS OF INTEREST

M.O. is a coinventor of US patents (US9970004 B2 and US10329566 B2) for the use of the RNAi method in the treatment of diseases induced by expansion of trinucleotide CAG repeats. M.O. is also an employee of Dystrogen Gene Therapies (part-time).

ACKNOWLEDGMENTS

The authors wish to thank Adam Ciesiolka for help in preparation of reporter constructs. This study was supported by research grants from the National Science Center, Poland (2015/18/E/NZ2/00678 and 2018/29/B/NZ1/00293), and funding for open access charge provided by the National Science Center (2015/18/E/NZ2/00678). The flow cytometry analyses were performed on Accuri C6 (BD Biosciences) in the Laboratory of Subcellular Structures Analysis at the Institute of Bioorganic Chemistry, PAS, in Poznan.

REFERENCES

- Ross, C.A. (2002). Polyglutamine pathogenesis: emergence of unifying mechanisms for Huntington's disease and related disorders. *Neuron* 35, 819–822.
- Fan, H.C., Ho, L.I., Chi, C.S., Chen, S.J., Peng, G.S., Chan, T.M., Lin, S.Z., and Harn, H.J. (2014). Polyglutamine (PolyQ) diseases: genetics to treatments. *Cell Transplant.* 23, 441–458.
- Sittler, A., Muriel, M.P., Marinello, M., Brice, A., den Dunnen, W., and Alves, S. (2018). Deregulation of autophagy in postmortem brains of Machado-Joseph disease patients. *Neuropathology* 38, 113–124.
- Seidel, K., Siswanto, S., Brunt, E.R., den Dunnen, W., Korf, H.W., and Rüb, U. (2012). Brain pathology of spinocerebellar ataxias. *Acta Neuropathol.* 124, 1–21.
- Tabrizi, S.J., Ghosh, R., and Leavitt, B.R. (2019). Huntingtin Lowering Strategies for Disease Modification in Huntington's Disease. *Neuron* 101, 801–819.
- Buijsen, R.A.M., Toonen, L.J.A., Gardiner, S.L., and van Roon-Mom, W.M.C. (2019). Genetics, Mechanisms, and Therapeutic Progress in Polyglutamine Spinocerebellar Ataxias. *Neurotherapeutics* 16, 263–286.
- Wild, E.J., and Tabrizi, S.J. (2017). Therapies targeting DNA and RNA in Huntington's disease. *Lancet Neurol.* 16, 837–847.
- Ashizawa, T., Öz, G., and Paulson, H.L. (2018). Spinocerebellar ataxias: prospects and challenges for therapy development. *Nat. Rev. Neurol.* 14, 590–605.
- Keiser, M.S., Kordasiewicz, H.B., and McBride, J.L. (2016). Gene suppression strategies for dominantly inherited neurodegenerative diseases: lessons from Huntington's disease and spinocerebellar ataxia. *Hum. Mol. Genet.* 25 (R1), R53–R64.
- Olejniczak, M., Urbanek, M.O., and Krzyzosiak, W.J. (2015). The role of the immune system in triplet repeat expansion diseases. *Mediators Inflamm.* 2015, 873860.
- Dickey, A.S., and La Spada, A.R. (2018). Therapy development in Huntington disease: From current strategies to emerging opportunities. *Am. J. Med. Genet. A.* 176, 842–861.
- Dickey, A.S., Pineda, V.V., Tsunemi, T., Liu, P.P., Miranda, H.C., Gilmore-Hall, S.K., Lomas, N., Sampat, K.R., Buttgerit, A., Torres, M.J., et al. (2016). PPAR- δ is repressed in Huntington's disease, is required for normal neuronal function and can be targeted therapeutically. *Nat. Med.* 22, 37–45.
- Esteves, S., Duarte-Silva, S., and Maciel, P. (2017). Discovery of Therapeutic Approaches for Polyglutamine Diseases: A Summary of Recent Efforts. *Med. Res. Rev.* 37, 860–906.
- Monteys, A.M., Ebanks, S.A., Keiser, M.S., and Davidson, B.L. (2017). CRISPR/Cas9 Editing of the Mutant Huntingtin Allele In Vitro and In Vivo. *Mol. Ther.* 25, 12–23.
- Dabrowska, M., Juzwa, W., Krzyzosiak, W.J., and Olejniczak, M. (2018). Precise Excision of the CAG Tract from the Huntingtin Gene by Cas9 Nickases. *Front. Neurosci.* 12, 75.
- Ouyang, S., Xie, Y., Xiong, Z., Yang, Y., Xian, Y., Ou, Z., Song, B., Chen, Y., Xie, Y., Li, H., and Sun, X. (2018). CRISPR/Cas9-Targeted Deletion of Polyglutamine in Spinocerebellar Ataxia Type 3-Derived Induced Pluripotent Stem Cells. *Stem Cells Dev.* 27, 756–770.
- Merienne, N., Vachey, G., de Longprez, L., Meunier, C., Zimmer, V., Perriard, G., Canales, M., Mathias, A., Herrgott, L., Beltraminelli, T., et al. (2017). The Self-Inactivating KamiCas9 System for the Editing of CNS Disease Genes. *Cell Rep.* 20, 2980–2991.
- Shin, J.W., Kim, K.H., Chao, M.J., Atwal, R.S., Gillis, T., MacDonald, M.E., Gusella, J.F., and Lee, J.M. (2016). Permanent inactivation of Huntington's disease mutation by personalized allele-specific CRISPR/Cas9. *Hum. Mol. Genet.* 25, 4566–4576.
- Tabrizi, S.J., Leavitt, B.R., Landwehrmeyer, G.B., Wild, E.J., Saft, C., Barker, R.A., Blair, N.F., Craufurd, D., Priller, J., Rickards, H., et al.; Phase 1–2a IONIS-HTTRx Study Site Teams (2019). Targeting huntingtin expression in patients with Huntington's disease. *N. Engl. J. Med.* 380, 2307–2316.
- Zeitler, B., Froelich, S., Marlen, K., Shivak, D.A., Yu, Q., Li, D., Pearl, J.R., Miller, J.C., Zhang, L., Paschon, D.E., et al. (2019). Allele-selective transcriptional repression of mutant HTT for the treatment of Huntington's disease. *Nat. Med.* 25, 1131–1142.
- Alterman, J.F., Godinho, B.M.D.C., Hassler, M.R., Ferguson, C.M., Echeverria, D., Sapp, E., Haraszti, R.A., Coles, A.H., Conroy, F., Miller, R., et al. (2019). A divalent siRNA chemical scaffold for potent and sustained modulation of gene expression throughout the central nervous system. *Nat. Biotechnol.* 37, 884–894.
- Hersch, S., Claassen, D., Edmondson, M., Wild, E., Guercioli, R., and Panzara, M. (2017). Multicenter, Randomized, Double-blind, Placebo-controlled Phase 1b/2a Studies of WVE-120101 and WVE-120102 in Patients with Huntington's Disease (P2.006). *Neurology* 2017, 88.
- Southwell, A.L., Skotte, N.H., Kordasiewicz, H.B., Østergaard, M.E., Watt, A.T., Carroll, J.B., Doty, C.N., Villanueva, E.B., Petoukhov, E., Vaid, K., et al. (2014). In vivo evaluation of candidate allele-specific mutant huntingtin gene silencing antisense oligonucleotides. *Mol. Ther.* 22, 2093–2106.
- Miller, V.M., Xia, H., Marrs, G.L., Gouvion, C.M., Lee, G., Davidson, B.L., and Paulson, H.L. (2003). Allele-specific silencing of dominant disease genes. *Proc. Natl. Acad. Sci. USA* 100, 7195–7200.
- Liu, J., Yu, D., Aiba, Y., Pendergraff, H., Swayze, E.E., Lima, W.F., Hu, J., Prakash, T.P., and Corey, D.R. (2013). ss-siRNAs allele selectively inhibit ataxin-3 expression: multiple mechanisms for an alternative gene silencing strategy. *Nucleic Acids Res.* 41, 9570–9583.
- Hu, J., Liu, J., Narayanannair, K.J., Lackey, J.G., Kuchimanchi, S., Rajeev, K.G., Manoharan, M., Swayze, E.E., Lima, W.F., Prakash, T.P., et al. (2014). Allele-selective inhibition of mutant atrophin-1 expression by duplex and single-stranded RNAs. *Biochemistry* 53, 4510–4518.
- Hu, J., Liu, J., and Corey, D.R. (2010). Allele-selective inhibition of huntingtin expression by switching to an miRNA-like RNAi mechanism. *Chem. Biol.* 17, 1183–1188.
- Hu, J., Liu, J., Yu, D., Aiba, Y., Lee, S., Pendergraff, H., Boubaker, J., Artates, J.W., Lagier-Tourenne, C., Lima, W.F., et al. (2014). Exploring the effect of sequence length and composition on allele-selective inhibition of human huntingtin expression by single-stranded silencing RNAs. *Nucleic Acid Ther.* 24, 199–209.
- Hu, J., Matsui, M., Gagnon, K.T., Schwartz, J.C., Gabillet, S., Arar, K., Wu, J., Bezprozvanny, I., and Corey, D.R. (2009). Allele-specific silencing of mutant huntingtin and ataxin-3 genes by targeting expanded CAG repeats in mRNAs. *Nat. Biotechnol.* 27, 478–484.
- Fischer, A., Olejniczak, M., Galka-Marciniak, P., Mykowska, A., and Krzyzosiak, W.J. (2013). Self-duplexing CUG repeats selectively inhibit mutant huntingtin expression. *Nucleic Acids Res.* 41, 10426–10437.
- Hu, J., Liu, J., Yu, D., Chu, Y., and Corey, D.R. (2012). Mechanism of allele-selective inhibition of huntingtin expression by duplex RNAs that target CAG repeats: function through the RNAi pathway. *Nucleic Acids Res.* 40, 11270–11280.
- Fischer, A., Wroblewska, J.P., Nowak, B.M., and Krzyzosiak, W.J. (2016). Mutant CAG repeats effectively targeted by RNA interference in SCA7 cells. *Genes (Basel)* 7, E132.
- Fischer, A., Ellison-Klimontowicz, M.E., and Krzyzosiak, W.J. (2016). Silencing of genes responsible for polyQ diseases using chemically modified single-stranded siRNAs. *Acta Biochim. Pol.* 63, 759–764.
- Fischer, A., Olejniczak, M., Switonski, P.M., Wroblewska, J.P., Wisniewska-Kruk, J., Mykowska, A., and Krzyzosiak, W.J. (2012). An evaluation of oligonucleotide-based therapeutic strategies for polyQ diseases. *BMC Mol. Biol.* 13, 6.
- Galka-Marciniak, P., Olejniczak, M., Starega-Roslan, J., Szczesniak, M.W., Makalowska, I., and Krzyzosiak, W.J. (2016). siRNA release from pri-miRNA scaffolds is controlled by the sequence and structure of RNA. *Biochim. Biophys. Acta* 1859, 639–649.

36. Monteys, A.M., Wilson, M.J., Boudreau, R.L., Spengler, R.M., and Davidson, B.L. (2015). Artificial miRNAs targeting mutant huntingtin show preferential silencing in vitro and in vivo. *Mol. Ther. Nucleic Acids* 4, e234.
37. Miniarikova, J., Zanella, I., Huseinovic, A., van der Zon, T., Hanemaaijer, E., Martier, R., Koornneef, A., Southwell, A.L., Hayden, M.R., van Deventer, S.J., et al. (2016). Design, Characterization, and Lead Selection of Therapeutic miRNAs Targeting Huntingtin for Development of Gene Therapy for Huntington's Disease. *Mol. Ther. Nucleic Acids* 5, e297.
38. Kozlowski, P., de Mezer, M., and Krzyzosiak, W.J. (2010). Trinucleotide repeats in human genome and exome. *Nucleic Acids Res.* 38, 4027–4039.
39. Hiby, S.E., Lough, M., Keverne, E.B., Surani, M.A., Loke, Y.W., and King, A. (2001). Paternal monoallelic expression of PEG3 in the human placenta. *Hum. Mol. Genet.* 10, 1093–1100.
40. Jiang, X., Yu, Y., Yang, H.W., Agar, N.Y., Frado, L., and Johnson, M.D. (2010). The imprinted gene PEG3 inhibits Wnt signaling and regulates glioma growth. *J. Biol. Chem.* 285, 8472–8480.
41. Paulson, H.L., Shakkottai, V.G., Clark, H.B., and Orr, H.T. (2017). Polyglutamine spinocerebellar ataxias - from genes to potential treatments. *Nat. Rev. Neurosci.* 18, 613–626.
42. Saudou, F., and Humbert, S. (2016). The Biology of Huntingtin. *Neuron* 89, 910–926.
43. Wood, J.D., Nucifora, F.C., Jr., Duan, K., Zhang, C., Wang, J., Kim, Y., Schilling, G., Sacchi, N., Liu, J.M., and Ross, C.A. (2000). Atrophin-1, the dentato-rubral and pallido-luysian atrophy gene product, interacts with ETO/MTG8 in the nuclear matrix and represses transcription. *J. Cell Biol.* 150, 939–948.
44. Grondin, R., Kaytor, M.D., Ai, Y., Nelson, P.T., Thakker, D.R., Heisel, J., Weatherspoon, M.R., Blum, J.L., Burrell, E.N., Zhang, Z., and Kaemmerer, W.F. (2012). Six-month partial suppression of Huntingtin is well tolerated in the adult rhesus striatum. *Brain* 135, 1197–1209.
45. Kaemmerer, W.F., and Grondin, R.C. (2019). The effects of huntingtin-lowering: what do we know so far? *Degener. Neurol. Neuromuscul. Dis.* 9, 3–17.
46. Naito, Y., and Ui-Tei, K. (2012). siRNA design software for a target gene-specific RNA interference. *Front. Genet.* 3, 102.
47. Kamola, P.J., Nakano, Y., Takahashi, T., Wilson, P.A., and Ui-Tei, K. (2015). The siRNA Non-seed Region and Its Target Sequences Are Auxiliary Determinants of Off-Target Effects. *PLoS Comput. Biol.* 11, e1004656.
48. Harper, S.Q., Staber, P.D., He, X., Eliason, S.L., Martins, I.H., Mao, Q., Yang, L., Kotin, R.M., Paulson, H.L., and Davidson, B.L. (2005). RNA interference improves motor and neuropathological abnormalities in a Huntington's disease mouse model. *Proc. Natl. Acad. Sci. USA* 102, 5820–5825.
49. Rodriguez-Lebron, E., Denovan-Wright, E.M., Nash, K., Lewin, A.S., and Mandel, R.J. (2005). Intrastratial rAAV-mediated delivery of anti-huntingtin shRNAs induces partial reversal of disease progression in R6/1 Huntington's disease transgenic mice. *Mol. Ther.* 12, 618–633.
50. Drouet, V., Perrin, V., Hassig, R., Dufour, N., Auregan, G., Alves, S., Bonvento, G., Brouillet, E., Luthi-Carter, R., Hantraye, P., and Déglon, N. (2009). Sustained effects of nonallele-specific Huntingtin silencing. *Ann. Neurol.* 65, 276–285.
51. Drouet, V., Ruiz, M., Zala, D., Feyeux, M., Auregan, G., Cambon, K., Troquier, L., Carpentier, J., Aubert, S., Merienne, N., et al. (2014). Allele-specific silencing of mutant huntingtin in rodent brain and human stem cells. *PLoS ONE* 9, e99341.
52. Nóbrega, C., Nascimento-Ferreira, I., Onofre, I., Albuquerque, D., Hirai, H., Déglon, N., and de Almeida, L.P. (2013). Silencing mutant ataxin-3 rescues motor deficits and neuropathology in Machado-Joseph disease transgenic mice. *PLoS ONE* 8, e52396.
53. Alves, S., Nascimento-Ferreira, I., Auregan, G., Hassig, R., Dufour, N., Brouillet, E., Pedroso de Lima, M.C., Hantraye, P., Pereira de Almeida, L., and Déglon, N. (2008). Allele-specific RNA silencing of mutant ataxin-3 mediates neuroprotection in a rat model of Machado-Joseph disease. *PLoS ONE* 3, e3341.
54. Scholefield, J., Watson, L., Smith, D., Greenberg, J., and Wood, M.J.A. (2014). Allele-specific silencing of mutant Ataxin-7 in SCA7 patient-derived fibroblasts. *Eur. J. Hum. Genet.* 22, 1369–1375.
55. McBride, J.L., Boudreau, R.L., Harper, S.Q., Staber, P.D., Monteys, A.M., Martins, I., Gilmore, B.L., Burstein, H., Peluso, R.W., Polisky, B., et al. (2008). Artificial miRNAs mitigate shRNA-mediated toxicity in the brain: implications for the therapeutic development of RNAi. *Proc. Natl. Acad. Sci. USA* 105, 5868–5873.
56. Grimm, D., Streetz, K.L., Jopling, C.L., Storm, T.A., Pandey, K., Davis, C.R., Marion, P., Salazar, F., and Kay, M.A. (2006). Fatality in mice due to oversaturation of cellular microRNA/short hairpin RNA pathways. *Nature* 441, 537–541.
57. Martin, J.N., Wolken, N., Brown, T., Dauer, W.T., Ehrlich, M.E., and Gonzalez-Alegre, P. (2011). Lethal toxicity caused by expression of shRNA in the mouse striatum: implications for therapeutic design. *Gene Ther.* 18, 666–673.
58. Boudreau, R.L., Monteys, A.M., and Davidson, B.L. (2008). Minimizing variables among hairpin-based RNAi vectors reveals the potency of shRNAs. *RNA* 14, 1834–1844.
59. Jiang, H., Lei, R., Ding, S.W., and Zhu, S. (2014). Skewer: a fast and accurate adapter trimmer for next-generation sequencing paired-end reads. *BMC Bioinformatics* 15, 182.
60. Koscianska, E., Starega-Roslan, J., Sznajder, L.J., Olejniczak, M., Galka-Marciniak, P., and Krzyzosiak, W.J. (2011). Northern blotting analysis of microRNAs, their precursors and RNA interference triggers. *BMC Mol. Biol.* 12, 14.

OMTN, Volume 19

Supplemental Information

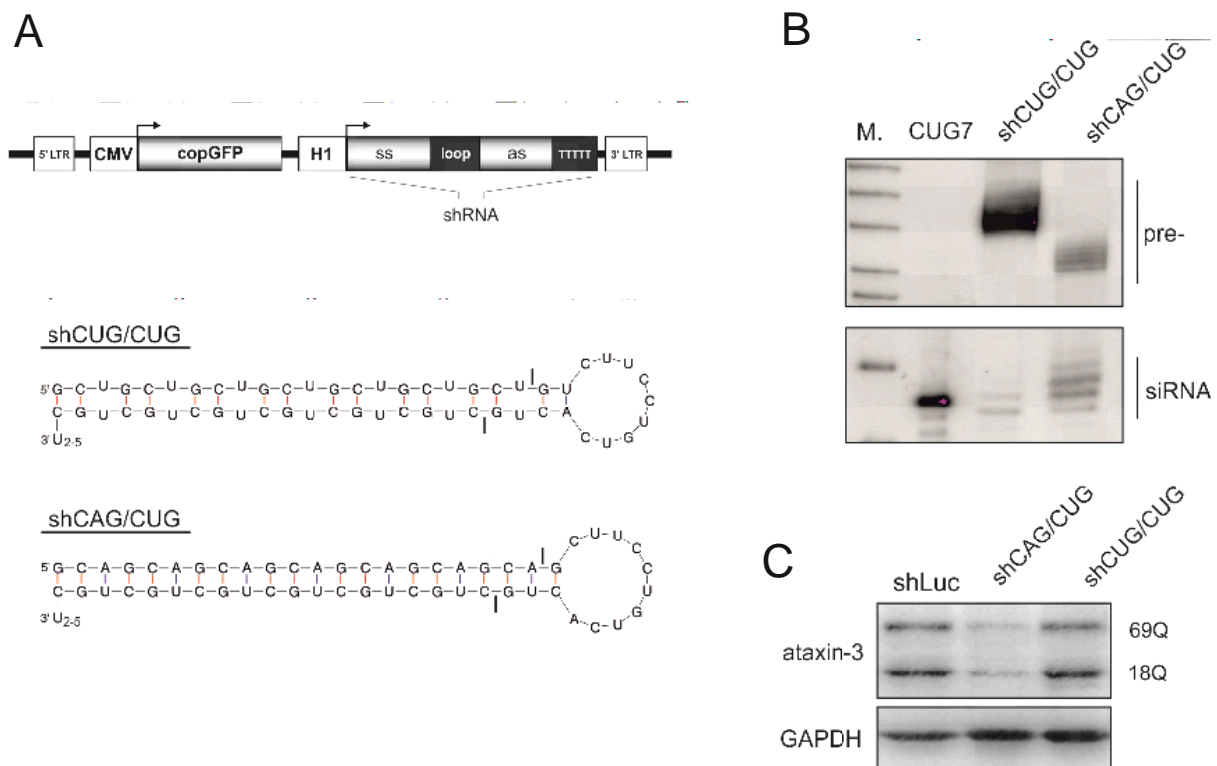
Universal RNAi Triggers for the Specific Inhibition of Mutant Huntingtin, Atrophin-1, Ataxin-3, and Ataxin-7 Expression

Anna Kotowska-Zimmer, Yuliya Ostrovska, and Marta Olejniczak

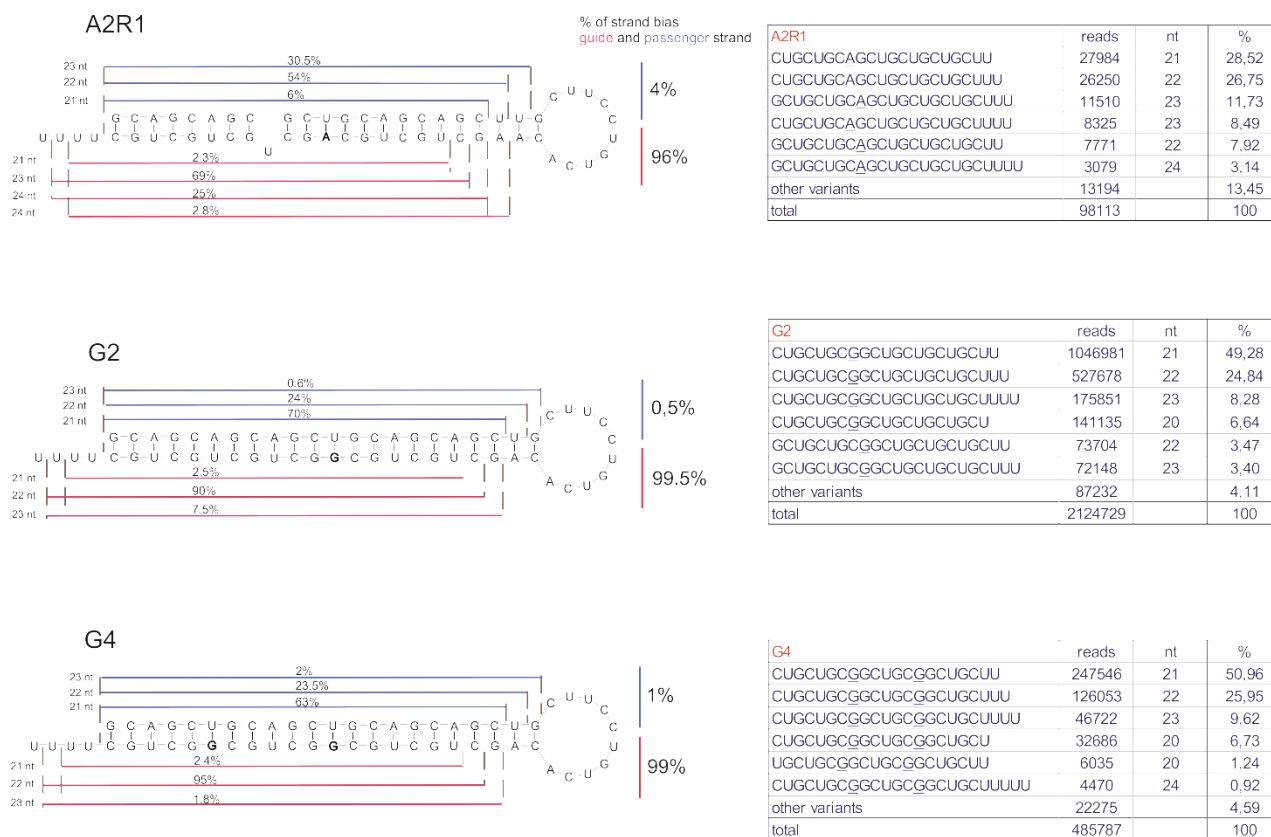
SUPPLEMENTAL INFORMATION

Universal RNAi triggers for the specific inhibition of mutant huntingtin, atrophin-1, ataxin-3 and ataxin-7 expression.

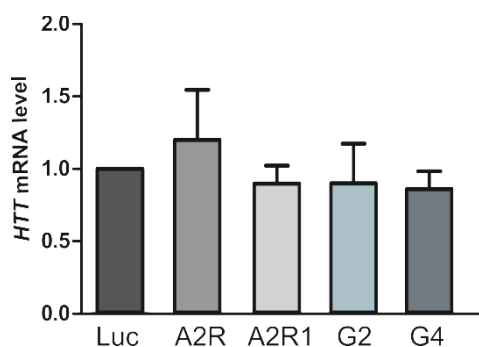
Anna Kotowska-Zimmer, Yuliya Ostrovska and Marta Olejniczak



Supplemental Figure S1. Cellular processing and activity of CUG/CUG and CAG/CUG shRNAs. (A) Lentiviral vector containing copGFP and shRNA expression cassettes and schematic structure of CUG/CUG and CAG/CUG shRNA structures. (B) High-resolution northern blot analysis of shRNA processing in HEK293T cells; M denotes RNA low molecular weight marker (USB), pre- denotes unprocessed shRNA. As a control of RNA migration and probe specificity synthetic 21 nt oligonucleotide (CUG7) was used. (C) Western blot analysis of ataxin-3 level in SCA3 fibroblasts (18/69Q, GM06153) transduced with LV - shRNAs. shLuc, negative control, shRNA targeting Luc gene. GAPDH was used as a reference protein.



Supplemental Figure S2. Cellular processing of shA2R1, shG2 and shG4. Next-generation sequencing analysis of the shRNA processing pattern in HEK293T cells. The guide strand is indicated in red and the passenger strand is indicated in blue. Cleavage sites are presented on both stands corresponding to the length of released siRNA variants (content and length are noted on the left site). The table presents the results of total quantity, length and percentage content of the sequence composition of released strands after NGS analysis.



Supplemental Figure S3. RT-qPCR analysis of HTT transcript levels in HD patient-derived fibroblasts (cell line GM04281, 17/68Q) at 7 days posttransduction with LV in MOI of 10, containing A2R, A2R1, G2 and G4 expression cassettes. Signal intensities were normalized to beta-actin protein level and compared using a one-sample t-test. The shLuc (Luc) construct was used as a control reference. The graph bars represent the mean value of transcript levels \pm SEM. All experiments were repeated at least three times.

	hsa-miR-221-3p	nt	No. of reads
1	AGCUACAUUGUCUGCUGGGUUUC	23	59672
2	AGCUACAUUGUCUGCUGGGUUU	22	36665
3	AGCUACAUUGUCUGCUGGGUUUCA	24	15677
4	AGCUACAUUGUCUGCUGGGUU	21	4500
5	AGCUACAUUGUCUGCUGGGU	20	962
6	AGCUACAUUGUCUGCUGGGUUUCAG	25	129
7	AGCUACAUUGUCUGCUGGG	19	120
	Total		117725

	hsa-miR-191-5p	nt	No. of reads
1	CAACGGAAUCCCAAAGCAGCU	22	74258
2	CAACGGAAUCCCAAAGCAGCUG	23	44852
3	CAACGGAAUCCCAAAGCAGCUGU	24	10035
4	CAACGGAAUCCCAAAGCAGC	21	4263
5	CAACGGAAUCCCAAAGCAG	20	846
6	CAACGGAAUCCCAAAGCA	19	123
	Total		134377

	hsa-miR-30a-5p	nt	No. of reads
1	UGUAAACAUCUCGACUGGAAGCU	24	181361
2	UGUAAACAUCUCGACUGGAAGC	23	33722
3	UGUAAACAUCUCGACUGGAAG	22	8986
4	UGUAAACAUCUCGACUGGAA	21	2925
5	UGUAAACAUCUCGACUGGA	20	219
6	UGUAAACAUCUCGACUGG	19	120
	Total		227333

	hsa-miR-26a-5p	nt	No. of reads
1	TTCAAGTAATCCAGGATAGGCT	22	287983
2	TTCAAGTAATCCAGGATAGGC	21	18487
3	TTCAAGTAATCCAGGATAGG	20	4915
4	TTCAAGTAATCCAGGATAGGCTG	23	668
5	TTCAAGTAATCCAGGATAGGCTGT	24	438
6	TTCAAGTAATCCAGGATAG	19	265
	Total		312756

Supplemental Figure S4. Endogenous miRNA levels in HEK293T cells treated with shA2R. The tables present the results of total quantity reads, length (nt) and the sequence composition of human miR-191-5p, miR-30a-5p, miR-221-3p and miR-26a-5p variants after small RNA NGS analysis. The sequence of the miRNA variant from the miRBase (<http://www.mirbase.org/>) is marked in bold.

Supplemental Table S1. Results of bioinformatics analysis of mRNA targets for the shA2R

	Gene name	Description	Transcript ID	Length [nt]	Localization		Expression*	
					Chr	Cytoband	Brain	Skin
1	<i>MYT1</i>	Myelin transcription factor 1	ENST00000650655.1	21	20	q13.33	low	low
2	<i>CCDC177</i>	Coiled-coil domain containing 177	ENST00000599174.3	21	14	q24.1	low	n/a
3	<i>PEG3</i>	Paternally expressed 3	ENST00000326441.15	21	19	q13.43	medium	low
4	<i>SLC16A2</i>	Solute carrier family 16 member 2	ENST00000587091.6	21	X	q13.2	medium	medium
5	<i>MINK1</i>	Misshapen-like kinase 1	ENST00000355280.11	21	17	p13.2	low	medium
6	Uncharacterized gene	AL121581.1-201	ENST00000625658.1	20	20	n/a	n/a	n/a
7	<i>TOX3</i>	TOX high mobility group box family member 3	ENST00000219746.14	20	16	q12.1	medium	n/d
8	<i>BSN</i>	Bassoon presynaptic cytomatrix protein	ENST00000296452.5	20	3	p21.31	high	n/d
9	<i>SOGA3</i>	SOGA family member 3	ENST00000525778.5	20	6	q22.33	medium	low
10	<i>BRD4</i>	Bromodomain containing 4	ENST00000263377.6	20	19	p13.12	medium	low
11	Uncharacterized gene	AL096711.2-201	ENST00000481848.6	20	6	n/a	n/a	n/a
12	<i>IGF2R</i>	Insulin-like growth factor 2 receptor	ENST00000356956.5	20	6	n/a	low	medium
13	<i>SLFNL1</i>	Schlafen-like protein	ENST00000359345.5	19	1	p34.2	low	low
14	<i>Z83838.1</i>	Ribosomal protein L6 (RPL6) pseudogene	ENST00000431036.1	18	22	n/a	n/a	n/a
15	<i>PBX2</i>	PBX homeobox 2	ENST00000453487.2	18	6	p21.32	low	low
16	<i>PTBP2</i>	Polypyrimidine tract binding protein 2	ENST00000609116.5	18	1	p21.3	low	low
17	<i>PIP4P2</i>	Phosphatidylinositol-4,5-bisphosphate 4-phosphatase 2	ENST00000285419.8	18	8	n/a	n/a	n/a
18	<i>KLHL42</i>	Kelch-like family member 42	ENST00000381271.7	18	12	p11.22	medium	medium
19	<i>PRPF40A</i>	Pre-mRNA processing factor 40 homolog A	ENST00000410080.6	18	2	q23.3	medium	medium
20	<i>ASXL3</i>	Additional sex combs-like 3, transcriptional regulator	ENST00000269197.12	18	18	q12.1	low	n/a

Blast (<https://blast.ncbi.nlm.nih.gov>) algorithm was used in search for complementary sequences for the A2R guide strand (100% complementarity to >17 nt) in human transcripts (refseq_rna). Analysis parameters: Organism: Homo sapiens (taxid:9606); Optimize for: Highly similar sequences (megablast); word size=16; Scoring parameter: Match/Mismatch: 4/-5. The results were confirmed by Ensembl Blast (<https://www.ensembl.org/>). *An information source: ww.proteinatlas.org.
n/a – not analyzed; n/d – not detected

Supplemental Table S2. Cell lines used in this study.

Cell line number	Cell type	Disease model	Organism	Affected gene	CAG repeats length
GM04208	fibroblast	HD	human	<i>HTT</i>	21/44
GM04281	fibroblast	HD	human	<i>HTT</i>	17/68
GM09197	fibroblast	HD	human	<i>HTT</i>	21/151
GM06153	fibroblast	SCA3	human	<i>ATXN3</i>	18/69
GM03561	fibroblast	SCA7	human	<i>ATXN7</i>	8/62
GM013717	fibroblast	DRPLA	human	<i>ATN1</i>	16/68
CH00096 (STHdh)	neuronally-derived precursor	HD	mouse	<i>HTT</i>	7/111

Supplemental Table S3. DNA oligonucleotides used for the generation of shRNA constructs: Luc, A2R, A2R1, G2, G4, CUG/CUG, CAG/CUG and Scr.

Name	Sequence 5'-3'
shLuc sense	GATCCGCTACTTGATCTGCGGCTTACCTGACCCAGTAAGCCGCAGATCAAGTAGCTTTTTG
shLuc antisense	AATTCAAAAAGCTACTTGATCTGCGGCTTACTGGGTCAGGGTAAGCCGCAGATCAAGTAGCG
shA2R sense	GATCCGCAGCAGCAGCTGCAGCAGCTGCTTCTGTACAGCTGCTGCAGCTGCTGCTGCTTTTTG
shA2R antisense	AATTCAAAAAGCAGCAGCAGCTGCAGCAGCTGTGACAGGAAGCAGCTGCTGCAGCTGCTGCTGCG
shA2R1 sense	GATCCGCAGCAGCGCTGCAGCAGCTTCTTCTGTACAAGCTGCTGCAGCTGCTGCTGCTTTTTG
shA2R1 antisense	AATTCAAAAAGCAGCAGCAGCTGCAGCAGCTTGTGACAGGAAGCAAGCTGCTGCAGCGCTGCTGCG
shG2 sense	GATCCGCAGCAGCAGCTGCAGCAGCTGCTTCTGTACAGCTGCTGCGGCTGCTGCTGCTTTTTG
shG2 antisense	AATTCAAAAAGCAGCAGCAGCCGCAGCAGCTGTGACAGGAAGCAGCTGCTGCAGCTGCTGCTGCG
shG4 sense	GATCCGCAGCAGCAGCTGCAGCAGCTGCTTCTGTACAGCGGCTGCGGCTGCTGCTGCTTTTTG
shG4 antisense	AATTCAAAAAGCAGCAGCAGCCGCAGCCGCTGTGACAGGAAGCAGCTGCTGCAGCTGCTGCTGCG
shCUG/CUG sense	GATCCGCTGCTGCTGCTGCTGCTGTCTTCTGTCACTGCTGCTGCTGCTGCTGCTGCTTTTTG
shCUG/CUG antisense	AATTCAAAAAGCAGCAGCAGCAGCAGCAGCAGTGTGACAGGAAGCAGCAGCAGCAGCAGCAGCAGCG
shCAG/CUG sense	GATCCGCAGCAGCAGCAGCAGCAGCAGCTTCTGTCACTGCTGCTGCTGCTGCTGCTGCTTTTTG
shCAG/CUG antisense	AATTCAAAAAGCAGCAGCAGCAGCAGCAGCAGTGTGACAGGAAGCTGCTGCTGCTGCTGCTGCTGCG
shScr sense	GATCCGGCCAGCCGTAGCCGAGTGAACCTTCTGTCACTCGGCTACGGCTGGGCCTTTTTG
shScr antisense	AATTCAAAAAGGCCAGCCGTAGCCGAGTGAATGACAGGAAGTTCCTCGGCTACGGCTGGGCCCG

Supplemental Table S4. Antibodies for the Western blot analysis.

Protein	Molecular weight [kDa]	Dilution	Supplier	Secondary antibody
ATXN3 (ataxin-3)	45	1:1000 in milk 5% TBS-T	Milipore (MAB5360)	R-POX Jackson, ImmunoResearch 1:1000, milk 5% TBS-T
ATXN7 (ataxin-7)	95	1:1000 in milk 5% TBS-T	Thermo Scientific (PA1-749)	R-POX Jackson, ImmunoResearch 1:1000, milk 5% TBS-T
ATN1 (atrophin-1)	190	1:1000 in BSA 5% TBS-T	Sigma-Aldrich (R30744)	R-POX Jackson ImmunoResearch, 1:1000, milk 5% TBS-T
HTT (huntingtin, N-terminal)	350	1:1000 in milk 5% PBS-T	Sigma-Aldrich (H7540)	M-POX Sigma-Aldrich, 1:1000, milk 5% PBS-T
FOXP2	70	1:1000 in milk 5% PBS-T	Santa Cruz Biotechnology (sc-517261)	M-POX Sigma-Aldrich, 1:1000, milk 5% PBS-T
RPL14	23	1:500 in milk 5% PBS-T	Santa Cruz Biotechnology (sc-100826)	M-POX Sigma-Aldrich, 1:1000, milk 5% PBS-T
TBP	36	1:1000 in milk 5% PBS-T	Santa Cruz Biotechnology (sc-421)	M-POX Sigma-Aldrich, 1:1000, milk 5% PBS-T
MINK1	150	1:1000 in milk 5% PBS-T	Proteintech (13137-1-AP)	R-POX Jackson ImmunoResearch, 1:1000, milk 5% PBS-T
SLC16A2	60	1:1000 in milk 5% PBS-T	Proteintech (20676-1-AP)	R-POX Jackson ImmunoResearch, 1:1000, milk 5% PBS-T
PEG-3	179	1:1000 in milk 5% PBS-T	Abcam (ab99252)	R-POX Jackson ImmunoResearch, 1:1000, milk 5% PBS-T
GAPDH	40	1:20000 in milk 5% PBS-T	Millipore (MAB 373)	M-POX Sigma-Aldrich, 1:1000, milk 5% PBS-T
Vinculin	125	1:1000 in BSA 5% TBS-T	Cell Signaling Technology (4650S)	R-POX Jackson ImmunoResearch, 1:1000, milk 5% TBS-T
Plectin	500	1:1000 in milk 5% PBS-T	Abcam (ab83497)	R-POX Jackson ImmunoResearch, 1:1000, milk 5% TBS-T

Supplemental Table S5. DNA oligonucleotides used as a PCR primers for RT-qPCR.

Name	Sequence 5'-3'
ATN1 F	TGCTATCCATGCAGCCTCTG
ATN1 R	AGCAAAGAGCTGGTGACGAA
ATXN3 F	GGAAGAGACGAGAAGCCTAC
ATXN3 R	TCACCTAGATCACTCCCAAGT
ATXN7 F	AGGTGTTCTTAGCGCATCCT
ATXN7 R	AGTGTGCCATCCATTTTCGG
HTT F	GTGCTGAGCGGCGCCGCGAGTC
HTT R	GGACTTGAGGGACTCGAAGGC
β -ACTIN F	TGAGAGGGAAATCGTGCCTG
β -ACTIN R	TGCTTGCTGATCCACATCTGC
GAPDH F	GAAGGTGAAGGTCGGAGTC
GAPDH R	GAAGATGGTGATGGGATTTC
MINK 1 F	ACTCTACGCCGGGAGTTTCT
MINK 1 R	GCAGCAGGTGTTTGATGTGT
PEG3 F	TGCAAGGATTGTGGTAAGTCC
PEG3 R	TTGTGGAACATGGACATTGG
SLC16A2 F	CTGCAGCAGCAGAAACAAGT
SLC16A2 R	CTGTTCTGGTCTGCCTCCT

Artificial miRNAs as therapeutic tools: Challenges and opportunities

Anna Kotowska-Zimmer | Marianna Pewinska  | Marta Olejniczak 

Department of Genome Engineering,
Institute of Bioorganic Chemistry PAS,
Poznan, Poland

Correspondence

Marta Olejniczak, Department of Genome
Engineering, Institute of Bioorganic
Chemistry PAS, Noskowskiego 12/14,
Poznan 61-704, Poland.
Email: marta.olejniczak@ibch.poznan.pl

Funding information

National Science Centre in Poland, Grant/
Award Numbers: 2015/18/E/NZ2/00678,
2019/35/O/NZ1/03535

Abstract

RNA interference (RNAi) technology has been used for almost two decades to study gene functions and in therapeutic approaches. It uses cellular machinery and small, designed RNAs in the form of synthetic small interfering RNAs (siRNAs) or vector-based short hairpin RNAs (shRNAs), and artificial miRNAs (amiRNAs) to inhibit a gene of interest. Artificial miRNAs, known also as miRNA mimics, shRNA-miRs, or pri-miRNA-like shRNAs have the most complex structures and undergo two-step processing in cells to form mature siRNAs, which are RNAi effectors. AmiRNAs are composed of a target-specific siRNA insert and scaffold based on a natural primary miRNA (pri-miRNA). siRNAs serve as a guide to search for complementary sequences in transcripts, whereas pri-miRNA scaffolds ensure proper processing and transport. The dynamics of siRNA maturation and siRNA levels in the cell resemble those of endogenous miRNAs; therefore amiRNAs are safer than other RNAi triggers. Delivered as viral vectors and expressed under tissue-specific polymerase II (Pol II) promoters, amiRNAs provide long-lasting silencing and expression in selected tissues. Therefore, amiRNAs are useful therapeutic tools for a broad spectrum of human diseases, including neurodegenerative diseases, cancers and viral infections. Recent reports on the role of sequence and structure in pri-miRNA processing may contribute to the improvement of the amiRNA tools. In addition, the success of a recently initiated clinical trial for Huntington's disease could pave the way for other amiRNA-based therapies, if proven effective and safe.

This article is categorized under:

RNA Processing > Processing of Small RNAs

Regulatory RNAs/RNAi/Riboswitches > RNAi: Mechanisms of Action

RNA in Disease and Development > RNA in Disease

KEYWORDS

artificial miRNA, gene therapy, miRNA, RNA interference, shRNA

1 | INTRODUCTION

RNA interference (RNAi) is a process in which small interfering RNAs (siRNAs) or endogenous microRNAs (miRNAs) with protein partners regulate cellular gene expression at the posttranscriptional level by the degradation of

complementary transcripts and/or inhibition of translation (Bartel, 2004; Elbashir et al., 2001; Zeng et al., 2003). This natural phenomenon has been used by researchers to develop technology allowing the expression of any gene of interest to be inhibited by small, designed RNAs (McManus et al., 2002; Silva et al., 2005). RNAi technology employs three kinds of tools: synthetic siRNAs, vector-based short hairpin RNAs (shRNAs), and artificial miRNAs (amiRNAs), which are processed in cells by miRNA biogenesis machinery to form mature siRNAs (Rao et al., 2009; Silva et al., 2005; Figure 1). Vector-based RNAi triggers vary in many ways. RNA polymerase III (Pol III)-driven shRNAs resemble endogenous miRNA precursors (pre-miRNAs), which have a characteristic stem-loop structure (Ma et al., 2014; Sheng et al., 2020). A target-specific siRNA sequence forms the stem of an ~60 nucleotide (nt) shRNA and is released as a result of single-step processing in the cytoplasm by the RNase DICER. Second-generation shRNAs (Silva et al., 2005), known as amiRNAs, miRNA mimics (Rossi, 2008), shRNA-miRs (Silva et al., 2005), or pri-miRNA-like shRNAs (Ros & Gu, 2016) enter the miRNA biogenesis pathway at an early stage and undergo two-step processing by the RNases DROSHA and DICER, similar to most endogenous mammalian miRNA transcripts (pri-miRNAs) (McBride et al., 2008; Zeng et al., 2002). In contrast to shRNAs, amiRNAs contain an siRNA sequence embedded within a complex endogenous pri-miRNA backbone (McManus et al., 2002; Zeng et al., 2002) transcribed by RNA polymerase II (Pol II) promoters. Thus, the levels of siRNAs, which are tightly regulated by endogenous machinery, are relatively low, and amiRNAs are considered safe and efficient RNAi triggers (R. Boudreau, et al., 2009; McBride et al., 2008). Delivered to cells as viral vectors, shRNAs and amiRNAs allow for prolonged silencing effects compared to the silencing effects of synthetic siRNAs or antisense oligonucleotides (ASOs) (Sliva & Schnierle, 2010; Van den Haute et al., 2003). In addition, amiRNAs can be precisely expressed in a tissue of interest by using tissue-specific RNA Pol II promoters and viral vectors with specific serotypes. This feature is of great importance in clinical applications, as it reduces the possibility of nonspecific effects (Evers et al., 2018; Pfister et al., 2017). Nevertheless, due to their simpler design and the more predictable results of their cellular processing, shRNAs are still the predominant molecules used for RNAi in mammalian cells (Moore et al., 2010). In contrast, plant research has readily taken advantage of amiRNAs to study gene functions, crop improvement and as antiviral agents (Carbonell & Daròs, 2019; Schwab et al., 2006).

Studies on miRNA biogenesis have provided the groundwork for amiRNA design, and recent years have brought many new reports on the role of sequence and structure in pri-miRNA processing (Fang & Bartel, 2015; Jin et al., 2020; Kwon et al., 2019; Liu et al., 2018; Wang et al., 2020). This may contribute to the improvement of amiRNA tools, which



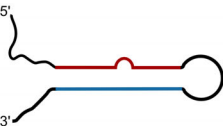
RNAi trigger	siRNA	shRNA	amiRNA
			
endogenous equivalent	miRNA	pre-miRNA	pri-miRNA
length	~21 nt	~60 nt	~60 nt + flanking sequences ~80-250 nt
processing	no	DICER	DROSHA and DICER
pairing	perfect complementarity	perfect complementarity	possible loops and bulges
expression	transient	transient/stable	transient/stable
source	synthetic	expression vectors, Pol III promoters	expression vectors, Pol II promoters
other	<ul style="list-style-type: none"> frequent dosing chemical modifications (↑stability, ↓toxicity) 	<ul style="list-style-type: none"> single administration saturation of the miRNA biogenesis machinery 	<ul style="list-style-type: none"> single administration low toxicity

FIGURE 1 Comparison of synthetic (siRNA) and vector-based (shRNA and amiRNA) RNAi triggers

have already been applied in biomedical research (Brendel et al., 2020; Spronck et al., 2019) and show promise in the clinic (NCT03282656, 2020; NCT04120493, 2020). Despite the problem of rational amiRNA design, RNAi technology has to manage other challenges of gene therapy, such as delivery and safety. To date, amiRNAs have been successfully used in preclinical studies for various disorders and the success of a recently initiated clinical trial for Huntington's disease (HD) could pave the way for other amiRNA-based therapies, if proven effective and safe.

Here, we present a comprehensive and updated overview of miRNA biogenesis for the design of efficient and specific amiRNAs. We have collected and summarized studies on the use of amiRNAs in the treatment of neurodegenerative diseases, cancers, viral infections, and other diseases. Moreover, we discuss the current limitations and challenges that RNAi technology must overcome before successful application of amiRNAs in the clinic.

2 | MiRNA BIOGENESIS

MiRNA biogenesis is a complex process that starts with the transcription of miRNA genes mostly by RNA Pol II, generating pri-miRNAs (Figure 2; Cai et al., 2004; Lee et al., 2002). Approximately half of all currently identified miRNAs are encoded in the introns of coding or noncoding genes and less frequently in the exons (intragenic). In addition, there is a group of intergenic miRNAs with their own promoters that are regulated independently of a host gene. MiRNA genes can be monocistronic and code only one miRNA or polycistronic and code a miRNA cluster. Long pri-miRNAs harbor a local stem-loop structure, which undergoes processing in a canonical or noncanonical pathway to release a mature ~22 nt miRNA (Bartel, 2018).

2.1 | Canonical miRNA biogenesis

The first step of the canonical pathway is catalyzed by the Microprocessor complex, which is composed of the nuclear RNase III enzyme DROSHA and two copies of the double-stranded RNA (dsRNA)-binding protein DiGeorge Syndrome Critical Region 8 (DGCR8) (Figure 2(b)). DROSHA contains two highly conserved RNase III domains, RIIIDa, and RIIIDb, which simultaneously cleave the 3p- and 5p- strands of pri-miRNAs, respectively. This step releases ~70 nt stem-loop precursors, termed pre-miRNAs, that contain 2 nt overhangs at the 3' end and a 5'-terminal phosphate group (Lee et al., 2003). Then, pre-miRNAs are exported from the nucleus to the cytoplasm by the Exportin-5 (XPO5)/Ran-GTP complex (Yi et al., 2003). The precise mechanism of pri-miRNA recognition and cleavage site selection is not fully understood. However, recent studies have shed light on this process (Kwon et al., 2019; Li et al., 2020; Nguyen et al., 2020; Roden et al., 2017). Notably, the miRNA sequence is embedded within a characteristic stem-loop structure composed of a basal junction, an ~13 nt lower stem, an ~22 nt upper stem and a loop (Figure 3). In addition, some sequence motifs located within different parts of the pri-miRNA influence its processing. DGCR8 recruits pri-miRNAs through its dsRNA-binding domain (dsRBD). Subsequently, recognition of the UG motif in the basal junction by DROSHA and the apical UGU motif by DGCR8 facilitates the positioning of pri-miRNAs. The correct orientation of DROSHA is also mediated by the cofactor SRSF3, which interacts with the CNNC motif in the 3' RNA-flanking sequence and recruits DROSHA to the basal junction (Kim et al., 2018; Nguyen et al., 2019). The precision of DROSHA cleavage strongly depends on the presence of a mismatched GHG motif (mGHG) within the lower stem of the pri-miRNA. In general, the cut site is determined by distances of ~13 base pairs (bp) (on the 5' side) and ~11 bp (3' side) from the basal junction. Recently, cryo-EM structures of human DROSHA and DGCR8 in complex with a pri-miRNA have explained how Microprocessor recognizes pri-miRNA and selects the cleavage site (Partin et al., 2020).

In the cytoplasm, pre-miRNAs undergo processing by a complex consisting of the RNase III-like enzyme DICER, its cofactor TAR RNA binding protein (TRBP) and protein kinase R-activating protein (PACT) (Chendrimada et al., 2005; Grishok et al., 2001; Hutvagner et al., 2001; Lee et al., 2006). DICER serves as a molecular ruler in this reaction, binding the basal ends of a pre-miRNA through its PAZ domain and measuring an ~22 nt distance from the 5' phosphate end to the pre-miRNA terminal loop (Park et al., 2011). Two catalytic RNase III domains cleave pre-miRNAs, removing the loop and imperfect ~22 nt miRNA duplex with characteristic 2 nt 3' overhangs (Zhang et al., 2004). The miRNA duplex is loaded onto an Argonaute protein (AGO1-4) with assistance from chaperone proteins (HSC70/HSP90), forming the RNA-induced silencing complex (RISC) (Iwasaki et al., 2010). Then, AGO unwinds the RNA duplex, and the passenger strand is removed from the complex. Selection of the strands is based in part on the thermodynamic stability of the 5' ends of the miRNA duplex. Therefore, some miRNAs originate from the 5' ends,

whereas other originate from the 3' ends. The less stable strand is preferentially loaded onto AGO and serves as a guide RNA that directs the activated RISC (miRISC) to the complementary target sequence in mRNA (Khvorova et al., 2003; Liu et al., 2004). This results in translation inhibition, mRNA destabilization and/or target mRNA degradation. The specificity of miRISC-target interactions depends mainly on nucleotides 2–8 from the 5' end of the miRNA, called the “seed sequence” (Bartel, 2018).

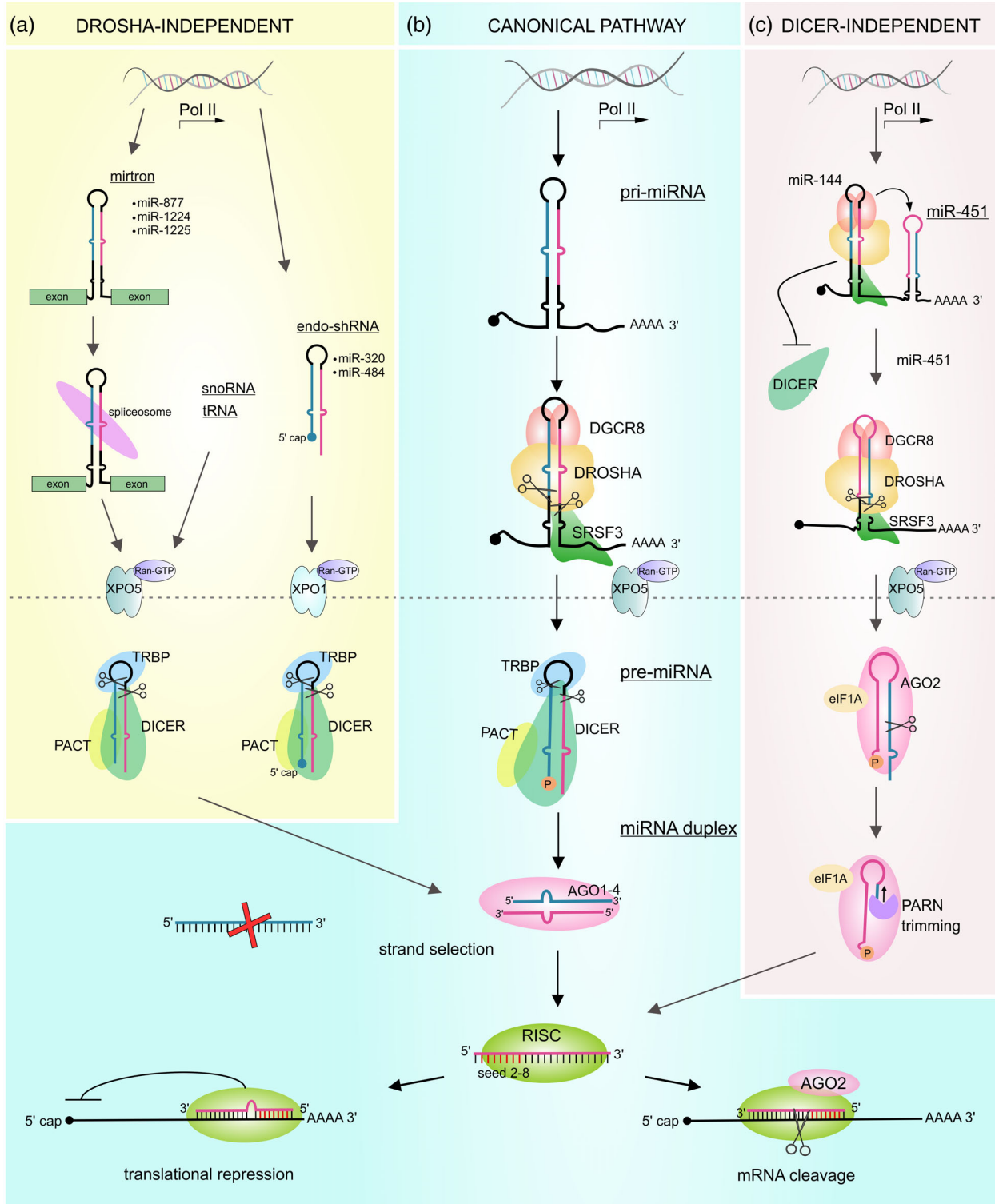


FIGURE 2 Legend on next page.

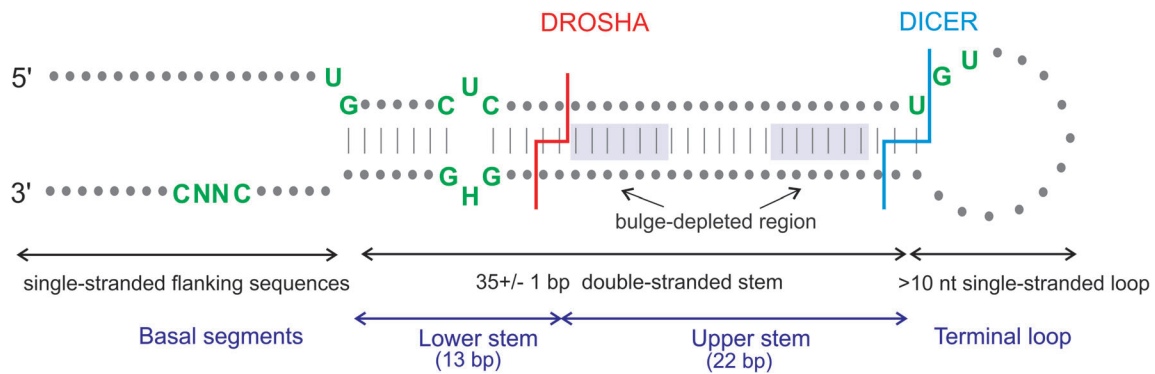


FIGURE 3 Structural features of canonical pri-miRNAs. Canonical pri-miRNAs are composed of single-stranded basal segments, a double-stranded stem and terminal loop. During pri-miRNA processing, the RNases DROSHA and DICER cleave the stem-loop structure at specific positions to form the mature miRNA. The presence of sequence motifs (green), such as CNNC, GHG, UG, and UGU, help to position the cleavage site and enhance processing. The optimal length of the stem is $\sim 35 \pm 1$ bp, and the stem is composed of the lower stem (13 bp), and upper stem (22 bp), which contains two bulge-depleted regions

2.2 | Noncanonical miRNAs

Some miRNAs undergo biogenesis in a noncanonical way. For example, mirtrons which are derived from short intronic hairpins, do not need Microprocessor (Figure 2(a)). Instead, mirtrons are processed by spliceosomes and debranching enzymes, which results in the production of pre-miRNAs that are exported to the cytoplasm by XPO5 and cut by DICER into ~ 22 nt RNAs (Okamura et al., 2007; Wen et al., 2015). Another group of DROSHA-independent miRNAs are small nucleolar RNA-derived miRNAs (snoRNAs) and tRNA-derived miRNAs (Figure 2(a)).

MiR-320 and miR-484 are other examples of noncanonical miRNAs that are DROSHA/DGCR8 independent (M. Xie et al., 2013). Their transcripts form hairpin structures known as endogenous short hairpin RNAs (endo-shRNAs). They lack the flanking sequences typical of canonical pri-miRNAs, which are helpful for the identification of pri-miRNAs by Microprocessor. Studies suggest that endo-shRNAs are generated directly by transcription and capped at the 5' end. Endo-shRNAs require XPO1 instead of XPO5 for nuclear transport. After DICER-mediated cleavage, ~ 20 nt RNAs are produced, and only 3p- miRNAs are loaded onto AGO proteins (Kim et al., 2016; M. Xie et al., 2013). One of the most highly conserved miRNA, muscle-specific miR-1, also does not require DROSHA for processing. Interestingly, there are two copies of miR-1 genes in zebrafish, mouse and human genomes encoding for ~ 70 nt precursors (miR-1-1 and

FIGURE 2 Canonical and noncanonical miRNA biogenesis. MiRNA genes are transcribed mostly by RNA Pol II. Then, depending on the substrate three different miRNA biogenesis pathways lead to the production of mature miRNAs: (a) the DROSHA-independent pathway, (b) canonical pathway, and (c) DICER-independent pathway. (a) Mirtrons derived from short intronic hairpins are processed into pre-miRNAs by spliceosomes and debranching enzymes, exported to the cytoplasm by XPO5 and cut by DICER into ~ 22 nt miRNAs. Endogenous short hairpin RNAs (endo-shRNAs) are generated directly by transcription, and require XPO1 for nuclear transport. After DICER-mediated cleavage, ~ 20 nt RNAs are produced, and only 3p- miRNAs are loaded onto AGO proteins. SnoRNA and tRNA-derived miRNA are processed by DICER, transported by XPO5 and loaded onto AGO proteins. (b) Primary miRNA transcripts (pri-miRNAs) undergo nuclear processing by the Microprocessor complex, which is composed of DROSHA, DGCR8, and SRSF3. RNase DROSHA cuts pri-miRNA to the miRNA precursor (pre-miRNA), which is transported to the cytoplasm by XPO5. In the cytoplasm, the pre-miRNA is processed by DICER, its cofactor TRBP and protein kinase R-activating protein (PACT). The RNase III-like enzyme DICER cleaves pre-miRNAs and generates an imperfect ~ 22 nt miRNA duplex that is loaded onto an ARGONAUTE protein (AGO1-4), forming the RNA-induced silencing complex (RISC). AGO unwinds the duplex, the passenger strand is removed from the complex and the guide strand directs the activated RISC to the complementary target sequence in the mRNA. Depending on the level of complementarity, this results in translation inhibition, mRNA destabilization (partial) and/or target mRNA degradation by AGO2 (full complementarity). Nucleotides 2–8 from the 5' end of the miRNA, called the “seed sequence,” are responsible for the specificity of the interactions. (c) MiR-451 is the only known DICER-independent miRNA. It is encoded in the same primary transcript as the DICER-dependent miR-144. DROSHA-mediated cleavage of pri-miRNA-451 generates a hairpin with a short stem that is not recognized by DICER. The pre-miRNA is loaded directly onto AGO2, which cleaves the 3' strand of the stem and generates an ~ 30 nt product that is trimmed by poly(A)-specific ribonuclease (PARN) to generate the mature miRNA. Translation initiation factor 1A (eIF1A) directly binds AGO2 and promotes miR-451 biogenesis

miR-1-2), which are processed by DICER to form identical 3' arm-derived mature miRNAs (J.-F. Chen et al., 2006; Zhao et al., 2005).

Vertebrate-specific miR-451 is the only known example of a miRNA that can be processed without DICER; instead, miR-451 relies on the slicing activity of AGO. After transcription, pri-miR-451 is cleaved in the nucleus by the Microprocessor complex (Figure 2(c)). This generates a hairpin with a stem 17 bp in length that is too short to be recognized and cleaved by DICER. The pre-miRNA is loaded directly onto AGO2, which cleaves the 3' strand of the stem at a position 10/11 nt from the end (Cheloufi et al., 2010). Furthermore, it has been shown that translation initiation factor 1A (eIF1A) directly binds to AGO2 and promotes miR-451 biogenesis (T. Yi et al., 2015). Cleavage by AGO2 generates a 30 nt product that is trimmed by poly(A)-specific ribonuclease (PARN) to generate a mature miRNA of 22–26 nt in length. After maturation, the miRNA duplex is loaded onto RISC, which unwinds the strands into guide and passenger strands (Cheloufi et al., 2010; J.-S. Yang et al., 2010; Yoda et al., 2013). Interestingly, miR-451 is encoded in the same primary transcript as the DICER-dependent miR-144 (Dore et al., 2008). A recent study demonstrated that miR-144 recruits Microprocessor and transfers it to miR-451, thus facilitating its processing (Shang et al., 2020). In addition, during erythropoiesis, miR-144 targets DICER in a negative feedback loop, leading to the inhibition of canonical miRNA processing. Otherwise, DICER-independent miR-451 processing is undisturbed (Kretov et al., 2020).

Both canonical and noncanonical miRNA biogenesis pathways generate a heterogeneous pool of miRNAs that differ mainly at their 3' ends. The main source of this variation is the imprecise cutting of pri- and pre-miRNA by the RNases DROSHA and DICER and posttranscriptional modifications. The functional consequence of 5' end heterogeneity is a shift of the seed sequence, leading to the regulation of different mRNAs. 3' IsomiRs can differ in their silencing efficacy and stability in cells. The interaction between the 3' end of a miRNA and its target is important for binding specificity because it can stabilize and enhance miRNA-target pairing, especially with imperfect seed complementarity (M. J. Moore et al., 2015).

3 | STRUCTURAL FEATURES OF ARTIFICIAL MiRNAs

AmiRNAs consist of two components: a pri-miRNA scaffold and siRNA insert. Because the sequence and structure of a pri-miRNA strongly influence its processing, it is difficult to predict the effects of replacement of the miRNA sequence with an exogenous siRNA sequence. In addition, miRNA biogenesis is controlled posttranscriptionally on multiple levels, and a number of cis- and trans-acting factors modulate this process (Ha & Kim, 2014; Michlewski & Cáceres, 2019). Improper amiRNA design may result in inefficient processing, the generation of siRNA variants with seed sequence changes or the induction of arm switching—a process that leads to the release of the passenger strand of siRNA (Medley et al., 2020).

The natural heterogeneity of miRNAs that emerge from one precursor (isomiRs) may be beneficial for cells and allows for the regulation of many transcripts (Nielsen et al., 2012). Precision and safety are the main principles of RNAi technology, and the improper processing of amiRNAs increases the risk of off-target effects (Galka-Marciniak et al., 2016). Therefore, the pri-miRNA backbone, length of the stem and flanking sequences, location of the siRNA insert or presence of structural and sequence motifs have to be chosen with caution to ensure the efficient and specific processing of an amiRNA. Application of the features of naturally occurring miRNAs to amiRNAs improves their processing and hence silencing efficiency (Ros et al., 2019; Ros & Gu, 2016; Box 1).

AmiRNAs mimic endogenous pri-miRNAs and consists of a double-stranded stem that is flanked by two single-stranded basal segments (5p- and 3p-) and an apical loop (Figure 3). The stem can be further divided into an upper stem consisting of approximately 22 bp from the terminal loop and a lower stem covering ~13 bp from the basal segments. The boundaries between these dsRNA and ssRNA regions are termed the basal and apical junctions. Stem length, apical loop size, and the presence of basal (CNNC and UG) and apical (UGU) motifs are well-known features that influence miRNA processing, and the combination of these features results in mature miRNAs. Because each pri-miRNA is unique in terms of its structure and sequence properties, there are no universal guidelines for the optimal design of amiRNAs. However, years of miRNA biogenesis studies and high-throughput analyses of hundreds of thousands of pri-miRNA variants have allowed the definition of simplified rules to guide the efficient and specific processing of amiRNAs (Fang & Bartel, 2015).

3.1 | Single-stranded basal segments

The presence of basal segments and their single-stranded nature are critical for pri-miRNA processing. *in vitro* processing of pri-miR-16 variants devoid of one or both basal segments was found to be disrupted or completely abolished, respectively (Han et al., 2006). Similarly, DROSHA-mediated cleavage of pri-miRNA mutants with double-stranded basal segments was blocked (Han et al., 2006). In general, the longer the flanking sequences are, the better the pri-miRNA processing is (Zeng & Cullen, 2005). The length of basal segments in endogenous pri-miRNAs varies considerably and can reach several hundred nucleotides. From a practical perspective, much shorter sequences are used in amiRNA constructs. For example, minimal pri-miR-16-1 and pri-miR-30a sequences containing ~20 nt outside of the DROSHA cleavage site were found to undergo processing *in vitro* (Han et al., 2004). However, a minimal pri-miR-31 sequence was ineffective for mature miRNA production when transcribed from the H1 promoter in transfected HEK293T cells (Zeng & Cullen, 2005). Therefore, to ensure efficient processing, 125 nt flanking sequences from the primary transcripts were used to generate libraries of miR-30-based constructs (Silva et al., 2005; Stegmeier et al., 2005).

In general, the nucleotide sequence of basal segments is not important for processing (Zeng & Cullen, 2005). The exception is the CNNC motif located in a 3' basal segment of ~60% of representative pri-miRNAs (Auyeung et al., 2013). This motif interacts with SRSF3, which recruits DROSHA to the basal junction, thus stimulating pri-miRNA processing. This effect only occurs when CNNC is located ~17 nt from the Microprocessor cleavage site (Kim et al., 2018). The Microprocessor complex recognizes the single-stranded basal segments and measures 11 bp from the basal junctions (Han et al., 2006).

3.2 | Double-stranded stem

Pri-miRNAs differ in terms of stem length and the variety of motifs that disturb the stem structure, including symmetric changes, which can form single mismatches or internal loops, and asymmetric changes, which are mainly single nucleotide bulges. In addition, natural pri-miRNA hairpins often contain G:U wobble base pairs at many positions of the stem. The lower stem is usually perfectly base-paired, and internal loops within this region downregulate miRNA expression (Nguyen et al., 2020). One of the most important features of amiRNAs is the optimal length of the stem.

BOX 1 NONSPECIFIC EFFECTS OF RNAi TECHNOLOGY

In addition to silencing selected targets, RNAi tools can also have unintended effects, including off-target activity, saturation of the miRNA biogenesis pathway, and an immune response. These effects can complicate the interpretation of phenotypic effects in gene-silencing experiments and lead to toxicity (Olejniczak et al., 2016).

Sequence-dependent off-target effects result from nonspecific interactions between siRNAs and other transcripts containing complementary sequences. Bioinformatic prediction of potential off-target interactions (e.g., BLAST NCBI and siSPOTR) during siRNA design can significantly reduce this risk. However, even partial sequence complementarity (within the “seed” sequence) to the 3' UTRs of some transcripts can induce miRNA-like gene silencing. Excess passenger strand or siRNA variants may also be responsible for the nonspecific inhibition of complementary transcripts.

Saturation of the miRNA biogenesis pathway results from overexpression of an RNAi trigger, which competes with endogenous miRNAs for the Microprocessor complex or XPO5, DICER, or AGO proteins. Small RNA sequencing analysis allows quantitative and qualitative evaluation of the processed siRNA content in relation to the endogenous miRNA content. This effect can be overcome by the use of weaker promoters, amiRNAs as RNAi triggers, or the lowest effective dose of viral vector.

Immune response Exogenous RNAi triggers can stimulate cellular sensors of foreign RNA and DNA, which recognize pathogen-associated molecular patterns (PAMPs). This effect depends mostly on the length, structure, concentration, and cellular localization of the molecule and leads to the production of proinflammatory cytokines and interferons. For example, the TLR9, AIM2, and ZBP1 sensors recognize foreign DNA that has been introduced into cells either as a plasmid or through a viral vector.

Naturally occurring pri-miRNAs have an imperfect stem structure consisting of 3 helical turns made of 35 ± 1 bp. Previous studies have demonstrated that a stem length of ~ 33 bp is optimal for the Microprocessor complex (Han et al., 2006; Nguyen et al., 2015). However, a study by the Lu group expanded the optimal range of the pri-miRNA stem length to 36 ± 3 bp. They modified the 35 bp stem of miR-125b by insertion/deletion of 1–4 bp near the apical loop, on the basal side or in the middle of the stem and demonstrated that 4 bp alterations reduced processing efficiency $\geq 80\%$. Otherwise, changes of 3 bp did not significantly impair processing. Their data highlight the presence of a range of optimal stem lengths that supports efficient pri-miRNA processing (Roden et al., 2017).

The presence and location of sequence motifs play an important role in pri-miRNA processing, and sequence motifs help Microprocessor in positioning pri-miRNAs with a nonoptimal stem length in the cleavage site (Auyeung et al., 2013). Several groups observed the enrichment of pri-miRNAs with a bulge at positions 5–9 nt from the base of the stem (Fang & Bartel, 2015; Han et al., 2006; Roden et al., 2017). By analysis of 40,000 pri-miRNA variants, the authors demonstrated that the presence of this bulge in the context of the GHG motif dictates the DROSHA cleavage site (Fang & Bartel, 2015). Cryo-EM structures confirmed that the GHG motif contributes to a unique RNA structure that supports the formation of a four-way junction (Partin et al., 2020). DROSHA also recognizes the UG motif within the 5' basal junction of some pri-miRNAs. In addition, Roden et al identified bulge-depleted regions at positions ~ 16 –21 and ~ 28 –32 nt from the base of the stem (Figure 3) (Roden et al., 2017). The authors propose that these regions may interact with DGCR8 and that bulges within these regions disturb processing.

Pri-miRNAs encode miRNAs in the 5' or 3' or both strands of the stem structure. 5' miRNAs are defined by DROSHA, in contrast to the 3' miRNAs, which are released by DROSHA and DICER. DROSHA is known to be more precise in cutting than DICER, leading to the generation of miRNAs with a predicted seed sequence. Therefore, the siRNA guide strand is usually inserted into the 5' amiRNA arm (Silva et al., 2005). In addition, most amiRNA stems are perfectly base-paired, facilitating amiRNA design and analysis. However, the transcription of such highly structured constructs can be prematurely terminated, leading to the generation of inactive viral vectors (J. Xie et al., 2017, 2020).

3.3 | Terminal loops

The presence of unstructured terminal loops is necessary for pri-miRNA recognition, positioning, and cutting. In addition, pre-miRNAs and shRNA loops are recognized by XPO5 and therefore necessary for nuclear-cytoplasmic transport. Terminal loops and basal segments derived from natural pri-miRNA scaffolds ensure the efficient processing of amiRNAs. Generally, pri-miRNAs contain loops 3–23 nt in length (Zeng & Cullen, 2003), and pri-miRNAs with loops >10 nt in length are processed efficiently (Ma et al., 2013). However, too large loops (>15 nt) were shown to be less efficiently processed because they can mimic the basal segment, leading to cleavage from the wrong end of the pri-miRNA (Han et al., 2006). Combination of the apical UGU motif with basal motifs helps to properly orient the cleavage site and enhance the processing of nonoptimal hairpins (Fang & Bartel, 2015). However, basal elements are more important than apical motif in cleavage site selection. DGCR8 recognizes the UGU motif, which is present in $>30\%$ of pri-miRNAs. The heme-binding region (HBR) is necessary for DGCR8 activation and terminal loop recognition (Nguyen et al., 2015; Partin et al., 2017).

4 | ARTIFICIAL MiRNA SCAFFOLDS

Pri-miRNA scaffold determines the way of amiRNA processing in a cell and production of siRNA which is an effector molecule in this system. The siRNA guide strand with perfect complementarity to the target mRNA directs the activated RISC to this sequence and induces cleavage of the mRNA by AGO2 (Figure 2). The first miRNA whose elements were used for siRNA expression was miR-26a. McManus et al. showed that their construct containing a 9 nt miR-26a loop, called a class II hairpin, effectively silenced target transcripts in human cells (McManus et al., 2002). The miR-26a loop was additionally modified, and a single C base was deleted to prevent unintended structural folding. In addition, the construct contained an asymmetric bulge within its stem structure, 19 nt of uninterrupted RNA duplex, and a 5 nt GC clamp. The authors demonstrated that even slight modification in the structure of the hairpins led to changes in silencing activity. Further studies confirmed that the design of miRNA hairpin mimics is critical for their silencing efficiency.

4.1 | Pri-miR-30a

Zeng et al. reported for the first time that the region of the primary hsa-miR-30a transcript corresponding to the mature miRNA can be replaced with a heterologous sequence without comprising activity (Zeng et al., 2002). Currently, pri-miR-30a is one of the best known and most commonly used siRNA scaffold. It belongs to the miR-30 family, which is composed of miR-30a, miR-30b, miR-30c, miR-30d, and miR-30e, the members of which play an important role in regulating tissue and organ development and disease pathogenesis (L. Mao et al., 2018). Pri-miR-30a contains a 15 nt loop, stem with an asymmetrical 2 nt bulge and G:U wobble base pairs, sequence motifs such as the basal CNNC and UG motifs and apical UGU(G) motif. Mature 22 nt miRNAs are derived from both the 5' and 3' ends, but the 5' products predominate (Figure 4).

MiR-30a-based amiRNA constructs have been optimized by many researchers. The main concerns regarding these constructs were the length of the flanking sequences, maintenance of structural and sequence motifs and choice of the optimal promoter for expression in cells. Generally, the more similar the structure of an amiRNA to pri-miR-30a is, the more efficient the silencing was. Most miR-30a-based amiRNAs contain the original loop sequence with an apical UGU(G) motif. Variation of the lengths of the flanking sequences from ~20 to 125 nt did not provide clear conclusions regarding their impact on processing or silencing efficiency.

Although preservation of the features of endogenous miRNAs in amiRNA constructs improves processing, the level of emerging siRNAs remains lower than siRNAs released from shRNAs. This directly influences silencing efficiency. Therefore, to further improve the processing of miR-30a-based amiRNAs, Fellmann et al. (2013) designed an experimental miR-30 backbone termed miR-E. The synthetic miR-30 stem was perfectly base-paired with a guide strand placed at the 3' arm. In addition, two conserved base pairs flanking the loop were mutated from CU/GG to UA/UA, changing the apical UGU(G) motif to AGU(G). The highly conserved 3' region of the basal stem was also changed by the introduction of XhoI/EcoRI restriction sites for shRNA cloning. These alterations had a positive impact on amiRNA knockdown efficiency. The level of mature siRNA was 10–30 times greater than that of unmodified miR-30-based amiRNA.

The miR-30 scaffold was used to generate a large-scale library of amiRNAs. This library covers the majority of human (34,711) and mouse (32,628) genes, and each target is represented by six different amiRNAs (Chang et al., 2006; Silva et al., 2005). Additionally, the same group designed another miR-30-based expression system called the PRIME (potent RNAi using microRNA expression) vector, which allows for the regulation of amiRNA expression by a

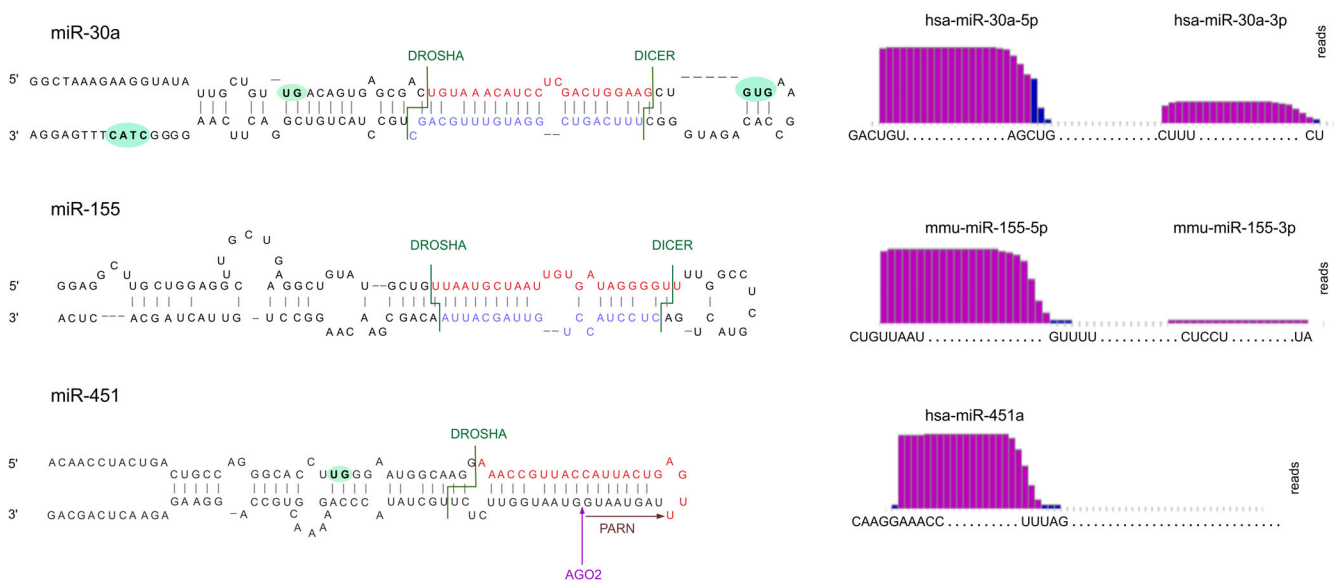


FIGURE 4 Commonly used amiRNA scaffolds. Pri-miR-30a is the most frequently used amiRNA scaffold. It contains basal CNNC, UG and terminal GUG motifs (highlighted in green). The mature 22 nt miRNAs are derived from both the 5' and 3' ends, with the 5' products predominating (from miRBase). Pri-mir-155 is the second most frequently used amiRNA scaffold. It does not contain sequence motifs that facilitate processing and generates miRNA from the 5' end. DICER-independent pri-miR-451 is processed by DROSHA, AGO2, and PARN, which does not generate a passenger strand

tetracycline (Tet)—responsive promoter (Stegmeier et al., 2005). This system allows for the tracking of amiRNA in cells by the coexpression of reporter genes and modulation of gene knockdown by using different dosages of doxycycline (DOX). There are three variants of the PRIME constructs: (i) the TET-ON system in which binding of DOX to reverse tet-controlled transcriptional activator (rtTA) activates transcription from the TET promoter; (ii) the TET-OFF system which is active in the absence of DOX; and (iii) the Tet-repressor-based expression system (TRES). A series of other lentiviral vectors to induce the Tet-responsive knockdown of gene expression such as pSLIK (single lentivector for inducible knockdown; Shin et al., 2006) or the constructs controlled by the ubiquitin C (UbiC) promoter (Xia et al., 2006; Zhou et al., 2005) were also developed (reviewed in Calloni & Bonatto, 2015).

4.2 | Pri-miR-155

Another widely used miRNA backbone is derived from mouse or human pri-miR-155 in the exon of a noncoding RNA and transcribed from the B-cell integration cluster (BIC). MiR-155 is highly conserved among humans, mice and chickens and participates in hematopoiesis, inflammation, and immunity. It is highly expressed in the thymus and spleen but has also been detected in other tissues (Faraoni et al., 2009; Mashima, 2015).

Pri-miR-155 contains a 13 nt loop that does not contain UG, GHG, CNNC and UGU motifs and the loops derived from humans and mice differ by 3 nt. The hairpin stem contains bulges and G:U wobble base pairs (Figure 4). The mature miRNA is generated from the 5' arm and consists of 24 nt. The 3' arm also generates a functional miRNA that is 22 nt in length (Y. Wang et al., 2018). Pri-miR-155 cassettes can be effectively designed to express single or multiple amiRNAs (Chung et al., 2006; X. Liu et al., 2012; Pfister et al., 2017).

Many researchers use the commercial plasmid pcDNA6.2-miR, which contains ~30–40-nt flanking sequences from mouse pri-miR-155. Expression of the corresponding amiRNA is driven by the cytomegalovirus (CMV) promoter. This construct allows for efficient silencing of the expression of a gene of interest in cultured cells and in vivo. MiR-155-based amiRNAs have been used in cellular and rodent models of cancers and viral and neurodegenerative diseases (X. Liu et al., 2012; Murphy et al., 2013; Sharma et al., 2018). Additionally, human pri-miR-155 has been used as an siRNA backbone. The Mueller group designed two amiRNA constructs using the hsa-miR-155 scaffold and HTT siRNA insert. One construct was driven by the U6 promoter and expressed one copy of the amiRNA. The second construct was driven by the chimeric CMV-chicken β -actin (CBA) promoter and expressed two copies of the amiRNA. The construct expressed from the U6 promoter produced the amiRNA at a supraphysiologic level, in contrast to the amiRNA driven by the Pol II promoter, which resulted in toxicity and abnormal behavior in mice. Expression of miR-155-based siRNA resulted in guide strand predominance (Pfister et al., 2017). Notably, the construct contained a modified loop and ~50 nt flanking sequences derived from hsa-pri-miR-155. An amiRNA cassette based on mmu-miR-155 could also be inserted inside an intron (Chung et al., 2006; Du et al., 2006). In this cassette, an almost 500 nt sequence from the third exon of mouse BIC, including the miR-155 sequence (149 nt), is embedded in an expression vector designated synthetic inhibitory BIC-derived RNA (SIBR). In place of the mature miR-155, a 22 nt duplex coding the chosen siRNA is inserted. The construct is under control of the simian CMV IE94 promoter (sCMV), and the cassette ends SV40 late polyadenylation. Northern blot analysis confirmed expression of the ~22 nt product from the vector. Luciferase assays and western blot analyses confirmed the silencing efficiency for different genes, such as the kinases B-Raf and c-Raf. The inclusion of multiple copies of this miRNA cassette (up to at least eight copies) can be used to increase the inhibition of a single target mRNA (Chung et al., 2006).

4.3 | Pri-miR-451

Noncanonical miR-451 participates in erythropoiesis and is most abundant in mature erythrocytes. The miRNA-451 gene is located on chromosome 17 in an intergenic region ~100 nt downstream of the DICER-dependent miR-144 gene. The pri-miR-451 structure contains a ~33 bp stem and 4 nt loop whose sequence is part of mature miR-451 (Figure 4). DROSHA-mediated cleavage generates the pre-miRNA, which contains a highly structured 17 bp stem and is cleaved by AGO2 to produce ~30 nt intermediates. These intermediates are trimmed to 20–26 nt mature miRNAs (Pan et al., 2015; Yoda et al., 2013). During biogenesis, the passenger strand is not generated, which makes this miRNA a promising tool due to its limited off-targets (Kretov et al., 2020). Konstantinova's group successfully used this backbone for the expression of siRNA targeting the HTT transcript, and a phase I/II clinical trial for this amiRNA in HD began

this year. The original pri-miRNA structure has been preserved in this construct, and the guide siRNA strand is incorporated in place of the mature miR-451. The flanking sequences consists of 200 nt and contain restriction sites for EcoRV and BamHI (J. Miniarikova et al., 2016, 2017). The amiRNA cassette was driven by the CMV or CMV- chicken β -actin-rabbit beta-globin (CAG) promoter in in vitro or in vivo studies, respectively. The amiRNA cassette also contains a human growth hormone polyadenylation (hGH polyA) signal. The results showed that depending on the siRNA sequence, the processing pattern can be different, generating siRNAs ranging in length from 19 to 31 nt (J. Miniarikova et al., 2016).

4.4 | Other amiRNA scaffolds

Other pri-miRNAs have been used as the backbone for amiRNA design, but less frequently than pri-miR-30a and pri-miR-155. One example is mouse pri-miR-33, which is encoded within intron 16 of the *SREBF2* gene and involved in cholesterol uptake and synthesis. MiR-33 was shown to regulate HDL biogenesis in the liver and cellular cholesterol efflux (Rayner et al., 2010). It was found that mmu-pri-miR-33 contains nearly all the features of an optimal miRNA, such as a 35 bp stem, UG motif in the basal junction region, mGHG in the stem, UGU(G) in the loop and CNNC motif in 3' flanking sequence. Gao et al. optimized this backbone to silence Apob and PC-1 (Gao et al., 2008).

The constructs, driven by the CB promoter, consisted of pre-miRNA loop and ~100 nt flanking sequences derived from pri-miR-33. The hairpin stem included bulges in the passenger strand to mimic the native structure. The introduction of bulges into the miR-33 scaffold significantly improved the rAAV genome integrity compared to that with fully complementary stems, which are responsible for the generation of truncated genomes during vector production. In cultured cells and mice, the constructs effectively mediated gene silencing at a level similar to the corresponding shRNA. Furthermore, miR-33-based amiRNAs were accurately processed, generating many more guide strand than passenger strand (J. Xie et al., 2020). This backbone and the rules applied to its design were also used in trials of osteoporosis therapies. In vivo studies have shown that it effectively silences expression of the key osteoclast regulators RANK (receptor activator for nuclear factor κ B) and cathepsin K (Yang et al., 2020).

Human pri-miR-31 is also used as an amiRNA backbone. Its gene is located on chromosome 9. MiR-31 is involved in diverse signaling pathways that exert effects on different types of cancers (Yu et al., 2018). Natural pri-miR-31 contains an apical UGU motif within a 17 nt loop and a CNNC motif in its 3' flanking sequence. Mature miRNAs are mainly derived from the 5' arm. Arbuthnot and colleagues designed an amiRNA based on this pri-miRNA (Ely et al., 2008, 2009). The natural sequence of pri-miR-31 was maintained, except the apical UGU motif was modified to GGU. The cassette contained 51 nt-long wild-type flanking sequences on each strand. Guide and passenger strands were replaced by sequences derived from a previously optimized shRNA to inhibit the hepatitis B virus. The construct was driven by the U6 or CMV promoter. Northern blot analysis confirmed the generation of 21 nt products corresponding to the mature miR-33. The additional presence of 20 and 22 nt products indicated that this shuttle can generate heterogeneous fragments. In vivo experiments confirmed the silencing efficiency measured in the cellular model.

The same group optimized the hsa-miR-122 backbone, whose sequence is derived from a liver-specific noncoding RNA. The length of the pri-miR-122 transcript is ~4.5 kb (Thakral & Ghoshal, 2015). Pri-miR-122 contains a 12 nt loop with a UGU motif, hairpin stem with symmetric bulges, basal CNNC motif and mature miRNA produced mainly from the 5' arm. Mir-122 is associated with cholesterol metabolism and hepatocellular carcinoma and promotes hepatitis C virus replication (Jopling, 2012). Anti-HBV amiRNA constructs efficiently inhibited HBV when driven by the U6 or CMV promoter. Cellular processing of the amiRNAs resulted in 21 nt products and was more efficient for the CMV-driven constructs than for those driven by the U6 promoter (Ely et al., 2008).

Other examples of miRNA backbones used in single studies to generate target-specific amiRNAs include hsa-miR-21 (Choi et al., 2015; Yue et al., 2010), gga-miR-126 (S. C.-Y. Chen et al., 2011), mmu-miR-144 (Walder et al., 2011), hsa-miR-221 (X. Huang & Jia, 2013), and miR-223 (Guda et al., 2015).

4.5 | MiRNA clusters

Approximately 40% of human miRNA genes are organized in clusters (Altuvia et al., 2005). Such clusters contain two or more miRNA genes that are transcribed in the same orientation. These genes are not separated by a transcription unit or miRNA in the opposite orientation. More miRNA clusters are located in intergenic regions than in introns and

exons. It has been hypothesized that the clustering of miRNA genes with similar biological functions improves the transcription efficiency of the miRNA genes within the cluster. Furthermore, genes within miRNA clusters can coregulate many biological processes (Kabekkodu et al., 2018). One such example is the miR-17-92 cluster, which naturally encodes six individual miRNAs (miR-17, miR-18a, miR-19a, miR-20a, miR-19b-1, and miR-92a; Concepcion et al., 2012; Y. P. Liu et al., 2008). The expression of four anti-HIV siRNAs from the miR-17-92 cluster backbone could inhibit the activity of the virus. This polycistronic construct increased silencing activity compared to that of the conventional construct (Y. P. Liu et al., 2008). Another group proposed the use of the miR-106b cluster for effective inhibition of viral activity. This cluster is tri-cistronic and endogenously expresses miR-106b, miR-93, and miR-25. The endogenous mature miRNA sequences were replaced by siRNAs targeting the tat and rev transcripts of HIV-1 (Aagaard et al., 2008).

The localization of miRNAs within introns inspired researchers to design amiRNAs expressed from polycistronic transcripts to obtain better silencing efficiency than that with a single amiRNA. One of the first polycistronic constructs was based on the miR-30 shuttle. In the corresponding study, two tandem shRNAs with flanking sequences derived from miR-30 were expressed with the CMV promoter. Unexpectedly, a construct in which two copies of the same shRNA were embedded into the background of the naturally occurring pri-miRNA showed lower efficiency than that consisting of a single amiRNA (Zhou et al., 2005). In turn, the use of the miR-155 backbone to generate tandem amiRNAs targeting different genes gave positive results. This construct was also driven by the CMV promoter. Even more interestingly, the embedding up to eight amiRNAs targeting the same gene turned out to be more effective than the embedding of one copy of this amiRNA. To obtain appropriate processing of the chimeric transcript, the secondary structure of one helical turn immediately before the DROSHA cleavage site must be maintained (Chung et al., 2006). Polycistronic amiRNAs can be especially useful in the treatment of viral diseases due to the mutability of viruses. A synergistic antiviral effect was obtained by the use of two miR-155-based amiRNAs targeting conserved sequences in human immunodeficiency virus (HIV) with tolerance for wobble base pairing. Flanking sequences and the stem-loop structure from pri-miR-155 were retained (Son et al., 2008).

5 | ARTIFICIAL MiRNA DELIVERY

The most common delivery system for amiRNAs is based on viral vectors. This system includes adenoviruses (Ads), lentiviruses (LVs), and adeno-associated viruses (AAVs) with different serotypes in which the pathogenic genes are replaced with expression cassettes. By combining different types of vectors and promoters, amiRNAs can be efficiently delivered to a tissue of interest and can provide stable or controlled expression of siRNA.

5.1 | Viral vectors

5.1.1 | Adenoviral vectors

Adenoviruses belong to the Adenoviridae family and represent the largest group of nonenveloped viruses. The adenovirus genome is linear, dsDNA that is between 26 and 48 kb in length. Replication takes place in the nuclei of vertebrate cells using the host's replication machinery. Binding to the cell occurs by interaction with the receptors CD46 for group B human adenovirus serotypes and coxsackievirus adenovirus receptor (CAR) for all other serotypes. Interestingly, human Ad virus-associated (VA) RNA inhibits RNAi by competing for binding to XPO5 and DICER, thus suppressing shRNA transport and the activity of RISC, respectively (Andersson et al., 2005; Lu & Cullen, 2004).

Adenoviral vectors are relatively easy to manipulate and can transduce dividing and nondividing cells without integrating their cargo into the host genome. They can be produced to a high vector titer. First-generation Ad vectors lack the viral E1 gene and are capable of packaging 8 kb. Second-generation Ad do not possess the E2, E3, and E4 genes to reduce the immune response. Third-generation Ad vectors lack all viral protein-coding genes and contain only the packaging signal and inverted terminal repeats (ITRs). The absence of viral proteins reduces the chance of evoking immunostimulatory responses, allowing prolonged expression of the transgene (H.-H. Chen et al., 1997; Herrera-Carrillo et al., 2017). These vectors are used to deliver shRNA and amiRNA expression cassettes into cells in vitro and in vivo, and studies have demonstrated the reduced expression of target genes (Ibrišimović, Kneidinger, et al., 2013; Pan et al., 2015).

5.1.2 | Lentiviral vectors

Lentiviruses belong to the subgroup of retroviruses. Their genome consists of two copies of single-stranded RNA. The best-known lentivirus is human immunodeficiency virus type 1 (HIV-1). Standard retroviral proteins, including Gag, Pol, Env, and the regulatory protein Tat, are responsible for the trans-activation of transcription and Rev-mediated export of spliced and unspliced HIV-1 transcripts from the nucleus. In lentiviral vectors, only the regulatory sequences remain and the capacity is approximately 10 kb. LVs can transduce dividing and nondividing cells allowing stable transgene expression by integrating into the host genome. Thus, transcriptional silencing can be stable for a long time. Lentiviruses can be pseudotyped, whereby their envelope is combined with foreign viral envelope proteins. This allows viral entry into cells that are refractory to infection, for example, hematopoietic and embryonic stem cells. A LV encoding three amiRNAs targeting the Bcl-Abl oncogene was shown to effectively alter leukemogenic potency in vitro and in vivo (McLaughlin et al., 2007). In the case of hepatocellular carcinoma, amiRNAs delivered by LV and targeting osteopontin inhibited cell proliferation (Sun et al., 2008). Positive in vitro results were also obtained with LV expressing anti-influenza virus amiRNAs that effectively inhibited influenza virus production (S. C.-Y. Chen et al., 2011).

5.1.3 | Adeno-associated viral vectors

Adeno-associated viruses belong to the *Parvoviridae* family. They are nonenveloped, and their genome is built of single-stranded DNA and approximately 4.7 kb in length. The DNA strands can be a plus (sense) or minus (anti-sense) strand. The genome contains two ITRs and two open reading frames for the *rep* and *cap* genes. *Rep* encodes a protein essential for the AAV life cycle, and *cap* encodes the capsid protein. Productive infection occurs when a helper virus, either adenovirus or herpesvirus, is present. In the absence of a helper virus, AAVs establish latency by integrating into chromosome 19q13.4 (Daya & Berns, 2008). In recombinant AAVs (rAAVs), the Rep protein is absent from the viral genome and can be supplied in trans. Therefore, viral integration is less efficient for rAAV than for wild-type AAV. There are 11 known AAV serotypes that manifest different host cell tropism and immunological properties. AAVs can be pseudotyped, allowing them to target nonnatural target cells and tissues. A large variety of capsids have been developed to prevent neutralization by antibodies targeting specific capsids, which improves the in vivo transduction efficiency (Dhungel et al., 2020; Wu et al., 2006).

AAVs are promising delivery vectors due to their lack of pathogenicity in humans, ability to facilitate long-term episomal expression, and minimal oncogenic potential and inflammatory response (D. Wang et al., 2019). AAVs are the leading platform for gene therapy delivery, and multiple clinical trials utilizing rAAVs are currently underway (D. Wang et al., 2019). AAVs are commonly used in preclinical studies for neurodegenerative disorders, cancers, muscular dystrophies, and viral infections. AAVs can infect postmitotic cells, and the effective transduction of neuronal cells in mouse, sheep and pig brains was obtained after rAAV2, rAAV5, and rAAV9 injection. Recombinant AAV9 efficiently transduces osteoclasts, and this advantage was used to treat osteoporosis. Systemic administration of rAAV9 carrying amiRNAs to silence the expression of key osteoclast regulators resulted in a significant increase in bone mass in mice (Y.-S. Yang et al., 2020).

5.2 | Expression cassettes

AmiRNAs can be expressed from their own promoters, can be located in the 3' UTRs of protein-coding genes (e.g., GFP) or embedded in an intron (Figure 5). They are mostly transcribed from Pol II promoters, such as the CMV promoter, CBA promoter, CAG promoter, UbiC promoter, phosphoglycerate kinase (PGK) promoter, and elongation factor 1 alpha (EF1A) promoter, leading to the production of transcripts with a 5' cap and poly(A) tail (Figure 5(a)). RNA Pol III promoters such as the U6 and H1 promoters are also used for the expression of amiRNA constructs (Figure 5(b)); however, they are a much more “natural” promoters for shRNA expression. RNA Pol III-derived transcripts contain a 5'ppp and 3' poly(U) tail resulting from the Pol III termination signal (usually 5–6 Ts). In the case of Pol III-regulated amiRNAs, stretches of ≥ 4 Ts should be avoided due to the risk of premature transcription termination. In addition, Pol II promoters allow for the expression of multiple amiRNAs as a polycistronic transcript (Figure 5(c)) and this feature is useful in the treatment of viral infections.

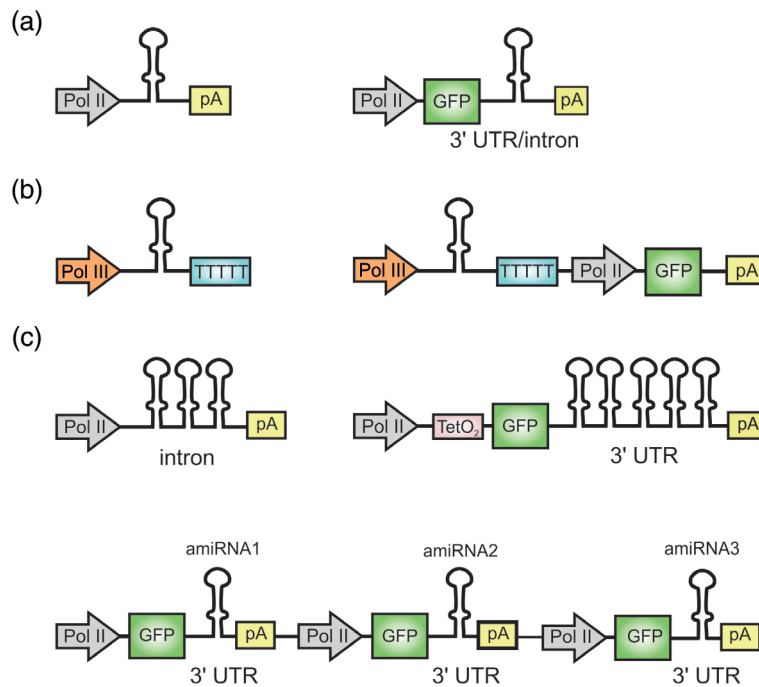


FIGURE 5 Schematic representation of amiRNA expression cassettes. (a) AmiRNAs are mostly transcribed from Pol II promoters. AmiRNA can be expressed from their own promoters or can be located in the 3' UTRs of protein-coding genes (e.g., GFP) or embedded in an intron. (b) RNA Pol III promoters are also used for the expression of amiRNA constructs and RNA Pol III-derived transcripts contain a 5'ppp and 3' poly(U) tail resulting from the Pol III termination signal (usually 5–6 Ts). (c) Pol II promoters allow for the expression of multiple amiRNAs as a polycistronic transcript, individual transcripts or inducible expression systems

There are several issues to consider when selecting a promoter, for example, the strength and activity of the promoter in the target cell or tissue. Direct comparison of the potency of a LV-derived amiRNA expressed from five different Pol II promoters in six human cell lines revealed a positive correlation between promoter strength, siRNA expression level, and protein target knockdown (Lebbink et al., 2011). In addition, the silencing efficiency was found to be cell type dependent. Strong viral promoters such as the CMV promoter, which is very efficient in fibroblasts and cancer cell lines, are not well expressed in lymphohematopoietic cells such as T, B and monocytic cells (Lebbink et al., 2011). Similarly, the CMV and MND promoters were found to induce the expression of transgenes in a limited number of primary cortical neurons, while the UbiC and PGK promoters ensured very high expression of the transgene in these cells. Notwithstanding, transgene expression driven by the CMV promoter in cerebellar granule cells and in neuroblastoma cultures was robust. For primary astrocyte cultures, the best choice was the PGK, CMV, or MND promoter (M. Li et al., 2010).

Although pri-miRNAs are mainly controlled by Pol II, Pol III promoters have also been tested in miR-30 based cassettes. The Hannon group cloned two different amiRNA cassettes downstream of the U6, H1, tRNA-val, MSCV-LTR, and CMV promoters and showed that the most consistent repression was achieved under the U6 and CMV promoters (Silva et al., 2005). Instead, the Davidson group demonstrated that U6 promoter-driven amiRNA vectors were more potent than corresponding CMV promoter-driven amiRNA vectors (R. L. Boudreau et al., 2008). These inconsistent results may suggest that besides the promoter type, other features influence amiRNA processing and silencing efficiency.

Notably promoters that are too strong, especially in the context of shRNA expression, can induce toxicity by oversaturation of the miRNA biogenesis pathway. In addition, the price paid for prolonged expression may be a lower silencing specificity because off-target effects are positively correlated with the level of RNAi triggers. Therefore, a good solution for safe RNAi therapeutic approaches is the use of the lowest effective doses of vectors and tissue-specific or inducible promoters rather than strong ubiquitous promoters. Compared to shRNAs, amiRNAs are more “natural” and safer and do not saturate the miRNA machinery even at a 10-fold higher vector dose (Bauer et al., 2009; R. L. Boudreau et al., 2009; McBride et al., 2008).

To facilitate the tracking of amiRNAs in cells, reporter genes are usually cotranscribed from the vector (Figure 5). Some studies have demonstrated that placing an amiRNA cassette directly upstream of the reporter gene in a monoclonic construct may lead to inefficient translation of the marker protein (Dickins et al., 2005). Therefore, the reporter gene should be placed between the CMV promoter and the miR-30-based amiRNA or should have its own promoter to ensure proper expression (Stegmeier et al., 2005). Otherwise, a miR-21-based amiRNA can be directly under control of a Pol II promoter or downstream of a reporter gene without the loss of knockout efficiency (Yue et al., 2010).

6 | THERAPEUTIC TOOLS TOWARD NEURODEGENERATIVE DISORDERS

Neurodegenerative diseases occur when neurons in the brain or peripheral nervous system irreversibly lose their function over time and finally die. These diseases are often connected with the progressive accumulation of dysfunctional proteins in cells. Examples of this type of disorder are HD; spinocerebellar ataxias (SCAs) type 1, 2, 3, 6, 7, and 17; Alzheimer's disease (AD); and amyotrophic lateral sclerosis (ALS). Current therapies for this type of disorder are directed to alleviate symptoms and maintain quality of life, not to correct the underlying pathogenic process.

6.1 | Polyglutamine disorders

HD and SCAs are genetically inherited autosomal dominant disorders caused by the expansion of unstable CAG triplet repeats in the coding regions of unrelated genes (Buijsen et al., 2019; Duyao et al., 1993). The fully penetrant alleles generally contain more than 40 CAG repeats; however, this feature is disease-specific. The main pathogenic factor in this type of disorder is toxic protein containing the polyglutamine (polyQ) domain (Zoghbi & Orr, 2000). Aggregates of polyQ-containing proteins may cause the degeneration of neurons in specific regions of the brain characteristic of each disorder, for example, the striatum and cerebral cortex (HD), cerebellum, basal ganglia, brainstem, and spinal cord (SCA3) or retina (SCA7) (Novak & Tabrizi, 2010; Paulson, 2009; Ross, 2002; Seidel et al., 2012; Sittler et al., 2018).

RNAi technology provides a great opportunity to decrease toxic protein levels due to the monogenic nature of these disorders (Ashizawa et al., 2018; J. Miniarikova et al., 2018). The main challenges are the delivery of RNAi triggers to the CNS, silencing specificity and selectivity toward the mutant variant. Long-term expression of a therapeutic molecule after a single administration would also be beneficial to patients because effective therapy should probably be introduced presymptomatically and last for decades. Therefore, AAV-based amiRNAs are ideal candidates due to their high potency, safety and long-term expression as episomal vectors, which have been confirmed in various preclinical studies (Table 1). The most advanced research, concerns the AMT-130 molecule, which targets exon 1 of the human huntingtin (*HTT*) gene, and entered phase I/II clinical study this year. The safety, tolerability and efficacy of AMT-130 will be analyzed in 26 HD patients after single intrastriatal injection of rAAV5 in two doses (NCT04120493).

A 21-nucleotide siRNA sequence is embedded within the noncanonical pri-miR-451 scaffold to reduce the risk of off-target effects caused by passenger strand activity. Pri-miR-451 was chosen through the analysis of many constructs including human miR-1-2, miR-16-1, miR-26a-1, miR-101-1, miR-122, miR-135b, miR-155, miR-203a, miR-335, and miR-451a, with 200 nt 5' and 3' flanking regions. The silencing efficacy and passenger strand activity were measured by a luciferase reporter system. Next generation sequencing (NGS) results demonstrated that miR-451-based amiRNA was processed to 30 nt species *in vitro* and *in vivo*, reaching ~60% and ~30% of all reads, respectively. The second most abundant variant contained a 31 nt species (~20% of all reads, *in vitro*) or a 23 nt species (~30% of all reads, *in vivo*) (J. Miniarikova et al., 2016). No full-length passenger strand was detected. The silencing efficiency and safety of AMT-130 were tested in various cellular and animal models of HD, such as cultured human neurons, rodents, transgenic minipigs and nonhuman primates, and a reduction in the total huntingtin level by 40%–80% was observed (Evers et al., 2018; Keskin et al., 2019; J. Miniarikova et al., 2017; Spronck et al., 2019; Table 1).

One of the first studies describing the use of amiRNAs toward the *HTT* gene used pri-miR-30a as an siRNA scaffold. Experiments performed in HEK293 cells and mouse models demonstrated that amiRNA expressed under the U6 promoter was almost as effective as the corresponding shRNA in *HTT* transcript reduction, despite the dramatic difference in expression levels (R. L. Boudreau et al., 2009; Dufour et al., 2014; McBride et al., 2008; Monteys et al., 2015). In addition, AAV-amiRNA was not toxic in the mouse striatum, unlike shRNAs. These results were confirmed by the same group using the SCA1 model and miR-30-based amiRNA (R. L. Boudreau et al., 2008). To evaluate the safety of partial wild-type huntingtin suppression in an animal model that is more similar to humans in terms of size and anatomy,

TABLE 1 AmiRNAs used in therapeutic approaches for neurodegenerative disorders

Disease	Target	Shuttle	Promoter	Vector	Cells/animals	Site of delivery	Processing	Results		Reference
								Molecular effects	Other	
HD	<i>HTT</i>	miR-451	CAG	AAV5	tgHD minipig	Injection to the striatum	NGS	<ul style="list-style-type: none"> Protein reduced by 50% in thalamus, putamen, and caudate, mRNA reduced by 70% in thalamus and 45% in caudate and putamen. 	<ul style="list-style-type: none"> Absence of widespread microgliosis 	Evers et al. (2018)
HD	<i>HTT</i>	miR-451	CAG	AAV5	Rat	Injection to the striatum	NGS	<ul style="list-style-type: none"> mRNA reduced by 70%, Reduction of HTT aggregates. 	<ul style="list-style-type: none"> Absence of astrogliosis and microgliosis 	Miniarikova et al. (2017)
HD	<i>HTT</i>	miR-451	CAG	AAV5	Q175 KI, R6/2 mice	Injection to the striatum	Previous studies	<ul style="list-style-type: none"> Protein reduced by 40%, Suppression of HTT aggregates in the striatum and cortex. 	<ul style="list-style-type: none"> Almost 60% rotarod improvement Beneficial effect on body weight 	Spronck et al. (2019)
HD	<i>HTT</i>	miR-451	CAG	AAV5	Hu128/21 mice	Injection to the striatum	NGS	<ul style="list-style-type: none"> Protein reduced by 70% in striatum and 50% in cortex. 		Miniarikova et al. (2016)
HD	<i>HTT</i>	miR-30	U6	AAV2/1	CAG140 KI mice	Injection to the striatum	Northern blot	<ul style="list-style-type: none"> mRNA reduced by 70%, Minimal induction of <i>CD11b</i> mRNA. 	<ul style="list-style-type: none"> No significant microglia activation 	McBride et al. (2008)
HD	<i>HTT</i>	miR-30	U6	AAV2/1	HD-N171-82Q mice	Injection to the striatum	Northern blot	<ul style="list-style-type: none"> mRNA reduced by 75% 	<ul style="list-style-type: none"> Improved motor coordination and survival 	R. L. Boudreau et al. (2009)
HD	<i>HTT</i>	miR-30	U6	AAV2/1	Rhesus	Injection to the striatum	No	<ul style="list-style-type: none"> mRNA reduced by 45% 	<ul style="list-style-type: none"> Lack of immune response, gliosis, and neuronal degeneration Skill deficits not induced 	McBride et al. (2011)
HD	<i>HTT</i>	miR-30	CBA	AAV2/1	YAC128 mice	Injection to the striatum	No	<ul style="list-style-type: none"> mRNA reduced by 50%, Protein reduced by 50%, Less aggregates and inclusions. 	<ul style="list-style-type: none"> Improvements in motor function and behavior, Lack of neurotoxicity 	Stanek et al. (2014)
HD	<i>HTT</i>	miR-30	U6	AAV9	C57BL/6, BACHD, and N171-82Q	Intravascular	Previous studies	<ul style="list-style-type: none"> BACH mice: mRNA reduced by 20%, but not significant, N171-82Q mice: mRNA reduced by 33% in striatum, Protein reduced by 65% in striatum, 34% hippocampus, and 32% in cortex. 	<ul style="list-style-type: none"> Lack of microglia activation, N171-82Q mice gained the weight. 	Dufour et al. (2014)
HD	<i>HTT</i>	miR-30	U6	AAV2/1	Double transgenic mice	Injection to the striatum	No	<ul style="list-style-type: none"> Significant reduction of mutant protein. 	<ul style="list-style-type: none"> Allele-selectivity depends on amiRNA dose. 	Monteys et al. (2015)
HD	<i>HTT</i>	miR-155	U6 and CBA	AAV9	YAC128 mice	Injection to the striatum	NGS	<ul style="list-style-type: none"> mRNA reduced by 50%. 	<ul style="list-style-type: none"> U6 promoter: toxicity observed, microglia activation, enlargement of the ventricle, loss of DARPP-32-positive neurons, and striatal shrinkage, Promoter CBA: no overt toxicity up to 6 months 	Pfister et al. (2017)
HD	<i>HTT</i>	miR-155	U6	scAAV9	YAC128 mice	Injection to the striatum	No	<ul style="list-style-type: none"> mRNA reduced by 30% in the striatum. 		W. Liu et al. (2016)

TABLE 1 (Continued)

Disease	Target Shuttle	Promoter	Vector	Cells/animals	Site of delivery	Processing	Results		Reference
							Molecular effects	Other	
HD	<i>HTT</i> miR-155	U6 and CBA	scAAV9	Sheep	Injection to the striatum	No	<ul style="list-style-type: none"> U6 promoter: mRNA reduced by >50% in the caudate and putamen, CBA promoter: mRNA reduced by >50% in the caudate, 35% in the putamen, and 20% in the anterior striatum, Protein reduced from 30% to 78% depending on the brain region. 	<ul style="list-style-type: none"> No influence on animal weight, Striatal volume unaffected, Transient microglia activation 	Pfister et al. (2018)
HD	<i>HTT</i> miR-155	CBA	AAV9	Q140/Q140 mice	Injection to the striatum	No	<ul style="list-style-type: none"> mRNA reduced by 40%–50%. Protein reduced by 25%–40% depending on the time of injection, mRNA foci reduced by 40%. 		Keeler et al. (2016)
SCA1	<i>ATXN1</i> miR-30	U6	AAV2/1	B05 mice	Injection to DCN	No	<ul style="list-style-type: none"> mRNA reduced by 70%. <i>Cjgap</i> mRNA level not significantly changed. 	<ul style="list-style-type: none"> Improved the balance, agility, and hindlimb musculature, Histological rescue of molecular layer width and Purkinje cell number. 	Keiser et al. (2013)
SCA1	<i>ATXN1</i> miR-30	U6	AAV2/5	154Q KI mice	Injection to DCN	No	<ul style="list-style-type: none"> mRNA reduced by 20%. Protein reduced by 58% in cerebellum and 72% in brainstem. 	<ul style="list-style-type: none"> No gial activation, Improved molecular layer widths. 	Keiser et al. (2014)
SCA1	<i>ATXN1</i> miR-30	U6	AAV1/2	Rhesus	Injection to DCN	No	<ul style="list-style-type: none"> mRNA reduced by >30% in the deep cerebellar nuclei, the cerebellar cortex, inferior olive, <i>Cjgap</i> mRNA not significantly changed. 		Keiser et al. (2015)
SCA1	<i>ATXN1</i> miR-30	U6	AAV2/1	B05 mice	Injection to DCN	No	<ul style="list-style-type: none"> mRNA level almost completely reduced in high dose, in medium by 70%. 	<ul style="list-style-type: none"> No changes in cerebellar metabolites, No microglia activation, Improved motor symptoms. 	Keiser et al. (2016)
SCA7	<i>ATXN7</i> miR-30	U6	AAV2/1	BAC Prp SCA7-92Q mice	Injection to DCN	No	<ul style="list-style-type: none"> mRNA reduced by 50%. Protein reduced by 35%. ATXN7 inclusions (NIs) reduced by 80%. 	<ul style="list-style-type: none"> Improved rotarod phenotype, stride length, and hindlimb clasping, No microglia activation 	Ramachandran, Boudreau, et al. (2014)
SCA7	<i>ATXN7</i> miR-30	U6	AAV2/1	BAC Prp SCA7-92Q mice	Injection to the eye	No	<ul style="list-style-type: none"> mRNA reduced by 60%. Mutant protein reduced by 50%. <i>Cjgap</i> mRNA not increased. 	<ul style="list-style-type: none"> No difference relative to wildtype mice in the optokinetic tracking response 	Ramachandran, Bhattarai, et al. (2014)
SCA3	<i>ATXN3</i> miR-451	CAG	AAV5	iPSC-neurons, SCA3 KI mice, and mimipig	Injection to DCN	NGS	<ul style="list-style-type: none"> mRNA reduced by 15%–20% in cerebellum and 40% in brainstem, Protein reduced by 65% in cerebellum and brainstem. 	<ul style="list-style-type: none"> No saturation of endogenous RNAi machinery 	Martier, Sogorb-Gonzalez, Stricker-Shaver, et al. (2019)

(Continues)

TABLE 1 (Continued)

Disease	Target	Shuttle	Promoter	Vector	Cells/animals	Site of delivery	Processing	Results		Reference
								Molecular effects	Other	
SCA3	<i>ATXN3</i>	miR-124	U6	AAV2/1	SCA3/MID84.2 mice	Injection to DCN	3'RACE	<ul style="list-style-type: none"> mRNA reduced by 70%, Protein reduced by 35%, <i>Gfap</i> and <i>Iba1</i> mRNA level not changed, ATXN3 nuclear accumulation reduced by 80%, A partial normalization of some of the altered miRNAs in SCA3 mice cerebella. 	<ul style="list-style-type: none"> No significant changes in the expression of off-target genes, Small number of altered miRNA steady-state levels in the cerebellum of SCA3/84.2 mice 	Rodríguez-Lebrón et al. (2013)
ALS	<i>SOD1</i>	miR-155	CBA	AAV9	B6SJL-Tg(SOD1-G93A)J(Gur/J, nontransgenic mice	Injection into the cerebral lateral ventricles	No	<ul style="list-style-type: none"> mRNA reduced by 50% in spinal cord, more than 80% in heart and gastrocnemius muscle, and unchanged in liver or lung, mRNA of potential off-target not changed. 	<ul style="list-style-type: none"> Improved survival and delays the onset of paralysis, Improved axonal integrity and motor neuron numbers. 	Stoica et al. (2016)
ALS	<i>SOD1</i>	miR-155	CBA and U6	AAVrh10	B6SJL.SOD1-G93A and marmosets	Intrathecal lumbar	No	<ul style="list-style-type: none"> mRNA reduced by 20% in the lumbar region, U6 promoter: mRNA reduced by 90% in lumbar region. 	<ul style="list-style-type: none"> Significantly delayed disease onset, Extended survival, Preserved limb strength and motor skills. 	Borel et al. (2016)
ALS	<i>SOD1</i>	miR-155	CBA and H1	AAVrh.10	Macaque	Intrathecal lumbar	NGS	<ul style="list-style-type: none"> mRNA reduced by 90% at the lumbar section with H1 promoter, mRNA reduced by 68% with CBA. 	<ul style="list-style-type: none"> Immune response not observed, Favorable guide/passenger strand ratio. 	Borel et al. (2018)
ALS, FTD	<i>C9orf72</i>	miR-101	CAG	AAV5	iPSC neurons, Tg(C9orf72_3) line 112 mice	Injection to the striatum	NGS	<ul style="list-style-type: none"> mRNA reduced by 20%–40% in cortex and striatum, 20% drop of cells containing RNA foci. 		Martier, Liefhebber, Garcia-Osta, et al. (2019)
ALS, FTD	<i>C9orf72</i>	miR-101, miR-451	CAG	AAV5	iPSC neurons, HEK293T	Transduction	NGS	<ul style="list-style-type: none"> Foci-positive cells reduced by 50%, mRNA reduced by 50% in frontal brain-like neurons. 		Martier, Liefhebber, Mimiarikova, et al. (2019)
AD	<i>ACAT1</i>	miR-155	CAG	AAV2	3xTg-AD mouse	Injection to the dorsal hippocampus	No	<ul style="list-style-type: none"> ACAT activity reduced by 45%, Aβ and hAPP significantly reduced. 		Murphy et al. (2013)

AAV2/1 carrying U6-amiRNA was injected into the rhesus putamen. AmiRNA injection caused a 45% reduction in HTT transcripts without motor skill deficits, an immune response, neuronal loss, or gliosis (McBride et al., 2011). AAV-amiRNA constructs were also efficient when expressed in vivo under control of the CBA promoter, reducing mutant huntingtin levels by ~50%, and Htt aggregates in the brains of YAC128 mice (Stanek et al., 2014). Direct comparison of the safety and efficiency of amiRNAs expressed under the U6 and CBA promoters was performed using miR-155-based constructs targeting the HTT transcript. Using a self-complementary AAV9 vector, amiRNA was injected into the striatum of an HD mouse model, and the human HTT mRNA was reduced by 50%. The U6 constructs produced the amiRNA at supraphysiologic levels, and cellular processing generated a high level of the passenger strand. This resulted in behavioral abnormalities and striatal damage 6 months after injection (W. Liu et al., 2016; Pfister et al., 2017). In contrast, CBA-amiRNA did not induce any toxicity (Keeler et al., 2016; Pfister et al., 2017). The effectiveness and safety of the construct were confirmed in transgenic sheep expressing full-length human *HTT* cDNA with 73 CAG repeats from the human *HTT* promoter. Six months post injection HTT mRNA and protein levels were decreased by 40%–80% depending on the brain region (Pfister et al., 2018).

Research on effective RNAi therapy for SCAs is less advanced than that for HD. Most approaches use pri-miR-30a as a backbone for the sequence targeting a particular region of specific *ATXN* genes (Table 1). In the case of SCA1, U6-amiRNA was delivered to the deep cerebellar nuclei of model mice by injection of pseudotyped AAV2 vectors (AAV2/1 and AAV2/5) (Keiser et al., 2013, 2014). This caused a significant reduction in *ATXN1* mRNA and protein levels as well as improvement shown by molecular and behavioral analyses (Keiser et al., 2013, 2014, 2016). Injection of the same construct into the rhesus deep cerebellar nuclei reduced *ATXN1* mRNA by >30% and was well tolerated (Keiser et al., 2015).

The same group designed amiRNA for the treatment of SCA7. Similar to the above, this construct was driven by the U6 promoter and packaged into the AAV2/1 vector. Injection into the deep cerebellar nuclei of SCA7 mice resulted in an approximately 50% reduction in the *ATXN7* mRNA level and a 35% reduction in *ATXN7* at the protein level without significant toxicity (Ramachandran, Boudreau, et al., 2014). SCA7 also affects the retina in the eye, and the injection of miR-30-based AAV-amiRNA into this structure in SCA7 mice significantly reduced *ATXN7* levels without altering retinal or visual function (Ramachandran, Bhattarai, et al., 2014).

In the case of SCA3, amiRNAs based on pri-miR-124 and pri-miR-451 backbones gave encouraging results. In the first construct, amiRNA was expressed from the U6 promoter (Rodríguez-Lebrón et al., 2013). AAV2/1 carrying the therapeutic RNA was injected into the deep cerebellar nuclei of SCA3 transgenic mice. The *ATXN3* mRNA level was suppressed by approximately 70%, and the *ATXN3* protein level was suppressed by 35%. Additionally, nuclear accumulation of *ATXN3* was reduced. This finding is important because the nuclear accumulation of proteins with polyQ stretches or even their fragments is thought to be a hallmark event in the pathogenicity of polyQ diseases (Koch et al., 2011). In the second study, pri-miR-451-based amiRNA constructs driven by the CAG promoter were designed and selected using luciferase reporter system and human iPSC-derived neurons. Small RNA sequencing confirmed that three amiRNA candidates were expressed within the range of endogenous miRNA expression and did not influence endogenous miRNA levels. In addition, the authors compared the results of bioinformatics predictions and RNA sequencing and did not find significant alterations in gene expression after treatment with the three amiRNAs. These results suggest that the risks for saturation of the miRNA biogenesis pathway and off-target effects are limited. Next, amiRNAs in AAV5 vectors were injected into the deep cerebellar nuclei of SCA3 knock-in mice. The *ATXN3* mRNA level was reduced by 15%–40%, and the *ATXN3* protein level was reduced by 64% depending on the brain region (Raygene Martier, Sogorb-Gonzalez, Stricker-Shaver, et al., 2019).

6.2 | ALS and frontotemporal dementia

ALS belongs to the group of motor neuron diseases, which result from degeneration and death of motor neurons. The symptoms of ALS are stiff muscles, muscle twitching, and gradually worsening weakness. Approximately 20% of familial ALS cases are caused by mutations in the superoxide dismutase (*SOD1*) gene, associated with the degeneration of neurons. There is evidence that the production of mutated *SOD1* protein can become toxic. Therefore, the silencing of *SOD1* gene expression by RNAi could be a therapy for ALS. Efficient knockout of *SOD1* by miR-155-based amiRNAs was demonstrated in a mouse model and nonhuman primates (Table 1). The first approach used a single-stranded AAV9 vector for the expression of two tandem amiRNAs under the CBA promoter. Bilateral injection into the cerebral lateral ventricles of ALS *SOD1*^{G93A} mice caused reductions in *SOD1* mRNA levels in the spinal cord by up to 50% and

in the heart and gastrocnemius muscles by more than 80% (Stoica et al., 2016). The same amiRNA expressed from the CAG or U6 promoter and packaged into the rAAVrh10 vector was injected intrathecally at the lumbar level into macaques. Higher silencing efficiency was observed after treatment with U6-amiRNA (decreases by 93% in the lumbar region, 65% in the thoracic region, and 92% in the cervical cord region) than with CAG-amiRNA (Borel et al., 2016). In the next study, the amiRNA was expressed from three different promoters, the H1, U6, and CBA promoters, and then administered through intrathecal lumbar injection to macaques. The silencing of *SOD1* expression was greatest in the lumbar section: up to 93% with the use of the H1 promoter. Depending on the promoter and region of the brain, the reduction in *SOD1* transcript levels varied from 40% to 90%. The safety of the construct was confirmed by RNA sequencing, which showed that the amiRNA was precisely processed and that the guide sequence was 100-fold more abundant than the passenger strand. Additionally, no off-target silencing was observed (Borel et al., 2018).

Frontotemporal dementia (FTD) is one of the most common types of dementia in people under 65, and 40% of FTD cases are familial (Ratnavalli et al., 2002). ALS and FTD involve similar genetic players, including an intronic hexanucleotide repeat expansion within chromosome 9 open reading frame 72 (*C9orf72*), which is the most frequent cause of these diseases. The production of RNA foci and dipeptide repeat (DPR) proteins by sense and antisense repeat-containing transcripts results in cellular toxicity leading to neuron death. A miR-101-based amiRNA construct delivered to iPSC neurons and the mouse model as the AAV5 vector reduced the *C9orf72* mRNA level by 60% and up to 40%, respectively (R. Martier, Liefhebber, García-Osta, et al., 2019; R. Martier, Liefhebber, Miniarikova, et al., 2019). In ALS/FTD mice, after bilateral injection of amiRNA into the striatum, a significant decrease in RNA foci was also demonstrated (R. Martier, Liefhebber, García-Osta, et al., 2019).

6.3 | Alzheimer's disease

AD is a progressive disorder characterized by the loss of memory and other cognitive functions in affected people. The causes of AD are complex and include age-related changes in the brain and genetic, environmental, and lifestyle factors. One biochemical characteristic of AD is the accumulation of plaques composed of amyloid- β ($A\beta$), an insoluble cleavage product of amyloid precursor protein (APP), in the brain (Tiwari et al., 2019). Some studies have linked AD with lipid metabolism in the brain, so one attempt to cure this disease could be targeting the acyl-CoA: cholesterol acyltransferase 1 (ACAT1) enzyme. Therefore, miR-155-based amiRNA targeting the *Acat1* (*Soat1*) gene was tested in cellular and animal models of AD (Table 1). The construct driven by the CAG promoter was injected into the dorsal hippocampus as an AAV2 vector, and a 45% decrease in ACAT activity in the whole-mouse brain was obtained. In addition, *Acat1* knockdown decreased $A\beta$ and human APP levels (Murphy et al., 2013).

7 | VIRAL INFECTIONS

AmiRNAs have also been used in the treatment of viral diseases (Table S1). Viruses, a group of pathogenic agents that cannot replicate outside a host organism, can cause many severe diseases (Girardi et al., 2018). Because of the ease of their transmission between organisms, which can promote pandemics, and the ease of viral genome alterations (mutations), they are hard to eradicate; therefore, there is still a growing need to find accurate treatments. To date, amiRNAs have been used to repress the replication of viruses including Chikungunya virus, HIV-1, hepatitis B, influenza, dengue virus, West Nile virus, and Japanese encephalitis virus (Gao et al., 2008; Karothia et al., 2020; Sharma et al., 2018; P. Xie et al., 2013; T. Zhang et al., 2012) (Table S1).

Despite its many advantages, the use of amiRNAs as therapeutic agents in the treatment of viral diseases may have several limitations. One such limitation is the fact that viruses can mutate very rapidly; therefore, it may be difficult to stably suppress a target gene. Hence, it is essential to target highly conserved regions of the viral genome and express more than one amiRNA sequence in one vector. Indeed, all researchers have used multiple amiRNAs to avoid viral escape resulting from the emergence of evading mutations. Furthermore, some viral proteins were discovered to have viral suppressor of RNAi (VSR) activity (Maillard et al., 2019). This phenomenon was observed, for example, in yellow fever virus (YFV) in 2016 by G.H. Samuel and colleagues. They discovered that the capsid protein of YFV interferes with DICER; therefore, it inhibits RNA silencing. The author also claimed that VSR activity is broadly conserved in the C proteins of other medically important flaviviruses (Samuel et al., 2016).

Analysis of publications on the use of amiRNAs for the treatment of viral diseases shows several common features, for example, amiRNAs were embedded mostly within the pri-miR-155 backbone, expressed under the CMV promoter and delivered via lipofection to cell cultures. Examination of the interferon response was the only method of off-target analysis used by all researchers. Cellular processing of amiRNAs was not analyzed, except four studies (S. C.-Y. Chen et al., 2011; Choi et al., 2015; Ely et al., 2009; Maepa et al., 2017). Ely et al. (2009) created anti-HBV multiple amiRNA cassettes to efficiently inhibit viral replication without off-target effects. For this purpose, pri-miR-31, miR-30a, and miR-122 were used as siRNA shuttles and expressed under the strong Pol II promoter. AmiRNA sequences were targeted to a conserved region within the HBV X (*HBx*) ORF. By determining secreted HBV surface antigen (HBsAg) levels, the authors demonstrated approximately 90% knockdown of the target. Nonspecific effects were excluded by analysis of the interferon response. The IFN- β mRNA concentration was measured in transfected cells, the results of which showed no immunostimulation. AmiRNA processing was analyzed by northern blot analysis. The obtained data showed the usefulness of pri-miR-31 for the production of Pol II trimeric cassettes. Moreover, coinjection of mice with HBV plasmid and miR-31-based amiRNA resulted in the remarkable knockdown of HBsAg. These findings confirmed the capability for pri-miR-31 to be used as a shuttle for trimeric amiRNAs to achieve effective silencing of HBV replication *in vivo*.

In vivo studies have also been conducted by H. Zhang et al. (2015). The aim of one of their studies was to suppress influenza A virus replication by amiRNAs targeting a highly conserved regions (the M1, M2, or nucleoprotein genes). The authors justified the importance of their research by noting the limitation of currently produced viral vaccines. For example, current viral vaccines do not guarantee cross-protection against antigenic variant strains and do not adequately protect immunocompromised or elderly people. Recombinant Ad was used to deliver agents to cells and mice, because of its tissue tropism and potent gene expression in cells of the lower respiratory tract. In transduced HEK293T cells, designed amiRNAs could inhibit viral replication up to 80%. Interestingly, coexpression of the most potent therapeutic agents in one vector failed to enhance this inhibition. Zhang and colleagues also showed that cross-protection was possible by the use of amiRNA. Vaccinated mice gained resistance to not only lethal influenza (A/PR8), but also two heterotypic viruses (H9N2 and H5N1). The authors summarized their experiments by suggesting that the targeting of conserved regions of influenza virus by amiRNAs can be considered an innovative way to prevent viral infection.

Another approach used a combinatorial gene expression cassette that included, in addition to multiple amiRNAs targeted to preterminal proteins, the gene encoding HSV thymidine kinase (HSV-TK). Gene expression was driven by the CMV promoter (amiRNAs) and E4 promoter (HSV-TK). Adenovirus replication in A549 cells was inhibited using this construct. HSV-TK is necessary to convert ganciclovir (GCV), an antiherpetic prodrug, to its active form. When activated, ganciclovir blocks viral and cellular DNA synthesis by acting as a competitive nucleotide analog. Interestingly, the authors inserted this cassette into replication-deficient Ad vector (in which the E1 and E3 genes had been deleted). Such Ad vectors ensure delivery of a therapeutic agent to the same location targeted by the wild-type Ad. The simultaneous treatment of cells with a single amiRNA, wt virus, and GCV resulted in a greater decrease in wt Ad genome copy number than treatment without GCV. There was an approximately 1.7 order of magnitude difference between the copy numbers of these two variants. The insertion of additional copies of the amiRNA reduced the dose of GCV required, because even at a lower concentration, the combination of GCV with multiple amiRNAs was more efficient than the combination of the highest dose of GCV with a single amiRNA. The authors claimed that the created combinatorial amiRNA/HSV-TK cassette might be a useful tool to inhibit Ad replication and spread (Ibrišimović, Lion, et al., 2013).

Combinatorial therapy was also investigated by Saha et al. (2016), who combined amiRNA treatment with several antivirals (chloroquine, ribavirin, and mycophenolic acid) to inhibit the replication of Chikungunya virus in Vero cells. These combination treatments noticeably reduced viral replication, but interestingly, only the combination of amiRNA with chloroquine inhibited replication more than amiRNA or the antiviral alone. The authors suspected that the combination of these two compounds arrested the viral life cycle at both the early and late stages. The undesirable effect of ribavirin-amiRNA was justified by the possible interference of ribavirin with the RNAi pathway.

8 | CANCER

According to the World Health Organization, in addition to cardiovascular diseases, cancer is one of the main causes of death worldwide. Cellular changes that determine carcinogenesis may have many causes, including genetic conditions as well as biological, physical or chemical carcinogens (Schulz, 2007). Based on the GLOBOCAN 2018 report, the most

common cancers are breast, prostate, lung and colorectal cancers. Every year, the number of cancer cases increases, and forecasts for future years are unsatisfactory; therefore, the most effective therapies are constantly sought. Despite the wide range of therapies for cancer, many cancers remain incurable, and treatment results are unsatisfactory. This is because of not only tumor metastasis, but also heterogeneity and resistance to chemotherapy (S. Wang et al., 2012).

Many scientists have invested their efforts in RNAi therapy. Thus far, researchers have designed amiRNAs to treat breast, pancreatic, gastric, and cervical cancers as well melanoma and hepatocellular carcinoma (Bonetta et al., 2015; Z. Li et al., 2006; Liang et al., 2007; C. Liu et al., 2016; X. Liu et al., 2012) (Table S2). Almost all of these amiRNAs have used the miR-155 backbone and CMV promoter. For example, pri-miR-155-based amiRNAs targeting vascular endothelial growth factor receptor (VEGFR) were designed to treat pancreatic ductal carcinoma. VEGFRs play a critical role in angiogenesis regulation and are overexpressed in cancer cells. Vectors containing amiRNAs homologous to the sequences of all three types of VEGFRs (VEGFR1, VEGFR2, and VEGFR3) were generated. Moreover, researchers designed an amiRNA vector that contained all three cassettes in tandem. The authors tested the efficacy of the vectors by transfecting pancreatic cell lines and by injecting SW1990 cells into athymic nude mice. The results showed that each amiRNA significantly reduced VEGFR1, 2, and 3 mRNA and protein levels by >50%, and the triple-amiRNA vector reduced the expression of all three genes. Moreover, the transfected cells were much less proliferative than mock-treated cells. Their invasive ability was inhibited up to 80%, and apoptosis in both the early and late stages was increased. In mice, treatment with the triple-amiRNA vector combined with cisplatin completely inhibited tumor growth. The authors did not analyze amiRNA processing or off-target effects in any way, but they confirmed the safety of the amiRNAs by analyzing the morphology and functionality of the mouse pancreas. Despite several limitations, the authors suggested that treatment with multiple amiRNAs is very promising (J. Huang et al., 2017).

A similar approach with three amiRNAs was used to target p21, a protein with an inhibitory effect on p53-mediated apoptosis. The authors confirmed that a tandem array suppressed the induction of p21 in HEK293T cells. Moreover, the simultaneous suppression of p21 and expression of p53 in cancer cells caused increase of apoptosis. Experiments were also performed *in vivo*. Intratumoral injection of therapeutic Ad-p53/amiRNA-p21 resulted in a smaller tumor volume. Notably, the authors also confirmed that p21 suppression in the absence of p53 overexpression increases the risk of cancer progression and should be considered important in future studies (Idogawa et al., 2009).

Pri-miR-30a was used as a shuttle for amiRNAs targeted to glyceraldehyde-3-phosphate dehydrogenase (GAPDH), eukaryotic translation initiation factor 4E (eIF4E), and DNA polymerase α . The aim of this study was to test the anti-tumor effect of the knockdown of essential genes for cell survival on hepatocellular carcinoma. All the constructs were expressed under the tissue-specific AFP promoter to ensure safety and delivered to cells and mice by recombinant Ad. The obtained data showed the efficient knockdown of target genes, which had an antitumor effect. Moreover, simultaneous infection with all amiRNAs significantly downregulated the target genes. The authors observed that ATP production and protein synthesis were inhibited and arrest of the cell cycle. The survival rate of the cells was lower than that of control cells. In mice, the delivery of amiRNA targeted to GAPDH caused destruction of the tumor. The authors also noted that, this treatment strategy may have few limitations, but despite these limitations, their results suggest a novel therapeutic approach (C. Mao et al., 2015).

In many other studies, genes related to the tumor progression and metastasis' pathways have been targeted by amiRNAs. For example, recombinant Ad was used to deliver CDH17-specific amiRNA to gastric cancer cells. CDH17, a type of cadherin, is correlated with tumor differentiation and lymph node metastasis. The treatment of cells with amiRNA reduced cancer cell motility and proliferation due to downregulation of the target gene (J. Zhang et al., 2011).

Notably, amiRNA treatment can be combined with another kind of therapy, such as radiation. With this approach, brain tumor and lung cancer cells were treated with amiRNA targeted to either a crucial factor for nonhomologous end joining (XRCC4) or a crucial factor for homologous recombination repair (XRCC2). Next, the cells were exposed to X-rays or ion (carbon) radiation. The results showed that targeting only the XRCC2 or HRR pathway sensitized tumor cells to high-LET radiation *in vitro* and *in vivo*, suggesting that this combination has therapeutic potential (Zheng et al., 2013).

9 | OTHER DISEASES

In addition to neurodegenerative diseases, viral infections, and cancers, amiRNAs have been used as therapeutic agents in the therapy of Pelizaeus–Merzbacher disease (PMD), osteoporosis, cardiovascular disorders, sickle cell disease (SCD), myotonic dystrophy (DM1), facioscapulohumeral muscular dystrophy (FSHD), hyperalgesia, familial

hypercholesterolemia (FH), and alcohol abuse (Table S3). PMD is a hypomyelinating leukodystrophy caused by overexpression of the proteolipid protein 1 (Plp1) gene in oligodendrocytes. This X-linked disorder is currently incurable. In 2019, H. Li et al. (2019) proposed scAAV-mediated gene-specific suppression as a potential treatment for PMD. Pri-miR-155-based amiRNA targeting Plp1 expressed under the human CNP promoter (chosen because of its size and high activity in oligodendrocytes) was injected into the corpus striatum and internal capsule of mice. In oligodendrocytes, Plp1 mRNA and protein levels were reduced by ~50% compared to those in controls. Moreover, the authors analyzed off-target effects by measuring the expression of eight genes with 60% or more complementarity to amiRNA seed sequences. Based on the lack of a significant difference in the expression of these genes and because their downregulation did not affect the expression of other oligodendrocyte-associated genes, the authors confirmed the safety of their therapeutic approach. Furthermore, they observed lifespan extension, bodyweight gain, and improved motor functions in treated mice. Although the myelin structure was preserved, an increased number of mature oligodendrocytes and suppression of astrogliosis and microgliosis were demonstrated.

An interesting method of off-target suppression was recently demonstrated by Y.-S. Yang et al. (2020). They created amiRNAs based on the pri-miR-33 backbone directed against two genes related to osteoporosis progression: cathepsin K (responsible for type 1 collagen degradation) and RANK (a tumor necrosis factor, crucial for the differentiation of monocytes to osteoclasts). The authors injected 2-month-old mice with AAV9 vector carrying the amiRNAs. Femur analysis showed that both amiRNAs suppressed expression of the rank and ctsk genes by approximately 60%. An increase in trabecular bone mass was also observed. The Yang group also noticed that treatment with the amiRNA targeted to rank caused a reduction in osteoclast differentiation, while osteoblast activity remained stable. In turn, targeting ctsk impaired bone resorption and caused bone formation (due to osteoblast activity) but did not affect osteoclasts. Finally, the authors concluded that targeting ctsk has more potential than targeting rank; therefore, they used this amiRNA for further experiments. To minimize off-target effects, which can be induced because cathepsin K is expressed in many nonskeletal organs, such as the heart or skin, the authors modified the viral capsid. They added two different peptide motifs, either (Asp-Ser-Ser)₆ or (Asp)₁₄, to the N-terminus of the VP2 capsid protein subunit. These motifs were reported to guide liposomes to either osteoblast-enriched surfaces or osteoclast-enriched surfaces, respectively. The authors showed that incorporation of these modifications did not reduce viral efficiency and concluded that addition of the (Asp-Ser-Ser)₆ motif improved bone-homing rAAV9 specificity by the observation that transduction to other tissues was reduced. Then, they packaged the amiRNA targeted to ctsk into a modified capsid and tested its final therapeutic potential. Injection of this agent protected against bone loss in the femurs of ovariectomized mice. In a rodent model of senile osteoporosis, virus injection resulted in reduced *ctsk* expression and increased trabecular bone mass in the femur and lumbar vertebrae. Through this research, the authors confirmed the clinical utility of an rAAV-mediated therapeutic agent for the treatment of postmenopausal and senile osteoporosis, which has advantages over conventional antiosteoporotic drugs (Y.-S. Yang et al., 2020).

Among cardiovascular diseases, hypertension and heart failure have been treated with amiRNAs (Fan et al., 2012; Größl et al., 2014). The aim of the first study was to determine whether mir-155-based AT1aR (angiotensin II type 1 receptor, overexpressed in spontaneously hypertensive rats) amiRNA could impair hypertension and improve cardiovascular remodeling in spontaneously hypertensive rats. Injection of rAd to the brain resulted in reduced target expression and therefore decreased arterial blood pressure, improved myocardial, and vascular remodeling and protection from hypertension (Fan et al., 2012).

The advantage of amiRNAs over shRNAs in terms of safety was demonstrated in another study that aimed to improve diminished Ca²⁺ homeostasis—a common cause of heart failure. In their previous research, the authors observed the toxicity of shRNA targeted to phospholamban (PLB). Therefore, they designed a miR-155-based amiRNA targeted to PLB expressed under a heart-specific promoter. The AAV6 vector was used as a vehicle for delivery because of its specificity to cardiac cells. Despite decreased amiRNA expression, both RNAi triggers reduced PLB expression equally and enhanced Ca²⁺ transport. Proteomic analysis showed that the shRNA induced the expression of interferon-regulated and proinflammatory genes whereas artificial miRNA did not induce any of them (Größl et al., 2014).

Currently a phase 1 of clinical trial for SCD is conducted (NCT03282656). Researchers are recruiting patients for treatment consisting of autologous transplantation of bone marrow derived CD34⁺ HSC cells transduced with the LV containing amiRNA targeting *BCL11A* gene. Previous research showed that downregulation of this gene results in activation of γ -globin which then induces fetal hemoglobin (HbF; Brendel et al., 2016; Guda et al., 2015; Sankaran et al., 2008). This in turn results in prevention from sickling of red blood cells which is characteristic hallmark of SCD. Therapeutic agent consists of miR-223-based amiRNA expressed under Pol II promoter (β -globin) and packed into

improved LV vector (BCH-BB694), which demonstrates enhanced titer characteristics (Brendel et al., 2020). Using this system, the authors achieved efficient knockdown of target in transduced CD34⁺ derived erythroid cells, γ -globin induction and more than 50% raised HbF level (Guda et al., 2015). In addition, they confirmed safety of the therapy in pre-clinical studies and its readiness to clinical trials (Brendel et al., 2020).

Promising results were also obtained with the use of miR-30-based amiRNAs for diseases related to muscle tissue, DM1 and FSHD (Bisset et al., 2015; Wallace et al., 2012, 2017). For the treatment of hyperalgesia, miR-144-based amiRNA was used to downregulate acid-sensing ion channel 3 (*ASIC3*) gene (Walder et al., 2011). AmiRNAs in a miR-155 backbone were successfully used in preclinical studies for familial hypercholesterolemia (Kerr et al., 2016) and even alcohol abuse (Baek et al., 2010).

10 | CONCLUSION

RNAi is a powerful technology used to study gene function, and siRNA/shRNA remain the first-choice molecules for the temporal knockdown of gene expression. The relatively decreased interest in amiRNAs and their decreased use compared to shRNA probably result from their more complex design and less predictable processing compared to those of shRNA, which may lead to lower silencing efficiency. However, well-designed amiRNAs are as effective as shRNAs (although they generate 10–80 times less siRNA), provide long-term silencing and, above all, are safer than other RNAi triggers. These features make amiRNAs ideal tools for gene therapy approaches, particularly for well-defined and incurable monogenic disorders.

Our knowledge regarding the rules governing miRNA biogenesis is constantly expanding; therefore, the rational design of amiRNAs seems to have become easier. The potency of amiRNAs as therapeutic RNAi triggers has been demonstrated in a number of preclinical studies for the treatment of different types of disorders. However, in the vast majority of studies, the specificity of amiRNA processing and amiRNA expression level were not tested. Detailed information on the siRNA variants resulting from amiRNA processing as well as the contribution of passenger and guide strands is necessary to assess the risk of off-target effects. In this regard, DICER-independent pri-miR-451 has advantages over other pri-miRNA backbones because it does not generate a passenger strand. However, it generates 3' isomiRs, which can theoretically interact nonspecifically in cells. The knowledge of mature siRNA levels in relation to endogenous miRNA levels helps to predict the risk of saturation of the miRNA biogenesis pathway. Research suggests that the use of tissue-specific Pol II promoters for amiRNA expression minimizes this risk. Obtaining the full safety profiles of amiRNA therapeutics requires detailed analysis of the transcriptome deregulation resulting from off-target interactions. This analysis should be performed in a relevant cellular and/or animal model by NGS and confirmed by other methods, such as qRT-PCR and western blotting. It is almost impossible to not disturb the physiological conditions of cells by virus transduction and the overexpression of exogenous material. However, amiRNAs are more “natural” than other gene therapy tools in terms of their structure, biogenesis, and expression levels.

In general, the safety of therapeutic tools as well as delivery issues are common problems in gene therapy. Recent years have yielded progress in the development of viral vectors; however, the effective delivery of amiRNAs to some tissues, for example, deep brain structures, remains a challenge. Stereotactic injection of AAV5 directly into the striatum is currently the best way to deliver HTT-targeting amiRNAs in clinical trials. Intravenous injection would not only be more comfortable to patients, but also reduce costs associated with complex brain surgery. In contrast to genome editing systems, such as the clustered regularly interspaced short palindromic repeats (CRISPR)-Cas9 or transcription activator-like effector nucleases (TALENs), amiRNA expression cassettes are much smaller and can be packaged into almost all known viral vectors. They also do not cause irreversible changes, unlike genome editing technology, and use the natural protein machinery of the cell.

Taken together, these studies show that all currently used therapeutic approaches, including ASOs, RNAi, and genome editing, have their advantages, but each also suffers from many limitations. The degree of its advancement depends on the time spent on the development of a particular technology, and ASOs have an advantage in this respect, which is confirmed in the number of approved therapies. Perhaps the time for RNAi is just arriving.

CONFLICT OF INTEREST

The authors have declared no conflicts of interest for this article.

AUTHOR CONTRIBUTIONS

Anna Kotowska-Zimmer: Visualization; writing-original draft. **Marianna Pewińska:** Conceptualization; writing-original draft. **Marta Olejniczak:** Conceptualization; resources; supervision; writing-original draft.

ORCID

Marianna Pewinska  <https://orcid.org/0000-0002-9298-1955>

Marta Olejniczak  <https://orcid.org/0000-0001-8471-6302>

RELATED WIREs ARTICLES

[RNA Interference to Treat Virus Infections](#)

[RNA Interference in Cancer Therapy](#)

REFERENCES

- Aagaard, L., Zhang, J., von Eije, K. J., Li, H., Sætrom, P., Amarzguioui, M., & Rossi, J. J. (2008). Engineering and optimization of the mir-106b-cluster for ectopic expression of multiplexed anti-HIV RNAs. *Gene Therapy*, *15*(23), 1536–1549. <https://doi.org/10.1038/gt.2008.147>
- Altuvia, Y., Landgraf, P., Lithwick, G., Elefant, N., Pfeffer, S., Aravin, A., Brownstein, M. J., Tuschl, T., & Margalit, H. (2005). Clustering and conservation patterns of human microRNAs. *Nucleic Acids Research*, *33*(8), 2697–2706. <https://doi.org/10.1093/nar/gki567>
- Andersson, M. G., Haasnoot, P. C. J., Xu, N., Berenjian, S., Berkhout, B., & Akusjärvi, G. (2005). Suppression of RNA interference by adenovirus virus-associated RNA. *Journal of Virology*, *79*(15), 9556–9565. <https://doi.org/10.1128/JVI.79.15.9556-9565.2005>
- Ashizawa, T., Öz, G., & Paulson, H. L. (2018). Spinocerebellar ataxias: Prospects and challenges for therapy development. *Nature Reviews. Neurology*, *14*(10), 590–605. <https://doi.org/10.1038/s41582-018-0051-6>
- Auyeung, V. C., Ulitsky, I., McGeary, S. E., & Bartel, D. P. (2013). Beyond secondary structure: Primary-sequence determinants license pri-miRNA hairpins for processing. *Cell*, *152*(4), 844–858. <https://doi.org/10.1016/j.cell.2013.01.031>
- Baek, M. N., Jung, K. H., Halder, D., Choi, M. R., Lee, B.-H., Lee, B.-C., Jung, M. H., Choi, I.-G., Chung, M.-K., Oh, D.-Y., & Chai, Y. G. (2010). Artificial microRNA-based neurokinin-1 receptor gene silencing reduces alcohol consumption in mice. *Neuroscience Letters*, *475*(3), 124–128. <https://doi.org/10.1016/j.neulet.2010.03.051>
- Bartel, D. P. (2004). MicroRNAs: Genomics, biogenesis, mechanism, and function. *Cell*, *116*(2), 281–297. [https://doi.org/10.1016/s0092-8674\(04\)00045-5](https://doi.org/10.1016/s0092-8674(04)00045-5)
- Bartel, D. P. (2018). Metazoan MicroRNAs. *Cell*, *173*(1), 20–51. <https://doi.org/10.1016/j.cell.2018.03.006>
- Bauer, M., Kinkl, N., Meixner, A., Kremmer, E., Riemenschneider, M., Förstl, H., Gasser, T., & Ueffing, M. (2009). Prevention of interferon-stimulated gene expression using microRNA-designed hairpins. *Gene Therapy*, *16*(1), 142–147. <https://doi.org/10.1038/gt.2008.123>
- Bisset, D. R., Stepniak-Konieczna, E. A., Zavaljevski, M., Wei, J., Carter, G. T., Weiss, M. D., & Chamberlain, J. R. (2015). Therapeutic impact of systemic AAV-mediated RNA interference in a mouse model of myotonic dystrophy. *Human Molecular Genetics*, *24*(17), 4971–4983. <https://doi.org/10.1093/hmg/ddv219>
- Bonetta, A., Maily, L., Robinet, E., Travé, G., Masson, M., & Deryckere, F. (2015). Artificial microRNAs against the viral E6 protein provoke apoptosis in HPV positive cancer cells. *Biochemical and Biophysical Research Communications*, *465*, 658–664. <https://doi.org/10.1016/j.bbrc.2015.07.144>
- Borel, F., Gernoux, G., Cardozo, B., Metterville, J. P., Toro Cabreja, G. C., Song, L., Su, Q., Gao, G. P., Elmallah, M. K., Brown, R. H., & Mueller, C. (2016). Therapeutic rAAVrh10 mediated SOD1 silencing in adult SOD1G93A mice and nonhuman Primates. *Human Gene Therapy*, *27*(1), 19–31. <https://doi.org/10.1089/hum.2015.122>
- Borel, F., Gernoux, G., Sun, H., Stock, R., Blackwood, M., Brown, R. H., & Mueller, C. (2018). Safe and effective superoxide dismutase 1 silencing using artificial microRNA in macaques. *Science Translational Medicine*, *10*(465), eaau6414. <https://doi.org/10.1126/scitranslmed.aau6414>
- Boudreau, R., Martins, I., & Davidson, B. L. (2009). Artificial microRNAs as siRNA shuttles: Improved safety as compared to shRNAs in vitro and in vivo. *Molecular Therapy: The Journal of the American Society of Gene Therapy*, *17*(1), 169–175. <https://doi.org/10.1038/mt.2008.231>
- Boudreau, R. L., McBride, J. L., Martins, I., Shen, S., Xing, Y., Carter, B. J., & Davidson, B. L. (2009). Nonallele-specific silencing of mutant and wild-type Huntingtin demonstrates therapeutic efficacy in Huntington's disease mice. *Molecular Therapy: The Journal of the American Society of Gene Therapy*, *17*(6), 1053–1063. <https://doi.org/10.1038/mt.2009.17>
- Boudreau, R. L., Monteys, A. M., & Davidson, B. L. (2008). Minimizing variables among hairpin-based RNAi vectors reveals the potency of shRNAs. *RNA*, *14*(9), 1834–1844. <https://doi.org/10.1261/rna.1062908>
- Brendel, C., Guda, S., Renella, R., Bauer, D. E., Canver, M. C., Kim, Y.-J., Heeney, M. M., Klatt, D., Fogel, J., Milsom, M. D., Orkin, S. H., Gregory, R. I., & Williams, D. A. (2016). Lineage-specific BCL11A knockdown circumvents toxicities and reverses sickle phenotype. *The Journal of Clinical Investigation*, *126*(10), 3868–3878. <https://doi.org/10.1172/JCI87885>
- Brendel, C., Negre, O., Rothe, M., Guda, S., Parsons, G., Harris, C., McGuinness, M., Abriss, D., Tsytsykova, A., Klatt, D., Bentler, M., Pellin, D., Christiansen, L., Schambach, A., Manis, J., Trebeden-Negre, H., Bonner, M., Esrick, E., Veres, G., ... Williams, D. A. (2020). Preclinical evaluation of a novel lentiviral vector driving lineage-specific BCL11A knockdown for sickle cell gene therapy. *Molecular Therapy—Methods & Clinical Development*, *17*, 589–600. <https://doi.org/10.1016/j.omtm.2020.03.015>

- Buijsen, R. A. M., Toonen, L. J. A., Gardiner, S. L., & van Roon-Mom, W. M. C. (2019). Genetics, mechanisms, and therapeutic progress in polyglutamine spinocerebellar ataxias. *Neurotherapeutics: The Journal of the American Society for Experimental Neurotherapeutics*, 16(2), 263–286. <https://doi.org/10.1007/s13311-018-00696-y>
- Cai, X., Hagedorn, C. H., & Cullen, B. R. (2004). Human microRNAs are processed from capped, polyadenylated transcripts that can also function as mRNAs. *RNA (New York, N.Y.)*, 10(12), 1957–1966. <https://doi.org/10.1261/rna.7135204>
- Calloni, R., & Bonatto, D. (2015). Scaffolds for artificial miRNA expression in animal cells. *Human Gene Therapy Methods*, 26(5), 162–174. <https://doi.org/10.1089/hgtb.2015.043>
- Carbonell, A., & Daròs, J.-A. (2019). Design, synthesis, and functional analysis of highly specific artificial small RNAs with antiviral activity in plants. *Methods in Molecular Biology (Clifton, N.J.)*, 2028, 231–246. https://doi.org/10.1007/978-1-4939-9635-3_13
- Chang, K., Elledge, S. J., & Hannon, G. J. (2006). Lessons from nature: MicroRNA-based shRNA libraries. *Nature Methods*, 3(9), 707–714. <https://doi.org/10.1038/nmeth923>
- Cheloufi, S., Dos Santos, C. O., Chong, M. M. W., & Hannon, G. J. (2010). A Dicer-independent miRNA biogenesis pathway that requires ago catalysis. *Nature*, 465(7298), 584–589. <https://doi.org/10.1038/nature09092>
- Chen, H.-H., Mack, L. M., Kelly, R., Ontell, M., Kochanek, S., & Clemens, P. R. (1997). Persistence in muscle of an adenoviral vector that lacks all viral genes. *Proceedings of the National Academy of Sciences of the United States of America*, 94(5), 1645–1650.
- Chen, J.-F., Mandel, E. M., Thomson, J. M., Wu, Q., Callis, T. E., Hammond, S. M., Conlon, F. L., & Wang, D.-Z. (2006). The role of microRNA-1 and microRNA-133 in skeletal muscle proliferation and differentiation. *Nature Genetics*, 38(2), 228–233. <https://doi.org/10.1038/ng1725>
- Chen, S. C.-Y., Stern, P., Guo, Z., & Chen, J. (2011). Expression of multiple artificial microRNAs from a chicken miRNA126-based lentiviral vector. *PLoS One*, 6(7), e22437. <https://doi.org/10.1371/journal.pone.0022437>
- Chendrimada, T. P., Gregory, R. I., Kumaraswamy, E., Norman, J., Cooch, N., Nishikura, K., & Shiekhattar, R. (2005). TRBP recruits the Dicer complex to Ago2 for microRNA processing and gene silencing. *Nature*, 436(7051), 740–744. <https://doi.org/10.1038/nature03868>
- Choi, J.-G., Bharaj, P., Abraham, S., Ma, H., Yi, G., Ye, C., Dang, Y., Manjunath, N., Wu, H., & Shankar, P. (2015). Multiplexing seven miRNA-based shRNAs to suppress HIV replication. *Molecular Therapy*, 23(2), 310–320. <https://doi.org/10.1038/mt.2014.205>
- Chung, K.-H., Hart, C. C., Al-Bassam, S., Avery, A., Taylor, J., Patel, P. D., Vojtek, A. B., & Turner, D. L. (2006). Polycistronic RNA polymerase II expression vectors for RNA interference based on BIC/miR-155. *Nucleic Acids Research*, 34(7), e53. <https://doi.org/10.1093/nar/gkl143>
- Concepcion, C. P., Bonetti, C., & Ventura, A. (2012). The miR-17-92 family of microRNA clusters in development and disease. *Cancer Journal (Sudbury, Mass.)*, 18(3), 262–267. <https://doi.org/10.1097/PPO.0b013e318258b60a>
- Daya, S., & Berns, K. I. (2008). Gene therapy using Adeno-associated virus vectors. *Clinical Microbiology Reviews*, 21(4), 583–593. <https://doi.org/10.1128/CMR.00008-08>
- Dhungal, B. P., Bailey, C. G., & Rasko, J. E. J. (2020). Journey to the center of the cell: Tracing the path of AAV transduction. *Trends in Molecular Medicine*. <https://doi.org/10.1016/j.molmed.2020.09.010>
- Dickins, R. A., Hemann, M. T., Zilfou, J. T., Simpson, D. R., Ibarra, I., Hannon, G. J., & Lowe, S. W. (2005). Probing tumor phenotypes using stable and regulated synthetic microRNA precursors. *Nature Genetics*, 37(11), 1289–1295. <https://doi.org/10.1038/ng1651>
- Dore, L. C., Amigo, J. D., dos Santos, C. O., Zhang, Z., Gai, X., Tobias, J. W., Yu, D., Klein, A. M., Dorman, C., Wu, W., Hardison, R. C., Paw, B. H., & Weiss, M. J. (2008). A GATA-1-regulated microRNA locus essential for erythropoiesis. *Proceedings of the National Academy of Sciences of the United States of America*, 105(9), 3333–3338. <https://doi.org/10.1073/pnas.0712312105>
- Du, G., Yonekubo, J., Zeng, Y., Osisami, M., & Frohman, M. A. (2006). Design of expression vectors for RNA interference based on miRNAs and RNA splicing. *The FEBS Journal*, 273(23), 5421–5427. <https://doi.org/10.1111/j.1742-4658.2006.05534.x>
- Dufour, B. D., Smith, C. A., Clark, R. L., Walker, T. R., & McBride, J. L. (2014). Intrajugular vein delivery of AAV9-RNAi prevents neuropathological changes and weight loss in Huntington's disease mice. *Molecular Therapy*, 22(4), 797–810. <https://doi.org/10.1038/mt.2013.289>
- Duyao, M., Ambrose, C., Myers, R., Novelletto, A., Persichetti, F., Frontali, M., Folstein, S., Ross, C., Franz, M., & Abbott, M. (1993). Trinucleotide repeat length instability and age of onset in Huntington's disease. *Nature Genetics*, 4(4), 387–392. <https://doi.org/10.1038/ng0893-387>
- Elbashir, S. M., Lendeckel, W., & Tuschl, T. (2001). RNA interference is mediated by 21- and 22-nucleotide RNAs. *Genes & Development*, 15(2), 188–200.
- Ely, A., Naidoo, T., & Arbuthnot, P. (2009). Efficient silencing of gene expression with modular trimeric Pol II expression cassettes comprising microRNA shuttles. *Nucleic Acids Research*, 37(13), e91. <https://doi.org/10.1093/nar/gkp446>
- Ely, A., Naidoo, T., Mufamadi, S., Crowther, C., & Arbuthnot, P. (2008). Expressed anti-HBV primary microRNA shuttles inhibit viral replication efficiently in vitro and in vivo. *Molecular Therapy: The Journal of the American Society of Gene Therapy*, 16(6), 1105–1112. <https://doi.org/10.1038/mt.2008.82>
- Evers, M., Miniarikova, J., Juhas, S., Vallès, A., Bohuslavova, B., Juhasova, J., Skalníková, H. K., Vodicka, P., Valekova, I., Brouwers, C., Blits, B., Lubelski, J., Kovarova, H., Ellederova, Z., van Deventer, S. J., Petry, H., Motlik, J., & Konstantinova, P. (2018). AAV5-miHTT gene therapy demonstrates broad distribution and strong human mutant Huntingtin lowering in a Huntington's disease Minipig model. *Molecular Therapy: The Journal of the American Society of Gene Therapy*, 26(9), 2163–2177. <https://doi.org/10.1016/j.yth.2018.06.021>
- Fan, Z.-D., Zhang, L., Shi, Z., Gan, X.-B., Gao, X.-Y., & Zhu, G.-Q. (2012). Artificial microRNA interference targeting AT1a receptors in paraventricular nucleus attenuates hypertension in rats. *Gene Therapy*, 19(8), 810–817. <https://doi.org/10.1038/gt.2011.145>

- Fang, W., & Bartel, D. P. (2015). The menu of features that define primary microRNAs and enable de novo design of microRNA genes. *Molecular Cell*, 60(1), 131–145. <https://doi.org/10.1016/j.molcel.2015.08.015>
- Faraoni, I., Antonetti, F. R., Cardone, J., & Bonmassar, E. (2009). miR-155 gene: A typical multifunctional microRNA. *Biochimica et Biophysica Acta (BBA) - Molecular Basis of Disease*, 1792(6), 497–505. <https://doi.org/10.1016/j.bbadis.2009.02.013>
- Fellmann, C., Hoffmann, T., Sridhar, V., Hopfgartner, B., Muhar, M., Roth, M., Lai, D. Y., Barbosa, I. A. M., Kwon, J. S., Guan, Y., Sinha, N., & Zuber, J. (2013). An optimized microRNA backbone for effective single-copy RNAi. *Cell Reports*, 5(6), 1704–1713. <https://doi.org/10.1016/j.celrep.2013.11.020>
- Galka-Marciniak, P., Olejniczak, M., Starega-Roslan, J., Szczesniak, M. W., Makalowska, I., & Krzyzosiak, W. J. (2016). SiRNA release from pri-miRNA scaffolds is controlled by the sequence and structure of RNA. *Biochimica et Biophysica Acta (BBA) - Gene Regulatory Mechanisms*, 1859(4), 639–649. <https://doi.org/10.1016/j.bbgrm.2016.02.014>
- Gao, Y.-F., Yu, L., Wei, W., Li, J.-B., Luo, Q.-L., & Shen, J.-L. (2008). Inhibition of hepatitis B virus gene expression and replication by artificial microRNA. *World Journal of Gastroenterology: WJG*, 14(29), 4684–4689. <https://doi.org/10.3748/wjg.14.4684>
- Girardi, E., López, P., & Pfeffer, S. (2018). On the importance of host MicroRNAs during viral infection. *Frontiers in Genetics*, 9, 439. <https://doi.org/10.3389/fgene.2018.00439>
- Grishok, A., Pasquinelli, A. E., Conte, D., Li, N., Parrish, S., Ha, I., Baillie, D. L., Fire, A., Ruvkun, G., & Mello, C. C. (2001). Genes and mechanisms related to RNA interference regulate expression of the small temporal RNAs that control *C. elegans* developmental timing. *Cell*, 106(1), 23–34. [https://doi.org/10.1016/s0092-8674\(01\)00431-7](https://doi.org/10.1016/s0092-8674(01)00431-7)
- Größl, T., Hammer, E., Bien-Möller, S., Geisler, A., Pinkert, S., Röger, C., Poller, W., Kurreck, J., Völker, U., Vetter, R., & Fechner, H. (2014). A novel artificial MicroRNA expressing AAV vector for phospholamban silencing in cardiomyocytes improves Ca²⁺ uptake into the sarcoplasmic reticulum. *PLoS One*, 9(3), e92188. <https://doi.org/10.1371/journal.pone.0092188>
- Guda, S., Brendel, C., Renella, R., Du, P., Bauer, D. E., Canver, M. C., Grenier, J. K., Grimson, A. W., Kamran, S. C., Thornton, J., de Boer, H., Root, D. E., Milsom, M. D., Orkin, S. H., Gregory, R. I., & Williams, D. A. (2015). MiRNA-embedded shRNAs for lineage-specific BCL11A knockdown and hemoglobin F induction. *Molecular Therapy: The Journal of the American Society of Gene Therapy*, 23(9), 1465–1474. <https://doi.org/10.1038/mt.2015.113>
- Ha, M., & Kim, V. N. (2014). Regulation of microRNA biogenesis. *Nature Reviews Molecular Cell Biology*, 15(8), 509–524. <https://doi.org/10.1038/nrm3838>
- Han, J., Lee, Y., Yeom, K.-H., Kim, Y.-K., Jin, H., & Kim, V. N. (2004). The Drosha-DGCR8 complex in primary microRNA processing. *Genes & Development*, 18(24), 3016–3027. <https://doi.org/10.1101/gad.1262504>
- Han, J., Lee, Y., Yeom, K.-H., Nam, J.-W., Heo, I., Rhee, J.-K., Sohn, S. Y., Cho, Y., Zhang, B.-T., & Kim, V. N. (2006). Molecular basis for the recognition of primary microRNAs by the Drosha-DGCR8 complex. *Cell*, 125(5), 887–901. <https://doi.org/10.1016/j.cell.2006.03.043>
- Herrera-Carrillo, E., Liu, Y. P., & Berkhout, B. (2017). Improving miRNA delivery by optimizing miRNA expression cassettes in diverse virus vectors. *Human Gene Therapy Methods*, 28(4), 177–190. <https://doi.org/10.1089/hgtb.2017.036>
- Huang, J., Mei, H., Tang, Z., Li, J., Zhang, X., Lu, Y., Huang, F., Jin, Q., & Wang, Z. (2017). Triple-amiRNA VEGFRs inhibition in pancreatic cancer improves the efficacy of chemotherapy through EMT regulation. *Journal of Controlled Release*, 245, 1–14. <https://doi.org/10.1016/j.jconrel.2016.11.024>
- Huang, X., & Jia, Z. (2013). Construction of HCC-targeting artificial miRNAs using natural miRNA precursors. *Experimental and Therapeutic Medicine*, 6(1), 209–215. <https://doi.org/10.3892/etm.2013.1111>
- Hutvagner, G., McLachlan, J., Pasquinelli, A. E., Bálint, E., Tuschl, T., & Zamore, P. D. (2001). A cellular function for the RNA-interference enzyme Dicer in the maturation of the let-7 small temporal RNA. *Science (New York, N.Y.)*, 293(5531), 834–838. <https://doi.org/10.1126/science.1062961>
- Ibrišimović, M., Kneidinger, D., Lion, T., & Klein, R. (2013). An adenoviral vector-based expression and delivery system for the inhibition of wild-type adenovirus replication by artificial microRNAs. *Antiviral Research*, 97(1), 10–23. <https://doi.org/10.1016/j.antiviral.2012.10.008>
- Ibrišimović, M., Lion, T., & Klein, R. (2013). Combinatorial targeting of 2 different steps in adenoviral DNA replication by herpes simplex virus thymidine kinase and artificial microRNA expression for the inhibition of virus multiplication in the presence of ganciclovir. *BMC Biotechnology*, 13, 54. <https://doi.org/10.1186/1472-6750-13-54>
- Idogawa, M., Sasaki, Y., Suzuki, H., Mita, H., Imai, K., Shinomura, Y., & Tokino, T. (2009). A single recombinant adenovirus expressing p53 and p21-targeting artificial microRNAs efficiently induces apoptosis in human cancer cells. *Clinical Cancer Research: An Official Journal of the American Association for Cancer Research*, 15(11), 3725–3732. <https://doi.org/10.1158/1078-0432.CCR-08-2396>
- Iwasaki, S., Kobayashi, M., Yoda, M., Sakaguchi, Y., Katsuma, S., Suzuki, T., & Tomari, Y. (2010). Hsc70/Hsp90 chaperone machinery mediates ATP-dependent RISC loading of small RNA duplexes. *Molecular Cell*, 39(2), 292–299. <https://doi.org/10.1016/j.molcel.2010.05.015>
- Jin, W., Wang, J., Liu, C.-P., Wang, H.-W., & Xu, R.-M. (2020). Structural basis for pri-miRNA recognition by Drosha. *Molecular Cell*, 78(3), 423–433.e5. <https://doi.org/10.1016/j.molcel.2020.02.024>
- Jopling, C. (2012). Liver-specific microRNA-122. *RNA Biology*, 9(2), 137–142. <https://doi.org/10.4161/rna.18827>
- Kabekkodu, S. P., Shukla, V., Varghese, V. K., Souza, J. D., Chakrabarty, S., & Satyamoorthy, K. (2018). Clustered miRNAs and their role in biological functions and diseases. *Biological Reviews*, 93(4), 1955–1986. <https://doi.org/10.1111/brv.12428>
- Karothia, D., Kumar Dash, P., Parida, M., Bhagyawant, S. S., & Kumar, J. S. (2020). Vector derived artificial miRNA mediated inhibition of West Nile virus replication and protein expression. *Gene*, 729, 144300. <https://doi.org/10.1016/j.gene.2019.144300>

- Keeler, A. M., Sapp, E., Chase, K., Sottosanti, E., Danielson, E., Pfister, E., Stoica, L., DiFiglia, M., Aronin, N., & Sena-Esteves, M. (2016). Cellular analysis of silencing the Huntington's disease gene using AAV9 mediated delivery of artificial micro RNA into the striatum of Q140/Q140 mice. *Journal of Huntington's Disease*, 5(3), 239–248. <https://doi.org/10.3233/JHD-160215>
- Keiser, M. S., Boudreau, R. L., & Davidson, B. L. (2014). Broad therapeutic benefit after RNAi expression vector delivery to deep cerebellar nuclei: Implications for spinocerebellar ataxia Type 1 therapy. *Molecular Therapy*, 22(3), 588–595. <https://doi.org/10.1038/mt.2013.279>
- Keiser, M. S., Geoghegan, J. C., Boudreau, R. L., Lennox, K. A., & Davidson, B. L. (2013). RNAi or overexpression: Alternative therapies for spinocerebellar ataxia Type 1. *Neurobiology of Disease*, 56, 6–13. <https://doi.org/10.1016/j.nbd.2013.04.003>
- Keiser, M. S., Kordower, J. H., Gonzalez-Alegre, P., & Davidson, B. L. (2015). Broad distribution of ataxin 1 silencing in rhesus cerebella for spinocerebellar ataxia type 1 therapy. *Brain*, 138(12), 3555–3566. <https://doi.org/10.1093/brain/awv292>
- Keiser, M. S., Monteys, A. M., Corbau, R., Gonzalez-Alegre, P., & Davidson, B. L. (2016). RNAi prevents and reverses phenotypes induced by mutant human ataxin-1. *Annals of Neurology*, 80(5), 754–765. <https://doi.org/10.1002/ana.24789>
- Kerr, A., Tam, L., Cioroch, M., Hale, A., Douglas, G., Channon, K., & Wade-Martins, R. (2016). A novel combinatorial non-viral vector to treat familial hypercholesterolaemia (FH). *Atherosclerosis*, 252, e238. <https://doi.org/10.1016/j.atherosclerosis.2016.07.018>
- Keskin, S., Brouwers, C. C., Sogorb-Gonzalez, M., Martier, R., Depla, J. A., Vallès, A., van Deventer, S. J., Konstantinova, P., & Evers, M. M. (2019). AAV5-miHTT lowers Huntingtin mRNA and protein without off-target effects in patient-derived neuronal cultures and astrocytes. *Molecular Therapy. Methods & Clinical Development*, 15, 275–284. <https://doi.org/10.1016/j.omtm.2019.09.010>
- Khvorova, A., Reynolds, A., & Jayasena, S. D. (2003). Functional siRNAs and miRNAs exhibit strand bias. *Cell*, 115(2), 209–216. [https://doi.org/10.1016/s0092-8674\(03\)00801-8](https://doi.org/10.1016/s0092-8674(03)00801-8)
- Kim, N., Nguyen, T. D., Li, S., & Nguyen, T. A. (2018). SRSF3 recruits DROSHA to the basal junction of primary microRNAs. *RNA*, 24(7), 892–898. <https://doi.org/10.1261/rna.065862.118>
- Kim, Y.-K., Kim, B., & Kim, V. N. (2016). Re-evaluation of the roles of DROSHA, Exportin 5, and DICER in microRNA biogenesis. *Proceedings of the National Academy of Sciences*, 113(13), E1881–E1889. <https://doi.org/10.1073/pnas.1602532113>
- Koch, P., Breuer, P., Peitz, M., Jungverdorben, J., Kesavan, J., Poppe, D., Doerr, J., Ladewig, J., Mertens, J., Tüting, T., Hoffmann, P., Klockgether, T., Evert, B. O., Wüllner, U., & Brüstle, O. (2011). Excitation-induced ataxin-3 aggregation in neurons from patients with Machado-Joseph disease. *Nature*, 480(7378), 543–546. <https://doi.org/10.1038/nature10671>
- Kretov, D. A., Walawalkar, I. A., Mora-Martin, A., Shafik, A. M., Moxon, S., & Cifuentes, D. (2020). Ago2-dependent processing allows miR-451 to evade the global microRNA turnover elicited during erythropoiesis. *Molecular Cell*, 78(2), 317–328. <https://doi.org/10.1016/j.molcel.2020.02.020>
- Kwon, S. C., Baek, S. C., Choi, Y.-G., Yang, J., Lee, Y.-S., Woo, J.-S., & Kim, V. N. (2019). Molecular basis for the single-nucleotide precision of primary microRNA processing. *Molecular Cell*, 73(3), 505–518.e5. <https://doi.org/10.1016/j.molcel.2018.11.005>
- Lebbink, R. J., Lowe, M., Chan, T., Khine, H., Wang, X., & McManus, M. T. (2011). Polymerase II promoter strength determines efficacy of microRNA adapted shRNAs. *PLoS One*, 6(10), e26213. <https://doi.org/10.1371/journal.pone.0026213>
- Lee, Y., Ahn, C., Han, J., Choi, H., Kim, J., Yim, J., Lee, J., Provost, P., Rådmark, O., Kim, S., & Kim, V. N. (2003). The nuclear RNase III Drosha initiates microRNA processing. *Nature*, 425(6956), 415–419. <https://doi.org/10.1038/nature01957>
- Lee, Y., Hur, I., Park, S.-Y., Kim, Y.-K., Suh, M. R., & Kim, V. N. (2006). The role of PACT in the RNA silencing pathway. *The EMBO Journal*, 25(3), 522–532. <https://doi.org/10.1038/sj.emboj.7600942>
- Lee, Y., Jeon, K., Lee, J.-T., Kim, S., & Kim, V. N. (2002). MicroRNA maturation: Stepwise processing and subcellular localization. *The EMBO Journal*, 21(17), 4663–4670. <https://doi.org/10.1093/emboj/cdf476>
- Li, H., Okada, H., Suzuki, S., Sakai, K., Izumi, H., Matsushima, Y., Ichinohe, N., Goto, Y.-I., Okada, T., & Inoue, K. (2019). Gene suppressing therapy for Pelizaeus-Merzbacher disease using artificial microRNA. *JCI Insight*, 4(10). <https://doi.org/10.1172/jci.insight.125052>
- Li, M., Husic, N., Lin, Y., Christensen, H., Malik, I., McIver, S., LaPash Daniels, C. M., Harris, D. A., Kotzbauer, P. T., Goldberg, M. P., & Snider, B. J. (2010). Optimal promoter usage for lentiviral vector-mediated transduction of cultured central nervous system cells. *Journal of Neuroscience Methods*, 189(1), 56–64. <https://doi.org/10.1016/j.jneumeth.2010.03.019>
- Li, S., Nguyen, T. D., Nguyen, T. L., & Nguyen, T. A. (2020). Mismatched and wobble base pairs govern primary microRNA processing by human microprocessor. *Nature Communications*, 11(1), 1926. <https://doi.org/10.1038/s41467-020-15674-2>
- Li, Z., Wenhua, Z., Zhao, W., Baohe, Z., Yulong, H., Junsheng, P., Shirong, C., & Jinping, M. (2006). Inhibition of PRL-3 gene expression in gastric cancer cell line SGC7901 via microRNA suppressed reduces peritoneal metastasis. *Biochemical and Biophysical Research Communications*, 348, 229–237. <https://doi.org/10.1016/j.bbrc.2006.07.043>
- Liang, Z., Wu, H., Reddy, S., Zhu, A., Wang, S., Blevins, D., Yoon, Y., Zhang, Y., & Shim, H. (2007). Blockade of invasion and metastasis of breast cancer cells via targeting CXCR4 with an artificial microRNA. *Biochemical and Biophysical Research Communications*, 363, 542–546. <https://doi.org/10.1016/j.bbrc.2007.09.007>
- Liu, C., Wang, S., Zhu, S., Wang, H., Gu, J., Gui, Z., Jing, J., Hou, X., & Shao, Y. (2016). MAP3K1-targeting therapeutic artificial miRNA suppresses the growth and invasion of breast cancer in vivo and in vitro. *Springerplus*, 5, 11. <https://doi.org/10.1186/s40064-015-1597-z>
- Liu, J., Carmell, M. A., Rivas, F. V., Marsden, C. G., Thomson, J. M., Song, J.-J., Hammond, S. M., Joshua-Tor, L., & Hannon, G. J. (2004). Argonaute2 is the catalytic engine of mammalian RNAi. *Science (New York, N.Y.)*, 305(5689), 1437–1441. <https://doi.org/10.1126/science.1102513>
- Liu, W., Pfister, E. L., Kennington, L. A., Chase, K. O., Mueller, C., DiFiglia, M., & Aronin, N. (2016). Does the mutant CAG expansion in huntingtin mRNA interfere with exonucleolytic cleavage of its first exon? *Journal of Huntington's Disease*, 5(1), 33–38. <https://doi.org/10.3233/JHD-150183>

- Liu, X., Fang, H., Chen, H., Jiang, X., Fang, D., Wang, Y., & Zhu, D. (2012). An artificial miRNA against HPSE suppresses melanoma invasion properties, correlating with a Down-regulation of chemokines and MAPK phosphorylation. *PLoS One*, 7(6), e38659. <https://doi.org/10.1371/journal.pone.0038659>
- Liu, Y. P., Haasnoot, J., ter Brake, O., Berkhout, B., & Konstantinova, P. (2008). Inhibition of HIV-1 by multiple siRNAs expressed from a single microRNA polycistron. *Nucleic Acids Research*, 36(9), 2811–2824. <https://doi.org/10.1093/nar/gkn109>
- Liu, Z., Wang, J., Cheng, H., Ke, X., Sun, L., Zhang, Q. C., & Wang, H.-W. (2018). Cryo-EM structure of human dicer and its complexes with a pre-miRNA substrate. *Cell*, 173(5), 1191–1203.e12. <https://doi.org/10.1016/j.cell.2018.03.080>
- Lu, S., & Cullen, B. R. (2004). Adenovirus VA1 noncoding RNA can inhibit small interfering RNA and MicroRNA biogenesis. *Journal of Virology*, 78(23), 12868–12876. <https://doi.org/10.1128/JVI.78.23.12868-12876.2004>
- Ma, H., Wu, Y., Choi, J.-G., & Wu, H. (2013). Lower and upper stem-single-stranded RNA junctions together determine the Drosha cleavage site. *Proceedings of the National Academy of Sciences of the United States of America*, 110(51), 20687–20692. <https://doi.org/10.1073/pnas.1311639110>
- Ma, H., Wu, Y., Dang, Y., Choi, J.-G., Zhang, J., & Wu, H. (2014). Pol III promoters to express small RNAs: Delineation of transcription initiation. *Molecular Therapy. Nucleic Acids*, 3(5), e161. <https://doi.org/10.1038/mtna.2014.12>
- Maepa, M. B., Ely, A., Grayson, W., & Arbuthnot, P. (2017). Sustained inhibition of HBV replication in vivo after systemic injection of AAVs encoding artificial antiviral primary microRNAs. *Molecular Therapy - Nucleic Acids*, 7, 190–199. <https://doi.org/10.1016/j.omtn.2017.04.007>
- Maillard, P. V., van der Veen, A. G., Poirier, E. Z., & Reis e Sousa, C. (2019). Slicing and dicing viruses: Antiviral RNA interference in mammals. *The EMBO Journal*, 38(8). <https://doi.org/10.15252/embj.2018100941>
- Mao, C., Liu, H., Chen, P., Ye, J., Teng, L., Jia, Z., & Cao, J. (2015). Cell-specific expression of artificial microRNAs targeting essential genes exhibit potent antitumor effect on hepatocellular carcinoma cells. *Oncotarget*, 6(8), 5707–5719. <https://doi.org/10.18632/oncotarget.3302>
- Mao, L., Liu, S., Hu, L., Jia, L., Wang, H., Guo, M., Chen, C., Liu, Y., & Xu, L. (2018). miR-30 family: A promising regulator in development and disease. *BioMed Research International*, 2018. <https://doi.org/10.1155/2018/9623412>
- Martier, R., Liefhebber, J. M., García-Osta, A., Miniarikova, J., Cuadrado-Tejedor, M., Espelosin, M., Ursua, S., Petry, H., van Deventer, S. J., Evers, M. M., & Konstantinova, P. (2019). Targeting RNA-mediated toxicity in C9orf72 ALS and/or FTD by RNAi-based gene therapy. *Molecular Therapy. Nucleic Acids*, 16, 26–37. <https://doi.org/10.1016/j.omtn.2019.02.001>
- Martier, R., Liefhebber, J. M., Miniarikova, J., van der Zon, T., Snapper, J., Kolder, I., Petry, H., van Deventer, S. J., Evers, M. M., & Konstantinova, P. (2019). Artificial MicroRNAs targeting C9orf72 can reduce accumulation of intra-nuclear transcripts in ALS and FTD patients. *Molecular Therapy. Nucleic Acids*, 14, 593–608. <https://doi.org/10.1016/j.omtn.2019.01.010>
- Martier, R., Sogorb-Gonzalez, M., Stricker-Shaver, J., Hübener-Schmid, J., Keskin, S., Klima, J., Toonen, L. J., Juhas, S., Juhasova, J., Ellederova, Z., Motlik, J., Haas, E., van Deventer, S., Konstantinova, P., Nguyen, H. P., & Evers, M. M. (2019). Development of an AAV-based microRNA gene therapy to treat Machado-Joseph disease. *Molecular Therapy - Methods & Clinical Development*, 15, 343–358. <https://doi.org/10.1016/j.omtm.2019.10.008>
- Mashima, R. (2015). Physiological roles of miR-155. *Immunology*, 145(3), 323–333. <https://doi.org/10.1111/imm.12468>
- McBride, J. L., Boudreau, R. L., Harper, S. Q., Staber, P. D., Monteys, A. M., Martins, I., Gilmore, B. L., Burstein, H., Peluso, R. W., Polisky, B., Carter, B. J., & Davidson, B. L. (2008). Artificial miRNAs mitigate shRNA-mediated toxicity in the brain: Implications for the therapeutic development of RNAi. *Proceedings of the National Academy of Sciences of the United States of America*, 105(15), 5868–5873. <https://doi.org/10.1073/pnas.0801775105>
- McBride, J. L., Pitzer, M. R., Boudreau, R. L., Dufour, B., Hobbs, T., Ojeda, S. R., & Davidson, B. L. (2011). Preclinical safety of RNAi-mediated HTT suppression in the rhesus macaque as a potential therapy for Huntington's disease. *Molecular Therapy*, 19(12), 2152–2162. <https://doi.org/10.1038/mt.2011.219>
- McLaughlin, J., Cheng, D., Singer, O., Lukacs, R. U., Radu, C. G., Verma, I. M., & Witte, O. N. (2007). Sustained suppression of Bcr-Abl-driven lymphoid leukemia by microRNA mimics. *Proceedings of the National Academy of Sciences of the United States of America*, 104(51), 20501–20506. <https://doi.org/10.1073/pnas.0710532105>
- McManus, M. T., Petersen, C. P., Haines, B. B., Chen, J., & Sharp, P. A. (2002). Gene silencing using micro-RNA designed hairpins. *RNA*, 8(6), 842–850.
- Medley, J. C., Panzade, G., & Zinovyeva, A. Y. (2020). microRNA strand selection: Unwinding the rules. *WIREs RNA*, e1627. <https://doi.org/10.1002/wrna.1627>
- Michlewski, G., & Cáceres, J. F. (2019). Post-transcriptional control of miRNA biogenesis. *RNA*, 25(1), 1–16. <https://doi.org/10.1261/rna.068692.118>
- Miniarikova, J., Zanella, I., Huseinovic, A., van der Zon, T., Hanemaaijer, E., Martier, R., Koornneef, A., Southwell, A. L., Hayden, M. R., van Deventer, S. J., Petry, H., & Konstantinova, P. (2016). Design, characterization, and Lead selection of therapeutic miRNAs targeting Huntingtin for development of gene therapy for Huntington's disease. *Molecular Therapy. Nucleic Acids*, 5, e297. <https://doi.org/10.1038/mtna.2016.7>
- Miniarikova, J., Zimmer, V., Martier, R., Brouwers, C. C., Pythoud, C., Richetin, K., Rey, M., Lubelski, J., Evers, M. M., van Deventer, S. J., Petry, H., Déglon, N., & Konstantinova, P. (2017). AAV5-miHTT gene therapy demonstrates suppression of mutant huntingtin aggregation and neuronal dysfunction in a rat model of Huntington's disease. *Gene Therapy*, 24(10), 630–639. <https://doi.org/10.1038/gt.2017.71>
- Miniarikova, J., Evers, M. M., & Konstantinova, P. (2018). Translation of microRNA-based Huntingtin-lowering therapies from preclinical studies to the clinic. *Molecular Therapy: The Journal of the American Society of Gene Therapy*, 26(4), 947–962. <https://doi.org/10.1016/j.ymthe.2018.02.002>

- Monteys, A. M., Wilson, M. J., Boudreau, R. L., Spengler, R. M., & Davidson, B. L. (2015). Artificial miRNAs targeting mutant Huntingtin show preferential silencing in vitro and in vivo. *Molecular Therapy - Nucleic Acids*, 4, e234. <https://doi.org/10.1038/mtna.2015.7>
- Moore, C. B., Guthrie, E. H., Huang, M. T.-H., & Taxman, D. J. (2010). Short hairpin RNA (shRNA): Design, delivery, and assessment of gene knockdown. *Methods in Molecular Biology (Clifton, N.J.)*, 629, 141–158. https://doi.org/10.1007/978-1-60761-657-3_10
- Moore, M. J., Scheel, T. K. H., Luna, J. M., Park, C. Y., Fak, J. J., Nishiuchi, E., Rice, C. M., & Darnell, R. B. (2015). MiRNA–target chimeras reveal miRNA 3′-end pairing as a major determinant of Argonaute target specificity. *Nature Communications*, 6(1), 8864. <https://doi.org/10.1038/ncomms9864>
- Murphy, S. R., Chang, C. C., Dogbevia, G., Bryleva, E. Y., Bowen, Z., Hasan, M. T., & Chang, T.-Y. (2013). Acat1 knockdown gene therapy decreases amyloid- β in a mouse model of Alzheimer's disease. *Molecular Therapy*, 21(8), 1497–1506. <https://doi.org/10.1038/mt.2013.118>
- NCT03282656. (2020). Clinical Trial Registration study/NCT03282656. [clinicaltrials.gov](https://clinicaltrials.gov/ct2/show/study/NCT03282656). <https://clinicaltrials.gov/ct2/show/study/NCT03282656>
- NCT04120493. (2020). Clinical Trial Registration No. NCT04120493. Available from clinicaltrials.gov. <https://clinicaltrials.gov/ct2/show/NCT04120493>
- Neilsen, C. T., Goodall, G. J., & Bracken, C. P. (2012). IsomiRs—The overlooked repertoire in the dynamic microRNAome. *Trends in Genetics: TIG*, 28(11), 544–549. <https://doi.org/10.1016/j.tig.2012.07.005>
- Nguyen, T. L., Nguyen, T. D., Bao, S., Li, S., & Nguyen, T. A. (2020). The internal loops in the lower stem of primary microRNA transcripts facilitate single cleavage of human microprocessor. *Nucleic Acids Research*, 48(5), 2579–2593. <https://doi.org/10.1093/nar/gkaa018>
- Nguyen, H. M., Nguyen, T. D., Nguyen, T. L., & Nguyen, T. A. (2019). Orientation of human microprocessor on primary MicroRNAs. *Biochemistry*, 58(4), 189–198. <https://doi.org/10.1021/acs.biochem.8b00944>
- Nguyen, T. A., Jo, M. H., Choi, Y.-G., Park, J., Kwon, S. C., Hohng, S., Kim, V. N., & Woo, J.-S. (2015). Functional anatomy of the human microprocessor. *Cell*, 161(6), 1374–1387. <https://doi.org/10.1016/j.cell.2015.05.010>
- Novak, M. J. U., & Tabrizi, S. J. (2010). Huntington's disease. *BMJ (Clinical Research Ed.)*, 340, c3109. <https://doi.org/10.1136/bmj.c3109>
- Okamura, K., Hagen, J. W., Duan, H., Tyler, D. M., & Lai, E. C. (2007). The mirtron pathway generates microRNA-class regulatory RNAs in drosophila. *Cell*, 130(1), 89–100. <https://doi.org/10.1016/j.cell.2007.06.028>
- Olejniczak, M., Urbanek, M. O., Jaworska, E., Witucki, L., Szczesniak, M. W., Makalowska, I., & Krzyzosiak, W. J. (2016). Sequence-non-specific effects generated by various types of RNA interference triggers. *Biochimica et Biophysica Acta*, 1859(2), 306–314. <https://doi.org/10.1016/j.bbagma.2015.11.005>
- Pan, Y., He, B., Chen, J., Sun, H., Deng, Q., Wang, F., Ying, H., Liu, X., Lin, K., Peng, H., Xie, H., & Wang, S. (2015). Gene therapy for colorectal cancer by adenovirus-mediated siRNA targeting CD147 based on loss of the IGF2 imprinting system. *International Journal of Oncology*, 47(5), 1881–1889. <https://doi.org/10.3892/ijo.2015.3181>
- Park, J.-E., Heo, I., Tian, Y., Simanshu, D. K., Chang, H., Jee, D., Patel, D. J., & Kim, V. N. (2011). Dicer recognizes the 5′ end of RNA for efficient and accurate processing. *Nature*, 475(7355), 201–205. <https://doi.org/10.1038/nature10198>
- Partin, A. C., Ngo, T. D., Herrell, E., Jeong, B.-C., Hon, G., & Nam, Y. (2017). Heme enables proper positioning of Drosha and DGCR8 on primary microRNAs. *Nature Communications*, 8, 1737. <https://doi.org/10.1038/s41467-017-01713-y>
- Partin, A. C., Zhang, K., Jeong, B.-C., Herrell, E., Li, S., Chiu, W., & Nam, Y. (2020). Cryo-EM structures of human Drosha and DGCR8 in complex with primary MicroRNA. *Molecular Cell*, 78(3), 411–422.e4. <https://doi.org/10.1016/j.molcel.2020.02.016>
- Paulson, H. L. (2009). The spinocerebellar ataxias. *Journal of Neuro-Ophthalmology: The Official Journal of the North American Neuro-Ophthalmology Society*, 29(3), 227–237. <https://doi.org/10.1097/WNO.0b013e3181b416de>
- Pfister, E. L., Chase, K. O., Sun, H., Kennington, L. A., Conroy, F., Johnson, E., Miller, R., Borel, F., Aronin, N., & Mueller, C. (2017). Safe and efficient silencing with a pol II, but not a pol III, promoter expressing an artificial miRNA targeting human Huntingtin. *Molecular Therapy. Nucleic Acids*, 7, 324–334. <https://doi.org/10.1016/j.omtn.2017.04.011>
- Pfister, E. L., DiNardo, N., Mondo, E., Borel, F., Conroy, F., Fraser, C., Gernoux, G., Han, X., Hu, D., Johnson, E., Kennington, L., Liu, P., Reid, S. J., Sapp, E., Vodicka, P., Kuchel, T., Morton, A. J., Howland, D., Moser, R., ... Aronin, N. (2018). Artificial miRNAs reduce human mutant Huntingtin throughout the striatum in a transgenic sheep model of Huntington's disease. *Human Gene Therapy*, 29(6), 663–673. <https://doi.org/10.1089/hum.2017.199>
- Ramachandran, P. S., Bhattarai, S., Singh, P., Boudreau, R. L., Thompson, S., LaSpada, A. R., Drack, A. V., & Davidson, B. L. (2014). RNA interference-based therapy for spinocerebellar ataxia type 7 retinal degeneration. *PLoS One*, 9(4), e95362. <https://doi.org/10.1371/journal.pone.0095362>
- Ramachandran, P. S., Boudreau, R. L., Schaefer, K. A., La Spada, A. R., & Davidson, B. L. (2014). Nonallele specific silencing of ataxin-7 improves disease phenotypes in a mouse model of SCA7. *Molecular Therapy*, 22(9), 1635–1642. <https://doi.org/10.1038/mt.2014.108>
- Rao, D. D., Vorhies, J. S., Senzer, N., & Nemunaitis, J. (2009). siRNA vs. shRNA: Similarities and differences. *Advanced Drug Delivery Reviews*, 61(9), 746–759. <https://doi.org/10.1016/j.addr.2009.04.004>
- Ratnavalli, E., Brayne, C., Dawson, K., & Hodges, J. R. (2002). The prevalence of frontotemporal dementia. *Neurology*, 58(11), 1615–1621. <https://doi.org/10.1212/wnl.58.11.1615>
- Rayner, K. J., Suárez, Y., Dávalos, A., Parathath, S., Fitzgerald, M. L., Tamehiro, N., Fisher, E. A., Moore, K. J., & Fernández-Hernando, C. (2010). MiR-33 contributes to the regulation of cholesterol homeostasis. *Science (New York, N.Y.)*, 328(5985), 1570–1573. <https://doi.org/10.1126/science.1189862>
- Roden, C., Gaillard, J., Kanoria, S., Rennie, W., Barish, S., Cheng, J., Pan, W., Liu, J., Cotsapas, C., Ding, Y., & Lu, J. (2017). Novel determinants of mammalian primary microRNA processing revealed by systematic evaluation of hairpin-containing transcripts and human genetic variation. *Genome Research*, 27(3), 374–384. <https://doi.org/10.1101/gr.208900.116>

- Rodríguez-Lebrón, E., Costa, M. d. C., Luna-Cancelon, K., Peron, T. M., Fischer, S., Boudreau, R. L., Davidson, B. L., & Paulson, H. L. (2013). Silencing mutant ATXN3 expression resolves molecular phenotypes in SCA3 transgenic mice. *Molecular Therapy*, 21(10), 1909–1918. <https://doi.org/10.1038/mt.2013.152>
- Ros, X. B.-D., & Gu, S. (2016). Guidelines for the optimal design of miRNA-based shRNAs. *Methods (San Diego, Calif.)*, 103, 157–166. <https://doi.org/10.1016/j.ymeth.2016.04.003>
- Ros, X. B.-D., Kasprzak, W. K., Bhandari, Y., Fan, L., Cavanaugh, Q., Jiang, M., Dai, L., Yang, A., Shao, T.-J., Shapiro, B. A., Wang, Y.-X., & Gu, S. (2019). Structural differences between Pri-miRNA paralogs promote alternative drosha cleavage and expand target repertoires. *Cell Reports*, 26(2), 447–459. <https://doi.org/10.1016/j.celrep.2018.12.054>
- Ross, C. A. (2002). Polyglutamine pathogenesis: Emergence of unifying mechanisms for Huntington's disease and related disorders. *Neuron*, 35(5), 819–822. [https://doi.org/10.1016/s0896-6273\(02\)00872-3](https://doi.org/10.1016/s0896-6273(02)00872-3)
- Rossi, J. (2008). Expression strategies for short hairpin RNA interference triggers. *Human Gene Therapy*, 19(4), 313–317. <https://doi.org/10.1089/hum.2008.026>
- Saha, A., Bhagyaawant, S. S., Parida, M., & Dash, P. K. (2016). Vector-delivered artificial miRNA effectively inhibited replication of Chikungunya virus. *Antiviral Research*, 134, 42–49. <https://doi.org/10.1016/j.antiviral.2016.08.019>
- Samuel, G. H., Wiley, M. R., Badawi, A., Adelman, Z. N., & Myles, K. M. (2016). Yellow fever virus capsid protein is a potent suppressor of RNA silencing that binds double-stranded RNA. *Proceedings of the National Academy of Sciences of the United States of America*, 113(48), 13863–13868. <https://doi.org/10.1073/pnas.1600544113>
- Sankaran, V. G., Menne, T. F., Xu, J., Akie, T. E., Lettre, G., Van Handel, B., Mikkola, H. K. A., Hirschhorn, J. N., Cantor, A. B., & Orkin, S. H. (2008). Human fetal hemoglobin expression is regulated by the developmental stage-specific repressor BCL11A. *Science (New York, N.Y.)*, 322(5909), 1839–1842. <https://doi.org/10.1126/science.1165409>
- Schulz, W. (2007). *Molecular biology of human cancers: An advanced student's textbook*. Springer. <https://doi.org/10.1007/978-1-4020-3186-1>
- Schwab, R., Ossowski, S., Rieger, M., Warthmann, N., & Weigel, D. (2006). Highly specific gene silencing by artificial microRNAs in Arabidopsis. *The Plant Cell*, 18(5), 1121–1133. <https://doi.org/10.1105/tpc.105.039834>
- Seidel, K., Siswanto, S., Brunt, E. R. P., den Dunnen, W., Korf, H.-W., & Rüb, U. (2012). Brain pathology of spinocerebellar ataxias. *Acta Neuropathologica*, 124(1), 1–21. <https://doi.org/10.1007/s00401-012-1000-x>
- Shang, R., Baek, S. C., Kim, K., Kim, B., Kim, V. N., & Lai, E. C. (2020). Genomic clustering facilitates nuclear processing of suboptimal Pri-miRNA loci. *Molecular Cell*, 78(2), 303–316.e4. <https://doi.org/10.1016/j.molcel.2020.02.009>
- Sharma, H., Tripathi, A., Kumari, B., Vradi, S., & Banerjee, A. (2018). Artificial microRNA-mediated inhibition of Japanese encephalitis virus replication in neuronal cells. *Nucleic Acid Therapeutics*, 28(6), 357–365. <https://doi.org/10.1089/nat.2018.0743>
- Sheng, P., Flood, K. A., & Xie, M. (2020). Short hairpin RNAs for strand-specific small interfering RNA production. *Frontiers in Bioengineering and Biotechnology*, 8. <https://doi.org/10.3389/fbioe.2020.00940>
- Shin, K.-J., Wall, E. A., Zavzavadjian, J. R., Santat, L. A., Liu, J., Hwang, J.-I., Rebres, R., Roach, T., Seaman, W., Simon, M. I., & Fraser, I. D. C. (2006). A single lentiviral vector platform for microRNA-based conditional RNA interference and coordinated transgene expression. *Proceedings of the National Academy of Sciences*, 103(37), 13759–13764. <https://doi.org/10.1073/pnas.0606179103>
- Silva, J. M., Li, M. Z., Chang, K., Ge, W., Golding, M. C., Rickles, R. J., Siolas, D., Hu, G., Paddison, P. J., Schlabach, M. R., Sheth, N., Bradshaw, J., Burchard, J., Kulkarni, A., Cavet, G., Sachidanandam, R., McCombie, W. R., Cleary, M. A., Elledge, S. J., & Hannon, G. J. (2005). Second-generation shRNA libraries covering the mouse and human genomes. *Nature Genetics*, 37(11), 1281–1288. <https://doi.org/10.1038/ng1650>
- Sittler, A., Muriel, M.-P., Marinello, M., Brice, A., den Dunnen, W., & Alves, S. (2018). Deregulation of autophagy in postmortem brains of Machado-Joseph disease patients. *Neuropathology: Official Journal of the Japanese Society of Neuropathology*, 38(2), 113–124. <https://doi.org/10.1111/neup.12433>
- Sliva, K., & Schnierle, B. S. (2010). Selective gene silencing by viral delivery of short hairpin RNA. *Virology Journal*, 7. <https://doi.org/10.1186/1743-422X-7-248>
- Son, J., Uchil, P. D., Kim, Y. B., Shankar, P., Kumar, P., & Lee, S.-K. (2008). Effective suppression of HIV-1 by artificial bispecific miRNA targeting conserved sequences with tolerance for wobble base-pairing. *Biochemical and Biophysical Research Communications*, 374(2), 214–218. <https://doi.org/10.1016/j.bbrc.2008.06.125>
- Spronck, E. A., Brouwers, C. C., Vallès, A., de Haan, M., Petry, H., van Deventer, S. J., Konstantinova, P., & Evers, M. M. (2019). AAV5-miHTT gene therapy demonstrates sustained Huntingtin lowering and functional improvement in Huntington disease mouse models. *Molecular Therapy. Methods & Clinical Development*, 13, 334–343. <https://doi.org/10.1016/j.omtm.2019.03.002>
- Stanek, L. M., Sardi, S. P., Mastis, B., Richards, A. R., Treleaven, C. M., Taksir, T., Misra, K., Cheng, S. H., & Shihabuddin, L. S. (2014). Silencing mutant Huntingtin by Adeno-associated virus-mediated RNA interference ameliorates disease manifestations in the YAC128 mouse model of Huntington's disease. *Human Gene Therapy*, 25(5), 461–474. <https://doi.org/10.1089/hum.2013.200>
- Stegmeier, F., Hu, G., Rickles, R. J., Hannon, G. J., & Elledge, S. J. (2005). A lentiviral microRNA-based system for single-copy polymerase II-regulated RNA interference in mammalian cells. *Proceedings of the National Academy of Sciences of the United States of America*, 102(37), 13212–13217. <https://doi.org/10.1073/pnas.0506306102>
- Stoica, L., Todeasa, S. H., Cabrera, G. T., Salameh, J. S., ElMallah, M. K., Mueller, C., Brown, R. H., & Miguel, S.-E. (2016). AAV delivered artificial microRNA extends survival and delays paralysis in an amyotrophic lateral sclerosis mouse model. *Annals of Neurology*, 79(4), 687–700. <https://doi.org/10.1002/ana.24618>

- Sun, B.-S., Dong, Q.-Z., Ye, Q.-H., Sun, H.-J., Jia, H.-L., Zhu, X.-Q., Liu, D.-Y., Chen, J., Xue, Q., Zhou, H.-J., Ren, N., & Qin, L.-X. (2008). Lentiviral-mediated miRNA against osteopontin suppresses tumor growth and metastasis of human hepatocellular carcinoma. *Hepatology*, *48*(6), 1834–1842. <https://doi.org/10.1002/hep.22531>
- Thakral, S., & Ghoshal, K. (2015). MiR-122 is a unique molecule with great potential in diagnosis, prognosis of liver disease, and therapy both as miRNA mimic and antimir. *Current Gene Therapy*, *15*(2), 142–150.
- Tiwari, S., Atluri, V., Kaushik, A., Yndart, A., & Nair, M. (2019). Alzheimer's disease: Pathogenesis, diagnostics, and therapeutics. *International Journal of Nanomedicine*, *14*, 5541–5554. <https://doi.org/10.2147/IJN.S200490>
- Van den Haute, C., Eggermont, K., Nuttin, B., Debyser, Z., & Baekelandt, V. (2003). Lentiviral vector-mediated delivery of short hairpin RNA results in persistent knockdown of gene expression in mouse brain. *Human Gene Therapy*, *14*(18), 1799–1807. <https://doi.org/10.1089/104303403322611809>
- Walder, R. Y., Gautam, M., Wilson, S. P., Benson, C. J., & Sluka, K. A. (2011). Selective targeting of ASIC3 using artificial miRNAs inhibits primary and secondary hyperalgesia after muscle inflammation. *Pain*, *152*(10), 2348–2356. <https://doi.org/10.1016/j.pain.2011.06.027>
- Wallace, L. M., Liu, J., Domire, J. S., Garwick-Coppens, S. E., Guckes, S. M., Mendell, J. R., Flanigan, K. M., & Harper, S. Q. (2012). RNA interference inhibits DUX4-induced muscle toxicity in vivo: Implications for a targeted FSHD therapy. *Molecular Therapy*, *20*(7), 1417–1423. <https://doi.org/10.1038/mt.2012.68>
- Wallace, L. M., Saad, N. Y., Pyne, N. K., Fowler, A. M., Eidahl, J. O., Domire, J. S., Griffin, D. A., Herman, A. C., Sahenk, Z., Rodino-Klapac, L. R., & Harper, S. Q. (2017). Pre-clinical safety and off-target studies to support translation of AAV-mediated RNAi therapy for FSHD. *Molecular Therapy. Methods & Clinical Development*, *8*, 121–130. <https://doi.org/10.1016/j.omtm.2017.12.005>
- Wang, D., Tai, P. W. L., & Gao, G. (2019). Adeno-associated virus vector as a platform for gene therapy delivery. *Nature Reviews Drug Discovery*, *18*(5), 358–378. <https://doi.org/10.1038/s41573-019-0012-9>
- Wang, J., Lee, J. E., Riemondy, K., Yu, Y., Marquez, S. M., Lai, E. C., & Yi, R. (2020). XPO5 promotes primary miRNA processing independently of RanGTP. *Nature Communications*, *11*(1), 1845. <https://doi.org/10.1038/s41467-020-15598-x>
- Wang, S., Shu, J.-Z., Cai, Y., Bao, Z., & Liang, Q.-M. (2012). Establishment and characterization of MTDH knockdown by artificial MicroRNA interference—Functions as a potential tumor suppressor in breast cancer. *Asian Pacific Journal of Cancer Prevention: APJCP*, *13*(6), 2813–2818. <https://doi.org/10.7314/apjcp.2012.13.6.2813>
- Wang, Y., Yan, L., Zhang, L., Xu, H., Chen, T., Li, Y., Wang, H., Chen, S., Wang, W., Chen, C., & Yang, Q. (2018). NT21MP negatively regulates paclitaxel-resistant cells by targeting miR-155-3p and miR-155-5p via the CXCR4 pathway in breast cancer. *International Journal of Oncology*, *53*(3), 1043–1054. <https://doi.org/10.3892/ijo.2018.4477>
- Wen, J., Ladewig, E., Shenker, S., Mohammed, J., & Lai, E. C. (2015). Analysis of nearly one thousand mammalian mirtrons reveals novel features of dicer substrates. *PLoS Computational Biology*, *11*(9), e1004441. <https://doi.org/10.1371/journal.pcbi.1004441>
- Wu, Z., Asokan, A., & Samulski, R. J. (2006). Adeno-associated virus serotypes: Vector toolkit for human gene therapy. *Molecular Therapy: The Journal of the American Society of Gene Therapy*, *14*(3), 316–327. <https://doi.org/10.1016/j.yymthe.2006.05.009>
- Xia, X.-G., Zhou, H., & Xu, Z. (2006). Multiple shRNAs expressed by an inducible pol II promoter can knock down the expression of multiple target genes. *BioTechniques*, *41*(1), 64–68. <https://doi.org/10.2144/000112198>
- Xie, J., Mao, Q., Tai, P. W. L., He, R., Ai, J., Su, Q., Zhu, Y., Ma, H., Li, J., Gong, S., Wang, D., Gao, Z., Li, M., Zhong, L., Zhou, H., & Gao, G. (2017). Short DNA hairpins compromise recombinant adeno-associated virus genome homogeneity. *Molecular Therapy*, *25*(6), 1363–1374. <https://doi.org/10.1016/j.yymthe.2017.03.028>
- Xie, J., Tai, P. W. L., Brown, A., Gong, S., Zhu, S., Wang, Y., Li, C., Colpan, C., Su, Q., He, R., Ma, H., Li, J., Ye, H., Ko, J., Zamore, P. D., & Gao, G. (2020). Effective and accurate gene silencing by a recombinant AAV-compatible microRNA scaffold. *Molecular Therapy*, *28*(2), 422–430. <https://doi.org/10.1016/j.yymthe.2019.11.018>
- Xie, M., Li, M., Vilborg, A., Lee, N., Shu, M.-D., Yartseva, V., Šestan, N., & Steitz, J. A. (2013). Mammalian 5'-capped MicroRNA precursors that generate a single MicroRNA. *Cell*, *155*(7), 1568–1580. <https://doi.org/10.1016/j.cell.2013.11.027>
- Xie, P., Xie, Y., Zhang, X., Huang, H., He, L., Wang, X., & Wang, S. (2013). Inhibition of dengue virus 2 replication by artificial microRNAs targeting the conserved regions. *Nucleic Acid Therapeutics*, *23*(4), 244–252. <https://doi.org/10.1089/nat.2012.0405>
- Yang, J.-S., Maurin, T., Robine, N., Rasmussen, K. D., Jeffrey, K. L., Chandwani, R., Papapetrou, E. P., Sadelain, M., O'Carroll, D., & Lai, E. C. (2010). Conserved vertebrate mir-451 provides a platform for Dicer-independent, Ago2-mediated microRNA biogenesis. *Proceedings of the National Academy of Sciences*, *107*(34), 15163–15168. <https://doi.org/10.1073/pnas.1006432107>
- Yang, Y.-S., Xie, J., Chaugule, S., Wang, D., Kim, J.-M., Kim, J., Tai, P. W. L., Seo, S., Gravallesse, E., Gao, G., & Shim, J.-H. (2020). Bone-targeting AAV-mediated gene silencing in osteoclasts for osteoporosis therapy. *Molecular Therapy - Methods & Clinical Development*, *17*, 922–935. <https://doi.org/10.1016/j.omtm.2020.04.010>
- Yi, R., Qin, Y., Macara, I. G., & Cullen, B. R. (2003). Exportin-5 mediates the nuclear export of pre-microRNAs and short hairpin RNAs. *Genes & Development*, *17*(24), 3011–3016. <https://doi.org/10.1101/gad.1158803>
- Yi, T., Arthanari, H., Akabayov, B., Song, H., Papadopoulos, E., Qi, H. H., Jedrychowski, M., Güttler, T., Guo, C., Luna, R. E., Gygi, S. P., Huang, S. A., & Wagner, G. (2015). EIF1A augments Ago2-mediated dicer-independent miRNA biogenesis and RNA interference. *Nature Communications*, *6*, 7194. <https://doi.org/10.1038/ncomms8194>
- Yoda, M., Cifuentes, D., Izumi, N., Sakaguchi, Y., Suzuki, T., Giraldez, A. J., & Tomari, Y. (2013). PARN mediates 3'-end trimming of Argonaute2-cleaved precursor microRNAs. *Cell Reports*, *5*(3), 715–726. <https://doi.org/10.1016/j.celrep.2013.09.029>
- Yu, T., Ma, P., Wu, D., Shu, Y., & Gao, W. (2018). Functions and mechanisms of microRNA-31 in human cancers. *Biomedicine & Pharmacotherapy*, *108*, 1162–1169. <https://doi.org/10.1016/j.biopha.2018.09.132>

- Yue, J., Sheng, Y., Ren, A., & Penmatsa, S. (2010). A miR-21 hairpin structure-based gene knockdown vector. *Biochemical and Biophysical Research Communications*, 394(3), 667–672. <https://doi.org/10.1016/j.bbrc.2010.03.047>
- Zeng, Y., & Cullen, B. R. (2003). Sequence requirements for micro RNA processing and function in human cells. *RNA (New York, N.Y.)*, 9(1), 112–123. <https://doi.org/10.1261/rna.2780503>
- Zeng, Y., & Cullen, B. R. (2005). Efficient processing of primary microRNA hairpins by Drosha requires flanking nonstructured RNA sequences. *The Journal of Biological Chemistry*, 280(30), 27595–27603. <https://doi.org/10.1074/jbc.M504714200>
- Zeng, Y., Wagner, E. J., & Cullen, B. R. (2002). Both natural and designed micro RNAs can inhibit the expression of cognate mRNAs when expressed in human cells. *Molecular Cell*, 9(6), 1327–1333. [https://doi.org/10.1016/S1097-2765\(02\)00541-5](https://doi.org/10.1016/S1097-2765(02)00541-5)
- Zeng, Y., Yi, R., & Cullen, B. R. (2003). MicroRNAs and small interfering RNAs can inhibit mRNA expression by similar mechanisms. *Proceedings of the National Academy of Sciences*, 100(17), 9779–9784. <https://doi.org/10.1073/pnas.1630797100>
- Zhang, H., Kolb, F. A., Jaskiewicz, L., Westhof, E., & Filipowicz, W. (2004). Single processing center models for human dicer and bacterial RNase III. *Cell*, 118(1), 57–68. <https://doi.org/10.1016/j.cell.2004.06.017>
- Zhang, H., Tang, X., Zhu, C., Song, Y., Yin, J., Xu, J., Ertl, H. C. J., & Zhou, D. (2015). Adenovirus-mediated artificial MicroRNAs targeting matrix or nucleoprotein genes protect mice against lethal influenza virus challenge. *Gene Therapy*, 22(8), 653–662. <https://doi.org/10.1038/gt.2015.31>
- Zhang, J., Liu, Q.-S., & Dong, W.-G. (2011). Blockade of proliferation and migration of gastric cancer via targeting CDH17 with an artificial microRNA. *Medical Oncology (Northwood, London, England)*, 28(2), 494–501. <https://doi.org/10.1007/s12032-010-9489-0>
- Zhang, T., Cheng, T., Wei, L., Cai, Y., Yeo, A., Han, J., Yuan, Y. A., Zhang, J., & Xia, N. (2012). Efficient inhibition of HIV-1 replication by an artificial polycistronic miRNA construct. *Virology Journal*, 9, 118. <https://doi.org/10.1186/1743-422X-9-118>
- Zhao, Y., Samal, E., & Srivastava, D. (2005). Serum response factor regulates a muscle-specific microRNA that targets Hand2 during cardiogenesis. *Nature*, 436(7048), 214–220. <https://doi.org/10.1038/nature03817>
- Zheng, Z., Wang, P., Wang, H., Zhang, X., Wang, M., Cucinotta, F. A., & Wang, Y. (2013). Combining heavy ion radiation and artificial microRNAs to target the homologous recombination repair gene efficiently kills human tumor cells. *International Journal of Radiation Oncology, Biology, Physics*, 85, 466–471. <https://doi.org/10.1016/j.ijrobp.2012.04.008>
- Zhou, H., Xia, X. G., & Xu, Z. (2005). An RNA polymerase II construct synthesizes short-hairpin RNA with a quantitative indicator and mediates highly efficient RNAi. *Nucleic Acids Research*, 33(6), e62. <https://doi.org/10.1093/nar/gni061>
- Zoghbi, H. Y., & Orr, H. T. (2000). Glutamine repeats and neurodegeneration. *Annual Review of Neuroscience*, 23, 217–247. <https://doi.org/10.1146/annurev.neuro.23.1.217>

SUPPORTING INFORMATION

Additional supporting information may be found online in the Supporting Information section at the end of this article.

How to cite this article: Kotowska-Zimmer A, Pewinska M, Olejniczak M. Artificial miRNAs as therapeutic tools: Challenges and opportunities. *WIREs RNA*. 2021;12:e1640. <https://doi.org/10.1002/wrna.1640>

Supplementary Table 1. AmiRNAs used in therapeutic approaches for viral infections

Disease	Target	Shuttle	Promoter	Multiple amiRNA	Cell line	In vivo	Delivery	Processing	Results		Reference
									Molecular effects	Other	
Hepatitis B	Hbx	miR-31 miR-30a miR-122	U6 CMV	Yes	Huh7	Mice	Lipofection, tail vein injection	Northern blot	<ul style="list-style-type: none"> 90% knockdown of target 	<ul style="list-style-type: none"> significant knockdown 3 and 5 days after injection, no interferon response 	Ely A., 2009
Hepatitis B	HBV S	miR-155	CMV	No	HepG2.2.15	No	Lipofection	No	<ul style="list-style-type: none"> mRNA reduced by ~47% 	<ul style="list-style-type: none"> HBeAg reduced by ~80%, copies of HBV DNA reduced by ~70% 	Gao Y., 2008
Hepatitis B	X sequence	miR-31	MTTR	Yes	Huh7	HBV mice	AAV2 AAV8	Northern blot	<ul style="list-style-type: none"> significant reduction of circulating viral particle equivalents 	<ul style="list-style-type: none"> HBsAg significantly reduced no toxicity no immune response 	Maepa M. B., 2017
Influenza A	NP M1 M2	miR-155*	CMV TK	Yes	HEK293T A549	ICR mice C57BL/6 mice	Ad, intranasally	No	<ul style="list-style-type: none"> ribonucleoprotein activity inhibited by 80%, viral replication inhibited 	<ul style="list-style-type: none"> cross-protection against heterotypic strains, multiple amiRNA failed in enhancement of inhibition 	Zhang H., 2015
Influenza	NP	miR-126	CAGGS	Yes	Vero DF-1	No	Lentivirus	Northern blot	<ul style="list-style-type: none"> virus production inhibited by 90% 	<ul style="list-style-type: none"> flanking sequences play important role in amiRNA processing, miR-126 is efficient for expression of amiRNA 	Chen S., 2011
Adenovirus infections	pTP	miR-155	CMV E4	Yes	T-Rex-293 A549	No	E1- deleted/E3- deleted Ad	No	<ul style="list-style-type: none"> adenovirus replication inhibited 	<ul style="list-style-type: none"> combination of amiRNA with GCV resulted in higher reduction rate than both approaches alone, multiple amiRNA inhibited virus replication even with low concentrations of GCV 	Ibrišimović M., 2013
Adenovirus infections	E1A pTP Iva2 hexon	miR-155	CMV	Yes	HeLa HepaRG	Syrian hamster s	AAV2 AAV9	No	<ul style="list-style-type: none"> virus replication decreased by ~90% using single and multiple amiRNA 	<ul style="list-style-type: none"> three copies of amiR-pTP and three copies of amiR-E1A_2 were not more efficient than six copies of amiR-pTP inhibition of Ad5-induced damages in liver 	Schaar K., 2017
Chikungunya virus	nsP1 nsP2 nsP2 capsid	miR-155*	CMV	Yes	Vero	No	Lipofection	No	<ul style="list-style-type: none"> CHIKV inhibited by 99,8% 	<ul style="list-style-type: none"> amiRNA with chloroquine inhibited replication more than amiRNA or antivirals alone 	Saha A., 2016

Supplementary Table 1. AmiRNAs used in therapeutic approaches for viral infections. Continued

HIV-1	<i>env</i>	miR-30a miR-155	CMV	Yes	293FT MT-4 TZM-bl	No	Lipofection	No	<ul style="list-style-type: none"> • multiple amiRNA more effective than single, • no interferon response, • prevention from viral escape 	Zhang T., 2012
HIV-1	CCR5 Tat	miR-30a miR-150 miR-21 miR-185 miR-20a miR-16-1	EF-1 α	Yes	TZM-bl PBMCs CD4T Jurkat	NOD/SCID IL2rycnu II mice Hu-PBL mice	Lentivirus	NGS	<ul style="list-style-type: none"> • virus replication inhibited 	Choi J., 2015
Japanese Encephalitis Virus	Highly conserved regions	miR-155	CMV	No	PS N2a HEK293T	No	Lipofection	No	<ul style="list-style-type: none"> • viral release reduced by 95%, • reduced viral NS1 expression in neuronal cells • reduced RNA and protein level, • reduced virus replication 	Sharma H., 2018
Dengue	Highly conserved regions	miR-155	CMV	Yes	BHK-21 Huh7 HEK293T	No	Lentivirus	No	<ul style="list-style-type: none"> • increase of cell survival rate 	Xie P., 2013
West Nile Virus	NS5 NS2A	miR-155	CMV	Yes	Vero	No	Lipofection	No	<ul style="list-style-type: none"> • concatenated amiRNA_1_2 showed more effective WNV inhibition as compared to individual amiRNA_2 but less effective than single amiRNA_1, • less cytopathic effect 	Karothia D., 2020

* presumably, GCV - ganciclovir

Supplementary Table 2. AmiRNAs used in therapeutic approaches for cancers

Disease	Target	Shuttle	Promoter	Multiple amiRNA	Cell line	In vivo	Delivery	Site of delivery	Results		Reference
									Molecular effects	Other	
Pancreatic cancer	VEGFR1 VEGFR2 VEGFR3	miR-155	CMV	Yes	HPDE6C7 BXP-3 MIAPACA2 PANC-1 SW1990	Athymic nude mice	Transfection	Front flank, subcutaneous	<ul style="list-style-type: none"> • VEGFR1 mRNA reduced by 43%, protein by 52%, • VEGFR2: mRNA reduced by 52% and protein by 75%, • VEGFR3: mRNA reduced by 36% and protein by 51% 	<ul style="list-style-type: none"> • inhibition of proliferation by 55%, • induced apoptosis, • reduced tumor growth, complete suppression after combination of DDP and triple amiRNA 	Huang J., 2017
									<ul style="list-style-type: none"> • augmented apoptosis, • decreased tumor volume, increased volume when p53 is absent 		Ilogawa M., 2009
Hepatocellular carcinoma, Colorectal cancer	p21	miR-155	CMV	Yes	HLF DLD-1 SW480 Hep3B HCT116 HEK293T	BALB/c nude mice	rAd	Intratumoral	<ul style="list-style-type: none"> • knockdown of target, • reduced protein level 	<ul style="list-style-type: none"> • inhibition of ATP production, • lower survival rate of cells, • blockade of cell cycle, • destruction of tumor 	Mao C., 2015
									<ul style="list-style-type: none"> • mRNA reduced by 98% • protein reduced by 78% • protein reduction 	<ul style="list-style-type: none"> • decrease of cell proliferation, migration • sensitization of cells to radiation by targeting HRR pathway, • reduction of tumor size 	Zhang J., 2011 Zheng Z., 2013
Gastric cancer	CDH17	miR-155*	CMV	No	BGC823	No	Lipofection Lentivirus	-	<ul style="list-style-type: none"> • CXCR4 reduced by 100% 	<ul style="list-style-type: none"> • cell migration 77% lower, invasion blocked by 84%, • fewer lung metastases • blockade of Akt phosphorylation • no apoptotic 	Liang Z., 2007
									<ul style="list-style-type: none"> • mRNA reduced by 		Liu C., 2016
Brain cancer Lung cancer	XRCC2 XRCC4	miR-155*	CMV	Comb. only	U87MG A549	Nude mice	Lipofection Lentivirus	Both hind leg, subcutaneous	<ul style="list-style-type: none"> • mRNA reduced by 	<ul style="list-style-type: none"> • CXCR4 reduced by 100% 	
									<ul style="list-style-type: none"> • CXCR4 reduced by 100% 		
Breast cancer	CXCR4	miR-155	CMV	No	MDA-MB-231	Mice	Lipofection	nd	<ul style="list-style-type: none"> • mRNA reduced by 	<ul style="list-style-type: none"> • CXCR4 reduced by 100% 	
									<ul style="list-style-type: none"> • mRNA reduced by 		
Breast cancer	MAP3K1	miR-155*	CMV	No	4T1	BALB/c-	Lentivirus	Fat pads	<ul style="list-style-type: none"> • mRNA reduced by 		

												response, <ul style="list-style-type: none"> impaired migration of cancer cells (from 80% to 20%), fewer tumors in lungs, suppression of tumor growth and metastasis 	
Breast cancer	<i>MTDH</i>	miR-155*	CMV	No	MDA-MB-231	No	Lipofection	-	80%, <ul style="list-style-type: none"> decreased level of ERK and p-38 	<ul style="list-style-type: none"> mRNA and protein reduced by more than 69% 	<ul style="list-style-type: none"> decreased migration, motility and proliferation of cells 	Wang S., 2012	
Melanoma	<i>HPSE</i>	miR-155	CMV	No	A375 HeLa	BALB/c-nu mice	Attractene Transfection Reagent	Tail vein (cell injection)		<ul style="list-style-type: none"> mRNA reduced by 70% 	<ul style="list-style-type: none"> no influence on apoptotic response, inhibition of proliferation, migration and invasion, suppression of lung metastasis, attenuation of MAPK phosphorylation 	Liu X., 2012	
Cervical cancer	<i>β-gal</i> <i>HPV16</i> <i>HPV18</i>	miR-155*	CMV	No	HeLa SiHa U2OS	Nude mice	AAV5	Intratumoral		<ul style="list-style-type: none"> 18E6 reduced by 62%, 16E6 reduced by 96% 	<ul style="list-style-type: none"> increase of p53, apoptosis, tumor inhibition 	Bonetta A. C., 2015	
Gastric cancer	<i>PRL-3</i>	miR-155	CMV	No	SGC7901	BALB/c nude mice	Lipofection	Peritoneal cavities		<ul style="list-style-type: none"> protein reduced by 3.7 fold, mRNA level reduced more than 80% 	<ul style="list-style-type: none"> decrease in cell migration and invasion, reduced peritoneal metastasis 	Li Z., 2006	

* presumably. Abbreviations: **AFP** - alpha-fetoprotein promoter, **DDP** – cisplatin, **HRR** – homologous recombination repair

Supplementary Table 3. AmiRNAs used in therapeutic approaches for other diseases

Disease	Target	Shuttle	Promoter	Cell line	In vivo	Vector	Site of delivery	Results		Refs
								Molecular effects	Other	
Pelizaeus-Merzbacher disease	<i>PLP1</i>	miR-155	CNP	No	Jcl:B6C3F1 mice Plp1-Tg mice Plp1-Tg/B6C3 backcross	AAV1/2	Corpus striatum, internal capsule	<ul style="list-style-type: none"> mRNA and protein reduced by 50% 	<ul style="list-style-type: none"> extension of lifespan, improved bodyweight gain, no off-target effects, reduced degeneration of oligodendrocytes, preservation of myelin structure, suppression of astrogliosis and microgliosis 	Li H., 2019
Osteoporosis	<i>Rank</i> <i>Ctsk</i>	miR-33	CB	No	C57BL/6J mice BALB/cJ mice	AAV9	Intravenously	<ul style="list-style-type: none"> mRNA reduced by 60% 	<ul style="list-style-type: none"> increase in trabecular bone mass and cortical thickness, relative increase in trabecular bone mass, no adverse effects and off-targets 	Yang Y., 2020
Hypertension	<i>AT_{1aR}</i>	miR-155	CMV	No	SHR rats Wistar rats	Ad	Paraventricular nucleus	<ul style="list-style-type: none"> mRNA reduced by 60% 	<ul style="list-style-type: none"> reduced blood pressure, blunt sympathetic activity improved myocardial and vascular remodeling 	Fan Z., 2012
Heart failure	<i>PLB</i>	miR-155	CMV ^{enh} / MLC0.26	HEK293T	No	AAV6	-	<ul style="list-style-type: none"> protein in cardiomyocytes reduced by 50% and 70%, similar efficiency as shRNA 	<ul style="list-style-type: none"> increase of SERCA2a-mediated Ca²⁺ transport, increased expression of miR-21, no induction of proinflammatory genes 	Gröbl T., 2014
Sickle cell disease	<i>BCL11</i> <i>A</i>	miR-223	U6 SFFV	MEL Jurkat K562 CD34 ⁺	No	LV	-	<ul style="list-style-type: none"> less efficient knockdown of target in cells expressing amiRNA under SFFV promoter than U6 promoter, hemoglobin F raised up to more than 50% 	<ul style="list-style-type: none"> induction of cytotoxicity in MIEL cells treated with amiRNAs expressed under U6 promoter reduced polymerization of sickle-containing hemoglobin reactivation of γ-globin 	Guda S., 2015
Sickle cell disease	<i>BCL11</i> <i>A</i>	miR-223	SFFV β -globin	CD34 ⁺ cells from Boyl and CD45.2 B6 mice	No	LV	-	<ul style="list-style-type: none"> protein reduced by 90% Hb F raised up by 70% in erythrocytes 	<ul style="list-style-type: none"> improvement of sickle-associated hemolytic anemia and reticulocytosis 	Brendel C., 2016

Supplementary Table 3. AmiRNAs used in therapeutic approaches for other diseases. Continued

Sickle cell disease	<i>BCL11A</i>	miR-223	β -globin	CD34 ⁺	B6 mice Boyl mice NSG mice	LV	Retro-orbitally	<ul style="list-style-type: none"> • HbF raised up by 74% 	<ul style="list-style-type: none"> • low genotoxicity of amiRNA • no engraftment defects • no LVV toxicity 	Brendel C., 2020
Myotonic dystrophy type 1	<i>HSA</i>	miR-30	U6	COS-1	HSA ^{IR} mice	AAV6	Tail vein	<ul style="list-style-type: none"> • HSA mRNA reduced by 95% 	<ul style="list-style-type: none"> • myotonia grade reduced • DM1 biomarkers decreased by 2-fold • nuclear foci decreased significantly 	Bisset D. R., 2015
Facioscapulo humeral muscular dystrophy	<i>DUX4</i>	miR-30	U6	HEK293T	C57BL/6 female mice	AAV6	Tibialis anterior	<ul style="list-style-type: none"> • protein level reduced by average 90% • mRNA reduced by average 64% • caspase-3 mRNA reduced by 77% 	<ul style="list-style-type: none"> • protection from muscle degeneration • no caspase-3 positive myofibers in muscles 	Wallace L. M., 2012
Facioscapulo humeral muscular dystrophy	<i>DUX4</i>	miR-30	U6	HEK293T	C57BL/6 mice	AAV6	Tibialis anterior	<ul style="list-style-type: none"> • mi1155 toxic to muscles • mi405 safe 	<ul style="list-style-type: none"> • changes in few non-target genes observed, but it was not caused by targeting 	Wallace L. M., 2017
Hyperalgesia	<i>ASIC3</i>	miR-144	CMV	CHO-K1	C57BL/6J mice	HSV	Left gastrocnemius muscle	<ul style="list-style-type: none"> • mRNA reduced by 90% • protein reduced in gastrocnemius muscle 	<ul style="list-style-type: none"> • reduced inflammatory hyperalgesia • inhibition of acid-sensing ion channel heteromeric channels 	Walder R. Y., 2011
Familial hypercholesterolemia	<i>Hmgcr</i>	miR-155*	CMV	Hepa 1-6	Ldlr ^{-/-} mice	-	Tail vein	<ul style="list-style-type: none"> • protein significantly reduced 	<ul style="list-style-type: none"> • LDLR protein level increased • atherogenic plasma lipids reduced by 32% • atherosclerosis reduced by 40% 	Kerr A. G., 2016
Alcohol abuse	<i>NK1R</i>	miR-155*	CMV*	NIH3T3	C57BL/6 mice	LV	Cerebellum	<ul style="list-style-type: none"> • mRNA reduced in hippocampus by 50% • protein reduced in hippocampus 	<ul style="list-style-type: none"> • lower consumption of alcohol in mice 	Baek M. N., 2010

* presumably.

Abbreviations: **CNP** - human 2',3'-cyclic nucleotide 3'-phosphodiesterase gene promoter, **CMVenh/MLC0.26** - cardiac-specific CMV-enhanced 0.26 kb rat MLC promoter, **LV** – lentivirus, **HSA** – human α -skeletal muscle actin

A CAG repeat-targeting artificial miRNA lowers the mutant huntingtin level in the YAC128 model of Huntington's disease

Anna Kotowska-Zimmer,¹ Lukasz Przybyl,² Marianna Pewinska,¹ Joanna Suszynska-Zajczyk,³ Dorota Wronka,² Maciej Figiel,⁴ and Marta Olejniczak¹

¹Department of Genome Engineering, Institute of Bioorganic Chemistry, Polish Academy of Sciences, Noskowskiego 12/14, 61-704 Poznan, Poland; ²Laboratory of Mammalian Model Organisms, Institute of Bioorganic Chemistry, Polish Academy of Sciences, Noskowskiego 12/14, 61-704 Poznan, Poland; ³Department of Biochemistry and Biotechnology, Poznan University of Life Sciences, 60-632 Poznan, Poland; ⁴Department of Molecular Neurobiology, Institute of Bioorganic Chemistry, Polish Academy of Sciences, Noskowskiego 12/14, 61-704 Poznan, Poland

Among the many proposed therapeutic strategies for Huntington's disease (HD), allele-selective therapies are the most desirable but also the most challenging. RNA interference (RNAi) tools that target CAG repeats selectively reduce the mutant huntingtin level in cellular models of HD. The purpose of this study was to test the efficacy, selectivity, and safety of two vector-based RNAi triggers in an animal model of HD. CAG repeat-targeting short hairpin RNA (shRNA) and artificial miRNA (amiRNA) were delivered to the brains of YAC128 mice via intrastriatal injection of AAV5 vectors. Molecular tests demonstrated that both the shRNA and amiRNA reduced the mutant huntingtin level by 50% without influencing endogenous mouse huntingtin. In addition, a concentration-dependent reduction in HTT aggregates in the striatum was observed. In contrast to the shRNA, the amiRNA was well tolerated and did not show signs of toxicity during the course of the experiment up to 20 weeks post injection. Interestingly, amiRNA treatment reduced the spleen weight to values characteristic of healthy (WT) mice and improved motor performance on the static rod test. These preclinical data demonstrate that the CAG-targeting strategy and amiRNA could make an original and valuable contribution to currently used therapeutic approaches for HD.

INTRODUCTION

Huntington disease (HD) is an inherited neurodegenerative disorder caused by the expansion of CAG repeats that encode a polyglutamine (polyQ) tract in the huntingtin protein (HTT). The underlying mutation is located in exon 1 of the 67-exon huntingtin (*HTT*) gene, and the presence of 36 or more CAG repeats is considered pathological.¹ A higher number of repeats results in earlier onset, faster progression, and increased severity of disease symptoms, with >60 CAG repeats leading to the juvenile form of HD.² Somatic CAG repeat instability further expands the CAG/polyQ tract and may serve as an important factor contributing to the selective vulnerability of brain tissues (e.g., the striatum and cortex) and cells (striatal medium spiny neurons) to

HD.^{3,4} Normal huntingtin is widely expressed and is essential for early embryogenesis and the development of the central nervous system.^{5–7} Mutant HTT acquires a toxic function and forms intracellular aggregates that are linked to neuronal dysfunction and degeneration.^{3,8,9} In addition, aberrant splicing of mutant HTT mRNA results in the production of the highly pathogenic exon 1 HTT protein.^{10,11}

Therapeutics that lower the mutant HTT level, such as antisense oligonucleotides (ASOs), RNA interference (RNAi) tools, zinc finger transcriptional repressors, or small molecule inhibitors have shown promising results in preclinical studies.¹² Nonselective approaches that target both mutant and normal HTT are much more prevalent than allele-selective strategies based on single nucleotide polymorphisms (SNPs) or CAG tract length. However, a growing body of evidence suggests that huntingtin plays important functions in the adult brain; thus, selective approaches are much safer.¹³ In 2021, three clinical trials of HTT-lowering ASOs, including allele-selective (NCT03225833 and NCT03225846) and nonselective (NCT03761849) ASOs, were terminated. Of special importance for the HD community is the discontinuation of a phase III study of tominersen (nonselective), which had been demonstrated to be safe, well tolerated, and efficient in reducing the HTT level in the cerebrospinal fluid during a previous phase I/IIa trial.¹⁴ Wave Life Sciences trials (allele-selective) were terminated due to the lack of significant change in the level of the mutant HTT in trial participants treated with WVE-120101 and WVE-120102, compared with those treated with placebo. In the case of Roche, patient groups treated with the tominersen were gradually but clearly starting to do worse than people in the group treated with a placebo. Therefore, there is a need for the development

Received 11 September 2021; accepted 29 April 2022;
<https://doi.org/10.1016/j.omtn.2022.04.031>

Correspondence: Marta Olejniczak, Department of Genome Engineering, Institute of Bioorganic Chemistry, Polish Academy of Sciences, Noskowskiego 12/14, 61-704 Poznan, Poland.

E-mail: marta.olejniczak@ibch.poznan.pl



of new therapeutic strategies for HD and their proper validation in preclinical studies.

RNAi technology uses exogenous small interfering RNA (siRNA) and cellular proteins (the RNA-induced silencing complex, RISC) for selective degradation of target transcripts. Chemical and structural modifications of siRNA (divalent siRNA) allowed potent and persistent silencing of huntingtin in the brains of HD mice, which lasted for at least 6 months.¹⁵ Longer silencing effects can be achieved by vector-based RNAi triggers, such as artificial microRNAs (amiRNAs) and short hairpin RNAs (shRNAs).¹⁶ These molecules resemble miRNA precursors (pri-miRNAs and pre-miRNAs, respectively) and undergo intracellular processing by the endonucleases Drosha and/or Dicer to form mature siRNAs. An amiRNA based on pri-miR-451 and delivered via an AAV5 vector (AMT-130) was demonstrated to be safe and efficient for allele-nonspecific silencing of huntingtin in a few animal models of HD.^{17–19} A phase I/IIa clinical trial (NCT0412049) was started this year to investigate the safety and persistence of AMT-130 in the brain. In other approaches, pri-miR-30- and pri-miR-155-based amiRNAs were used to lower the HTT level using AAV2/1 and AAV9 vectors, respectively.^{20–22} However, all the above examples are nonselective approaches that target both mutant and normal HTT.

In our previous studies, we demonstrated that shRNAs targeting CAG repeats are selective for mutant huntingtin in cellular models of HD.^{23,24} Allele selectivity was achieved by the introduction of mismatches to the siRNA:target duplexes, which changed the mechanism of action from transcript degradation (siRNA-like) to translation inhibition (miRNA-like).^{25,26} In addition, the same shRNAs were efficient in selective inhibition of mutant proteins in other polyQ models,²⁴ thus supporting the idea of using universal CAG-targeting therapeutics for the treatment of polyQ diseases.

Here, we designed and characterized a CAG-targeting amiRNA vector based on a novel pri-miR-136 backbone. Then, we compared the efficacy, selectivity, and safety of the most universal CAG-targeting shRNA (shA2) and corresponding amiRNA in an animal model of HD. RNAi tools were delivered to the brains of YAC128 mice via intrastriatal injection of AAV5 vectors. Regarding the two molecules tested, the amiRNA was efficient, showed allelic preference for the mutant HTT, and was well tolerated for up to 20 weeks post injection. It reduced the number of polyQ aggregates in the striatum, a major hallmark of HD. This preclinical study is an important step in the clinical translation of the RNAi-based CAG-targeting strategy.

RESULTS

Design and characteristics of the CAG repeat-targeting artificial miRNA

The most efficient and allele-selective shRNAs targeting the CAG tract were selected from our previous study²⁴ and used to design more complex amiRNA molecules composed of a siRNA insert and a pri-miRNA scaffold. siRNA inserts contain a single A (A2) and a double G (G4) interruption within a CUG sequence, which generate

A:A and G:A mismatches with a target sequence in the transcript (Figure 1A). CAG-targeting siRNAs were embedded within four naturally occurring pri-miRNA backbones: human pri-miR-451, pri-miR-122, and pri-miR-136 and mouse pri-miR-155 (Figure 1A). The cellular processing of these pri-miRNAs is well characterized.^{20,27–29} Based on miRBase (<http://www.mirbase.org/>)³⁰ analysis and our previous study,²⁸ these pri-miRNAs show high guide-to-passenger strand ratios. In addition, pri-miR-451 undergoes non-canonical, Dicer-independent processing, which does not result in the formation of a passenger strand.³¹ In the amiRNAs based on pri-miR-155 and pri-miR-451, the stem contains the bulges that exist in naturally occurring pri-miRNAs to improve their processing, while the amiRNAs based on shmiR-136 and shmiR-122 exhibit full base complementarity within the hairpin stem (Figure 1A). amiRNA expression cassettes driven by the cytomegalovirus (CMV) promoter were inserted upstream of the copepod GFP (copGFP) reporter gene expressed under the control of the EF-1 α promoter. Lentiviral vectors encoding amiRNAs and control vectors were generated.

In the first step, we analyzed the silencing efficiency of the amiRNAs in a cellular model of HD. Patient-derived fibroblasts (GM04281; 17/68 CAG repeats) were transduced with lentiviral particles at an MOI of 10, and the HTT protein level was analyzed by western blotting. The most effective reagents (amiR136-A2 and amiR451-A2) decreased the mutant HTT protein level by approximately 50%, leaving normal huntingtin level unchanged (Figure 1B). The less effective amiRNAs based on pri-miR-122 and pri-miR-155 caused a 20% to 40% reduction in the mutant HTT level. They also showed worse selectivity. The most allele-selective construct based on pri-miR-136 was chosen for further analysis as a potential candidate for HD therapy. Then amiR136-A2 was tested in other HD patient-derived cell line containing shorter CAG repeat tract in the mutant *HTT* allele (GM04869; 15/47 CAG repeats) (Figure 1C). With the use of two anti-HTT antibodies, we demonstrated that amiR136-A2 significantly decreased the mutant HTT protein level. However, the allele-discriminating properties of the tested reagent were lower than those observed for longer mutant *HTT* alleles. The allele-selective potential of amiR136-A2 was analyzed by a luciferase assay using *HTT* exon 1 containing 16, 40, and 57 CAG repeats as targets (Figure 1D). We observed a repeat length-dependent silencing by amiR136-A2. An HTT silencing efficiency of approximately 50% was achieved for the target sequence with 40 CAG repeats, which is one of the shortest mutant variants observed in patients. Given that the expression of the normal *HTT* variant with 16 CAG repeats was reduced by approximately 20%, this result confirmed the allelic preference of amiR136-A2.

To better characterize this molecule, we analyzed the products of amiR136-A2 processing by Drosha and Dicer. HEK293T cells were transfected with plasmids encoding amiR136-A2, and small RNA-sequencing analysis was performed. The reagent exhibited predominance of the guide siRNA strand originating from the 5' arm, reaching more than 80% of the reads (Figure 1E). Nearly 70% of the molecules contained an A substitution at position 8 relative to

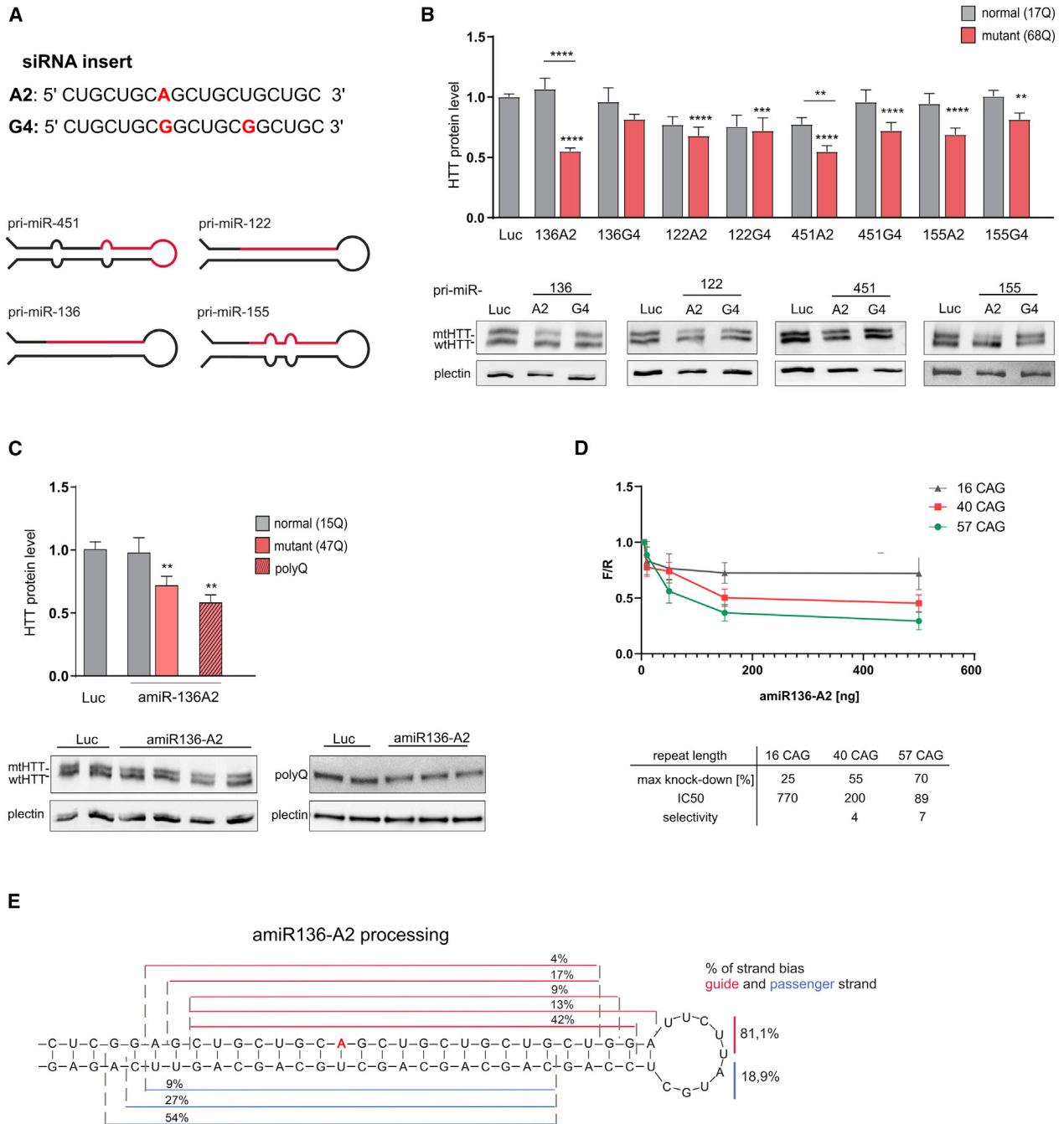


Figure 1. *In vitro* analysis of the efficiency and allele selectivity of different amiRNAs

(A) Schematic representation the siRNA inserts and the pri-miRNA shuttles used to construct the amiRNAs. (B) Western blot analysis of HTT levels in HD patient-derived fibroblasts (cell line GM04281, 17/68Q) 7 days posttransduction with lentiviral particles (MOI of 10), containing expression cassettes with amiRNAs based on the pri-miR-136, pri-miR-122, pri-miR-155, and pri-miR-451 shuttles. Signal intensities of the protein bands were normalized to those of plectin and compared using a one-sample t test. The bars on the graph indicate the mean protein levels \pm SEMs (from at least three biological and technical replicates, $n = 9$). p values are indicated by asterisks ($p < 0.03$, $**p < 0.002$, $***p < 0.0002$, $****p < 0.0001$). (C) Western blot analysis of HTT levels in HD patient-derived fibroblasts (cell line GM04869, 15/47Q) 7 days posttransduction with lentiviral particles (MOI of 10), containing expression cassette with amiR136-A2. Signal intensities of the protein level were normalized to plectin protein levels and compared using a one-sample t test. The graph bars represent the mean value of protein levels \pm SEM (from at least three biological and technical replicates, $n = 9$). p values are

(legend continued on next page)

the 5' end, and the predominant length of the product was 22 nt. A similar pattern of processing was also observed for the shA2 molecule in our previous studies^{23,24}; however, the number of reads representing mature siRNA molecules for the amiRNA was approximately 10 times lower than that for the shRNA and was comparable to the endogenous miRNA level (Figure S1).

ShA2 and amiR136-A2 reduce the mutant HTT level *in vivo* in an allele-selective manner

Two types of vector-based RNAi tools—shRNAs and amiRNAs—can be used to achieve long-lasting silencing effects *in vivo*. Therefore, to directly compare the efficiency and allele selectivity of the CAG-targeting RNAi triggers, shA2 and amiR136-A2 constructs were generated in AAV5 vectors for direct delivery to the striatum of mice. The shRNA and amiRNA were expressed under the control of the Pol III promoter (H1 promoter) and Pol II promoter (a CAG promoter consisting of the cytomegalovirus immediate-early enhancer fused to the chicken β -actin promoter), respectively (Figure 2A). Transgenic YAC128 mice, which express full-length human HTT with 125 CAG repeats interrupted by nine CAA repeats, were used as the HD model³² (Figure 2B). The CAA CAA CAG CAA interruptions are located at repeats 24–28, 109–113, and a single CAA triplet is located at repeat 124. This structure of interruptions still leaves 80 pure CAG repeats and allows the study of CAG repeat-targeting strategies. The presence of mouse Htt (mHtt) with 7 CAG repeats allows indirect analysis of allele selectivity in this model. It is worth noting that the expression level of human HTT is approximately 75% that of endogenous mHtt.³³

To investigate the distribution of AAV5 in the brains of YAC128 mice, we injected AAV5-GFP unilaterally into the striatum at three doses: 1×10^9 , 1×10^{10} , and 1×10^{11} gc/animal ($n = 3$ mice per dose). One month post injection, mice were killed, and coronal and sagittal sections of their brains were prepared for fluorescence microscopy. For the highest concentration of AAV5-GFP, we observed widespread distribution of vector at the injection site and in surrounding regions. The GFP signal was observed in the striatum as well as in the hippocampus. Deeper layers of the cortex were also transduced (Figure 2C).

In the next step, AAV5 vectors expressing shA2 or amiR136-A2 were injected unilaterally into the striatum of 16- or 12-week-old mice, respectively ($n = 10$ mice per vector). Scramble shRNA (shSCR) and amiRNA (amiR136-SCR) were used as controls. GFP was excluded from the expression cassettes to eliminate the risk of inducing the host immune response. Mice received 1×10^{11} gc of AAV5-shRNA or 3×10^{11} gc of AAV5-amiRNA. One month post injection, mice were killed, and their brains were processed to assess the

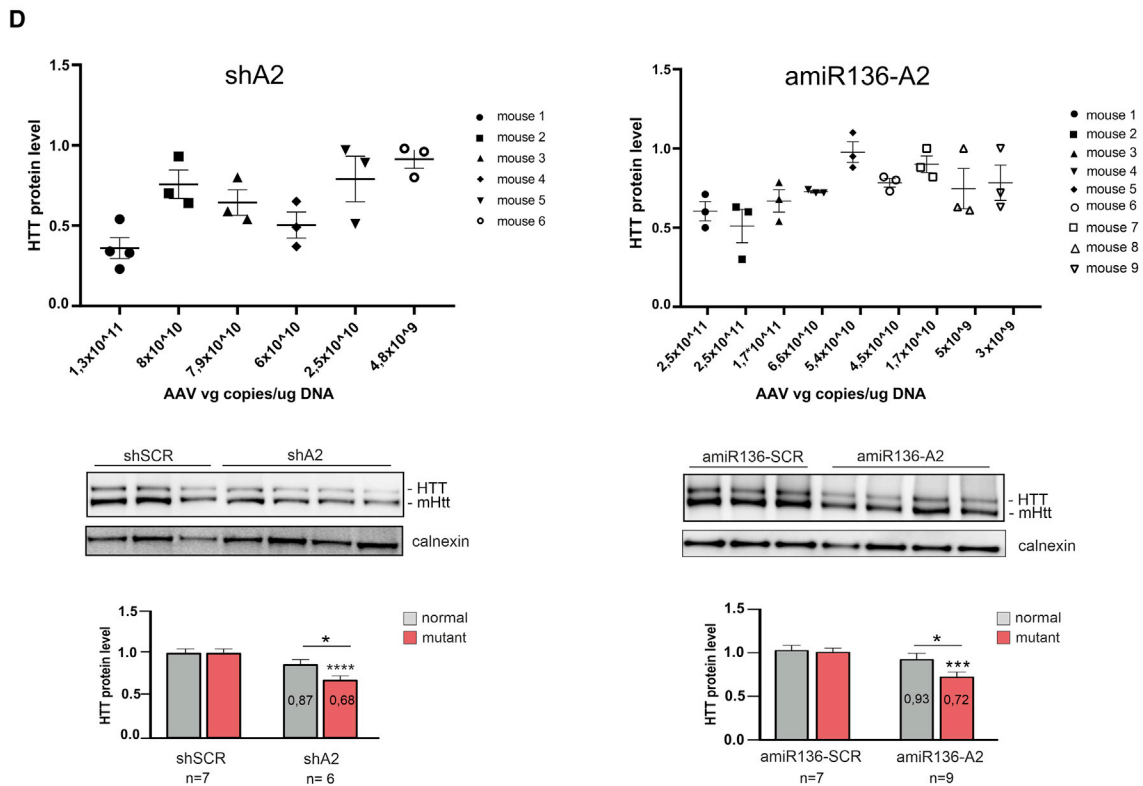
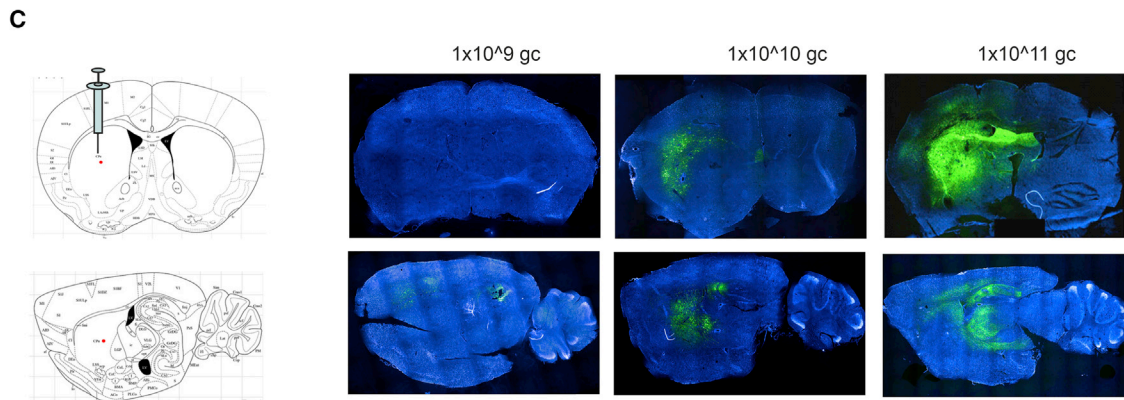
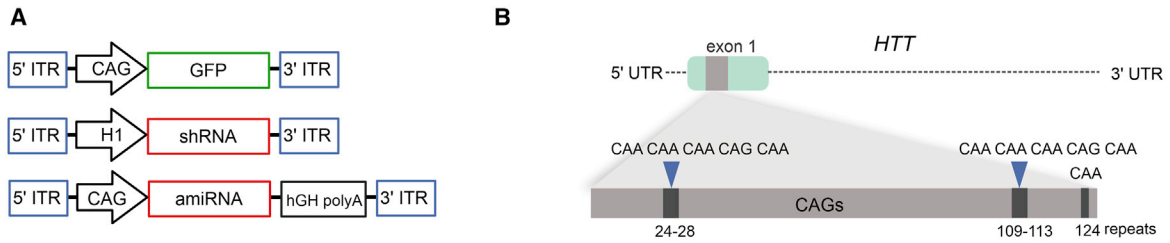
silencing efficiency and the presence of vector DNA. To quantify AAV5 genome copies in the striatum, hippocampus and cortex we performed RT-qPCR with primers specific for the H1 or CAG promoter, depending on the construct. The vector DNA levels in homogenates from injected mice correlated with the silencing efficiency of the HTT protein (Figure 2D). Generally, animals that showed the strongest vector transduction (more than 1×10^{11} vector genome copies per microgram of DNA) showed the greatest reduction in the HTT protein level relative to the SCR control-treated group. A similar average silencing efficiency was observed for shA2 and amiR136-A2 in the striatum (~30%). We also analyzed each sample individually, and the maximum efficiency of HTT silencing in the striatum was ~65% and ~50% for shA2 and amiR136-A2, respectively. The endogenous mHtt level was not significantly reduced. In the other brain regions, the silencing of HTT was also noticeable. In the hippocampus, the silencing efficiency was similar to that in the striatum, possibly due to the proximity of these two regions, and was 30% and 20% for shA2 and amiR136-A2, respectively. The smallest effect was observed in the cortex; a silencing efficiency of 20% was achieved only by amiR136-A2 (Figure S2A). In addition, in some animals, we observed greater HTT silencing in the hippocampus and cortex than in the striatum (Figure S2B). The high variability of HTT silencing between individuals can be partially explained by the uneven distribution of AAV5 (Figure S3).

Efficacy comparison of shA2 and amiR136-A2 in a long-term experiment

To evaluate the efficacy of HTT silencing over an extended period, adult mice (12–14 weeks old) received bilateral intrastriatal injections of AAV5 carrying shA2 or amiR136-A2 at low and high doses ($n = 10$ mice). Every 5 weeks post injection, the body weights of the mice were evaluated, and behavioral tests were performed (Figure 3A). Twenty weeks post injection, the mice were killed, and the brains, hearts, and spleens were removed, weighed, and snap frozen for further molecular analysis. DNA, protein, and RNA were isolated from the striatum, hippocampus, and cortex for analysis of vector genome copies, analysis of protein levels by western blotting, and analysis of transcript levels by RT-qPCR, respectively. Two animals from each group were also subjected to perfusion for further immunohistochemical analysis of brain tissues.

Western blot analysis revealed that the HTT protein level in the striatum was significantly reduced by 50% in both the low- and high-dose shA2-treated groups compared with the SCR control-treated group (Figure 3B). Similar silencing efficiencies were achieved using amiR136-A2 at the high dose (~45% and ~50% using a polyQ-specific antibody) (Figure 3C). The low dose of amiR136-A2 caused a decrease of 30% in the HTT level. Both molecules silenced the

indicated by asterisks (** $p < 0.002$). (D) The graph shows the results of Luc reporter knockdown by the amiR136-A2 construct. HEK293T cells were co-transfected with 50 ng of Luc reporters and 5, 10, 50, 150, or 500 ng of amiRNA constructs. The maximal knockdown efficiency achieved with amiR136-A2 (%); the half-maximal inhibitory concentration (IC50) and allele selectivity are shown in the table. (E) Next-generation sequencing analysis of the amiR136-A2 processing pattern in HEK293T cells. The guide strand is indicated in red, and the passenger strand is indicated in blue. Cleavage sites are shown on both strands corresponding to the length of released siRNA variants.



(legend on next page)

expression of HTT in an allele-selective manner, and there was no statistically significant silencing of mHtt with a normal-length-CAG tract. Allele-selective silencing of HTT by shA2 was also observed in the hippocampus and cortex, with silencing efficiencies of approximately 30% and 20%, respectively (Figure S4A). Interestingly, amiR136-A2 reduced the HTT level in the hippocampus by 45% at the low dose and by 35% at the high dose (Figure S4B). Similar to the observations in the short-term experiment, we observed interindividual variability in HTT silencing, and a difference was also observed between brain hemispheres (Figure S5). Analysis of the *HTT* transcript level did not reveal any differences between control- and amiR136-A2-treated animals, confirming translation inhibition mechanism of action (Figure 3D). YAC128 mice exhibit age-dependent neuropathology manifested as whole brain atrophy including striatal loss and the presence of HTT aggregates. We observed a dose-dependent reduction in the number of polyQ aggregates in the striata of amiR136-A2-treated mice (Figure 4).

amiR136-A2 is well tolerated for up to 20 weeks post injection

It has been previously demonstrated that shRNA vectors can be toxic *in vivo*.^{34–36} During the course of the experiment, we observed abnormal behavior of animals treated with AAV5-shRNAs, and some of them had to be killed before termination of the study, specifically, five mice treated with shA2 at the high dose, 3 mice treated with shA2 at the low dose, and one mouse treated with shSCR (control). Consequently, the number of animals per group decreased over time, and some analyses could not be performed. In contrast, amiRNA treatment did not induce any abnormalities, and no signs of toxicity were observed.

YAC128 mice exhibit a characteristic body weight increase starting at the age of 2 months.³⁷ Interestingly, mice injected with the low dose of shA2 weighed less and did not gain weight over time, in contrast to mice in all other groups (Figure S6A). There was no difference in body weight among wild-type (WT), amiR136-SCR-treated, and amiR136-A2-treated animals (Figure 5A).

Expression of mutant huntingtin has been previously shown to increase organ weight.³⁷ Therefore, after the experiment, hearts, brains, and spleens were weighed. Significant differences in organ weights between amiR136-SCR control- and amiR136-A2-treated animals were found only for the spleen (Figures 5A and S6B). Both groups treated with amiR136-A2 showed significantly smaller spleens (SCR = 0.135 g versus 0.105 g versus 0.102 g), resembling spleen weights characteristic of healthy (WT) mice (0.106 ± 0.002).³⁷

To evaluate whether injection of AAV5-amiR136-A2 induces neuroinflammation, striatal tissue sections were stained with antibodies against Iba-1 (a marker of microglia), GFAP (a marker of astrocytes), NeuN (a marker of neurons), and DARPP-32 (a marker of medium spiny neurons). We did not observe histopathologic changes in the injected brain regions (Figure 5B). These results were also confirmed by RT-qPCR analysis of the *Gfap* and *Iba-1* transcript levels, which were similar to those in SCR control-treated mice (Figure 5C).

We evaluated the selectivity of amiR136-A2 for mutant HTT by analyzing the levels of proteins encoded by other genes containing long CAG tracts, including *Rbm33* (10 CAG repeats) and *Hcn1* (>30 CAG repeats with a 4xCAA). Western blot analysis did not reveal any differences in these protein levels between SCR control-treated and amiR136-A2-treated animals (Figure 5D). Then, using bioinformatic analysis, we selected transcripts with full complementarity to A2 siRNA (Table S2). These transcripts included *Golga4*, *Soga3*, *Maml1*, *Ccdc177*, *Th*, and *Ppp1r3f*. Only one (*Golga4*) of the six tested transcripts was downregulated by amiR136-A2 at the high dose; however, this downregulation was statistically insignificant (Figure 5E). The human counterpart does not contain a sequence fully complementary to A2 siRNA.

ShA2 and amiR136-A2 improve some motor and cognitive deficits

YAC128 mice exhibit progressive motor, cognitive, and psychiatric abnormalities.^{38,38–41} During the course of the experiment, mice were subjected to an accelerated rotarod test to assess motor deficit improvement (5, 10, 15, and 20 weeks post injection). Throughout the experiment, mice treated with the high dose of shA2 performed significantly better than mice treated with control shSCR ($p = 0.0398$) (Figure S6C). Although mice injected with the low dose of shA2 performed similarly throughout the course of the experiment, the differences were not significant in comparison with performance in the shSCR group due to the smaller numbers of animals tested. In addition, these mice did not show significant differences compared with mice treated with the high dose. However, treatment with the low dose of shA2 significantly influenced the learning capabilities of YAC128 mice when the performance on each of the 3 days of testing was compared separately at 15 weeks after surgery ($p = 0.0444$). Mice that received the high dose of shA2 behaved similarly at that time point, and the improvement was not significant; however, 5 weeks later, the difference in performance was significant ($p = 0.0158$). In addition to the latency to fall, the distance, number of rotations to

Figure 2. Analysis of the distribution of AAV5-GFP in the YAC128 mouse brain and analysis of the efficiency and allele selectivity of CAG-targeting RNAi triggers *in vivo* in a short-term experiment

(A) Schematic representation of AAV5 vectors encoding GFP, shRNA, or amiRNA. (B) Representation of the YAC128 HTT transgene sequence and location of the CAA interruptions within the CAG tract. (C) Coronal and sagittal sections of mouse brains after intrastriatal injection of AAV5-GFP at three increasing doses: 1×10^9 , 1×10^{10} , and 1×10^{11} gc/mouse. (D) Analysis of HTT protein silencing and the number of AAV5 vector genome copies in the striatum of YAC128 mice. qPCR was used to quantify AAV5 genome copies in the brain structures of shA2- and amiR136-A2 injected mice ($n = 6$ and $n = 9$, respectively) 1 month post injection. Primers specific for the H1 and CAG promoters were used, and the gc values were calculated based on the standard curve. Western blots show examples of the results. Signal intensities of the protein bands were normalized to those of calnexin and compared using Student's *t* test. The bars on the graph indicate the mean protein levels \pm SEMs ($n = 6$ for shRNA, $n = 9$ for amiRNA). *p* values are indicated by asterisks (* $p < 0.03$, ** $p < 0.002$, *** $p < 0.0002$, **** $p < 0.0001$).

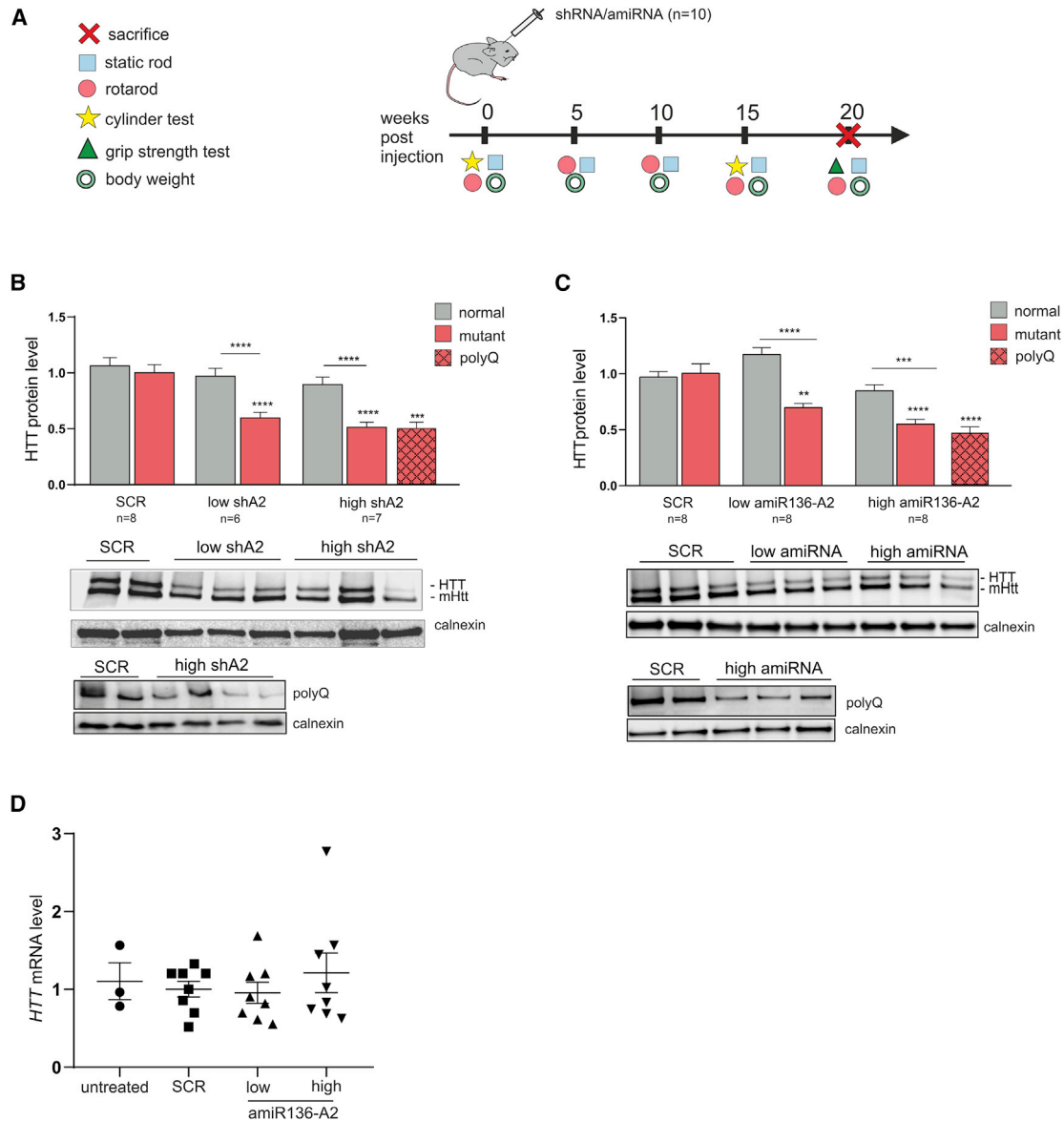


Figure 3. Analysis of HTT protein and mRNA levels 20 weeks post intrastratial injection of mice with A2 shRNA and amiRNA

(A) Overview of the study design showing the timeline of AAV5-shA2 and amiR136-A2 injections, behavioral tests, and experimental endpoints. (B) Western blot analysis of the HTT level in the striatum after shA2 treatment. (C) Western blot analysis of the HTT level in the striatum after amiR136-A2 treatment. Signal intensities of the protein bands were normalized to those of calnexin and compared using Student's *t* test. Two antibodies were used to visualize HTT: one detecting both forms of protein, mutant and normal, and the second detecting only mutant protein (polyQ antibody). The bars on the graph indicate the mean protein levels \pm SEMs (n = 8 for shSCR, 6 for shA2 low dose, 7 for shA2 high dose; 8 for amiR136-A2). *p* values are indicated by asterisks (**p* < 0.03, ***p* < 0.002, ****p* < 0.0002, *****p* < 0.0001). (D) Analysis of the *HTT* mRNA level after amiR136-A2 treatment.

fall, and speed at falling were measured. All of the measurements showed similar results (data not shown).

To further assess the motor performance of mice, a static rod test was performed. Every 5 weeks, mice were placed facing outward on a rod of a certain diameter ranging from 28 to 10 mm, and the time the mouse needed to turn around and traverse the rod

was measured. The most relevant rod has a diameter of 17 mm. Wider rods are easily traversed by mice, and a 10-mm rod is highly challenging for small rodents. Mice treated with shA2 traversed the 17 mm rod even more quickly than WT mice and exhibited a significant performance difference compared with shSCR control-treated animals 15 weeks after treatment (Figure S6D). The time to turn showed a similar trend, but the difference was not

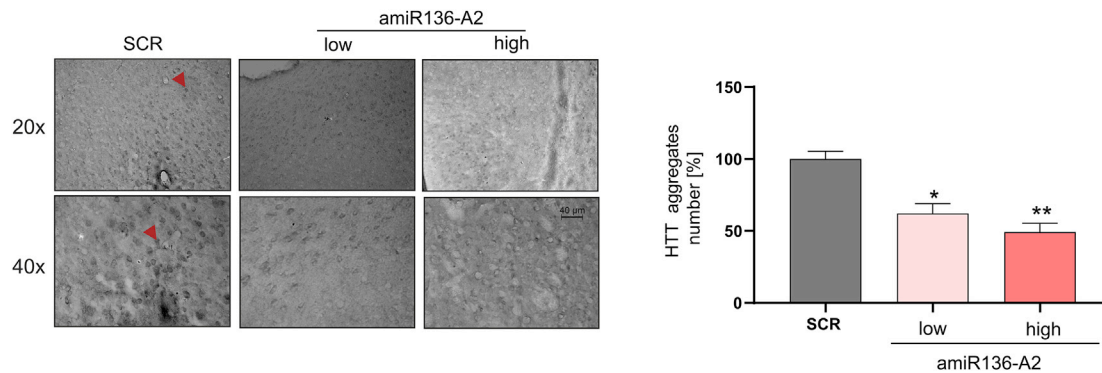


Figure 4. Reduction of the number of HTT aggregates 20 weeks post injection with amiR136-A2

Immunohistochemical (IHC) staining of the striatum using the EM48 antibody, which specifically reacts with intranuclear mutant HTT aggregates. Representative aggregates are indicated by the red arrow. The bars on the graph show the percentage reduction in HTT aggregates after amiR136-A2 treatment. The data were analyzed using one-way ANOVA. p values are indicated by asterisks (*p < 0.03, **p < 0.002). The bars on the graph show the mean protein levels \pm SEMs (n = 2 for amiR136-SCR, 4 for amiR136-A2).

statistically significant. Similar trends were observed for other rod diameters and experimental time points.

Similar to shA2-treated animals, amiR136-A2-treated animals were evaluated using a battery of behavioral tests, including rotarod, static rod, grip strength, and cylinder tests. In the assessment of motor and learning capabilities using the rotarod test, the performance of mice treated with either amiR136-A2 concentration did not differ significantly compared with that of SCR control-treated mice. In contrast, on the static rod test, amiR136-A2-treated mice exhibited a significant improvement in the time to turn on the 17-mm diameter rod 15 weeks after treatment (3.9 versus 1.25 versus 1.76 s) (Figure S6E). Animals did not show any differences on the cylinder or grip strength tests (data not shown).

DISCUSSION

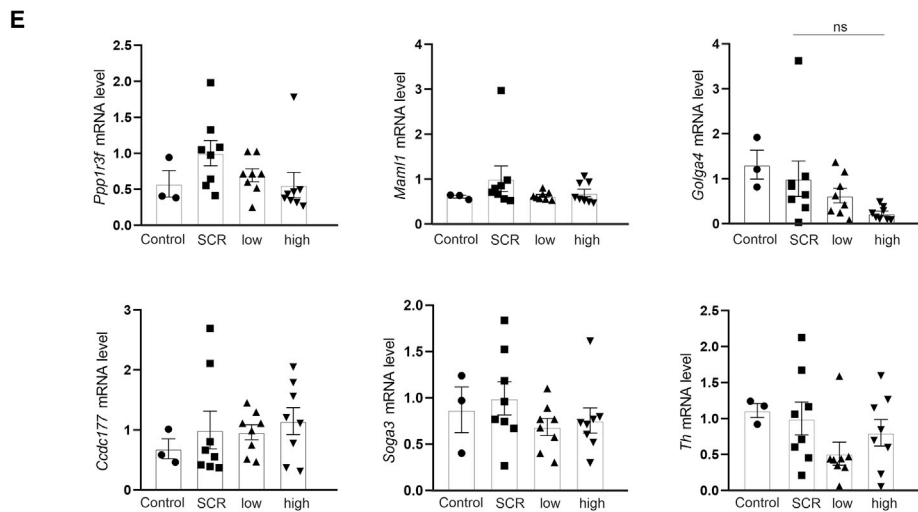
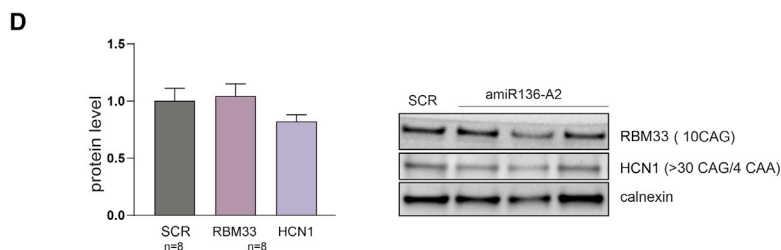
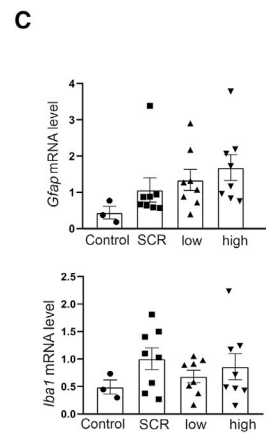
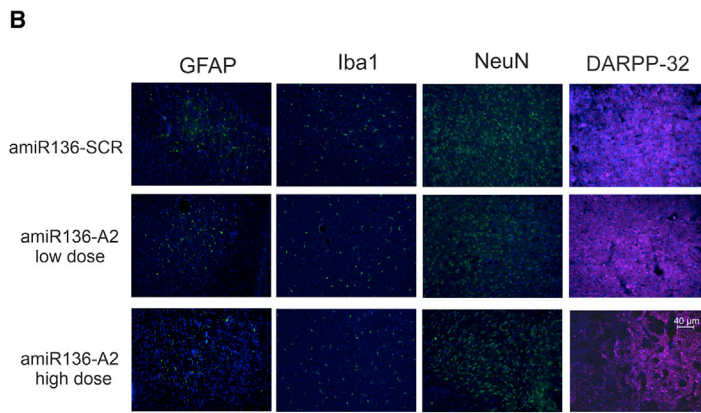
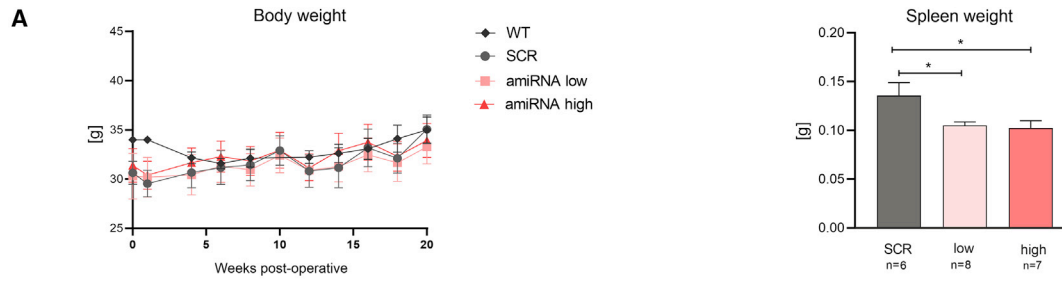
Therapeutic strategies that lower the HTT level have been used in a number of preclinical studies and have demonstrated promising results in decreasing HD pathology.¹⁴ However, apart from ZF transcription inhibitors,⁴² there are no allele-selective approaches based on viral delivery and single administration of therapeutic agents.

Here, we developed a CAG-targeting amiRNA that efficiently and preferentially reduced the mutant HTT level in an animal model of HD. Because cellular biogenesis of vector-based RNAi triggers is difficult to predict, their selectivity with respect to the original siRNA can be reduced or lost.^{43,44} Our previous efforts to find a pri-miRNA scaffold that generates homogeneous siRNA products,²⁸ and detailed analysis of pri-miR-136 processing allowed us to preserve the selectivity and efficacy of the amiR136-A2 vector. By direct comparison of the corresponding shRNA and amiRNA, we confirmed that shRNA can be toxic *in vivo*, probably due to saturation of the miRNA biogenesis pathway.⁴⁵ In contrast, amiR136-A2, which enters the miRNA biogenesis pathway at an early step and generates quantity of mature siRNA approximately 10 times lower than that generated by shA2, did not cause any overt symptoms of toxicity. However,

both the shRNA and amiRNA variants reduced the mutant HTT level by \sim 50% 20 weeks post injection when administered at the high dose. This efficiency of HTT silencing was sufficient to observe a reduction in the number of polyQ aggregates in the striatum, improvements in some motor and learning deficits, and a reduction in the spleen weight to values characteristic of those in healthy mice. It has been postulated that mutant huntingtin expression increases organ weights (except those of the brain and testis), perhaps via a central mechanism originating in the brain.^{33,37,39} This suggests the possibility that a reduction in the mutant HTT level in the brain may influence the spleen weight, but this hypothesis requires further investigation.

In general, CAG repeat-targeting strategies carry a risk of unintended targeting of other genes. Because of the miRNA-like translation inhibition mechanism, only transcripts containing long, uninterrupted CAG repeats can be efficiently silenced by amiR136-A2. In addition, transcripts with full complementarity to the A2 molecule (especially in the 3'UTR) can be degraded by a siRNA-like mechanism. Analysis of selected proteins and transcripts did not reveal any significant off-target effects. Since there is little similarity between the repeated sequences of mice and humans, further analyses in human neurons are necessary. The role of the mutant HTT transcript, which is not degraded by amiR136-A2, also requires further clarification. The toxicity of RNA containing long CAG repeats is mainly correlated to the production of the toxic forms of proteins.^{10,11,46–48} Since our therapeutic agent blocks translation, we can assume that it prevents the formation of toxic proteins, and thus the negative effects mentioned in these studies.

Previous studies demonstrated that direct injection of AAV5 into the parenchyma ensures widespread distribution of the vector in the CNS and sufficient transduction of deep brain structures.^{17,49,50} In addition, a recent study confirmed that amiRNAs are present in vesicles 2 years post injection into the brains of NHPs.⁵¹ These results support the choice of AAV5 as a delivery vehicle for amiR136-A2; however, the high variability in the silencing efficiency between individuals



(legend on next page)

and the low silencing efficiency in the cortex suggest that the delivery and distribution of RNAi vectors in the brain should be improved. The uneven distribution of amiR136-A2 may be a cause of the weak improvements in motor deficits. YAC128 mice represent a “late-onset” model, and it is possible that examination at later time points (e.g., in ≥ 9 -month-old animals) may reveal more behavioral improvements (our tested animals were 8 months old).

The most advanced RNAi-based approach using nonselective amiRNA and AAV5 vectors (AMT-130) is currently in a phase I/IIa clinical trial (NCT0412049). The main advantages of this approach compared with more advanced ASOs are the possibility of a single administration and the long-term effects. Our strategy gives an additional benefit of allele selectivity and possible universality for the treatment of other polyQ disorders. Overall, this preclinical study is an important step in the clinical translation of vector-based CAG repeat-targeting strategies.

MATERIALS AND METHODS

Cell culture

Fibroblasts from HD patients (GM04281 and GM04869) were obtained from Coriell Cell Repositories (Camden, NJ) and grown in minimal essential medium (MEM) (Sigma-Aldrich, St. Louis, MO) supplemented with 10% fetal bovine serum (FBS) (Sigma-Aldrich) and antibiotics (Sigma-Aldrich). HEK293T cells were grown in Dulbecco's modified Eagle's medium (DMEM) (Sigma-Aldrich) supplemented with 8% FBS, antibiotics, and L-glutamine (Sigma-Aldrich).

Plasmids and viral vectors

For experiments performed in cell cultures, the amiRNA expression cassettes were generated from DNA oligonucleotides (Sigma-Aldrich, see the sequences in [Table S1](#)). Pairs of oligonucleotides were annealed and ligated into the pCDH-CMV-MCS-EF1-Puro (System Biosciences, Palo Alto, CA) expression plasmid and verified through sequencing. For lentivirus production, the plasmids were cotransfected with the packaging plasmids pPACKH1-GAG, pPACKH1-REV, and pVSVG (System Biosciences) into HEK293TN cells. The medium was collected on days 2 and 3, and the viral supernatants were passed through 0.45- μ m filters and concentrated using PEGit Virus Precipitation Solution (System Biosciences). The lentiviral vectors were resuspended in Opti-MEM (GIBCO, Invitrogen, Carlsbad, CA), and the virus titers (TU/mL) were determined through flow cytometry (Accuri C6, BD Biosciences, San Jose, CA) based on copGFP expression. Transduction of fibroblasts was performed at MOI of 10 in the presence of polybrene (4 μ g/mL). Total protein was harvested

7 days post transduction. The luciferase (Luc) construct was used as a negative control.

For *in vivo* experiments, the shRNA and amiRNA constructs were used for the production of the AAV5 vectors. The shRNAs were expressed under the control of the H1 Pol III promoter and they contained a 22-base pair stem and a 10-nt miR-23 loop; the amiRNAs were expressed under the control of the CAG Pol II promoter. We used shSCR (scramble) and amiR136-SCR constructs as negative controls for silencing. AAV5 vectors were produced in the HEK293 cell system by Vigene Biosciences (Rockville, MD).

Luciferase assays

For luciferase assays, HEK293T cells were cultured in 24-well plates in DMEM supplemented with 10% FBS. The next day, the cells were cotransfected with two types of plasmids: constructs containing exon 1 of the *HTT* gene with defined numbers of CAG repeats (16, 40 and 57) with Renilla and firefly luciferase sequences,²⁴ and constructs containing amiR136-A2, using Lipofectamine 2000 (Invitrogen, Thermo Fisher Scientific, Carlsbad, CA). Cells were cotransfected with 50 ng of the *HTT* target reporter plasmid, and 5, 10, 50, 150, or 500 ng of the amiRNA construct. Forty-eight hours after transfection, cells were harvested and lysed using Passive Lysis Buffer (Promega, Madison, WI). The bioluminescence assay was performed using a Dual-Luciferase Reporter Assay System (Promega) and Victor $\times 4$ Multilabel Plate Reader (PerkinElmer, Waltham, MA) according to the manufacturer's instructions. Empty plasmid was used as the negative control, and the fluorescence intensity of firefly luciferase was normalized to the fluorescence intensity of Renilla luciferase. The values of the half-maximal inhibitory concentrations (IC₅₀) were calculated with the use of the GraphPad/SPSS software.

RNA isolation and RT-qPCR

Total RNA was isolated using TRIzol Reagent (Thermo Fisher Scientific) and Phenol equilibrated, stabilized chloroform:isoamyl alcohol 25:24:1 (PanReac AppliChem, Barcelona, Spain). A DeNovix Nanodrop Spectrophotometer was used to measure the RNA concentration. A total of 500 ng of total RNA was transcribed to cDNA using SuperScript III Reverse Transcriptase (Invitrogen) at 55°C. RT-qPCR was performed in a the CFX Connect Real-Time PCR Detection System (Bio-Rad, Hercules, CA) using SsoAdvanced Universal SYBR Green Supermix (Bio-Rad) with β -actin as the reference gene under the following thermal cycling conditions: denaturation at 95°C for 30 s followed by 40 cycles of denaturation at 95°C for 15 s and annealing at 60°C for 30 s. Sequences of specific primers are listed

Figure 5. Lack of significant off-target effects after intrastriatal injection of amiR136-A2

(A) Body weight was measured twice at 5-week intervals throughout the experimental period. No differences between the treated groups were observed in the amiRNA experiment. amiR136-A2 treatment decreased the weight of the spleen at both doses; p values: * <0.05; ** <0.01; **** <0.0001 (n = 8). For body weight analysis, two-way ANOVA was used, and for spleen weight analysis, one-way ANOVA was used; both were followed by Tukey's test. (B) IHC staining for Iba1 to show microglial activation, with GFAP to show astrocyte activity, with NeuN as a marker for neurons and with DARPP-32, which is specific for medium spiny neurons (MSNs). (C) RT-qPCR analysis of *Gfap* and *Iba1* transcript levels. (D) Western blot analysis of RBM33 and HCN1 proteins containing pure or interrupted CAG repeats in the corresponding genes. The signal intensities of the protein bands were normalized to those of calnexin (n = 8). (E) Analysis of the mRNA transcript level of the predicted off-target genes *Ppp1r3f*, *Mam11*, *Golga4*, *Ccdc177*, *Soga3*, and *Th*. The bars on the graph show the mean mRNA levels \pm SEMs. Control – untreated YAC128 mice.

in Table S3. Gene expression levels were normalized to those in SCR-treated mice.

Bioinformatic analysis

To identify A2 off-target sequences, we mapped the A2 sequence to the mouse genome. We used bowtie (version 1.2.3) with the *-a* (all alignments) and *-v 3* (max 3 mismatches) options. The MM10 genome assembly from University of California, Santa Cruz (UCSC) was used as the reference assembly. Python scripts were used to filter the results. By this analysis, we selected six genes (see Table S2) with full complementarity to A2.

Western blotting

Western blot analysis for HTT protein expression isolated from cell culture was performed as previously described.²⁴ Briefly, 30 μ g of total protein was separated on a Tris-acetate SDS-polyacrylamide gel (1.5 cm, 4% stacking gel/4.5 cm, 5% resolving gel, acrylamide:bis-acrylamide ratio of 49:1) in XT Tricine buffer (Bio-Rad) at 135 V in an ice-water bath. For proteins isolated from mouse brains, NuPAGE Tris-Acetate 3%–8% Protein Gel (Thermo Fisher Scientific) in NuPAGE Tris-Acetate SDS Running Buffer (Thermo Fisher Scientific) were used. After electrophoresis, the proteins were transferred overnight to a nitrocellulose membrane (Sigma-Aldrich) by the wet transfer method. The primary and secondary antibodies were used in PBS/0.1% Tween 20 buffer containing 5% nonfat milk. Immunoreactions were detected using Western Bright Quantum HRP Substrate (Advanta, Menlo Park, CA). Protein bands were scanned directly from the membrane using a camera, and band densities were quantified using a Gel-Pro Analyzer (Media Cybernetics). Plectin or calnexin was used as the reference protein. A list of all antibodies used is provided in Table S4.

Small RNA next-generation sequencing and data analysis

Total RNA was isolated (TRI reagent) from HEK293T cells at 24 h post transfection, and the RNA quality was analyzed with an Agilent 2100 Bioanalyzer (RNA Nano Chip, Agilent, Santa Clara, CA). Small RNA sequencing was performed by CeGaT (Tubingen, Germany) using an Illumina HiSeq2500 with 1×50 base pair reads. Demultiplexing of the sequencing reads was performed with Illumina bcl2fastq (2.19) software. Adapter trimming was performed with Skewer (version 0.2.2).⁵²

The reads in FASTQ format were then subjected to length filtering using a custom Python script, retaining only sequences longer than 15 nucleotides. Then, the reads were filtered for quality using the fastq_quality_filter tool in the FASTX-Toolkit package (http://hannonlab.cshl.edu/fastx_toolkit/). We applied the parameters *-q20* and *-p9*, with which only reads having 95% of the bases with a Phred quality score ≥ 20 were retained. Through quality filtering, between 5% and 6% of the reads from each sample were discarded. Then, we removed redundant data with the fastx_collapse tool in the same package. The reads were finally mapped against the sequences of our shRNA constructs using bowtie, with no mismatches allowed. Finally, with an in-house Python script, the alignments were parsed and displayed in a graphical form for manual inspection.

Animal model and housing

All experiments were performed on YAC128 transgenic (FVB-Tg(YAC128)53Hay/J) and WT (FVB/NJ) mice maintained on the FVB/NJ strain background.⁵³ Mice were acquired from The Jackson Laboratory and bred in the animal facility of Center for Advanced Technologies Adam Mickiewicz University in Poznan (CAT AMU) where the experiments were conducted. All experiments were approved by the Local Ethical Committee for Animal Experiments (approval no. 45/2018 given on 22.11.2018). Animals were housed under specific pathogen-free conditions, and their health was monitored on a 3-month basis. Mice were housed in individually ventilated cages with access to water and food *ad libitum*.

Intrastriatal delivery of AAVs

In the treated groups, we stereotaxically injected 3 μ L of AAV5 vectors into the striatum of both hemispheres at specific coordinates (AP + 0.7 mm, ML \pm 1.7 mm, and DV -3.5 mm from the bregma) using a Hamilton gauge syringe over a 10-min period (0.3 μ L/min). In the pilot experiment ($n = 10$ per construct), mice were injected with 3 μ L of AAV5 vectors unilaterally into the right hemisphere. All surgeries were performed under inhaled isoflurane anesthesia, and mice were placed on a heating pad to prevent hypothermia. The wound was covered with antibiotics to prevent infection. After surgery, mice were injected subcutaneously with a nonsteroidal anti-inflammatory drug (meloxicam) and transferred to preheated cages for recovery. The health of mice was monitored for at least 2 h postsurgery and afterward on a daily basis. WT littermate mice were used as healthy controls in the shA2 experiment.

Animal perfusion and tissue collection

Mice were subjected to cardiac perfusion with PBS to remove all blood and were then perfused with 4% paraformaldehyde solution. After 24 h, brains were transferred to 30% sucrose for 72 h. Then, tissues were sectioned into 25- μ m sections using a cryostat at -16°C and mounted on SuperFrost Plus slides (Thermo Scientific).

Immunohistochemistry

Heat-induced antigen retrieval was performed. Sections were incubated in citrate buffer (pH 6.0) for 30 min in a boiling water bath and were then placed in ice-cold TBS-T. Then, sections were blocked with 4% normal goat serum in TBS-T for 1 h. For immunofluorescence staining, sections were incubated overnight at 4°C with the primary antibodies (listed in Table S4) and subsequently with the corresponding secondary antibodies. Sections were mounted using ProLong Gold Antifade mounting reagent with DAPI (Thermo Fisher P36941).

For aggregate staining, EM48 primary antibody (Sigma-Aldrich) and an ImmPRESS Horse Anti-Mouse IgG PLUS Polymer Kit (Vector Laboratories, Burlingame, CA) were used according to the manufacturer's instructions. Images were acquired with a Leica SP5 confocal microscope. ImageJ Software (NIH, Bethesda, MD) was used for aggregate quantification. The counts were made from eight images from each hemisphere (sections separated by 50 μ m).

Behavioral tests

We performed motor function tests (rotarod, static rod, cylinder, grip strength tests) for 20 weeks post injection to evaluate the effect of pre-symptomatic treatment on the HD phenotype.

Rotarod test

We used an accelerating rotarod protocol (Ugo-Basile) to test motor coordination and learning capabilities. The acceleration ranged from 3 to 40 rpm over 5 min. After the training period (three trials per day for 3 days), mice were tested with three consecutive trials in a single day. The rotarod was wiped clean with ethanol between each subject and trial.

Static rod test

To further assess motor deficits in treated YAC128 animals, a static rod test was employed. Mice were placed on four different rods with a specific diameter (28 mm, 21 mm, 17 mm, and 10 mm) and a length of 60 cm facing outward and 100 cm above the bottom surface. Fall protection was provided by a soft cushion below the rod. The time to turn to safety and time to traverse the rod were recorded. The test was repeated two times on consecutive days.

Cylinder (beaker) test

Mice were placed in a transparent beaker with a 90-mm diameter and a height of 125 mm for 3 min. During that time, rearings were counted. For rearing, an animal must be standing on two paws and standing straight with at least one paw touching the wall of the glass cylinder.

Statistical analysis (behavioral)

Statistical analysis of the obtained data was performed with GraphPad/SPSS software. Based on experience and the literature, the majority of experiments would have a power of 80% to achieve a significance level of 0.05. Data are presented as the SEM. Tests to check for a normal distribution were performed. If a normal distribution was confirmed, the data were analyzed by ANOVA or a t test; if the normality assumption was violated, the data were analyzed using Kruskal-Wallis and Mann-Whitney tests, with $p < 0.05$ considered significant. For behavioral testing, when time dependency was considered, two-way ANOVA was performed with additional correction for multiple comparisons with the Holm-Sidak test.

Statistical analysis (molecular)

All experiments were repeated at least three times. The statistical significance of silencing was assessed using a one-sample t test, with an arbitrary value of 1 assigned to the cells treated with control. Selected data were compared using an unpaired t test. Two-tailed p values of < 0.05 were considered significant. Signal intensities of the protein bands were normalized to those of calnexin and compared using Student's t test. The bars on the graphs indicate the mean protein levels \pm SEM. p values are indicated by asterisks (* $p < 0.03$, ** $p < 0.002$, *** $p < 0.0002$, **** $p < 0.0001$).

SUPPLEMENTAL INFORMATION

Supplemental information can be found online at <https://doi.org/10.1016/j.omtn.2022.04.031>.

ACKNOWLEDGMENTS

This study was supported by research grants from the National Science Center PL [2015/18/E/NZ2/00678; 2016/21/D/NZ4/00478; 2019/35/O/NZ1/03535] and Dystrogen Gene Therapies Inc, Chicago, IL. We thank Magdalena Otrocka, Gabriela Kramer-Marek, and Adam Plewinski for technical support. The microscopy analysis was performed in the Laboratory of Subcellular Structures Analysis at the Institute of Bioorganic Chemistry, PAS, in Poznan.

AUTHOR CONTRIBUTIONS

M.O., M.F., L.P., J.S.Z., and A.K.Z. designed the research; A.K.Z., L.P., M.P., J.S.Z., and D.W. performed the experiments; A.K.Z., L.P., M.P., and M.O. analyzed the data and interpreted the results of the experiments; A.K.Z. and L.P. prepared the figures; M.O., A.K.Z., and L.P. drafted, edited, and revised the manuscript; A.K.Z., L.P., M.P., J.S.Z., D.W., M.F., and M.O. approved the final version of manuscript.

DECLARATION OF INTERESTS

Marta Olejniczak (MO) is a coinventor on patents (US9970004B2 and US10329566B2) for the use of the RNAi approach in the treatment of diseases induced by expansion of trinucleotide CAG repeats.

REFERENCES

- MacDonald, M.E., Ambrose, C.M., Duyao, M.P., Myers, R.H., Lin, C., Srinidhi, L., Barnes, G., Taylor, S.A., James, M., Groot, N., et al. (1993). A novel gene containing a trinucleotide repeat that is expanded and unstable on Huntington's disease chromosomes. *Cell* 72, 971–983. [https://doi.org/10.1016/0092-8674\(93\)90585-e](https://doi.org/10.1016/0092-8674(93)90585-e).
- Ross, C.A. (2002). Polyglutamine pathogenesis: emergence of unifying mechanisms for Huntington's disease and related disorders. *Neuron* 35, 819–822. [https://doi.org/10.1016/s0896-6273\(02\)00872-3](https://doi.org/10.1016/s0896-6273(02)00872-3).
- Duyao, M., Ambrose, C., Myers, R., Novelletto, A., Persichetti, F., Frontali, M., Folstein, S., Ross, C., Franz, M., and Abbott, M. (1993). Trinucleotide repeat length instability and age of onset in Huntington's disease. *Nat. Genet.* 4, 387–392. <https://doi.org/10.1038/ng0893-387>.
- Monckton, D.G. (2021). The contribution of somatic expansion of the CAG repeat to symptomatic development in Huntington's disease: a historical perspective. *J. Huntingtons Dis.* 10, 7–33. <https://doi.org/10.3233/JHD-200429>.
- Zeitlin, S., Liu, J.P., Chapman, D.L., Papaioannou, V.E., and Efstratiadis, A. (1995). Increased apoptosis and early embryonic lethality in mice nullizygous for the Huntington's disease gene homologue. *Nat. Genet.* 11, 155–163. <https://doi.org/10.1038/ng1095-155>.
- Nasir, J., Floresco, S.B., O'Kusky, J.R., Diewert, V.M., Richman, J.M., Zeisler, J., Borowski, A., Marth, J.D., Phillips, A.G., and Hayden, M.R. (1995). Targeted disruption of the Huntington's disease gene results in embryonic lethality and behavioral and morphological changes in heterozygotes. *Cell* 81, 811–823. [https://doi.org/10.1016/0092-8674\(95\)90542-1](https://doi.org/10.1016/0092-8674(95)90542-1).
- Van Raamsdonk, J.M., Murphy, Z., Slow, E.J., Leavitt, B.R., and Hayden, M.R. (2005). Selective degeneration and nuclear localization of mutant huntingtin in the YAC128 mouse model of Huntington disease. *Hum. Mol. Genet.* 14, 3823–3835. <https://doi.org/10.1093/hmg/ddi407>.
- Novak, M.J.U., and Tabrizi, S.J. (2010). Huntington's disease. *BMJ* 340, c3109. <https://doi.org/10.1136/bmj.c3109>.
- Gutekunst, C.-A., Li, S.-H., Yi, H., Mulroy, J.S., Kuemmerle, S., Jones, R., Rye, D., Ferrante, R.J., Hersch, S.M., and Li, X.-J. (1999). Nuclear and neuropil aggregates in Huntington's disease: relationship to neuropathology. *J. Neurosci.* 19, 2522–2534. <https://doi.org/10.1523/jneurosci.19-07-02522.1999>.
- Sathasivam, K., Neueder, A., Gipson, T.A., Landles, C., Benjamin, A.C., Bondulich, M.K., Smith, D.L., Faull, R.L.M., Roos, R.A.C., Howland, D., et al. (2013). Aberrant

- splicing of HTT generates the pathogenic exon 1 protein in Huntington disease. *PNAS* 110, 2366–2370. <https://doi.org/10.1073/pnas.1221891110>.
11. Neueder, A., Landles, C., Ghosh, R., Howland, D., Myers, R.H., Faull, R.L.M., Tabrizi, S.J., and Bates, G.P. (2017). The pathogenic exon 1 HTT protein is produced by incomplete splicing in Huntington's disease patients. *Sci. Rep.* 7, 1307. <https://doi.org/10.1038/s41598-017-01510-z>.
 12. Pan, L., and Feigin, A. (2021). Huntington's disease: new frontiers in therapeutics. *Curr. Neurol. Neurosci. Rep.* 21, 10. <https://doi.org/10.1007/s11910-021-01093-3>.
 13. Dietrich, P., Johnson, I.M., Alli, S., and Dragatsis, I. (2017). Elimination of huntingtin in the adult mouse leads to progressive behavioral deficits, bilateral thalamic calcification, and altered brain iron homeostasis. *PLoS Genet.* 13, e1006846. <https://doi.org/10.1371/journal.pgen.1006846>.
 14. Tabrizi, S.J., Leavitt, B.R., Landwehrmeyer, G.B., Wild, E.J., Saft, C., Barker, R.A., Blair, N.F., Craufurd, D., Priller, J., Rickards, H., et al. (2019). Targeting huntingtin expression in patients with Huntington's disease. *N. Engl. J. Med.* 380, 2307–2316. <https://doi.org/10.1056/nejmoa190907>.
 15. Alterman, J.F., Godinho, B.M.D.C., Hassler, M.R., Ferguson, C.M., Echeverria, D., Sapp, E., Haraszti, R.A., Coles, A.H., Conroy, F., Miller, R., et al. (2019). A divalent siRNA chemical scaffold for potent and sustained modulation of gene expression throughout the central nervous system. *Nat. Biotechnol.* 37, 884–894. <https://doi.org/10.1038/s41587-019-0205-0>.
 16. Kotowska-Zimmer, A., Pewinska, M., and Olejniczak, M. (2021). Artificial miRNAs as therapeutic tools: challenges and opportunities. *Wiley Interdiscip. Rev. RNA* 12, e1640.
 17. Evers, M.M., Miniarikova, J., Juhas, S., Vallès, A., Bohuslavova, B., Juhasova, J., Skalnikova, H.K., Vodicka, P., Valekova, I., Brouwers, C., et al. (2018). AAV5-miHTT gene therapy demonstrates broad distribution and strong human mutant huntingtin lowering in a Huntington's disease minipig model. *Mol. Ther.* 26, 2163–2177. <https://doi.org/10.1016/j.jymthe.2018.06.021>.
 18. Miniarikova, J., Zimmer, V., Martier, R., Brouwers, C.C., Pythoud, C., Richetin, K., Rey, M., Lubelski, J., Evers, M.M., van Deventer, S.J., et al. (2017). AAV5-miHTT gene therapy demonstrates suppression of mutant huntingtin aggregation and neuronal dysfunction in a rat model of Huntington's disease. *Gene Ther.* 24, 630–639. <https://doi.org/10.1038/gt.2017.71>.
 19. Caron, N.S., Southwell, A.L., Brouwers, C.C., Cengio, L.D., Xie, Y., Black, H.F., Anderson, L.M., Ko, S., Zhu, X., van Deventer, S.J., et al. (2020). Potent and sustained huntingtin lowering via AAV5 encoding miRNA preserves striatal volume and cognitive function in a humanized mouse model of Huntington disease. *Nucleic Acids Res.* 48, 36–54. <https://doi.org/10.1093/nar/gkz976>.
 20. Pfister, E.L., Chase, K.O., Sun, H., Kennington, L.A., Conroy, F., Johnson, E., Miller, R., Borel, F., Aronin, N., and Mueller, C. (2017). Safe and efficient silencing with a Pol II, but not a Pol III, promoter expressing an artificial miRNA targeting human huntingtin. *Mol. Ther. Nucleic Acids* 7, 324–334. <https://doi.org/10.1016/j.omtn.2017.04.011>.
 21. Stanek, L.M., Sardi, S.P., Mastis, B., Richards, A.R., Treleaven, C.M., Taksir, T., Misra, K., Cheng, S.H., and Shihabuddin, L.S. (2014). Silencing mutant huntingtin by adeno-associated virus-mediated RNA interference ameliorates disease manifestations in the YAC128 mouse model of Huntington's disease. *Hum. Gene Ther.* 25, 461–474. <https://doi.org/10.1089/hum.2013.200>.
 22. McBride, J.L., Pitzer, M.R., Boudreau, R.L., Dufour, B., Hobbs, T., Ojeda, S.R., and Davidson, B.L. (2011). Preclinical safety of RNAi-mediated HTT suppression in the rhesus macaque as a potential therapy for Huntington's disease. *Mol. Ther.* 19, 2152–2162. <https://doi.org/10.1038/mt.2011.219>.
 23. Fiszer, A., Olejniczak, M., Galka-Marciniak, P., Mykowska, A., and Krzyzosiak, W.J. (2013). Self-duplexing CUG repeats selectively inhibit mutant huntingtin expression. *Nucleic Acids Res.* 41, 10426–10437. <https://doi.org/10.1093/nar/gkt825>.
 24. Kotowska-Zimmer, A., Ostrovska, Y., and Olejniczak, M. (2020). Universal RNAi triggers for the specific inhibition of mutant huntingtin, atrophin-1, ataxin-3, and ataxin-7 expression. *Mol. Ther. Nucleic Acids* 19, 562–571. <https://doi.org/10.1016/j.omtn.2019.12.012>.
 25. Ciesiolka, A., Stroynowska-Czerwinska, A., Joachimiak, P., Ciolak, A., Kozłowska, E., Michalak, M., Dabrowska, M., Olejniczak, M., Raczynska, K.D., Zielinska, D., et al. (2021). Artificial miRNAs targeting CAG repeat expansion in ORFs cause rapid deadenylation and translation inhibition of mutant transcripts. *Cell Mol. Life Sci.* 78, 1577–1596. <https://doi.org/10.1007/s00018-020-03596-7>.
 26. Hu, J., Liu, J., and Corey, D.R. (2010). Allele-selective inhibition of huntingtin expression by switching to an miRNA-like RNAi mechanism. *Chem. Biol.* 17, 1183–1188. <https://doi.org/10.1016/j.chembiol.2010.10.013>.
 27. Yoda, M., Cifuentes, D., Izumi, N., Sakaguchi, Y., Suzuki, T., Giraldez, A.J., and Tomari, Y. (2013). Poly(A)-Specific ribonuclease mediates 3'-end trimming of argonaute2-cleaved precursor MicroRNAs. *Cell Rep.* 5, 715–726. <https://doi.org/10.1016/j.celrep.2013.09.029>.
 28. Galka-Marciniak, P., Olejniczak, M., Starega-Roslan, J., Szczesniak, M.W., Makalowska, I., and Krzyzosiak, W.J. (2016). siRNA release from pri-miRNA scaffolds is controlled by the sequence and structure of RNA. *Biochim. Biophys. Acta* 1859, 639–649. <https://doi.org/10.1016/j.bbagr.2016.02.014>.
 29. Jopling, C. (2012). Liver-specific microRNA-122: biogenesis and function. *RNA Biol.* 9, 137–142. <https://doi.org/10.4161/rna.18827>.
 30. Kozomara, A., Birgaoanu, M., and Griffiths-Jones, S. (2019). miRBase: from microRNA sequences to function. *Nucleic Acids Res.* 47, D155–D162. <https://doi.org/10.1093/nar/gky1141>.
 31. Cheloufi, S., Dos Santos, C.O., Chong, M.M.W., and Hannon, G.J. (2010). A Dicer-independent miRNA biogenesis pathway that requires Ago catalysis. *Nature* 465, 584–589. <https://doi.org/10.1038/nature09092>.
 32. Pouladi, M.A., Stanek, L.M., Xie, Y., Franciosi, S., Southwell, A.L., Deng, Y., Butland, S., Zhang, W., Cheng, S.H., Shihabuddin, L.S., and Hayden, M.R. (2012). Marked differences in neurochemistry and aggregates despite similar behavioural and neuropathological features of Huntington disease in the full-length BACHD and YAC128 mice. *Hum. Mol. Genet.* 21, 2219–2232. <https://doi.org/10.1093/hmg/ddg037>.
 33. Slow, E.J., van Raamsdonk, J., Rogers, D., Coleman, S.H., Graham, R.K., Deng, Y., Oh, R., Bissada, N., Hossain, S.M., Yang, Y.-Z., et al. (2003). Selective striatal neuronal loss in a YAC128 mouse model of Huntington disease. *Hum. Mol. Genet.* 12, 1555–1567. <https://doi.org/10.1093/hmg/ddg169>.
 34. McBride, J.L., Boudreau, R.L., Harper, S.Q., Staber, P.D., Monteys, A.M., Martins, I., Gilmore, B.L., Burstein, H., Peluso, R.W., Polisky, B., et al. (2008). Artificial miRNAs mitigate shRNA-mediated toxicity in the brain: implications for the therapeutic development of RNAi. *Proc. Natl. Acad. Sci. U S A* 105, 5868–5873. <https://doi.org/10.1073/pnas.0801775105>.
 35. Grimm, D. (2011). The dose can make the poison: lessons learned from adverse in vivo toxicities caused by RNAi overexpression. *Silence* 2, 8. <https://doi.org/10.1186/1758-907x-2-8>.
 36. Martin, J.N., Wolken, N., Brown, T., Dauer, W.T., Ehrlich, M.E., and Gonzalez-Alegre, P. (2011). Lethal toxicity caused by expression of shRNA in the mouse striatum: implications for therapeutic design. *Gene Ther.* 18, 666–673. <https://doi.org/10.1038/gt.2011.10>.
 37. Van Raamsdonk, J.M., Gibson, W.T., Pearson, J., Murphy, Z., Lu, G., Leavitt, B.R., and Hayden, M.R. (2006). Body weight is modulated by levels of full-length Huntingtin. *Hum. Mol. Genet.* 15, 1513–1523. <https://doi.org/10.1093/hmg/ddl072>.
 38. Van Raamsdonk, J.M., Pearson, J., Slow, E.J., Hossain, S.M., Leavitt, B.R., and Hayden, M.R. (2005). Cognitive dysfunction precedes neuropathology and motor abnormalities in the YAC128 mouse model of Huntington's disease. *J. Neurosci.* 25, 4169–4180. <https://doi.org/10.1523/jneurosci.0590-05.2005>.
 39. Van Raamsdonk, J.M., Murphy, Z., Selva, D.M., Hamidzadeh, R., Pearson, J., Petersén, Á., Björkqvist, M., Muir, C., Mackenzie, I.R., Hammond, G.L., et al. (2007). Testicular degeneration in Huntington disease. *Neurobiol. Dis.* 26, 512–520. <https://doi.org/10.1016/j.nbd.2007.01.006>.
 40. Southwell, A.L., Ko, J., and Patterson, P.H. (2009). Intrabody gene therapy ameliorates motor, cognitive, and neuropathological symptoms in multiple mouse models of Huntington's disease. *J. Neurosci.* 29, 13589–13602. <https://doi.org/10.1523/jneurosci.4286-09.2009>.
 41. Pouladi, M.A., Graham, R.K., Karasinska, J.M., Xie, Y., Santos, R.D., Petersén, A., and Hayden, M.R. (2009). Prevention of depressive behaviour in the YAC128 mouse model of Huntington disease by mutation at residue 586 of huntingtin. *Brain* 132, 919–932. <https://doi.org/10.1093/brain/awp006>.
 42. Zeitler, B., Froelich, S., Marlen, K., Shivak, D.A., Yu, Q., Li, D., Pearl, J.R., Miller, J.C., Zhang, L., Paschon, D.E., et al. (2019). Allele-selective transcriptional repression of

- mutant HTT for the treatment of Huntington's disease. *Nat. Med.* 25, 1131–1142. <https://doi.org/10.1038/s41591-019-0478-3>.
43. Monteyts, A.M., Wilson, M.J., Boudreau, R.L., Spengler, R.M., and Davidson, B.L. (2015). Artificial miRNAs targeting mutant huntingtin show preferential silencing in vitro and in vivo. *Mol. Ther. Nucleic Acids* 4, e234. <https://doi.org/10.1038/mtna.2015.7>.
 44. Miniarikova, J., Zanella, I., Huseinovic, A., van der Zon, T., Hanemaaijer, E., Martier, R., Koornneef, A., Southwell, A.L., Hayden, M.R., van Deventer, S.J., et al. (2016). Design, characterization, and lead selection of therapeutic miRNAs targeting huntingtin for development of gene therapy for Huntington's disease. *Mol. Ther. Nucleic Acids* 5, e297. <https://doi.org/10.1038/mtna.2016.7>.
 45. Grimm, D., Streetz, K.L., Jopling, C.L., Storm, T.A., Pandey, K., Davis, C.R., Marion, P., Salazar, F., and Kay, M.A. (2006). Fatality in mice due to oversaturation of cellular microRNA/short hairpin RNA pathways. *Nature* 441, 537–541. <https://doi.org/10.1038/nature04791>.
 46. Krauß, S., Griesche, N., Jastrzebska, E., Chen, C., Rutschow, D., Achmüller, C., Dorn, S., Boesch, S.M., Lalowski, M., Wanker, E., et al. (2013). Translation of HTT mRNA with expanded CAG repeats is regulated by the MID1-PP2A protein complex. *Nat. Commun.* 4, 1511. <https://doi.org/10.1038/ncomms2514>.
 47. Wojciechowska, M., Olejniczak, M., Galka-Marciniak, P., Jazurek, M., and Krzyzosiak, W.J. (2014). RAN translation and frameshifting as translational challenges at simple repeats of human neurodegenerative disorders. *Nucleic Acids Res.* 42, 11849–11864. <https://doi.org/10.1093/nar/gku794>.
 48. Ghosh, R., Wood-Kaczmar, A., Dobson, L., Smith, E.J., Sirinathsinghji, E.C., Kriston-Vizi, J., Hargreaves, I.P., Heaton, R., Herrmann, F., Abramov, A.Y., et al. (2020). Expression of mutant exon 1 huntingtin fragments in human neural stem cells and neurons causes inclusion formation and mitochondrial dysfunction. *FASEB J.* 34, 8139–8154. <https://doi.org/10.1096/fj.201902277rr>.
 49. Burger, C., Gorbatyuk, O.S., Velardo, M.J., Peden, C.S., Williams, P., Zolotukhin, S., Reier, P.J., Mandel, R.J., and Muzyczka, N. (2004). Recombinant AAV viral vectors pseudotyped with viral capsids from serotypes 1, 2, and 5 display differential efficiency and cell tropism after delivery to different regions of the central nervous system. *Mol. Ther.* 10, 302–317. <https://doi.org/10.1016/j.ymthe.2004.05.024>.
 50. Pietersz, K.L., Martier, R.M., Baatje, M.S., Liefhebber, J.M., Brouwers, C.C., Pouw, S.M., Fokkert, L., Lubelski, J., Petry, H., Martens, G.J.M., et al. (2021). Transduction patterns in the CNS following various routes of AAV-5-mediated gene delivery. *Gene Ther.* 28, 435–446. <https://doi.org/10.1038/s41434-020-0178-0>.
 51. Sogorb-Gonzalez, M., Vendrell-Tornero, C., Snapper, J., Stam, A., Keskin, S., Miniarikova, J., Spronck, E.A., de Haan, M., Nieuwland, R., Konstantinova, P., et al. (2021). Secreted therapeutics: monitoring durability of microRNA-based gene therapies in the central nervous system. *Brain Commun.* 3. <https://doi.org/10.1093/braincomms/fcab054>.
 52. Jiang, H., Lei, R., Ding, S.-W., and Zhu, S. (2014). Skewer: a fast and accurate adapter trimmer for next-generation sequencing paired-end reads. *BMC Bioinf.* 15, 182. <https://doi.org/10.1186/1471-2105-15-182>.
 53. Hodgson, J.G., Agopyan, N., Gutekunst, C.A., Leavitt, B.R., LePiane, F., Singaraja, R., Smith, D.J., Bissada, N., McCutcheon, K., Nasir, J., et al. (1999). A YAC mouse model for Huntington's disease with full-length mutant huntingtin, cytoplasmic toxicity, and selective striatal neurodegeneration. *Neuron* 23, 181–192. [https://doi.org/10.1016/s0896-6273\(00\)80764-3](https://doi.org/10.1016/s0896-6273(00)80764-3).

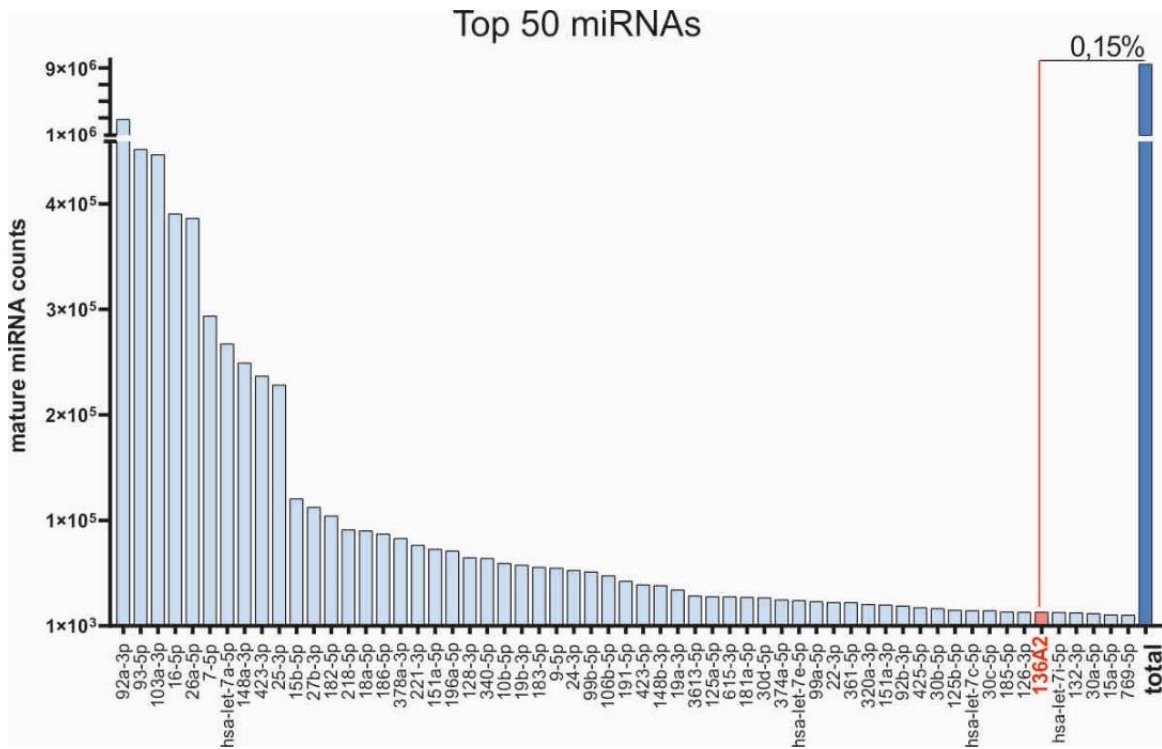
OMTN, Volume 28

Supplemental information

**A CAG repeat-targeting artificial miRNA
lowers the mutant huntingtin level in the YAC128
model of Huntington's disease**

Anna Kotowska-Zimmer, Lukasz Przybyl, Marianna Pewinska, Joanna Suszynska-Zajczyk, Dorota Wronka, Maciej Figiel, and Marta Olejniczak

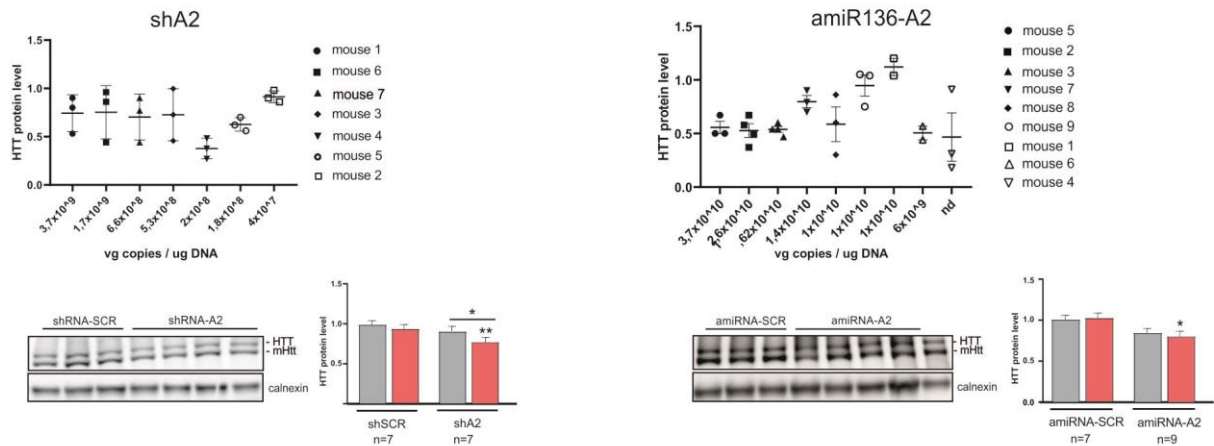
SUPPLEMENTAL INFORMATION



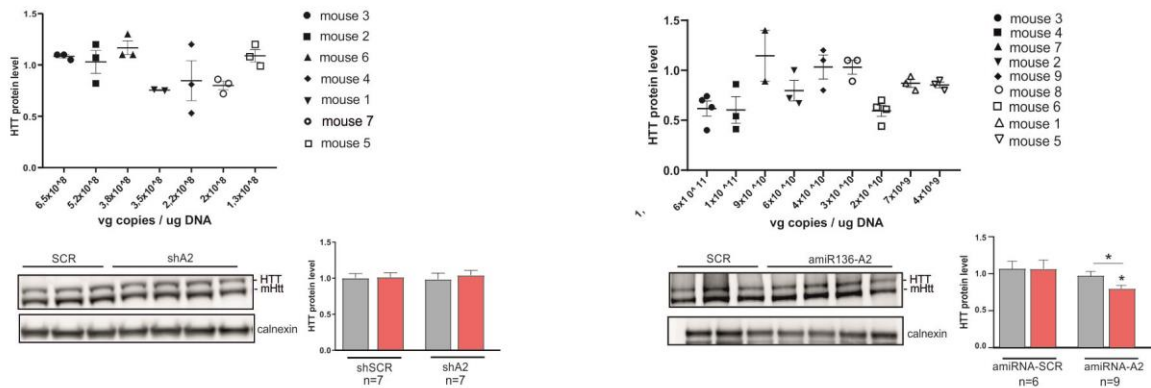
Supplemental Figure S1. Small RNA sequencing analysis of amiR136-A2-treated HEK293T cells. Top 50 most abundant miRNAs. The red bar indicates the mature amiR136-A2 count, and the last bar indicates the total mature miRNA count.

A

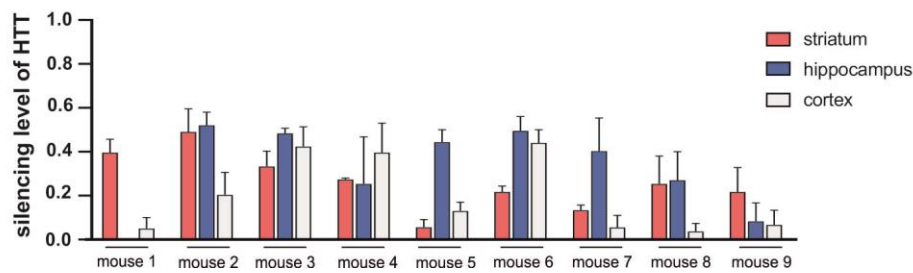
Hippocampus



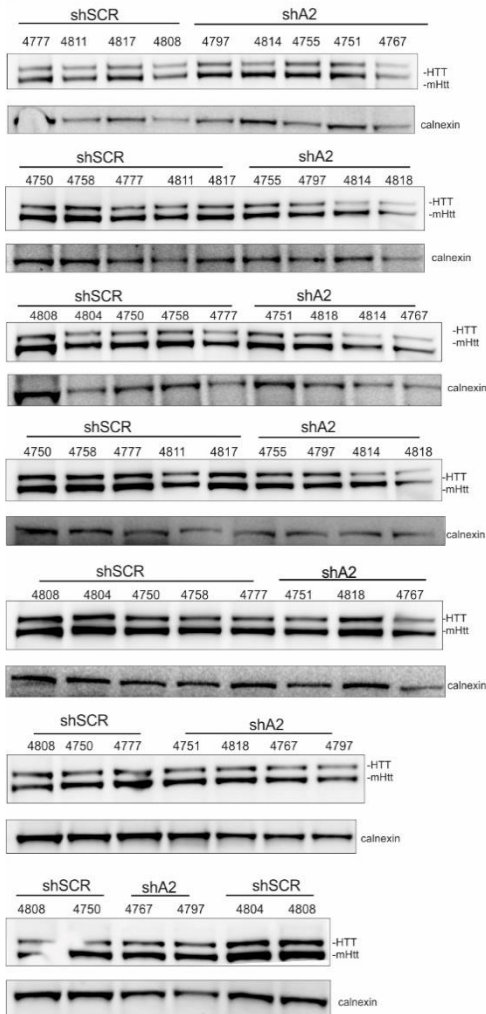
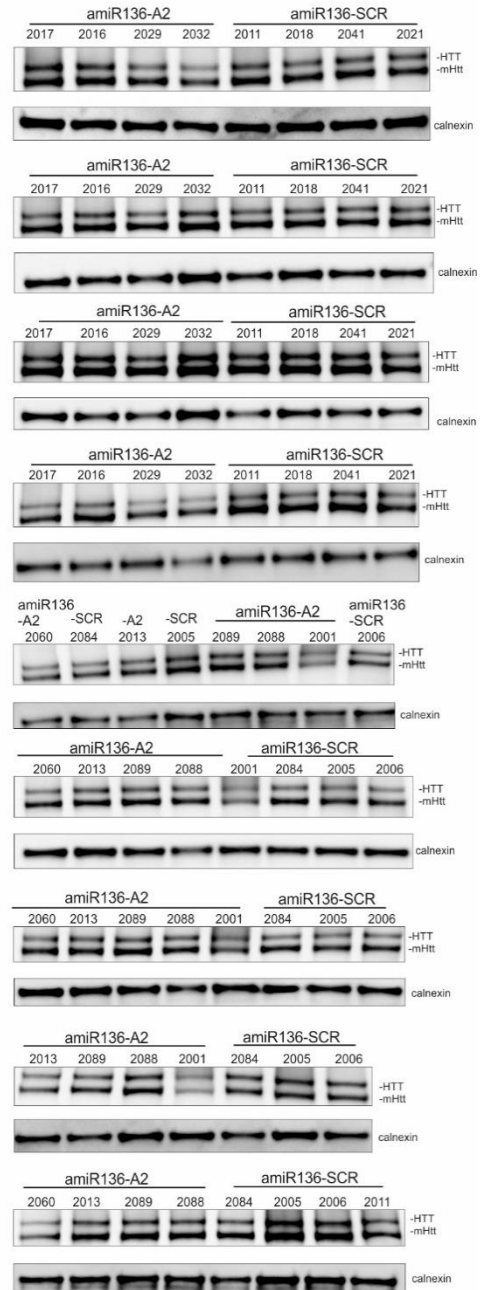
Cortex



B

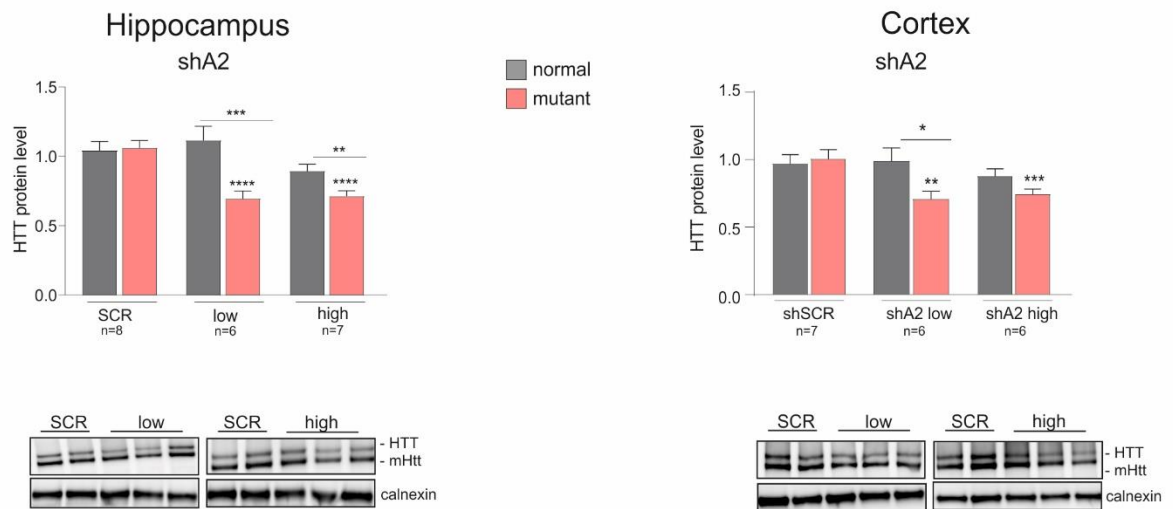


Supplemental Figure S2. Analysis of HTT protein silencing and AAV5 vector genome copies in the hippocampus and cortex of YAC128 mice. (A) qPCR to determine AAV5 genome copies (gc) in the brain structures of shA2- and amiR136-A2-injected mice (n=7 and n=9, respectively), one month post injection. Primers specific for the H1 and CAG promoters were used, and the gc values were calculated based on the standard curve. Western blot analysis of the HTT protein level. (B) Comparison of silencing efficiency in the striatum, hippocampus and cortex in amiR136-A2-treated mice. Signal intensities of the protein bands were normalized to those of calnexin and compared using Student's t-test. The bars on the graph indicate the mean protein levels \pm SEMs. P values are indicated by asterisks (*p < 0.03, **p < 0.002).

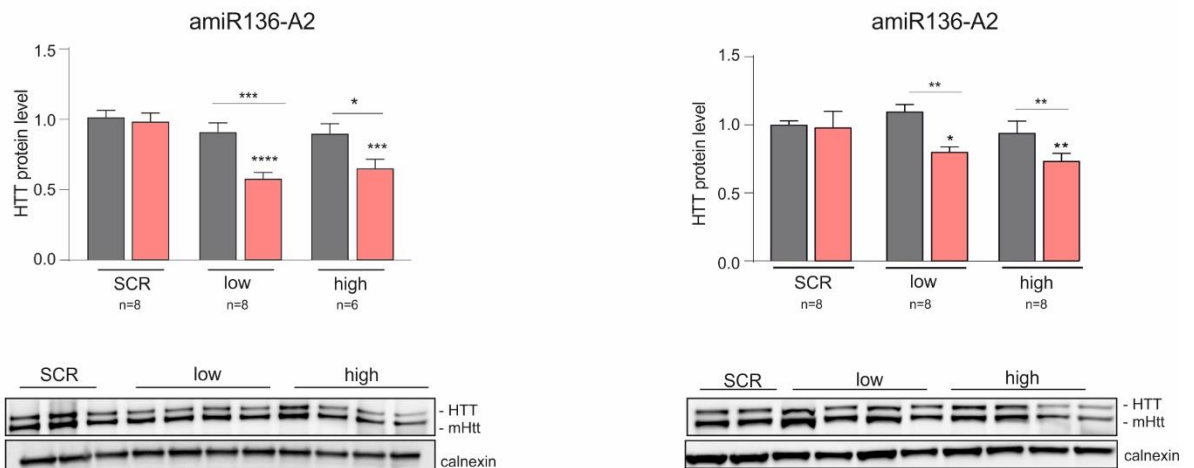
A**B**

Supplemental Figure S3. Western blots used for quantification of HTT suppression in the striatum one month post injection of (A) AAV5-shA2 and (B) amiR136-A2.

A

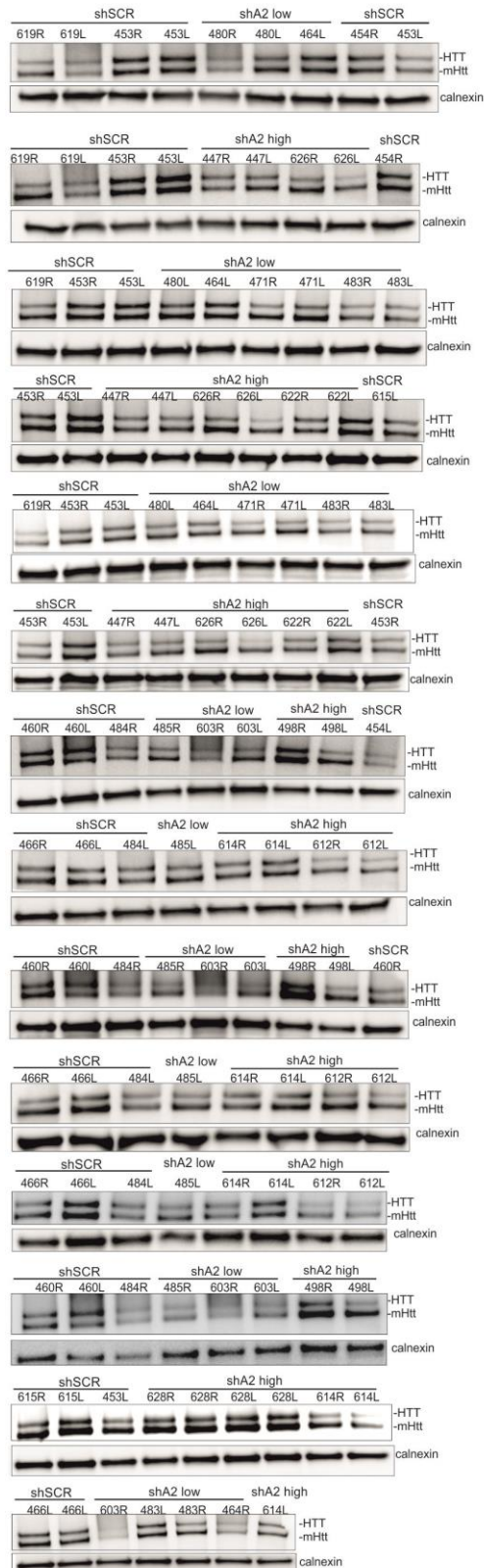


B

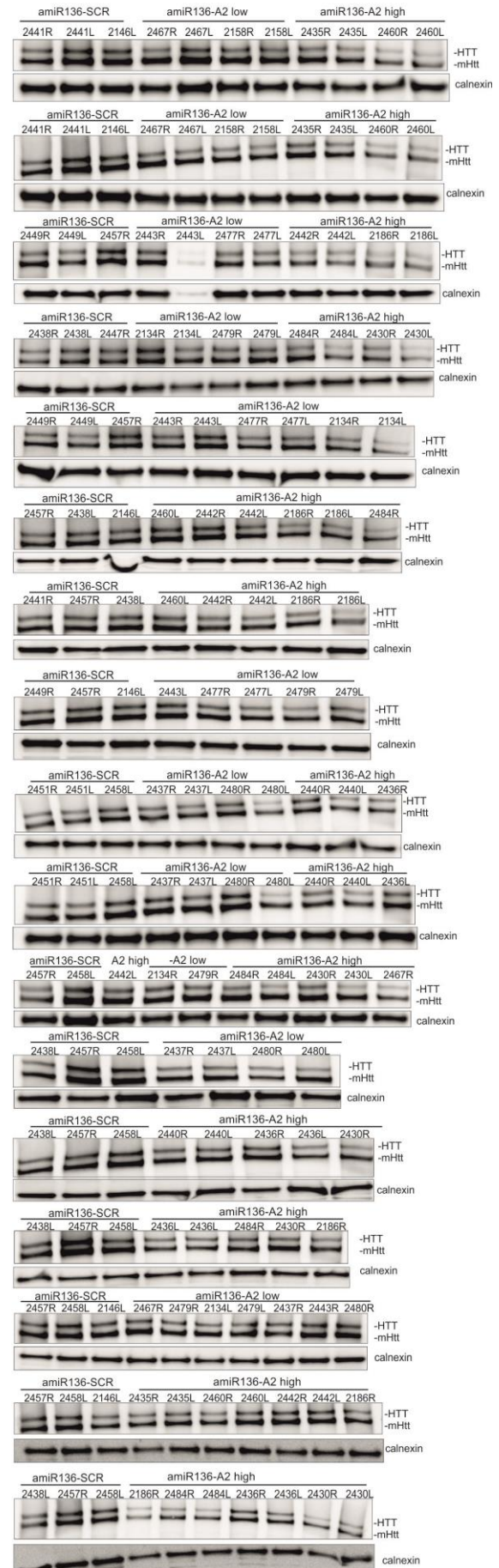


Supplemental Figure S4. Long-term analysis of the efficacy and allele selectivity of shA2 and amiR136-A2 in the hippocampus and cortex in treated mice. **(A)** Western blot analysis of the HTT protein level in the hippocampus and cortex 20 weeks post injection with AAV5-shA2. The shSCR construct was used as the reference control. **(B)** Western blot analysis of the HTT protein level in the hippocampus and cortex 20 weeks post injection with AAV5-amiR136-A2. The amiR136-SCR construct was used as the reference control. The bars on the graph indicate the mean protein levels \pm SEMs. P values are indicated by asterisks (* $p < 0.03$, ** $p < 0.002$, *** $p < 0.0002$, **** $p < 0.0001$).

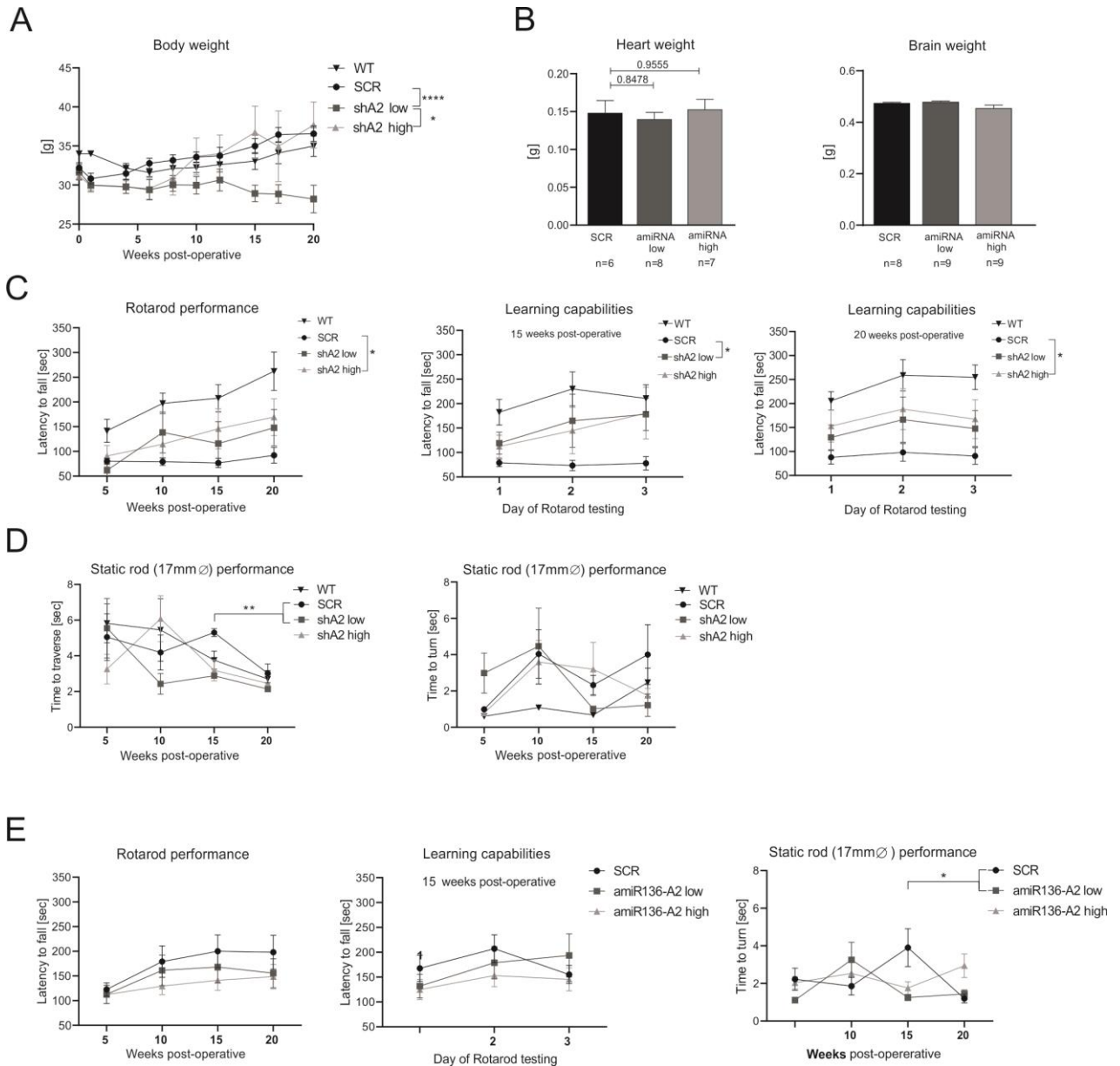
A



B



Supplemental Figure S5. Western blots used for quantification of HTT suppression in the striatum 20 weeks post injection with (A) AAV5-shA2 and (B) amiR136-A2. L- left hemisphere, R – right hemisphere



Supplemental Figure S6. The effects of shA2 and amiR136-A2 administration on body and organ weight and on behavior in YAC128 mice. **(A)** Body weight was measured twice at 5 week intervals throughout the experimental period and showed significant differences between the SCR- and shRNA-treated groups at both the low and high doses. WT animals were used as healthy controls. **(B)** The heart weight and brain weight did not change after amiR136-A2 treatment **(C)** When tested for 3 consecutive days, mice showed improvement in learning on the rotarod test toward the performance of healthy animals 15 weeks after injection with the low dose of shRNA **(D)** The results of the static rod test. Mice treated with shA2 traversed the 17 mm rod more quickly than WT mice and exhibited a significant performance difference compared to shSCR control-treated animals 15 weeks after treatment. There was no significant difference in time to turn parameter **(E)** YAC128 mice treated with amiR136-A2 did not show any improvement in performance in either motor performance or learning capabilities on the rotarod test; mice treated with the low dose of amiRNA showed an improvement in time turn on the 17-mm rod 15 weeks after injection. P values are indicated by asterisks (* < 0.05; ** < 0.01; **** < 0.0001). For body weight 2-way ANOVA was employed and for the spleen weight 1-way ANOVA was used, both with the Tukey's test.

Supplemental Table S1. Oligonucleotides used for the generation of amiRNA constructs.

Pri-miRNA shuttle	Insert	Oligonucleotide sequences 5'->3'
451	A2	CCCAAGAAGCTCTCTGCTCAGCCTGTCAACCTACTGACTGCCAGGGCACTTGGGAATGGCAAGGGCTGCTGCAGCTGCTGCTGCTGCAGCAGCTGCAGCAGATCTTGCTATAACCAAGAAACGTGCCAGGAAGAGAACTCAGGACCCTGAAGCAGACTACTGGAAGGG
	G4	CCCAAGAAGCTCTCTGCTCAGCCTGTCAACCTACTGACTGCCAGGGCACTTGGGAATGGCAAGGGCTGCTGCGGCTGCGGCTGCTGCCGCAGC CGCAGCAGATCTTGCCATTCCAAGAAACGTGCCAGGAAGAGAACTCAGGACCCTGAAGCAGACTACTGGAAGGG
136	A2	CACTCCACTGCCCAGCTCGCCTCGGTGGTGGTGGATGAGCCCTCGGAGGGCTGCTGCAGCTGCTGCTGCTCGATTCTTATGCTCGAGCAGCAGCA GCTGCAGCAGTTCAGAGGGTTCTATCATTTTCGTCGGATGGAAAGGAGTGTATTCTGAAGAT
	G4	CACTCCACTGCCCAGCTCGCCTCGGTGGTGGTGGATGAGCCCTCGGAGGGCTGCTGCGGCTGCGGCTGCTCGATTCTTATGCTCGAGCAGCcGCA GCcGCAGCAGTTCAGAGGGTTCTATCATTTTCGTCGGATGGAAAGGAGTGTATTCTGAAGAT
122	A2	GACAATGGTGGAAATGTGGAGGTGAAGTAAACACCTTCGTGGCTACACCTTAGCAGAGCTGGCTGCTGCAGCTGCTGCTGCTTGTCTAAACTATAGC AGCAGCAGCTGCAGCAGCCAGCTACTGCTAGGCTGTCTTGGCATCGTTTGCTTTGAGCAAGAAGGTTTCATCT
	G4	GACAATGGTGGAAATGTGGAGGTGAAGTAAACACCTTCGTGGCTACACCTTAGCAGAGCTGGCTGCTGCGGCTGCGGCTGCTTGTCTAAACTATAG CAGCCGCAGCCGCAGCAGCCAGCTACTGCTAGGCTGTCTTGGCATCGTTTGCTTTGAGCAAGAAGGTTTCATCT
155	A2	GCCTGGAGGCTTGCTTTGGGCTGTATGCTGGCTGCTGCAGCTGCTGCTGCTGTTTTGGCCACTGACTGACAGCAGCAGCAGCTGCAGCAGCCAGG ACACAAGGCCCTTTATCAGCACTCACATGGAACAAATGGCCC
	G4	GCCTGGAGGCTTGCTTTGGGCTGTATGCTGGCTGCTGCGGCTGCGGCTGCTGTTTTGGCCACTGACTGACAGCAGCcGCAGCcGCAGCAGTCAGG ACACAAGGCCCTTTATCAGCACTCACATGGAACAAATGGCCC

Supplemental Table S2. Off-targets with full complementarity to the A2 insert.

Gene ID	Gene name	Localization	Expression in brain	Expression in other tissues
Golga4	Golgi autoantigen, golgin subfamily a, 4	ORF, 3' UTR*	Low**	High
Soga3	SOGA family member 3	ORF	High	Low
Maml1	Mastermind like transcriptional coactivator 1	ORF	Low	Low
Ccdc177	Coiled-coil domain containing 177	ORF	High	Low
Th	Tyrosine hydroxylase	ORF	High	Low
Ppp1r3f	Protein phosphatase 1, regulatory subunit 3F	ORF	Low	Low

* 3'UTR in transcript ENSMUST00000212593.1. ** based on publication Guo S. et al., DOI: 10.1016/j.bbrc.2020.05.170

Supplemental Table S3. Sequences of primers used for RT-qPCR and genotyping.

Gene	Primer orientation	Sequence
<i>β-actin</i>	F	AGAGCTACGAGCTGCCTGAC
	R	AGCACTGTGTTGGCGTACAG
<i>Cccdc177</i>	F	TCGGACAGGTAGAAAGAGCCAC
	R	CTGTTCTGGCGGAAGCTCGA
<i>Cnr1</i>	F	ATCGGAGTCACCAGTGTGCTGT
	R	CCTTGCCATCTTCTGAGGTGTG
<i>Darpp32</i>	F	TCTCAGAGCACTCCTCACCAGA
	R	CACTCAAGTTGCTAATGGTCTGC
<i>Drd2</i>	F	CCTGTCCTTCACCATCTCTTGC
	R	TAGACCAGCAGGGTGACGATGA
<i>Gfap</i>	F	CACCTACAGGAAATTGCTGGAGG
	R	CCACGATGTTCTCTTGAGGT
<i>Golga4</i>	F	GCAAATGGACCAGCAAGCAA
	R	GGGTTTTAGCGGAAGTCCCA
<i>HTT</i>	F	GTGCAGTGATGACGCAGAGT
	R	TCTTCGGGTCTCTTGCTTGT
<i>Htt</i> (for genotyping)	F	CCGCTCAGGTTCTGCTTTTA
	R	TGGACAGGGAACAGTGTGG
<i>HTT</i> (for genotyping)	F	CCGCTCAGGTTCTGCTTTTA
	R	GGCTGAGGAAGCTGAGGAG
<i>Iba1</i>	F	TCTGCCGTCCAACTTGAAGCC
	R	CTCTTCAGCTCTAGGTGGGTCT
<i>Maml1</i>	F	TCACAAGCAAGATGATGAGCACAG
	R	GCACGGAAGTCACTCCAGCA
<i>Ppp1r3f</i>	F	CCTGATGTTGAGAGTCACTAGG
	R	TGCTGGTCAACATAACTTCGGGC
<i>Soga3</i>	F	AGATGGAGAAGCTGAGGGAAGAG
	R	AGTTGACAGGCATCCTCCTCGA
<i>Th</i>	F	GCCAAGGACAAGCTCAGGAA
	R	CTCAGTGCTTGGGTCAGGGT

Supplemental Table S4. Antibodies used for Western blot analysis and immunohistochemistry.

Protein	Dilution	Supplier	Secondary antibody
HTT (total)	1:2000 in milk 5% PBS-T	Abcam (ab109115)	R-POX Jackson, ImmunoResearch 1:1000, milk 5% PBS-T
polyQ	1:1000 in milk 5% PBS-T	Sigma-Aldrich (P1874)	M-POX Jackson, ImmunoResearch 1:1000, milk 5% PBS-T
plectin	1:1000 in milk 5% PBS-T	Cell Signaling (#12254)	R-POX Jackson, ImmunoResearch 1:1000, milk 5% TBS-T
calnexin	1:2000 in milk 5% PBS-T	Sigma-Aldrich (C4731)	R-POX Jackson, ImmunoResearch 1:1000, milk 5% PBS-T
HCN1	1:500 in milk 5% PBS-T	Abcam (ab176304)	R-POX Jackson, ImmunoResearch 1:1000, milk 5% PBS-T
RBM33	1:1000 in milk 5% PBS-T	Bethyl Laboratories (A303-926A)	R-POX Jackson, ImmunoResearch 1:1000, milk 5% PBS-T
HTT (aggregates)	1:50 in 4% NGS PBS-T	Sigma-Aldrich (MAB5374)	Anti-mouse, Vector Laboratories (MP-7802)
NeuN	1:500 in 4% NGS PBS-T	Millipore (MAB377)	Anti-mouse, Thermo Scientific, 1:1000, 4% NGS TBS-T
IBA1	1:1000 in 4% NGS PBS-T	WAKO (019-19741)	Anti-rabbit, Thermo Scientific, 1:1000, 4% NGS TBS-T
GFAP	1:400 in 4% NGS PBS-T	Millipore (MAB3402)	Anti-mouse, Thermo Scientific, 1:1000, 4% NGS TBS-T
DARPP-32	1:500 in 4% NGS PBS-T	R&D Systems (MAB4230)	Anti-rat, Thermo Scientific, 1:1000, 4% NGS TBS-T